To the Graduate Council:

I am submitting herewith a dissertation written by Ashesh S. Belapure entitled “Catalytic applications of 1,2,4-triazoles in oxidative processes”. I have examined the final electronic copy of this dissertation for form and content and recommend that it be accepted in partial fulfillment of the requirements for the degree of Doctor of Philosophy, with a major in Chemistry.

Shane Foister, Major Professor

We have read this dissertation and
recommend its acceptance:

Shawn R. Campagna

Craig E. Barnes

Thomas A. Zawodzinski

Accepted for the Council:

Carolyn R. Hodges

Vice Provost and Dean of the Graduate School

(Original signatures are on file with official student records.)

Synthesis and Catalytic Applications of 1,2,4-Triazoles in Oxidative Processes

A Dissertation

Presented for the

Doctor of Philosophy

Degree

The University of Tennessee, Knoxville

Ashesh Shirish Belapure

August 2012

Dedication

For my parents

Acknowledgements

The road to getiing a PhD is filled with many obstacles and cannot be completed without the guidance, help and constant encouragement of many. I would like to thank my parents who inculcated the values of education, honesty and perseverance in me. My mother and father have always been my strongest supporters. They are my role models and I can only hope to be as good as them one day. I would also like to express my deepest gratitude to my gradmother who has been a teacher her whole life. She has helped countless students achieve their goals and I count myself fortunate to be one of them.

My road to PhD actually began when I joined Garware College for pursuing M.Sc. It was the teachers that I met there who encouraged me to continue my academic journey and not be satisfied until I achieved the highest education possible. I must thank Dr. Arun Natu, Dr. Suhas Gadre, Dr. Hari Damle and Dr. Paradkar for showing me how exciting the world of organic chemistry was.

Of course, the actual graduate school would have been impossible to complete if not for the guidance of my advisor Dr. Shane Foister. His enthusiasm, knowledge and constant push has helped me continue to drive myself towards the eventual goal. Dr. Ramez ElgammaI, the post doc researcher in our group has been a great help to me throughout this journey. I would like to thank him for his constant support. I would also like thank my committee, Dr. Shawn Campagna, Dr. Craig Barnes and Dr. Thomas Zawodzinski. I am priviledged to have such distinguished committee members, who

despite their busy schedules have always extended their help to me. The support staff at the Department of chemistry at UT has been instrumental in making my life much easier and I would like to offer my sincerest thanks to them.

I wish to thank all former and current members of the Foister Groups. Thank you, Dr. Jeremiah Harden, Dr. Ashleigh Prince, Dave Schneider, Rachel Glazener, Belinda Lady, Chinmay Dabke for your constant support and helpful discussions. I would like to extend special thanks to Belinda Lady and Chinmay Dabke who have helped me beyond what was expected of them. I wish you all the best in your future plans.

My sincerest thanks to Dr. Gabriel Goenaga and Dr. Alex Papandrew for their help on the ORR project. A lot was achieved in a short time because of them.

Last but not the least, none of this would have been possible without the constant and loving support of my dear wife, Sneha. Thank you for always thinking about me and being there for me. You are the best companion one could hope for.

Abstract

Pollution due to use of fossil fuels is a growing problem in today's world. In recent years, chemical research has been focused on catalysis as the possible means of providing economical alternatives to conventional energy sources. Enhanced capabilities in the area of chemical catalysis could play a significant role that can extend from more efficient production of low or non-carbon fuels (e.g., water-splitting, electrolysis, methane oxidation), to more efficient fuel and electrolytic cells. This dissertation describes the homogeneous as well as heterogeneous synthesis of 1,2,4-triazole complexes with transiton metals. The application of these complexes for catalysis of hydrocarbon oxidation, ORR (oxygen reduction reaction) and aziridination are described. Extensive studies into effects of ligand topology and electronics are described. Metal complexes involving 1,2,4-triazole ligands showed remarkable selectivity and activity for hydrocarbon oxidation. These observations led to further exploration of the applications of these catalysts for ORR in fuel cells. Research efforts led to the identification of carbon black immobilized 1,2,4-triazole based catalysts as a potential alternatives for current platinum based catalysts. Finally, the utility of triazole catalysts was extended to the aziridination reaction. Reaction parameter optimization studies led to the discovery of a relatively mild Ni(II)-1,2,4-triazole based catalytic system. A broad substrate scope is observed for this system making it a potent synthetic tool for organic chemists.

Table of Contents

List of Figures

List of Tables

Abbreviations and Acronyms

3,5$Py_2$4atrz	3,5-dipyridyl-4-amino-1,2,4-triazole
3,5Py_2trz	3,5-dipyridyl-1,2,4-triazole
ACN	Acetonitrile
AcOH	Acetic Acid
Atrz	Aminotriazole
BP-2K	Black pearls 2000
DCE	Dichloroethane
DCM	Dichloromethane
DMF	N,N-Dimethylfomamide
CuAAC	Copper-Catalyzed Azide-Alkyne Cycloaddition
DART-TOFMS	Direct analysis in real time, time of flight mass spectrometer
ESI-MS	Electrospray ionization mass spectrometer
Et_2O	Diethyl ether
Et_3N	Triethylamine
EtOAc	Ethyl acetate
EtOH	Ethanol
EWG	Electron withdrawing group
EDG	Electron donating group
Fmoc	Fluorenylmethyloxycarbonyl
GC-MS	Gas chromatography – mass spectroscopy
HBTU	O-Benzotriazole-N,N,N’,N’-tetramethyl-uronium-hexafluoro-phosphate
HDAC	Histone deacetylase
HMPA	Hexamethyl phosphoramide
HOBt	1-Hydroxybenzotriazole hydrate
HPLC	High-pressure liquid chromatography
Htrz	1,2,4-triazole
ICP-OES	Inductively coupled plasma – optical emission spectroscopy
IR	Infrared spectroscopy
LC/MS	Liquid chromatography-mass spectroscopy

MeCN	Acetonitrile
MeOH	Methanol
MOF	Metal-organic framework
MW	Microwave
NMP	N-Methylpyrolidinone
NMR	Nuclear magnetic resonance
NPM	Non-precious metal
ORR	Oxygen reduction reaction
PPA	Polyphosphoric Acid
RDE	Rotating disk electrode
RHE	Reversible hydrogen electrode
RRDE	Rotating ring disk electrode
SHE	Standard hydrogen electrode
TBAB	Tetrabutylammonium bromide
TBAF	Tetrabutylammonium fluoride
TBAI	Tetrabutylammonium iodide
TBTA	Tris(benzyltriazolylmethyl)amine
TFA	Trifluoroacetic acid
TFAA	Trifluoroacetic anhydride
THF	Tetrahydrofuran
TLC	Thin-layer chromatography
UV-Vis	Ultraviolet – visible spectroscopy
XPS	X-ray photoelectron spectroscopy

1. *Catalytic applications of 1,2,4-triazoles in oxidative processes*

1.1. Introduction

As the population of the world is growing, the consumption of fossil based fuels has increased accordingly. Carbon dioxide is one of the main byproducts of fossil fuel burning, which in turn contributes to the greenhouse effect. Over the past few decades, the awareness about the harmful effects of greenhouse gases, in particular carbon dioxide; has increased exponentially.[1] Harmful effects of fossil fuels notwithstanding, they continue to be the primary source of energy generation. A critical reason behind this is the lack of viable alternatives. In recent years the cost, scarcity and the possible depletion of natural sources are creating an acute sense of need for alternative fuels.

In recent years, chemical research has been focused on catalysis as the possible solution to the above mentioned problems. Enhanced capabilities in the area of chemical catalysis could play a significant role that can extend from more efficient production of low or non-carbon fuels (e.g., water-splitting, electrolysis, methane oxidation), to more efficient fuel and electrolytic cells.[2]

The search for better ligands for catalysis of oxidative processes continues relentlessly. This dissertation describes advances made towards developing better catalysts for oxidative processes such as hydrocarbon oxidation, oxygen reduction reaction (ORR) and aziridination.

1.2. Inspirations from nature

Multiple examples of oxidation of organic molecules catalyzed by naturally occurring metalloenzymes are known. Metalloenzyme catalyzed oxidation reactions demonstrate remarkable substrate specificity and regioselectivity. These processes operate under very mild conditions, especially when compared to the analogous industrial processes.[3-5]

Metalloenzymes often act in a way that is difficult to replicate using traditional synthetic chemistry.[6] A good example of this phenomenon is the oxidation of methane to methanol. Traditional approaches toward activation of C-H bonds require extreme reactions conditions such as high temperatures and/or pressures or the use of large excesses of strong oxidants.[7] In nature, metalloenzymes such as the multicopper oxidases catalyze a variety of different oxidation reactions, including alkane hydroxylation, under ambient conditions. Advancements in protein X-ray crystallography have significantly advanced our understanding of the how these enzymes function. **Figure 1-1** shows binding modes of some O_2-derived metalloenzyme intermediates that have been structurally characterized by X-ray crystallography.[8-10] **Figure 1-2** shows metalloenzymes active sites in laccase as well as Cytochrome C Oxidase. While the debate on the particulars of the mechanism still continues, knowing the metalloenzyme structure and function has allowed researchers to design synthetic catalysts. This 'biomimetic' approach allows for tuning of catalyst for activity, selectivity and scale of the reaction.[11-13] The usual oxygen sources used in these reactions are (O_2) and hydrogen peroxide.[13]

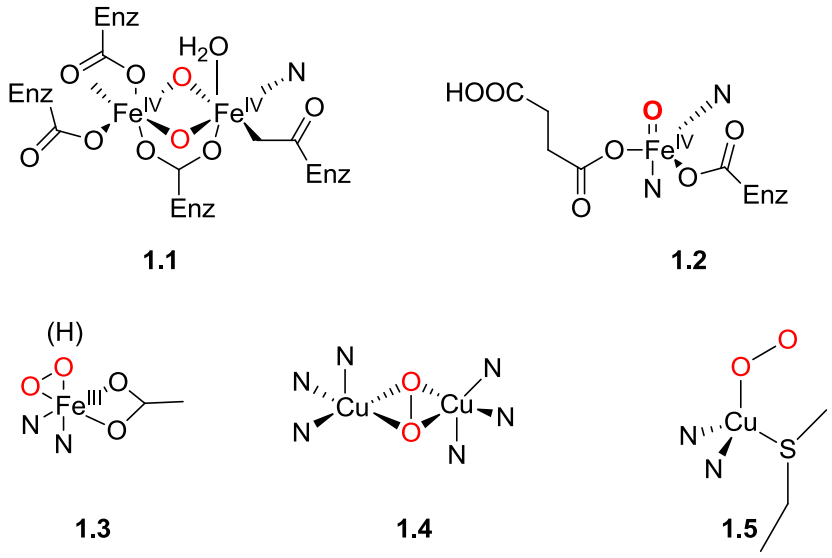

Figure 1-1 - Structurally characterized O_2 derived metalloenzyme intermediates. N represents histidine imidazolyl donor ligands. Key oxygen atoms involved in the process are marked red[13]

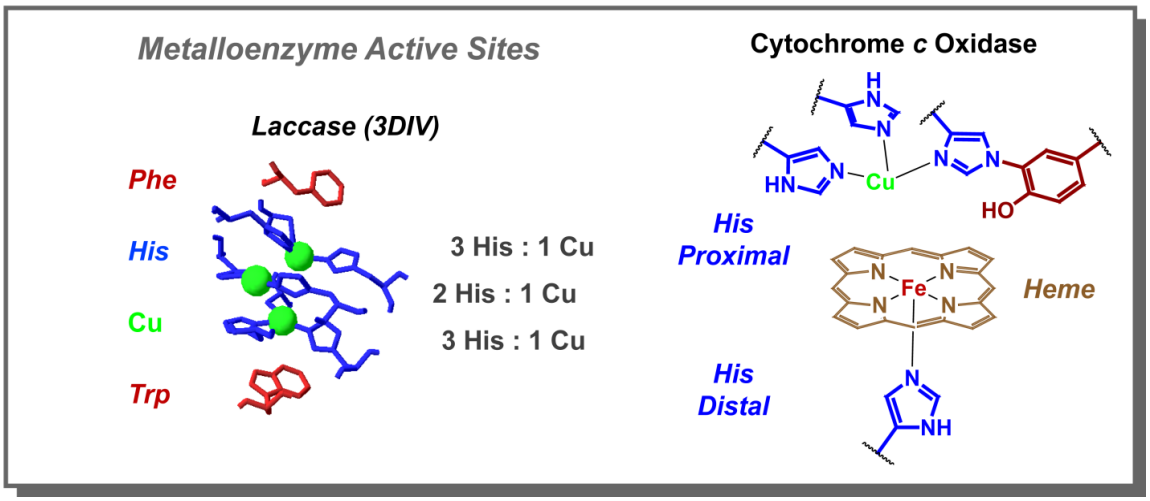

Figure 1-2 – Metalloenzyme active sites[14-15]

Various ligands have been developed that mimic natural metalloenzymes. Heterocycles such as imidazoles, pyrazoles, phenanthrolines, porphyrins, phthalocyanines and pyridines are commonly incorporated in the ligand structures designed for catalyzing oxidation reactions.[16-20] **Figure 1-3** depicts some the commonly used ligands in copper, iron and manganese catalyzed oxidation reactions. As can be seen from these examples, nitrogen containing heterocycles play an important role in oxidation catalysis. Following the biological leads as well as examples of previously developed ligands, we decided to explore alternative ligands that could be used to catalyze oxidative processes.

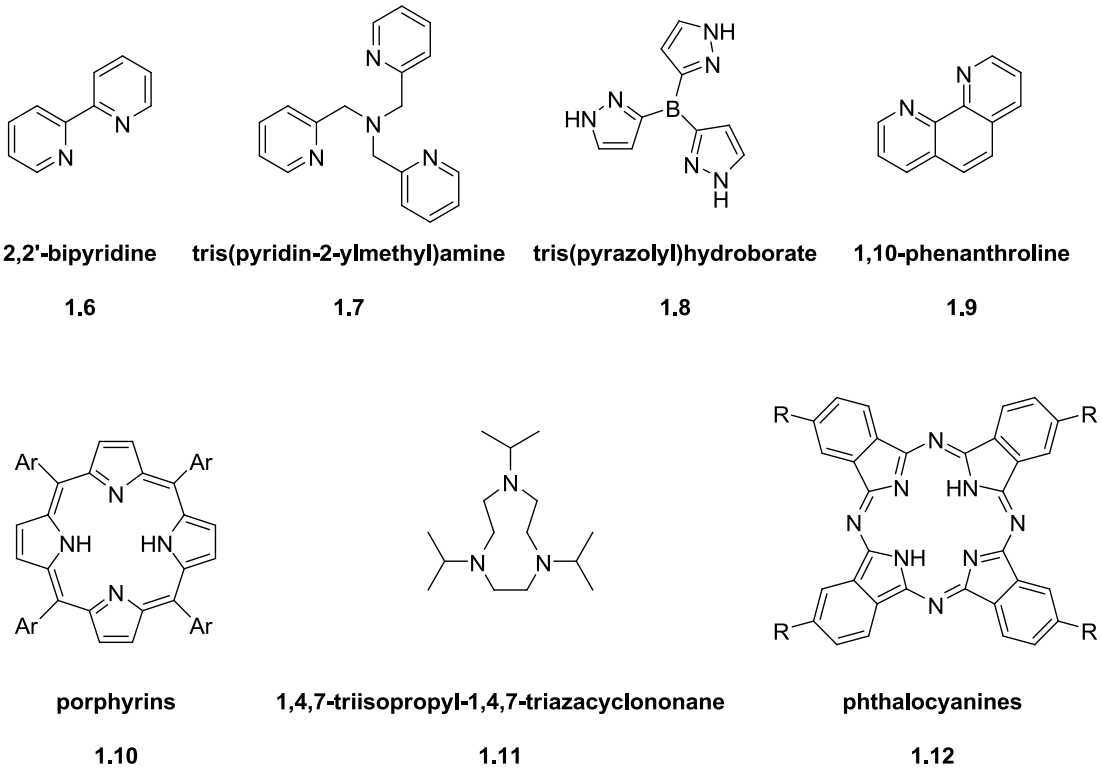

Figure 1-3 - commonly used ligands in copper, iron and manganese catalyzed oxidation reactions

1.3. Choice of 1,2,4-triazoles as ligands for oxidative catalytic processes

1,2,4-Triazoles and its derivatives were first described by Bladin in 1885.[21] Over the past few decades, interest in 1,2,4-triazoles has grown exponentially due to their observed antifungal activity.[22] Fluconazole and Itraconazole are two well known examples of antifungal drug molecules containing 1,2,4-triazole moiety, that are currently marketed **(figure 1-4)**. 1,2,4-triazoles also show herbicidal and antimicrobial activities making them a popular target for new drug development.[23] In fact, just the commerical 3-amino-1,2,4-triazole by itself has been shown to be a potent herbicide. It has been observed that the antifungal and antimicrobial activities are enhanced if the triazole exists as a salt or a metallic complex.[24]

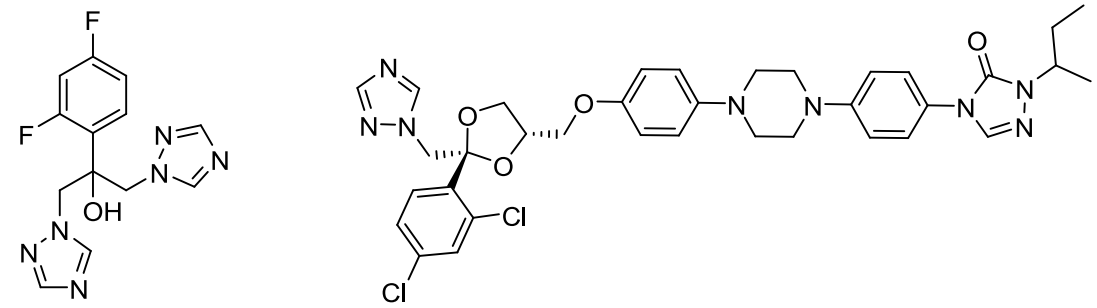

Figure 1-4 - Biologically active 1,2,4-triazoles

1,2,4-Triazoles exist in two tautomeric forms: 1H-form and 4H-form as shown in **figure 1-5**. It must be noted that this distinction is not observed for 1,2,4-triazoles that lack substitution on nitrogen atoms. Experiments designed to give isomeric C-monosubstituted and C-disubstituted triazoles always yield only one product, the 1H isomer.[25] DFT studies on various C-substituted 1,2,4-triazole systems show that the 4H-

form is the least stable form and is thus not observed.[26] However, isomeric forms of N-substituted triazoles are known, and thus this distinction becomes important when considering highly substituted 1,2,4-triazoles.

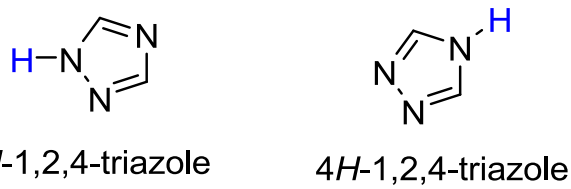

1*H*-1,2,4-triazole 4*H*-1,2,4-triazole

Figure 1-5 - Tautomerism in unsubstituted 1,2,4-triazole

In addition to the biological activity, 1,2,4-triazoles show remarkable potential towards metal binding. The primary reason for their affinity towards metal is the presence of multiple hetero-atoms that can coordinate the metal easily.

Because of the position of the donor atoms in the five-membered ring, the triazoles appear to possess the possibility of linking (transition) metal ions together. The triazole ligands thereby constitute a bridge between the metal ions. This bridge can be of several different geometries, depending on the donor atoms of the ligand and the properties of the metal. This phenomenon is particularly important since pairs or frameworks of metal ions mediate reactions in a different manner than the complexes of isolated metal centers.[27]

The fact that 1,2,4-triazoles are quite similar in geometry to imidazoles, which occur overwhelmingly in nature, is a second property that has made the triazoles and triazole complexes much sought after compounds to mimic natural processes. They are also used to mimic imidazoles in model compounds for such processes.[27] **Table 1-1**

lists examples of metal-1,2,4-triazole frameworks that have been characterized by X-ray crystallography.

Advancements in X-ray crystallography of particulate methane monooxygenase (pMMO)[5], have indicated that di-, tri-, or polynuclear copper centers are present in the active sites. Subsequently, there has been considerable study of polynucleating ligands[28-32] for copper as well as the development of ligands that mimic the coordination sphere of pMMO[33], which contains pendant histidines. As a model for an imidazole-containing histidine residue, we chose 1,2,4-triazoles because i) 1,2,4-triazoles are structurally similar to imidazoles but allow for an additional nitrogen containing coordination site, ii) syntheses of 1,2,4-triazoles requires few steps and are readily amenable to structure-activity relationship studies through control of ligand topology and electronics, iii) copper complexes of 1,2,4-triazoles have been shown to adopt a myriad of structures including di-, tri-, or polynuclear metal centers[34-36], motifs that are present in multicopper oxidases and iv) transition metal complexes of 1,2,4-triazoles adopt various geometries depending on the choice of the metal, thus altering their catalytic properties. Furthermore, while there are many examples of 1,2,4-triazole-metal complexes, the full extent of their catalytic activity has not yet been explored.[37-43]

In order to expore the potential of 1,2,4-triazoles in catalytic processes, we synthesized multiple triazole ligands and screened their complexes with various transition metals for catalytic acitvity. The synthetic strategies applied for this purpose are discussed in chapter 2. An extension of this work involved synthesis of 1,2,4-triazoles immobilized on solid supports such as polystyrene and silica, via solid phase synthesis. Chapter 3 details the synthesis of these entities. It should be noted that the

nature of the triazoles synthesized was largely dictated by the catalytic activity observed, which is described in detail in chapters 4, 5 and 6.

Table 1-1 – Structures of 1,2,4-triazole complexes with different transition metals, deciphered on the basis of x-ray crystallography

Entry	Compound	Structure
1	$CuCl_2(Htrz)$	Polynuclear chain with triple bridges of two chlorides and one N1,N2 triazole[37]
2	$[Ni_3(Htrz)_6(H_2O)_6](NO_3)_6 \cdot 2H_2O$	Trinuclear, triple bridges of three triazoles[38-39]
3	$[Ni_2(3,5Py_2 4atrz)_2Cl_2(H_2O)_2]Cl_2 \cdot 4H_2O$	Dinuclear with planar double N1, N2-triazole bridge[40]
4	$[Cu_2(3,5Py_2trz)_2(NO_3)_2(H_2O)_2] \cdot 1{:}2H_2O$	Dinuclear, planar double N1, N2 triazole bridge[41]
5	HCA II 1,2,4-triazole complex. HCA II = human carbonic anhydrase isoenzyme II	Zinc in tetrahedral coordination, triazole monodentate N4[42]
6	$[Cu(4atrz)Cl_2]$	1D polynuclear, bridges consist of two chlorides and one N1,N2 triazole[43]

1.4. Ligand accelerated copper catalyzed hydrocarbon oxidation reactions

The development of catalysts for mild and selective hydrocarbon oxidation has been a long-standing goal in both synthetic chemistry and industrial processes[44]. Development of biomimetic catalysts has yielded rather elegant systems exhibiting good selectivity towards oxidation of C-H bonds and offer a means of tuning selectivity and activity by judicious choice of ligand sets, solvent, oxidant, and other experimental conditions.[6, 13, 45] These successes have provided a framework for future improvements and may ultimately lead to an efficient method for the oxidation of natural gas to methanol and other valuable chemicals, thereby creating alternatives to petroleum as a primary fuel source.

Despite being thermodynamically favorable, the large BDE of methane, 104 kcal/mol, and high activation energy make this transformation unfavorable. The conventional synthesis of methanol from methane is a multi-step process, typically requiring high temperatures (700 C) and pressures (200-300 atm). Therefore, methods to develop catalysts that operate under mild conditions, thus preventing overoxidations to HCHO, COx, etc., are highly sought.[7]

In Nature, this transformation is catalyzed by iron and copper enzymes, soluble and particulate methane monooxygenase (sMMO and pMMO) respectively, under physiological conditions and efforts to develop functional models based upon MMOs have been met with limited success. While the active site of sMMO, a diiron enzyme, has been well-studied and characterized, the active site of pMMO has yet to be identified. Two recent crystal structures of pMMO, cutaways shown in **Figure 1-6**, have provided some insight.[5, 46] The X-ray data has revealed the presence of a dinuclear

copper cluster bound by histidine imidazoles. Activation of the dicopper center by O_2 likely leads to a species responsible for the alkane hydroxylation observed by pMMO. Of particular interest is the bis(μ-oxo) dicopper core which has an oxygen-centered σ* LUMO consistent with the selectivity of C-H attack.[47]

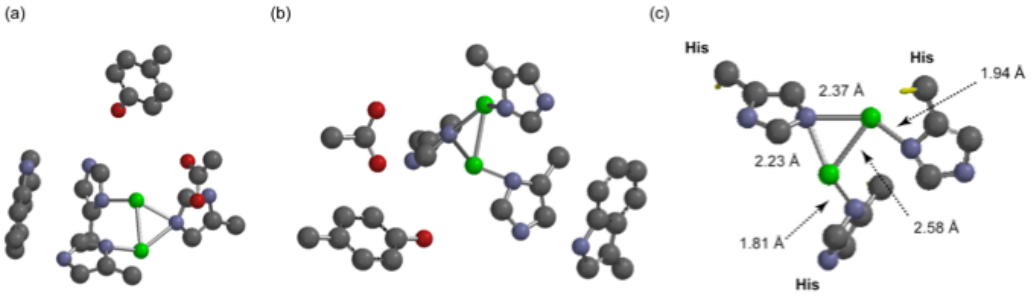

Figure 1-6 - X-ray crystallographic structure of pMMO illustrating pendant histidine ligands and tyrosine and aspartic acid residues. (a) Top-view of 10 Å cutaway of the dicopper site.(b) Side-view of 10 Å cutaway. (c) Distances of histidine ligands from the copper centers and the copper-copper distance[5] (green spheres represent copper)

The catalyst precursors reported in literature range from simple salts to more elaborate copper complexes, in most cases the oxidation state of the metal being +2. It is also worth mentioning that all the complexes employed contain N-donor ligands, a common feature in this catalytic system.

Barton et. al. published a series of contributions related to the use of copper(II), in a pyridine:acetic acid medium, as catalysts for the oxidation of hydrocarbons with hydrogen peroxide, in the early 1990s.[48-53] Conversions observed were always lower than 30% for an array of substrates, the selectivity being also quite low. For example, using $Cu(ClO_4)_2$ as the catalyst precursor, adamantane could be converted into a

mixture of several compounds, including adamantone, adamantoles, as well as other compounds derived from the incorporation of pyridine into the hydrocarbon skeleton.

Recently, Pombeiro and co-workers[28, 54-56] have reported one of the most active to date copper catalytic system for hydrocarbon oxidation. Several multinuclear copper complexes containing the tetradentate triethanolamine ligands were prepared and tested as catalysts for the oxidation of cyclohexane in acetonitrile, using hydrogen peroxide as the oxidant. Such combination of reactants and solvents originate a biphasic reaction medium, acidic in nature by action of HNO_3. The study of several reaction conditions and catalysts showed that the complex $Cu_3(H_2tea)2(4\text{-}HOC_6H_4COO))_2(H_2O)]$ provided the best conversions in the oxidation of cyclohexane, up to 32%, using a 1:800 [catalyst]:[H_2O_2] ratio. Cyclohexanol and cyclohexanone were obtained in nearly 53:47 ratio.

The direct oxidation of methane with non precious metal catalysts has been scarcely reported. Periana and co-workers[57] described the use of metallic gold as catalyst precursor in a 3 M solution of H_2SeO_4 in 96% H_2SO_4 for the conversion of methane into methanol. The reaction is carried out at 180 °C. Se(VI) is required as a stoichiometric oxidant. The catalytic species seems to be cationic gold derived from the solution of the initial gold metal by action of selenic acid. A different approach has been reported by Lee and co-workers[58] that employed copper salts for the methane oxidation by in situ generated hydrogen peroxide. The latter is formed by reacting H_2 and O_2 over Pd/C, and H_2O_2 is then used as the oxidant in the reaction of trifluoroacetic acid and methane. **Figure 1-7** shows schematic representation of these examples.

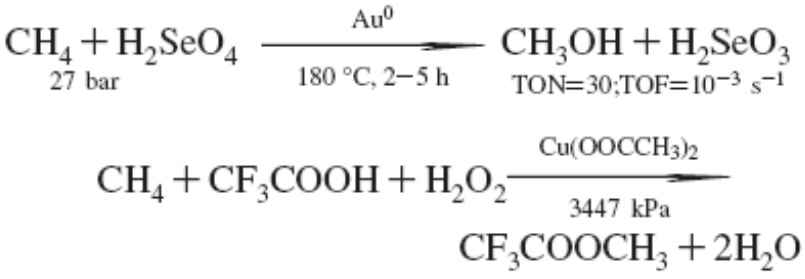

Figure 1-7 – Literature examples of methane oxidation

Based on the previous examples it can be seen that while there are numerous instances of copper-promoted oxidation of organic substrates, they are in general unselective and typically operate via autooxidation and radical mechanisms.[59] These catalysts often employ harsh reaction conditions (high temperature, large excess of oxidant, strongly acidic media, etc.) and from both the standpoint of practicality and environmental friendliness, it would be prudent to harness the dioxygen-activating ability of copper to use O2 as a terminal oxidant.

Our efforts towards development of mild, selective and efficient catalytic system began once we identified 1,2,4-triazoles as potential ligands for metal catalyzed oxidation reactions. We designed a set of experiments to carry out a SAR (structure activity relationship) study. In particular, we wished to examine the effects of change in ligand topology and electronics on the catalytic activity of 1,2,4-triazole ligands.

Scheme 1-8 shows the model system chosen for this study. Hydrogen peroxide and cyclohexane were chosen as the oxidant and the substrate, respectively. While C-H bond activation in methane is considerably more difficult than C-H bond activation in cyclohexane, the latter remains a good benchmarking standard for assessing the potential of catalytic systems. Cyclohexane oxidation can also result in two products, cyclohexanol and cyclohexanone. The alcohol/ketone (A/K) ratio in the oxidation of

cyclohexane is a simple test that reflects the lifetime of alkyl radicals. An A/K ratio of 1 suggests that long-lived alkyl radicals, such as the cyclohexyl radical, are trapped by O_2 at a diffusion-controlled rate to form alkylperoxyl radicals. Following a Russell-type termination step, recombination of these radicals will result in formation of equimolar amounts of cyclohexanol and cyclohexanone. When A/K > 1, the HO radicals formed by a metal-based oxidant react quickly to form the alcohol as the main product.[60-62] Radical chain autooxidation processes typically have A/K < 1.[61]

Figure 1-9 depicts representative examples of 1,2,4-triazole ligands used for this study, as well as the general conditions applied to the synthesis of copper-1,2,4-triazole complexes. Four different classes of 1,2,4-triazole ligands were used in this study.

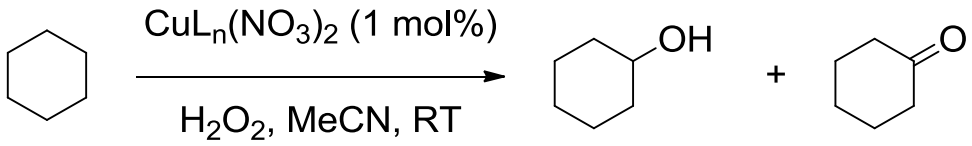

Scheme 1-8 - Model system for SAR study of 1,2,4-triazole ligands. (L_n represents ligands)

Chapter 4 of this dissertation includes the detailed summary of observations, results and discussions related to the oxidation experiments

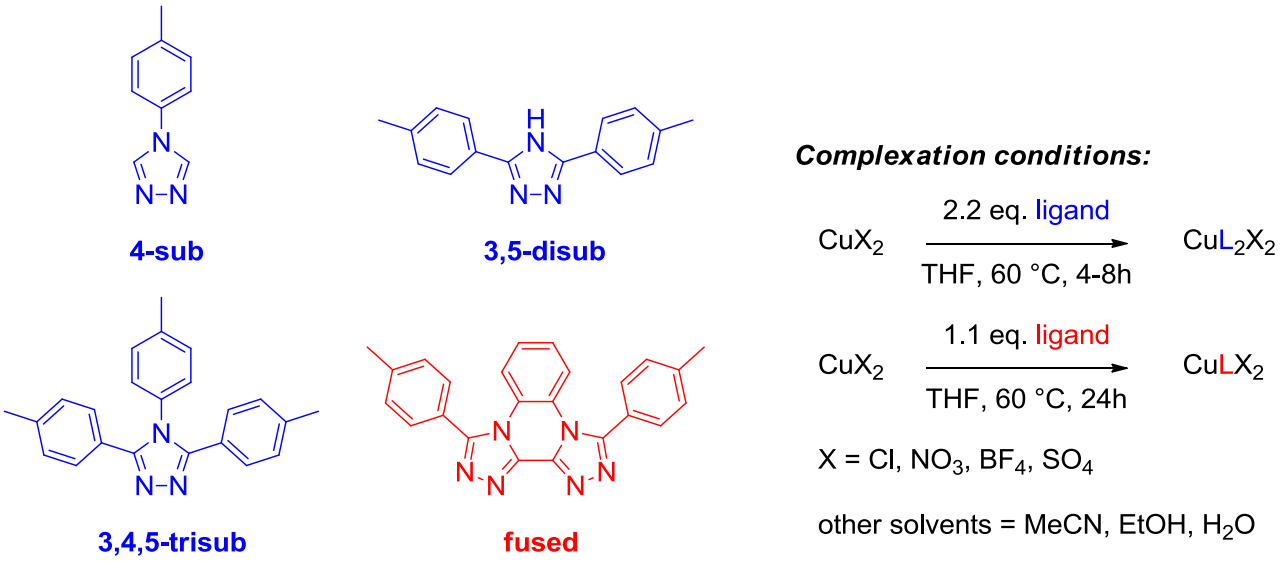

Figure 1-9 – Representative examples of 1,2,4-triazole ligands used in the catalysis of oxidation reactions

1.5. Oxygen reduction reaction (ORR)

A logical extension of the observed catalytic potential of 1,2,4-triazoles, was their application to the catalysis of oxygen reduction reaction in fuel cells. Fuel cells primarily consist of two electrodes, a cathode and an anode which is separated by an electrolyte. An oxidation reaction occurs at the anode while reduction reaction takes place at the cathode. The ions generated in these reactions are transferred from one electrode to the other through the ionically conductive but electronically insulating electrolyte. The electrons generated at the anode travel through the external electric circuit to the cathode, and are responsible for generating power from the fuel cell **(figure 1-10)**. [63]

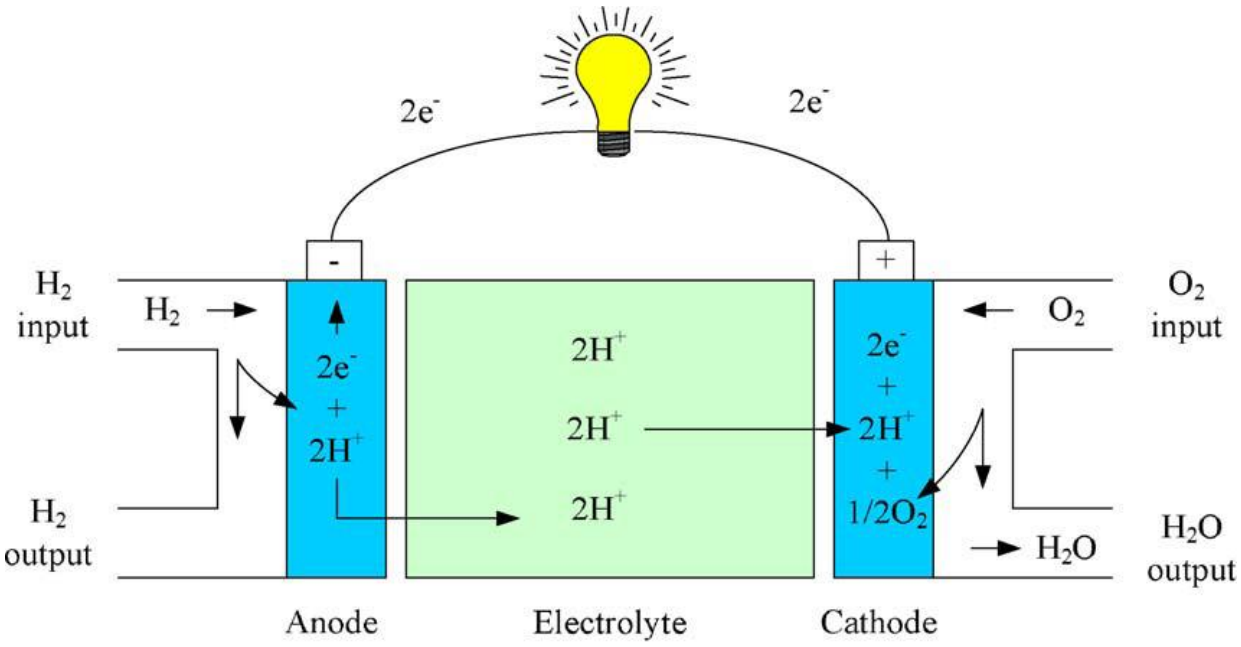

Figure 1-10 – Schematic representation of a typical PEMFC [64]

Fuel cells are generally classified on the basis of the electrolyte used in the cell. Some of the different types of fuel cells are polymer electrolyte membrane fuel cells (PEMFCs), molten carbonate fuel cells (MCFCs), direct methanol fuel cells (DMFCs) etc. [63]

For the last 20 years, the primary applications of fuel cells have been replacing internal combustion engines and providing power in stationary and portable power applications. Apart from this, fuel cells are being used in forklifts, vending machines, traffic signals etc. Fuel cells are also being developed for portable electronic devices like mobile phones and laptops. [64]

A hydrogen-oxygen fuel cell is one of the most popular types of fuel cell. In this particular fuel cell, hydrogen is oxidized at the anode and oxygen is reduced at the cathode. The reaction at the cathode is called the Oxygen Reduction Reaction (ORR).

Reactions in a Hydrogen-Oxygen Fuel Cell

At the **anode**:

$$H_2 \rightarrow 2H^+ + 2e^-$$

At the **cathode**:

$$O_2 + 4H^+ + 4e^- \rightarrow H_2O$$

The cathode is fed oxygen, and these oxygen molecules break up into atomic oxygen when they come into contact with the catalyst. This atomic oxygen then combines with the protons generated at the anode and the electrons freed at the anode, in turn producing water. This is the primary by-product of the oxygen reduction reaction **(ORR)**.

Depending upon the process, two reactions can take place at the cathode. One is the four electron process, which gives water, while the two electron process gives hydrogen peroxide, as shown below. Water is the desired product in this reaction, as hydrogen peroxide is detrimental for the membrane as well as the cathode catalyst[65].

$$O_2 + 4H^+ + 4e^- \rightarrow H_2O$$

$$O_2 + 4H^+ + 2e^- \rightarrow H_2O_2$$

Hydrogen oxidation is known to be a fast process; however, the oxygen reduction reaction (ORR) is a sluggish reaction at any pH[66].

The current mainstream proton exchange membrane fuel cells (PEMFCs) are based on platinum and platinum alloy catalysts for the relatively slow kinetics of the oxygen reduction reaction (ORR). Platinum group metals (PGM) are one of the most expensive components of the PEMFC. The high cost of the catalyst is one important barrier to the mass commercialization of fuel cell technology. Lower cost non-PGM catalysts for ORR are therefore an important development target. While platinum is currently used as a catalyst at both electrodes, significantly more catalyst is required for the ORR. Replacing platinum with a non-PGM catalyst at the cathode would significantly reduce the amount of platinum required for fuel cell operation[67]. In the past decades, particular interest has focused on Fe and Co based materials, with recent significant improvement reported by Zelenay and Dodelet groups on materials prepared with high temperature treatment[68-69]. However, the use of pyrolysis in the synthesis of these materials makes it difficult to decipher the nature of the ORR catalytic center.

Substantial amount of research has been carried out with a view to replace platinum completely as the catalyst at the cathode for ORR, but with little to moderate success. There have been 3 primary approaches taken to remedy this problem:

1. **Metal composites** – Using other non precious metals with platinum. This includes using Pt monolayered materials[70-71] or Pt alloys with other non precious metals[72-73]. Another strategy to improve the performance of Pt catalysts in fuel cells is to increase the effective surface area of the catalyst. Increasing the surface area is known to improve catalytically activity substantially[74].
2. **Bio inspired materials** – Enzymes like Cytochrome *c* oxidases (C*c*Os), and multicopper oxidases (MCOs) are known to catalyze the four-electron reduction

of oxygen to water. Due to their ability to catalyze this oxygen reduction reaction, they are being actively investigated as possible catalysts for the ORR at the cathode of a commercial fuel cell[75].

3. **Surface supported/non supported organic-metal chelates** – Jasinski first reported the catalytic activity of Metal-Nitrogen ($M-N_4$) type of chelates for the catalysis of ORR[76]. Following this discovery, there have been multiple attempts to use tetraphenlyporphyrins (TPP) and phthalocyanine (Pc) based macrocycles, complexed with transition metals like cobalt and iron to catalyze the ORR reactions. These metal chelates are generally supported on high surface area carbon, and pyrolyzed in order to improve their performance as catalysts in the ORR[68, 77].

Despite these efforts, attaining the activity of platinum, with a 4-electron process and achieving durability which will suffice commercial purposes has not yet been attained.

Naturally occurring multicopper oxidase enzymes (e.g. laccase) are observed to be very efficient ORR catalysts. Such copper oxidases are known to reduce oxygen at approximately 1.2 V vs. RHE[78]. These enzymes are characterized by a three or four Cu-atom active site where the ORR is known to occur[14]. These active sites have been used to inspire the development of a series of copper triazole based complexes for ORR. 1,2,4-Triazoles are potent ligands for non-PGM metals and the resulting complexes have demonstrated the ability to catalyze a wide range of reactions including the ORR[79]. The structural diversity of different 1,2,4- triazole-copper complexes is striking, with slight changes in stoichiometry, solvent conditions, and temperature exerting powerful

influences on the molecular features of a given complex[80-81]. As explained in the previous section, one recurring structural theme inherent to 1,2,4-triazole complexes with copper is the presence of multiple bridged metal ions in proximities defined by the chemical features of the ligand. This feature of 1,2,4-triazole-containing structures is particularly advantageous from the standpoint of developing redox catalysts.

We decided to adopt a diversity-oriented approach for heterogeneous catalyst discovery (**Figure 1-11**). This approach offers a means of controlling the reactivity of multifunctional ligands by spatially addressing them in a reaction medium. Controlled immobilization strategies also allow the design of chemical processes composed of multiple reactions catalyzed by combinations of ligands and non-precious metals.

The development of ORR catalysts and the synthetic approaches for the immobilization of 1,2,4-triazoles on carbon black supports is explained in chapter 5 of this dissertation The text of Chapter 5 was taken in part from a manuscript coauthored with Zawodzinski Group (University of Tennessee, Knoxville)).

Electrochemical Characterization of Adsorbed and Immobilized Cu TriazoleComplexes: Some Mechanistic Aspects

Gabriel A. Goenagaa, Ashesh Belapure, Congling Zhang, Alex Papandrew, Shane Foister and Tom Zawodzinski

ECS Transactions, 41 (1) 1193-1205 (2011)

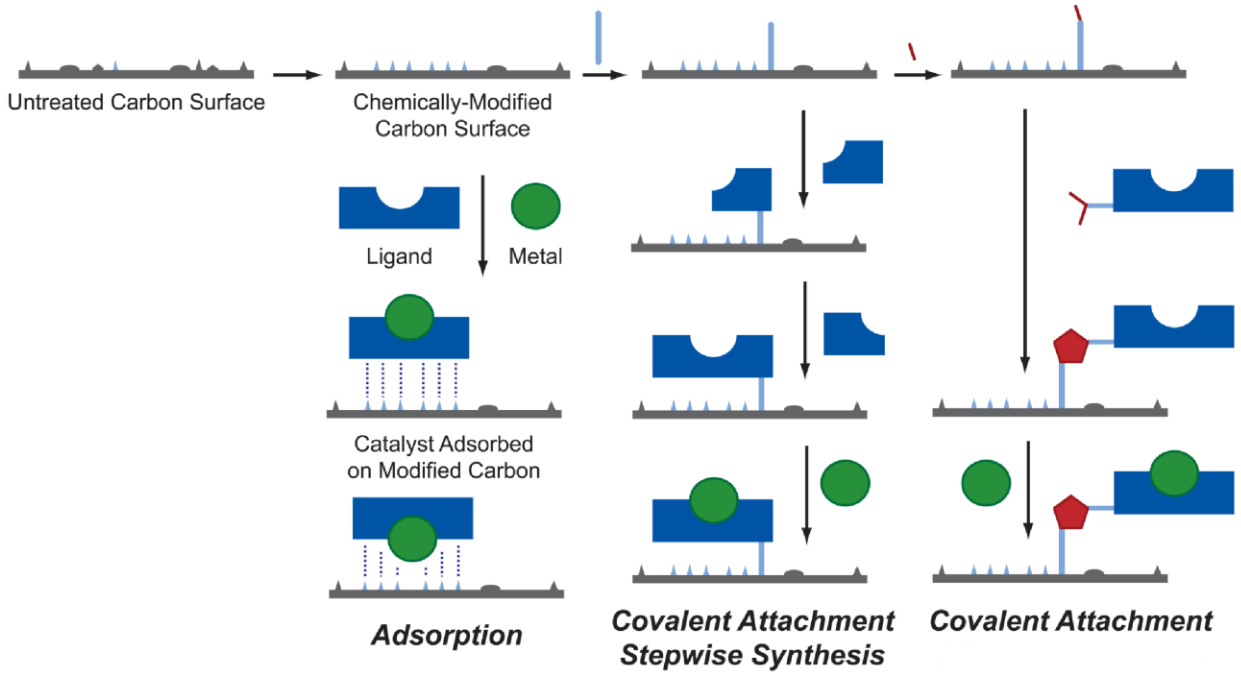

Figure 1-11 – Diversity oriented approach for catalyst discovery

1.6. Aziridination

Aziridines are organic compounds characterized by presence of an aziridine functional group, which consists of a three membered heterocyclic ring containing a nitrogen atom bonded to two methylene groups. These molecules are nitrogenated analogues of epoxides and are sometimes referred to as the ugly cousins of the epoxides due to considerably higher challenges encountered during their synthesis[82]. Despite this fact, there are certain common motifs present in the strategies used to synthesize aziridines and epoxides. Essentially, both epoxides and aziridines are synthesized by oxidation of alkenes, an oxygen source is used in the first case whereas the latter is synthesized using a suitable nitrogen source. Having observed the activity of 1,2,4-triazole based ligands in the transition-metal catalyzed oxidative processes, we

decided to explore the possible use of these ligands in the catalysis of aziridination reactions.

Aziridines represent an important class of organic molecules, serving as reactive precursors to a variety of natural products and pharmaceuticals[83]. The significance of aziridines is highlighted by their function as building blocks for numerous chemical transformations. Aziridines have natural susceptibility to nucleophilic ring opening leading to various synthetically important intermediates as illustrated in **figure 1-12**. Many naturally occurring molecules that contain an aziridine ring display potent biological activity which is closely associated with the strained nature of the heterocycle. A good example is that of mitosanes **(Figure 1-13)**, which possess anti-tumor and antibiotic activity[84-85].

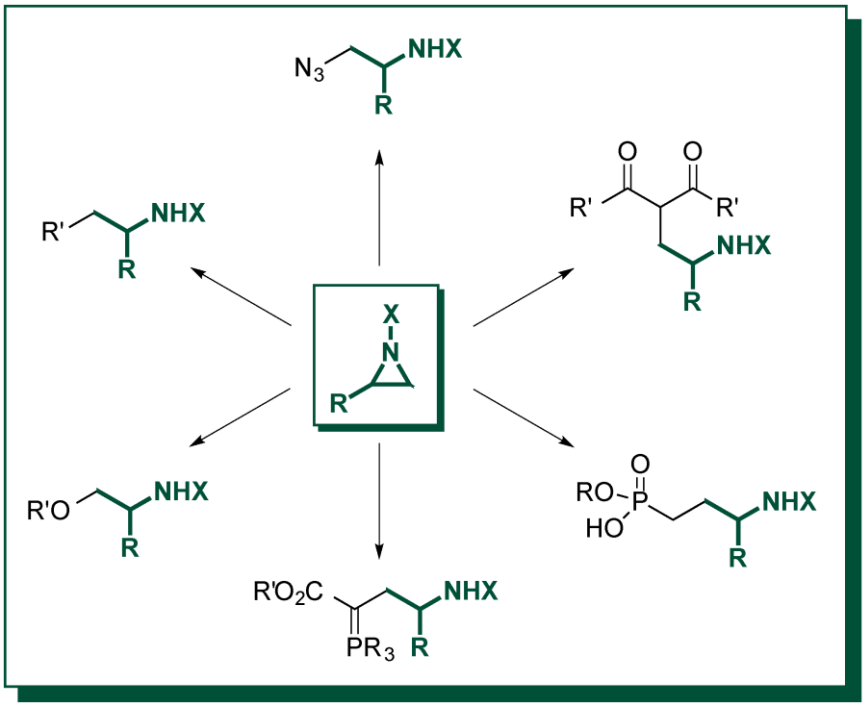

Figure 1-12 – Synthetic utility of aziridine molecules

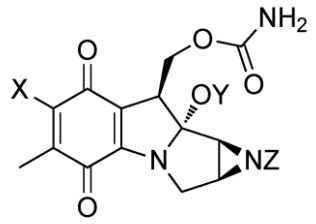

Mitosanes

Figure 1-13 – Mitosanes - naturally occurring aziridines

Over the past decade, synthetic methodologies employing transition metal-catalyzed routes to aziridines have been developed that primarily utilize iminoiodiane compounds[86-90], chloramine T/bromamine-T3[91-92], and sulfonyl azides[93-94] as nitrogen transfer reagents. In all cases, the product is an *N*-protected sulfonyl derivative which requires cumbersome and low-yielding deprotection steps **(scheme 1-14)**.

There have been few reports of aziridination reactions involving organic azides as atom transfer reagents with $–N_2$ as a byproduct, resulting in improved atom economy[95-96]. However, most of these methodologies use great excesses of alkene, sometimes using them as solvents and are thus limited by the number of alkenes that can be utilized. These reactions also suffer from low yields, which when coupled with the need for expensive ligands, metals and rigorously maintained inert conditions, lead to the significant reduction of their practical applicability.

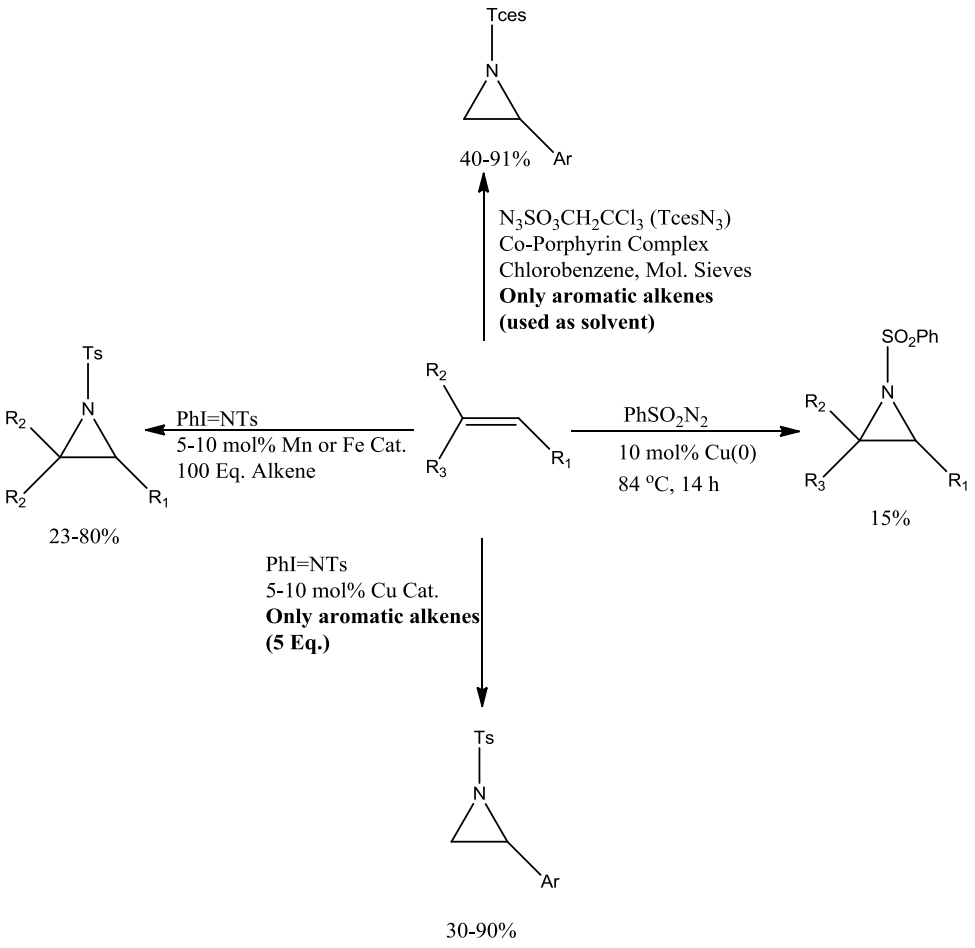

Scheme 1-14 – Literature examples of aziridination methologies[97-99]

In light of the continued need of efficient and practical route to synthesizing aryl aziridines with wide substrate scope, we have explored the application of Ni(II)-1,2,4-triazole complexes as catalysts for aziridination of alkenes with organic azides. **Scheme 1-15** shows the general reaction strategy for synthesis of aziridines using 1,2,4-triazole based metal complexes as catalysts. Chapter 6 of this dissertation details the development of this methodology.

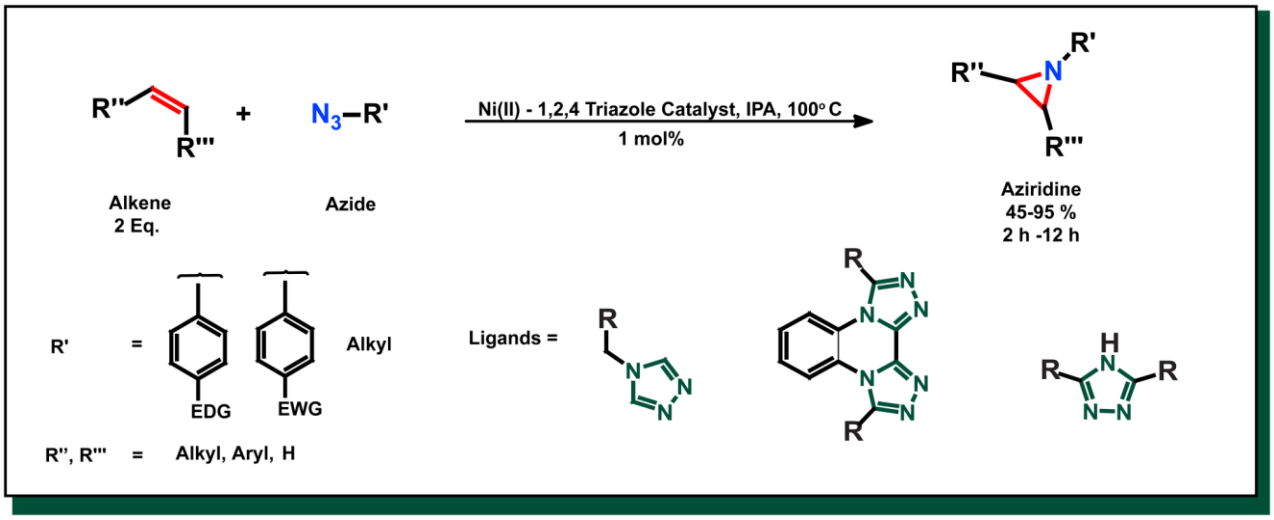

Scheme 1-15 – Ni(II)-1,2,4-triazoles catalyzed aziridination reactions

Scope of this work

This dissertation describes research directed toward the application of 1,2,4-triazoles in the catalysis of oxidative processes. These include hydrocarbon oxidation, oxygen reduction reactions (ORR) and aziridination. Chapter 2 and 3 are focused on solution phase as well as solid phase synthesis of 1,2,4-triazoles and derivatives thereof, respectively. Chapter 4 discusses the research carried out for the development of catalytic systems for hydrocarbon oxidation. Chapter 5 details the synthetic approaches towards immobilization of 1,2,4-triazoles on carbon black surface and the electrochemical activity of the carbon black supported ligands in the catalysis of ORR. Finally, chapter 6 describes the method development of Ni(II)-1,2,4-triazole catalyzed aziridination reactions.

2. *Homogeneous 1,2,4-triazole synthesis*

2.1. Introduction

We came across the catalytic activity of 1,2,4-triazole complexes through what can only be described as a serendipitous discovery. Our original research project involved synthesis of small molecule mimics of HDAC (Histone deacetylase) inhibitors. This involved probing into possible use of 1,2,4-triazoles as zinc binding groups. It was during this project that we recognized that copper complexes of 1,2,4-triazoles showed remarkable potential towards hydrocarbon oxidation. This prompted us to launch a systematic investigation into possible use of similar metal complexes for multiple other chemical transformations such as aziridination and click reactions. In order to investigate the effects of ligand topology and electronics on the catalytic activity, we synthesized various analogues of 1,2,4-triazoles The synthetic strategies applied for this purpose are described herein. It should be noted that the nature of the triazoles synthesized was largely dictated by the catalytic activity observed, which is described in detail in the latter chapters.

2.2. Synthesis of substituted 1,2,4-triazole derivatives

Synthetic approaches towards 1,2,4-triazoles have been under investigation for more than a century, yet this remains a challenging task. This is partly due to the use of archaic methods employing very high temperatures that often result in tedious workups and very low yields[21, 100]. Additionally, very high polarity of many 1,2,4-triazoles makes the chromatographic separation a challenging task, often forcing chemists to rely solely

on purification techniques such as recrystallization. Moreover, the synthetic methods are not general and vary greatly depending upon the nature of the substituents and the pattern of substitution present in the target triazole[101-107]. Generally, 1,2,4-triazoles can be classified into seven major classes based solely on the substitution pattern as shown in **figure 2-1**. The next few sections describe details of the synthetic pathways adopted and optimized by us towards preparation of various 1,2,4-triazoles as well as provide more information on synthetic routes reported in literature thus far.

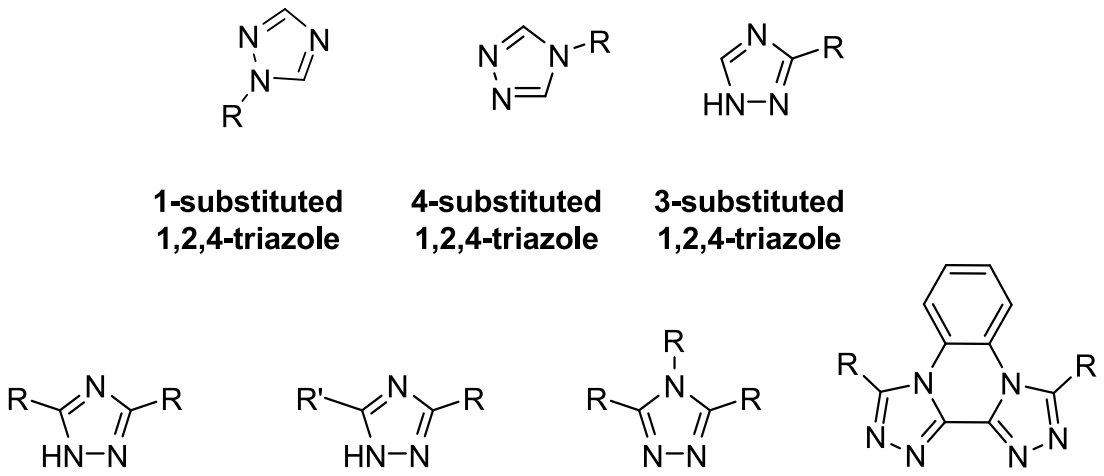

Figure 2-1 - Structural classes of 1,2,4-triazoles. R = Ar, Alkyl, NH_2

2.2.1. Synthesis of 4-substituted 1,2,4-triazoles

In order for us to carry out a systematic study of catalytic activity of 1,2,4-triazoles, it was necessary to evaluate effects of different substitutions at different positions. Substitution at N-4 of 1,2,4-triazoles essentially blocks of one of the free nitrogen atoms thereby exerting a profound effect on the possible metal coordination model.

We also believed that electronic effects generated by varying the nature of substituents at the 4-position can influence the eventual activity. Thus, we planned to synthesize a variety of 4-subsituted 1,2,4-triazoles with varying electronic and structural properties.

Direct substitution on nitrogen at the 4-position of 1,2,4-triazoles is difficult due to the prevalence of the 1H-isomer of 1,2,4 triazoles, which results in almost exclusive substitution at 1-position. Thus, carrying out the substitution at 4-postion of triazole involves a series of steps starting with protection of the more nucleophilic 1-position. This is followed by substitution at 4-position and subsequent removal of the protecting group at 1-position, prolonging the synthesis and lowering the yield. These tranformations are usually achieved through formation of isolable quaternary salts.[108-109] **Scheme 2-2** displays this strategy.

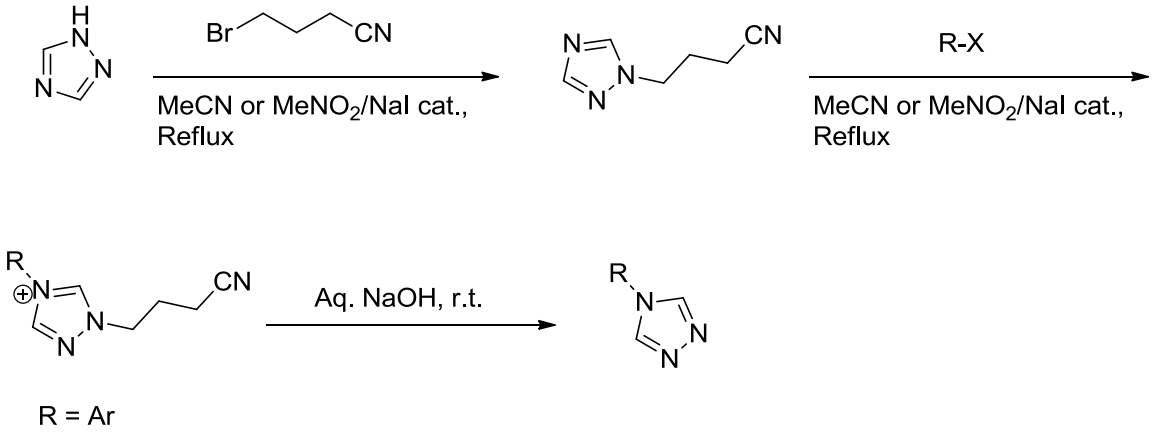

Scheme 2-2 – Multistep synthesis of 4-substituted-1,2,4-triazoles

In light of this, the preferred route to forming 4-substituted 1,2,4-triazoles is synthesizing the triazole directly from a suitably substituted amine. **Figure 2-3** lists all the 4-substituted triazoles synthesized in our laboratory.

One of the most commonly used methods to synthesize 4-substituted triazoles is a patented procedure from Bayer et al[24]. The first step in this method is the reaction of formic acid hydrazide with triethyl orthoformate leading to the intermediate which is then subjected to the reaction with primary amine. This one-pot synthesis affords 4-substituted 1,2,4-triazoles in moderate yields depending on the nature of the substituent **(Scheme 2-4)**.

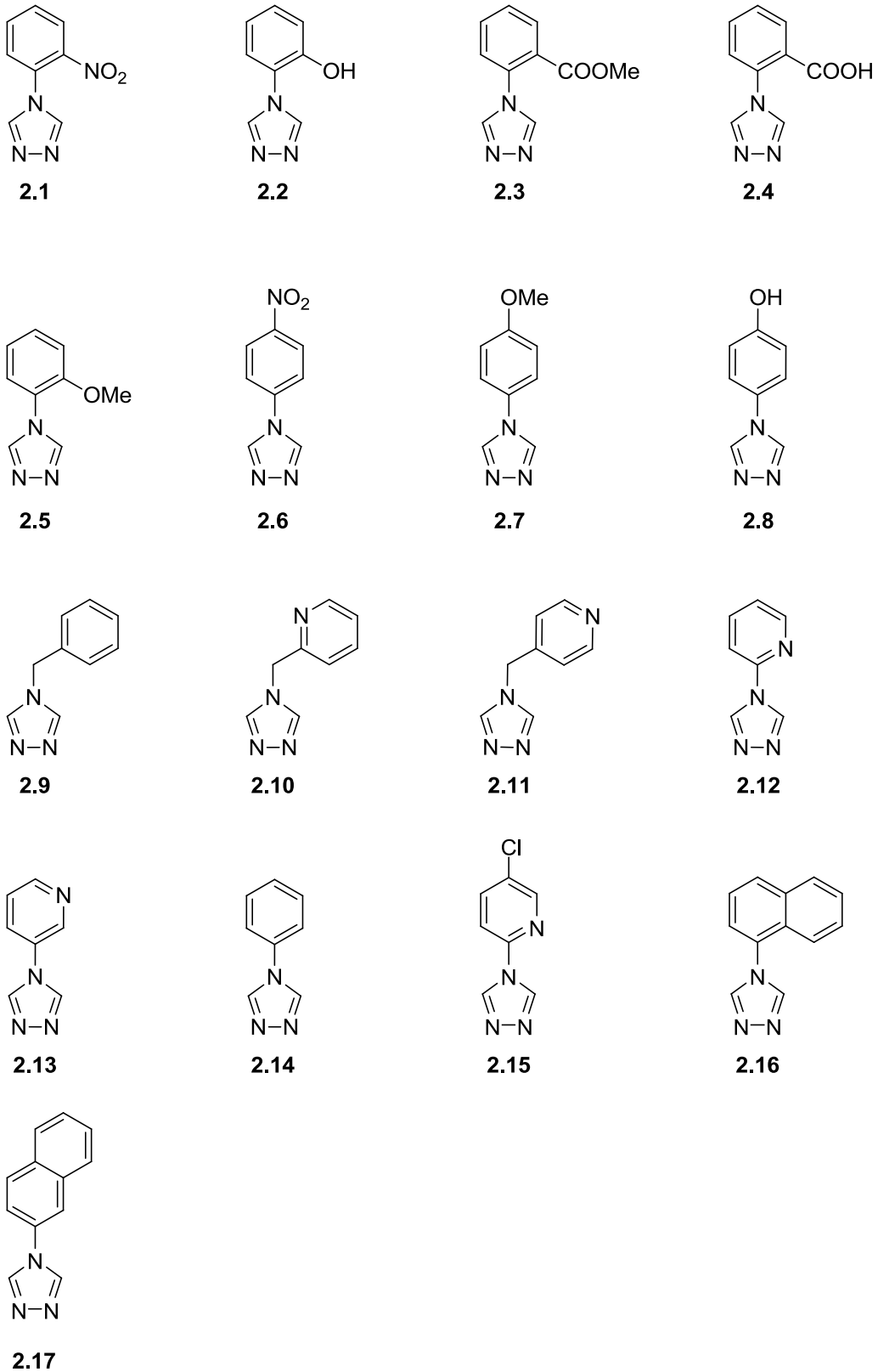

Figure 2-3 – List of 4-substituted triazoles synthesized

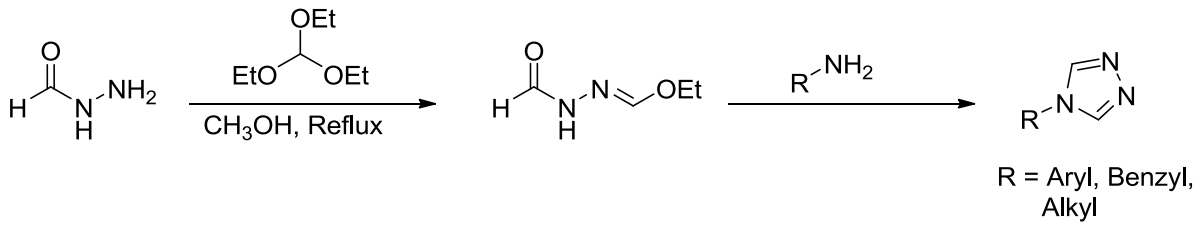

Scheme 2-4 - Synthesis of 4-substituted-1,2,4-triazoles from primary amines utilizing triethyl orthoformate

Haasnoot and Groeneveld were also credited for their report on the direct approach[110] to the synthesis of 4-substituted-1,2,4-triazoles by a one-step reaction between substituted amines and diformylhydrazine.

Nevertheless, both these methods suffer from several drawbacks such as low yields (25-50%), high temperatures for the reaction, tedious workups, and uncertainties in reproducibility.

In 1967, Bartlett and Humphrey reported a multi-step synthesis of 4,4-bis-1,2,4-triazole by the transamination of *N*,*N*-dimethylformamide azine with 4-amino-1,2,4 triazole in the presence of a catalytic amount of *p*-toluenesulfonic acid in refluxing toluene for 72 hours, in appreciable yield (64%)[111]. The reactive agent (chloromethylene) dimethylammonium chloride $[Me_2N^+=CHCl]Cl$, which was proposed to be generated from a solution of thionyl chloride in DMF, reacts with hydrazine to produce *N*,*N*-dimethylformamide azine dihydrochloride (**Scheme 2-6**). We chose to utilize this direct transamination route to form 4-substituted-1,2,4-triazoles. This methodology was found to be suitable towards synthesis of multiple different triazole systems, often resulting in fairly high yields.

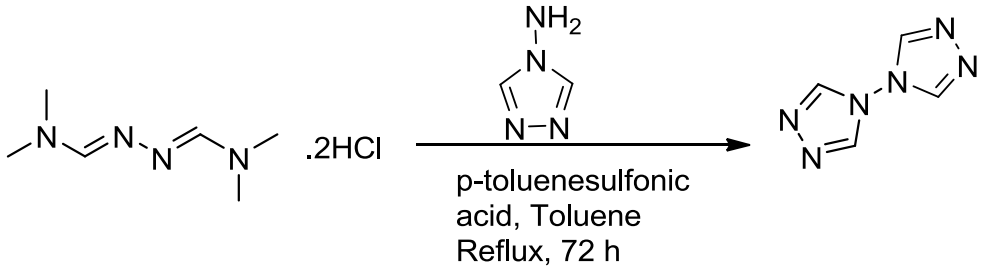

Scheme 2-5 - Synthesis of 4,4-bis-1,2,4-triazole by transamination of *N,N*-dimethylformamide azine

Despite the utility of this method, we were concerned about safety hazards posed by the use of benzene as the solvent. Thus, we attempted to change the solvent system to a more innocuous solvent **(table 2-1)**. These efforts resulted in the identification toluene or acetonitrile as exchangeable solvent systems while maintaining the high yields. Later on it was found that carrying out these reactions in a microwave reactor resulted in much shorter reaction times while also improving the yields **(Table 2-1, and Scheme 2-6)**.

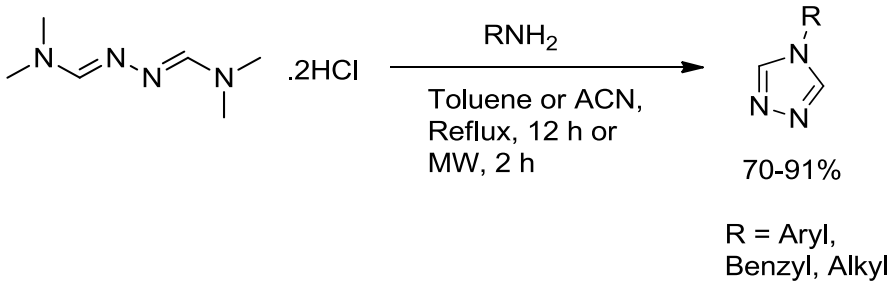

Scheme 2-6 - Optimized synthesis of 4-substituted triazoles utilizing dimethylformamide azine dihydrochloride

The workup on these reactions proved to be simple too, since the triazole product often falls out of the reaction mixture after the completion of the reaction. The

precipitated crude product could then be recrystallized from ethanol to obtain an analytically pure sample.

Table 2-1 - Evaluation of alternate solvents and conditions for the synthesis of 4-substituted-1,2,4-triazoles

Entry[a]	Solvent	Conditions	Time	% Yield[b]
1	Benzene	Reflux	12 h	70%
2	Toluene	Reflux	12 h	65%
3	Acetonitrile	Reflux	12 h	66%
4	Acetonitrile	Microwave, 150 ^{o}C	4 h	91%

a) Aniline was used in all cases as the amine component b) percent yield based on isolated yield of 4-phenyl-1,2,4-triazole

A modification of Haasnoot and Groeneveld's method[110] involved the solvent free fusion of primary amines with diformylhydrazine under microwave radiation in the presence of silica gel. This method also results in fair to high yield while affording an easy workup **(Scheme 2-7)**. As with the examples before, this methodology was compatible with alkyl, aryl and benzyl amines.

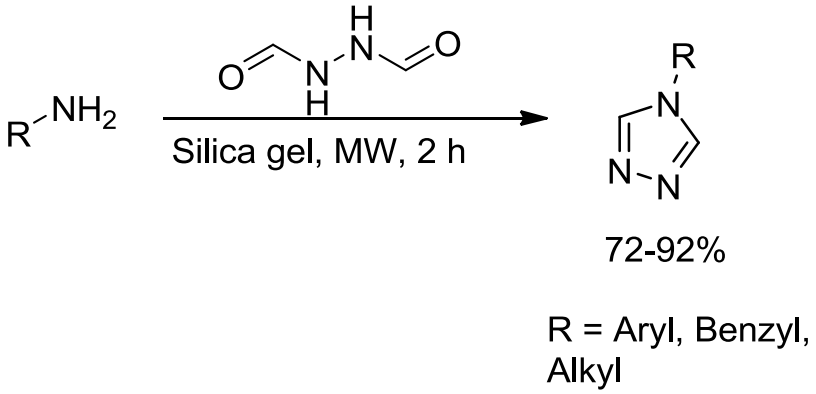

Scheme 2-7 – Synthesis of 4-substituted-1,2,4-triazoles using diformylhydrazine under microwave irradiation

2.2.2. Synthesis of 1-substituted triazoles

Synthesis of 1-substituted triazoles poses less of a challenge than the 4-substituted analogues, mainly because they can be efficiently synthesized via selective alkylation of the simple 1,2,4-1H-triazole. With the 1H-tautomer being the predominant form, it takes precedence in the substitution reaction, delivering 1-substituted triazoles as major products in most cases. This selectivity is further enhanced due to the greater nucleophilicity of the N-N linkage in comparison with that of standalone 4-nitrogen atom[112]. **Figure 2-8** shows the list of various 1-substituted triazoles that we prepared. Thus, triazoles can be activated for a nucleophilic reaction with alkyl halides by exposure to sodium alkoxides. In our hands this method resulted in 70-80% yields depending on the substrates **(Scheme 2-9)**.

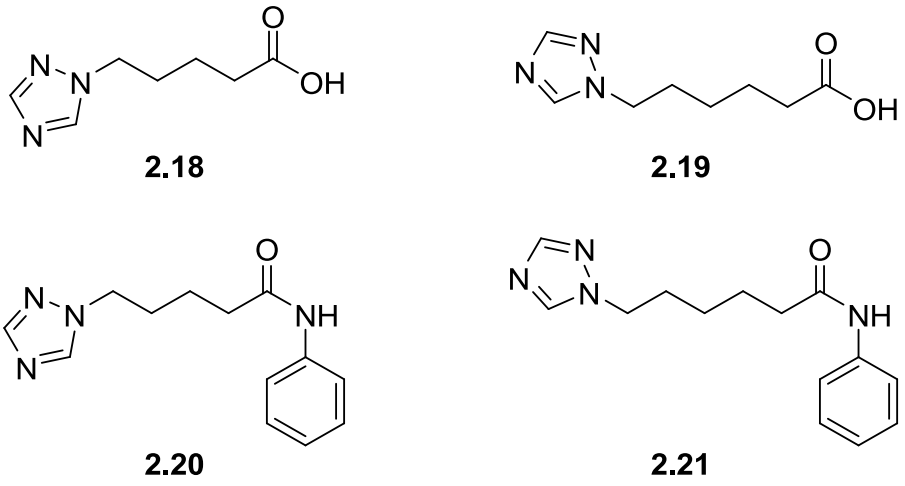

Figure 2-8 - List of 1-subtituted triazoles synthesized

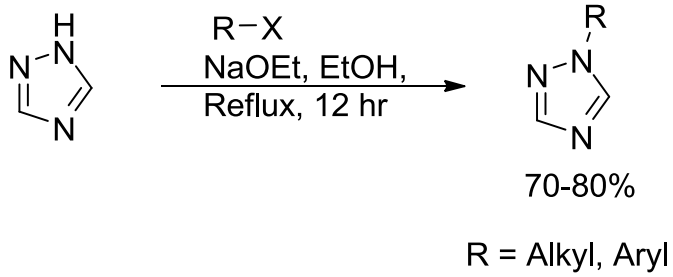

Scheme 2-9 - N-alkylation of 1,2,4-triazoles

Utilizing a microwave reactor can lead to further improvements in the yield and the required reaction time. We observed that the substitution reactions of 1,2,4-trizoles take place rapidly and in 90-95% yields under microwave irradiation. This was our preferred route of synthesizing 1-substituted triazoles **(Scheme 2-10)**.

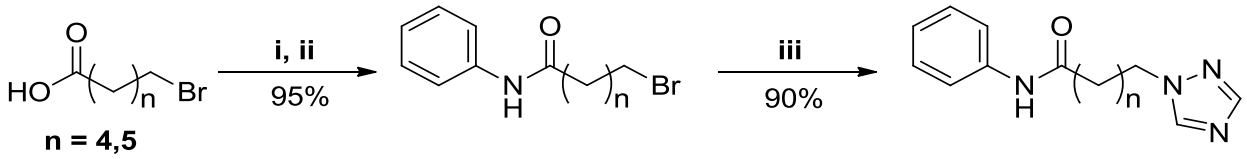

Scheme 2-10 - Alkylation reactions under microwave irradiation. i) oxalyl chloride, DCM, DMF, 0 ^{o}C, 1h, ii) aniline, DCM, 0 ^{o}C-1h, RT-2h, iii) 1H-1,2,4-triazole, DMF, K_2CO_3, Microwave- 150 ^{o}C, 2h

The molecules depicted in the **figure 2-8** were originally synthesized as zinc binding HDAC inhibitors and were found to be ineffective as catalysts for oxidative processes. Therefore, no further development was carried out for this class of 1,2,4-triazoles.

2.2.3. Synthesis of 3,5-disubstituted triazoles

3,5-Disubstituted-1,2,4-triazoles constitute an important class of 1,2,4-triazoles due to markedly different characteristics from 1- or 4-substituted triazoles. In this class the carbon atoms are substituted, as opposed to N-substitution in 1- or 4-subtituted triazoles. Thus 3,5-disubstituted-1,2,4-triazoles have an additional free ring nitrogen atom that can potentially participate in metal coordination. Furthermore, appropriate 3,5-substituents can also participate in coordination due to the proximity of these substituents to ring nitrogen atoms **(Figure 2-11)**. **Figure 2-12** lists all the 3,-5-disubstituted triazoles that were prepared in our laboratory.

Symmetrical 3,5-disubstituted triazoles can be prepared through a two step sequence starting with the reaction of aromatic nitriles with excess hydrazine

hydrochloride and hydrazine hydrate[101]. This leads to the formation of 4-amino-3,5-disubstituted triazole. Subsequent deamination by treatment of sodium nitrite in hypophosphorous acid leads to the desired product **(Scheme 2-13)**.

Figure 2-11 – Possible interactions of metal with substituents on the triazole ring

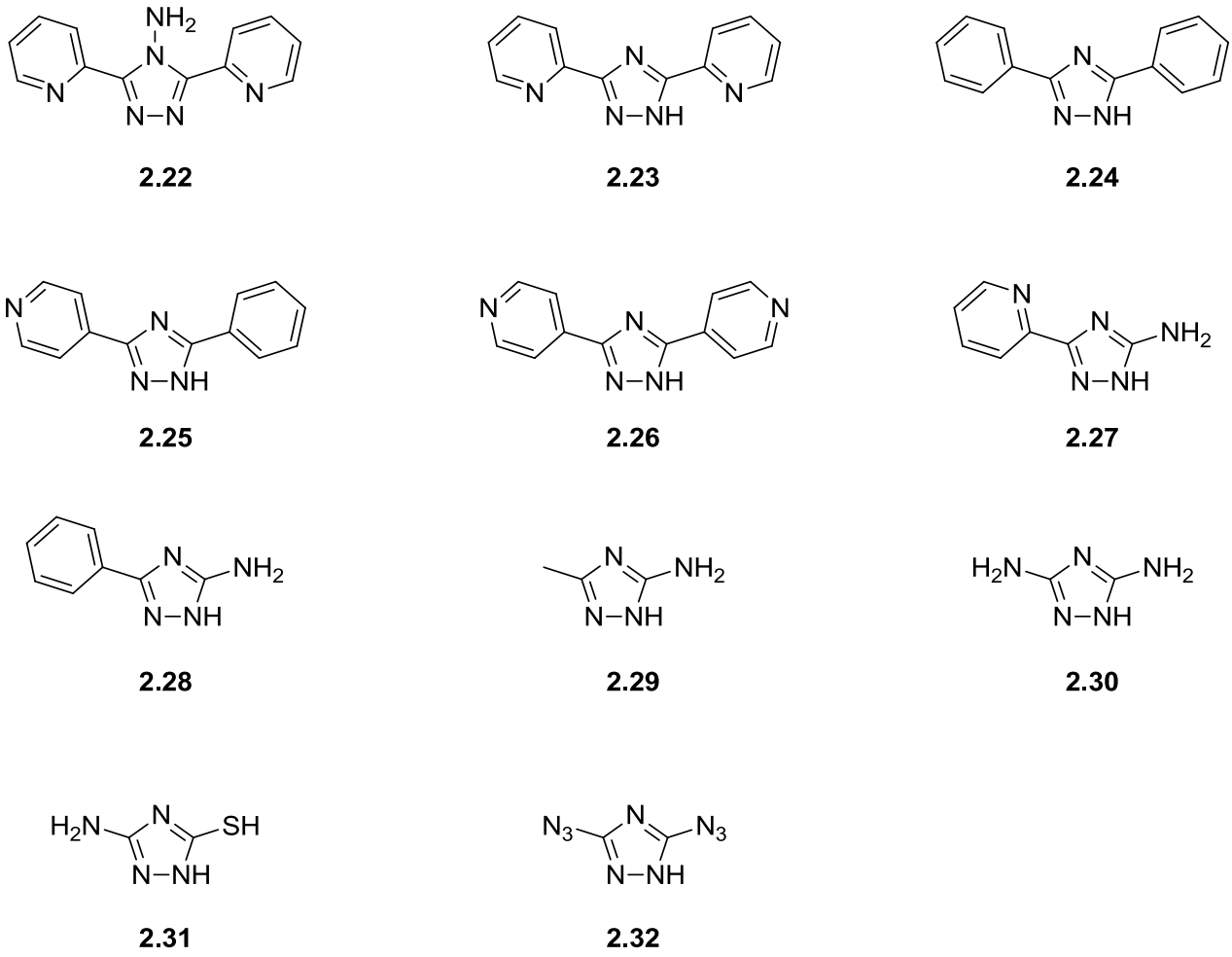

Figure 2-12 - List of 3,5-disubtituted triazoles synthesized

However, the workup of this reaction is fairly complicated. The product triazoles (in particular, the 3,5-dipyridyl-1,2,4-triazole) is highly soluble in water. The literature example claims that the product falls out of the reaction mixture upon basification, however no such precipitation was observed in our hands. The only possible workup was evaporation of water followed by column chromatography which resulted in low yields (20-25%). This led us to explore alternate synthetic pathways that would result in higher yields.

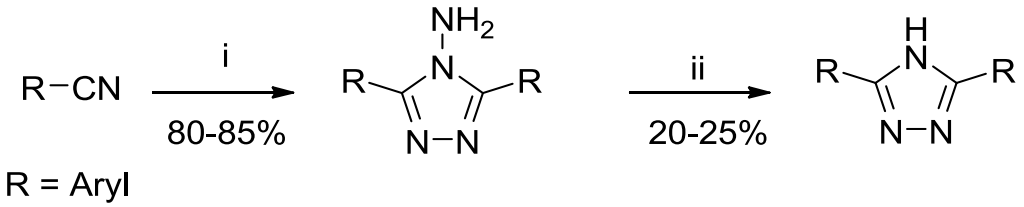

Scheme 2-13 - Synthesis of symmetric 3,5-disubstituted triazoles via deamination reaction. i) N_2H_4.HCl, N_2H_4. H_2O, EtOH, reflux, 24 h ii) $NaNO_2$, H_3PO_2, H_2O, RT, 1 h

One of the promising synthetic strategies that we came across in the literature was the reaction between an aromatic hydrazide and aromatic nitrile that leads to the formation of 3,5-disubstituted triazoles[102]. This methodology has a broad substrate scope and both symmetric and asymmetric products can be obtained with this method. Like previous instances microwave irradiation can be efficiently applied in lieu of thermal conditions to improve yields and reaction parameters **(Scheme 2-14)**. This method resulted in fairly high yields of the products (75-85%). In all cases, product triazoles were insoluble in n-butanol leading to easy recoveries by filtration. Isolated crude materials could then be recrystallized in ethanol to give analytically pure products.

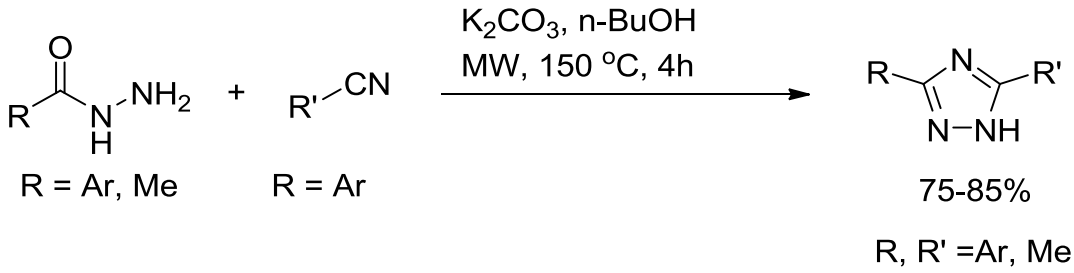

Scheme 2-14 - Hydrazide - nitrile condensation under microwave irradiation

The substituted aromatic hydrazides were prepared in a single step from either the carboxylic acid precursor or the ester precursor depending on the commercial availability **(Scheme 2-15)**. These hydrazides were isolated by standard aqueous

workup and characterized by HRMS (DART or ESI). Thin layer chromatography was used to determine the purity. The crude products were found to be pure enough to be carried on to the triazole formation step. Aliphatic hydrazides, with the exception of acetic hydrazide, were found to be incompatible with this method, often resulting in very low yields.

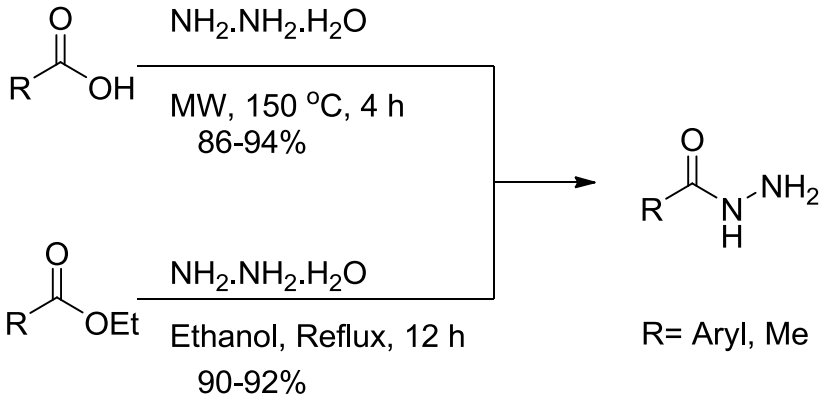

Scheme 2-15 - Synthesis of substituted hydrazide precursors

Synthesis of 5-amino-3-substituted triazoles differs slightly from the above described methods. The nitrile component was replaced with S-methylthiourea in the reaction with the hydrazide. All other conditions were kept identical. This procedure was based on the method described by Dolzhenko et al[113]. However, our method was carried out in one pot as opposed to the two step synthesis in the reported method **(Scheme 2-16)**. No impact on purity or yield was observed when using single pot reaction conditions.

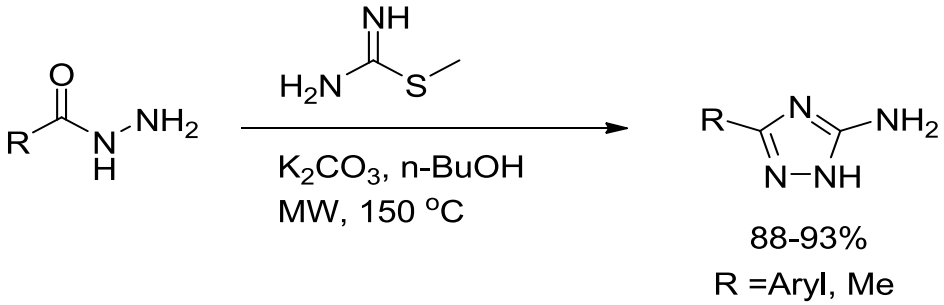

Scheme 2-16 - Synthesis of 5-amino-3-sub-1,2,4-triazoles

2.2.4. Synthesis of 3,4,5-trisubstituted-1,2,4-triazoles

A simple two step procedure can be used to synthesize tri-substituted triazoles. Aromatic carboxylic acids can be converted to substituted diacylhydrazines by reaction with hydrazine hydrate[114]. Substituted diacylhydrazines can be smoothly converted to trisubstituted-1,2,4-triazoles upon reaction with aromatic amines in the presence of phosphoryl chloride. 3,4,5-Tritolyl-1,2,4-triazole was prepared as shown in **scheme 2-17.** These reactions were not as amenable as the ones previously described. Attempts to synthesize similar triazoles with pyridine substituents were met with failure.

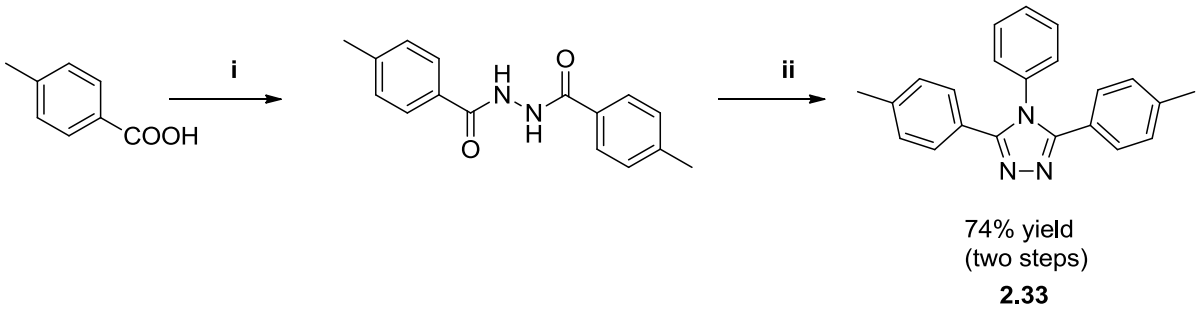

Scheme 2-17 - Synthesis of 3,4,5-tritolyl-1,2,4-triazole. i) $NH_2NH_2.H_2O$, PPA, 12h, 120°C, ii) $POCl_3$, xylenes 0 °C→140 °C, 4h

2.2.5. Synthesis of fused-1,2,4-triazoles

Given the excellent metal coordinating ability of 1,2,4-triazoles[27], the next logical step in the 1,2,4-triazole synthesis was to incorporate more than one triazole in the same molecule. We synthesized a variety of molecules containing more than one triazole moiety. **Figure 2-18** lists all of these molecules.

Compounds **2.34** through **2.37** were prepared using the same strategy[115]. This involved thermal fusion of hydrazides with dichloroquinoxalines, which led to the formation of tetracyclic molecules containing two triazoles fused with the quinoxaline ring system. The required dichloroquinoxaline precursors can be prepared over two steps starting from 1,2-diamines, as depicted in the **scheme 2-19**. 1,2-diamines were subjected to cyclization reaction with oxalic acid in acidic medium leading to diones. The diones upon treatment with thionyl chloride under reflux were converted to the dichloroquinoxalines.

The fusion reaction with hydrazide takes place only if hexamethyl phospharamide is used as a solvent. Due to high toxicity of this solvent we attempted to use various other solvents as substitutes for this reaction. However, none of the other solvents tested were successful in delivering the desired results. Overall yields for this reaction sequence range from 25-35% depending upon substitution. Use of microwave synthesizer did not result in any improvements. Despite the low yields, this was found to be the only plausible pathway towards fused quinoxalino triazole systems.

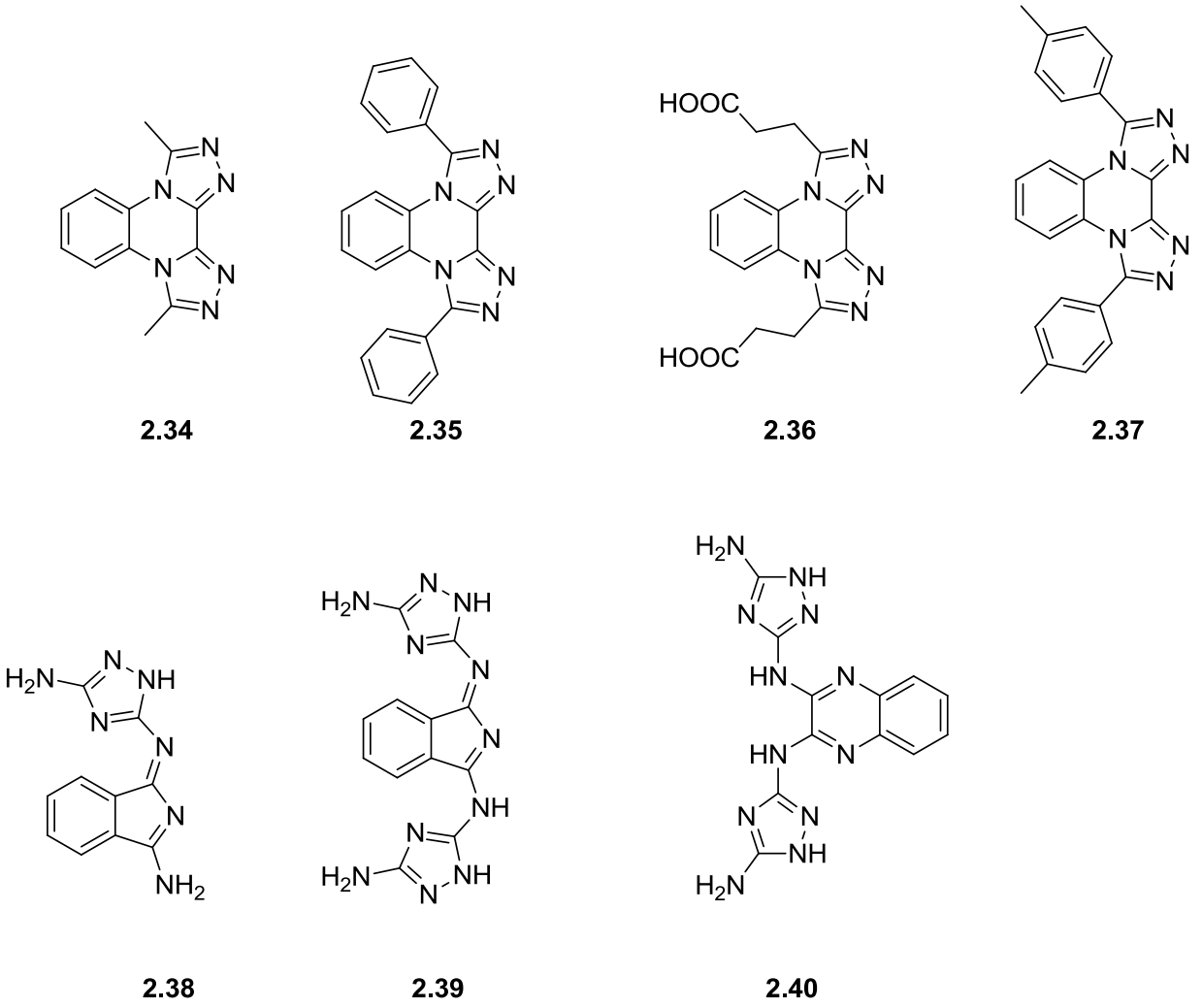

2.34 **2.35** **2.36** **2.37**

2.38 **2.39** **2.40**

Figure 2-18 - Molecules containing more than one 1,2,4-triazole moiety

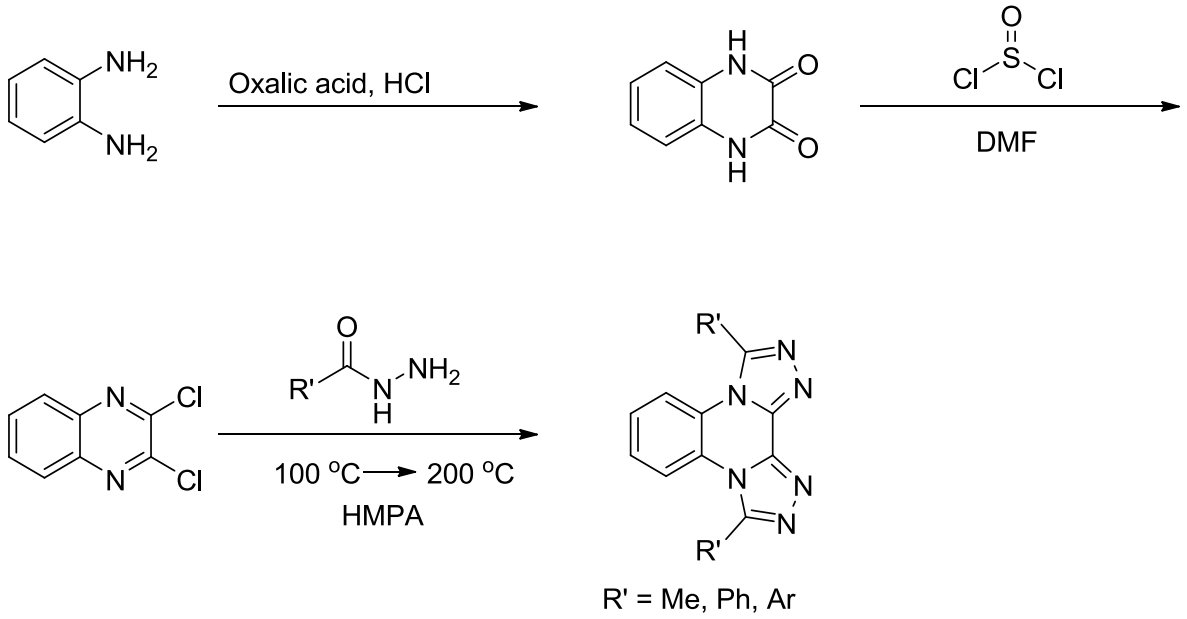

Scheme 2-19 - Synthesis of fused 1,2,4-triazoles

The other class of molecules containing more than one 1,2,4-triazole moiety that we synthesized was hemiphthalocyanine mimics. Phthalocyanines **(Figure 2-20)** are macrocyclic compounds containing multiple heterocycles. These molecules are well known for their ability to coordinate and sequester transition metals[20].

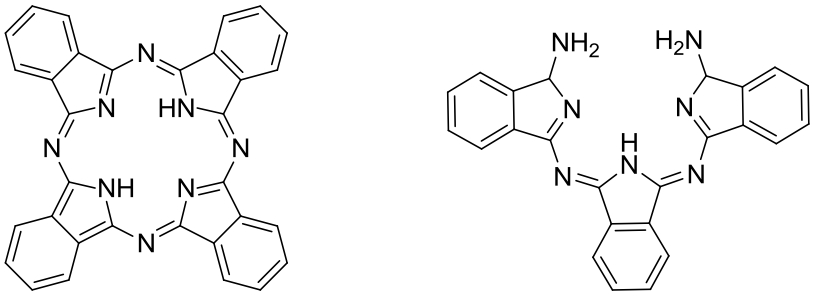

Phthalocyanine **Hemiphthalocyanine**

Figure 2-20 – Examples of phthalocyanine and hemiphthalocyanine

Typical molecules belonging to phthalocyanine family are comprised of four isoindolinone cores connected through bridging nitrogen atoms. Hemiphthalocyanines represent non-cyclic systems comprising of three isoindolinone cores. We planned to synthesize hemiphthalocyanine analogues with the difference being that the terminal isoindolinones would be replaced with 1,2,4-triazoles.

Usually, phthalocyanines and hemiphthalocyanines are synthesized from phthalonitriles or diiminoisoindolines by treatment with suitable nucleophiles. Formation of fully closed phthalocyanines is usually achieved through metal templated reactions. Our target was to form similar compounds without requiring metal templated closure. This would allow flexibility to construct various metal complexes at a latter stage without having to repeat the entire syntheis. We tested various literature protocols to identify the one that was best suited to prepare triazolo-hemiphthalocyanines[116-123]. **Table 2-2** lists the details and results from this study. We observed that it was not possible to form the fully closed phthalocyanine-mimics without the use of a metal. However, triazole-hemiphthalocyanines (entries 1,2,3,4) could be efficiently formed without using metal. Thus, we synthesized molecules **2.38** and **2.39** using the conditions from entry 2 (table 2-2). These molecules were synthesized through sequential substitution of 3,5-diamino-1,2,4-triazoles on 1,3-Diiminoisoindoline. Reaction of excess 3,5-diaminotriazole with 1,3-Diiminoisoindoline, designed to give the di-substituted product in a single step resulted in formation of mixture of both mono- and di–substituted products, thereby requiring another substitution step to effect complete formation of di-substituted product **(Scheme 2-21)**.

Table 2-2 - Synthetic study of triazolo-hemiphthalocyanine formation

Entry	Reactant A	Reactant B	Product[a]	Conditions	Remarks[b]
1	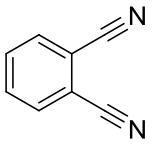	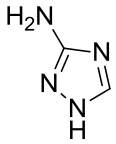 (2.5 Eq.)	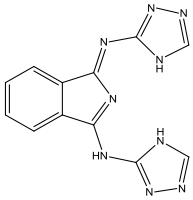	$CaCl_2$, Cyclo-hexanol,	Complete Conversion
2	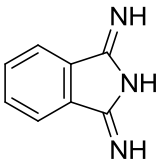 (2.5 Eq.)	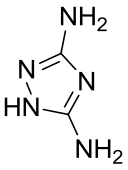	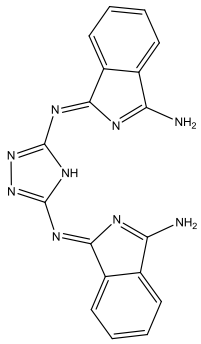	Ethanol, MW, 2 h	Complete Conversion
4	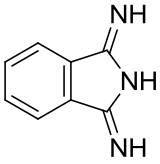	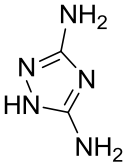 (2.5 Eq.)	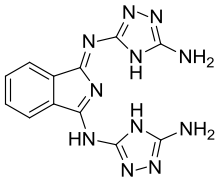	Ethanol, MW, 12 h	Complete Conversion
5	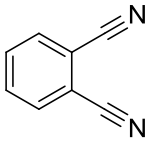	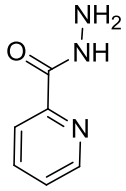	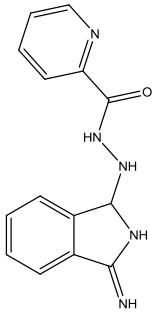	n-Butanol, Potassium Carbonate, MW, 6 h	Inseparable mixture of products (unidentifiable)

Table 2-2 - Continued

Entry	Reactant A	Reactant B	Product[a]	Conditions	Remarks[b]
6	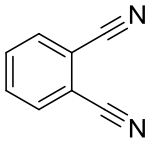	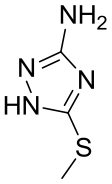	Products could not be identified	DCE, MW, 12 h	Decomposition
7	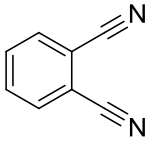	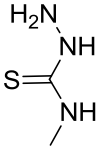	Products could not be identified	Methyl Iodide, Ethanol, MW, 12 h	Decomposition
8	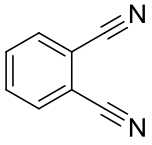	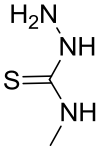	Products could not be identified	Ethanol MW, 12 h	Decomposition

a) Products were identified using HRMS (DART and ESI) b) reaction monitoring and quantitation was carried out using HPLC

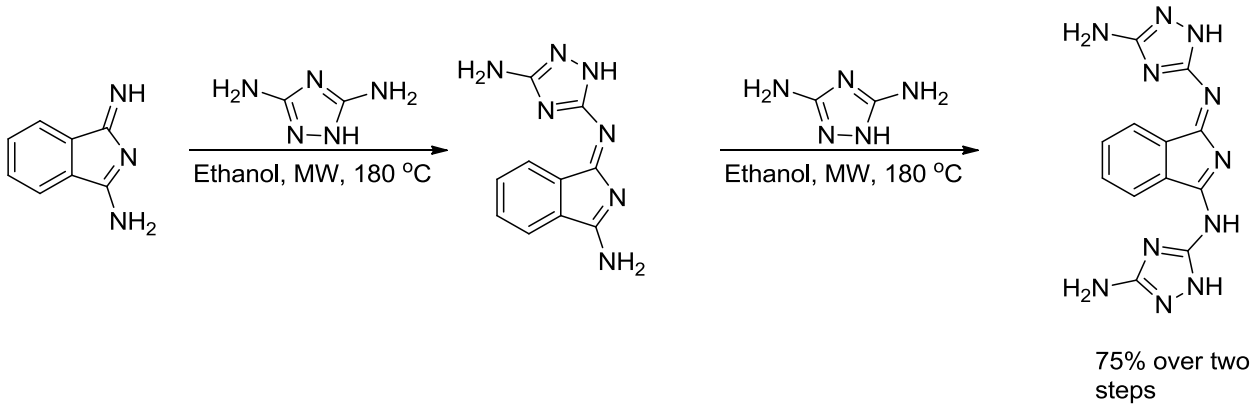

Scheme 2-21 - Synthesis of hemiphthalocyanine mimics from 1,3-diiminoisoindoline

Another series was prepared from dichloroquinoxaline in a similar fashion. This reaction resulted in exclusive formation of the di-substituted product in a single step, presumably due to use of the better leaving group (chloride). **Scheme 2-22** depicts this transformation.

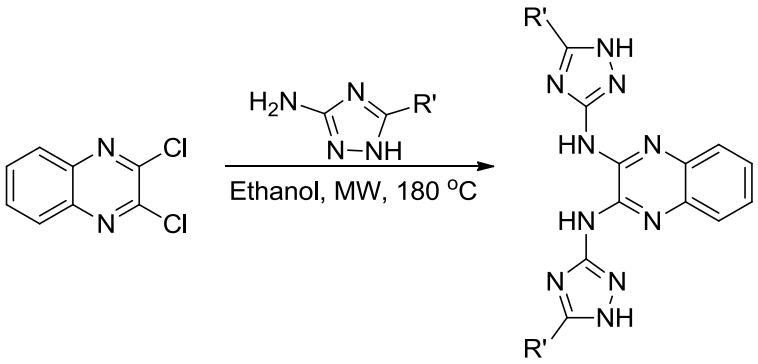

Scheme 2-22 - Synthesis of hemiphthalocyanine mimics from dichloroquinoxalines

2.2.6. Synthesis of 3-substituted triazoles by diazotiation

Organic chemists have long utilized diazotization reactions of aromatic amines to generate a strong electrophile that can subsequently undergo nucleophilic attack to

transform aromatic systems[124-125]. This same strategy can be used to generate aromatic azides by reaction with sodium azide. Our interest in preparing the azido substituted triazole stemmed from the idea that azide functionalities could be exploited efficiently to react with substituted alkynes in a 1,3 dipolar cyclo-addition reaction (click reaction) to generate a novel class of molecules encompassing both 1,2,4-triazole and 1,2,3-triazoles connected together. To our dismay, we discovered that while the diazotization chemistry used to generate the azide functional group worked efficiently the subsequent click reaction failed to work, despite trying variety of conditions. However, while carrying out the diazotization reaction we made a serendipitous discovery. We observed that if the diazo intermediate was allowed to react with another equivalent of amino triazole it led to the formation of the self-coupling product. Amino triazoles were found to be susceptible to diazotiation reaction conditions leading to formation of various substituted products. It is important to note that while halogenation and azide formation reactions through the application of diazotization chemistry are widely reported[126-127], very few examples of use of other nucleophiles exist[128-129]. On the other hand, virtually no reports exist of C-N bond formation through use of primary amines as nucleophiles. **Scheme 2-23** depicts the application of the diazotization strategy towards carrying out modifications at 3-position. This reaction was also found to work with other aromatic amines as well as aliphatic amines. Further optimization of this new class of reaction is currently underway.

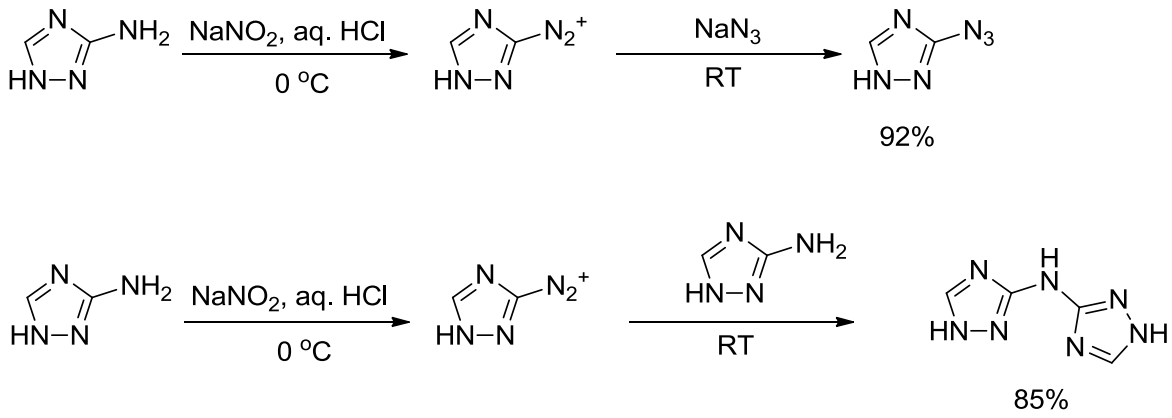

Scheme 2-23 - Application of diazotization reaction to the synthesis of 3-substituted-1,2,4-triazoles

One of our long standing goals was to synthesize triazoles with an aldehyde at the 3- position. The presence of an aldehyde group provides a highly reactive handle that can be further functionalized in multiple ways. Attempts to carry out either reduction of commercially available ester with DIBAL-H or oxidation of alcohol precursor resulted in failure **(Scheme 2-24)**. Starting materials were recovered in both cases. This wasn't surprising as we have observed multiple times that the reactivity of substituents on 3- or 5-positions of 1,2,4-triazoles is greatly decreased. In fact, this was one of the main reasons for the synthesis of formyl triazole, which we believed would have higher reactivity compared to its ester analogue.

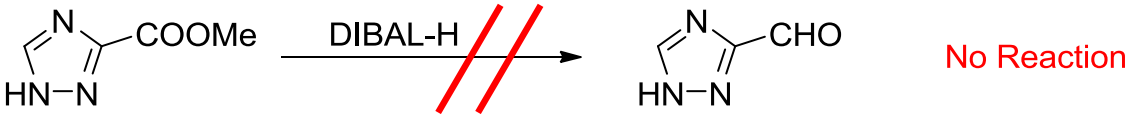

Scheme 2-24 - Attempted synthesis of formyl triazole from the ester precursor

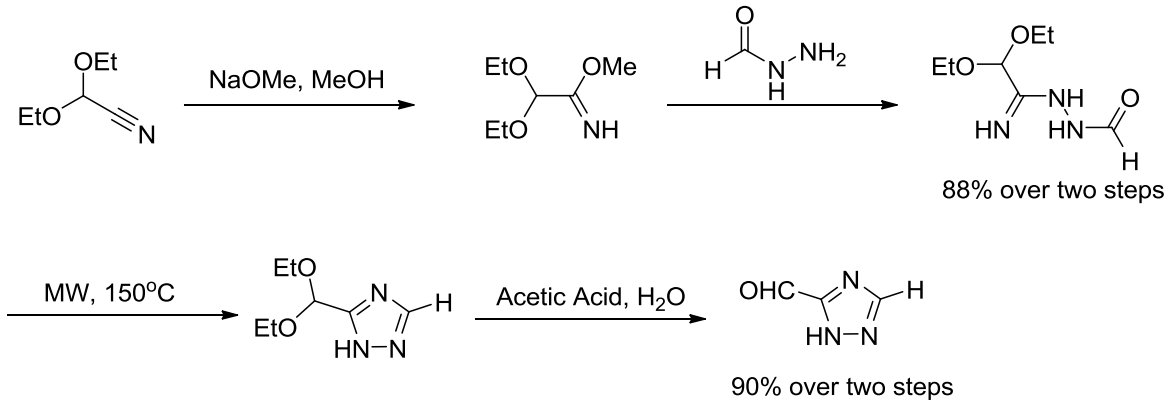

Scheme 2-25 - Successful Synthesis of 3-formyl-1,2,4-triazole

Eventually, 3-formyl-1,2,4-triazole was synthesized via a three step process starting from commercially available diethoxyacetonitrile. The diethoxy group acts as an aldehyde synthon. Thus, diethoxyacetonitrile when treated with sodium methoxide at room temperature led to the formation of the imidate intermediate that was treated with formyl hydrazine insitu. The adduct formed, underwent cyclization under microwave irradiation leading to the diethoxy triazole. Target formyl triazole was obtained when the diethoxy precursor was treated with acetic acid in water **(scheme 2-25)**. **Figure 2-26** depicts the 3-substituted triazoles synthesized in our lab

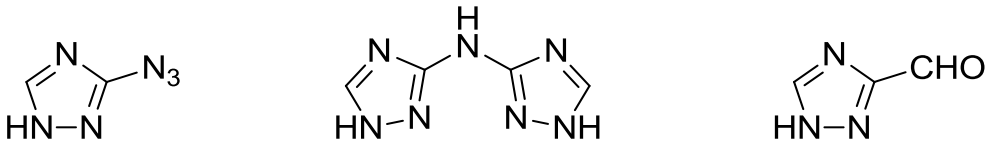

2.41 **2.42** **2.43**

Figure 2-26 – List of 3-substituted-1,2,4-triazoles synthesized

2.3. Conclusions

In conclusion, various 1,2,4-triazole molecules were successfully synthesized. Although most of the molecules were synthesized according to literature precedents, considerable improvements in the methodology were achieved through application of updated techniques. In particular, the use of a microwave synthesizer led to significant reduction in reaction times and improvement in yields. A novel way of synthesizing 3-substituted-1,2,4-triazoles by application of diazotization chemistry was also discovered. Further investigation into this chemistry is currently underway.

2.4. Experimental

Materials- Reagents and solvents were purchased from various commercial sources and used without further purification unless otherwise stated. Anhydrous solvents were purified using a Grubbs solvent system. Deuterated solvents were purchase from Cambridge Isotopes. Microwave reactions were carried out using Biotage Initiator 2.5 microwave synthesizer. Analytical thin-layer chromatography (TLC) was performed using aluminum backed silica gel TLC plates with UV indicator from Sorbent Technologies. Flash column chromatography was performed using 40-63 μm (230 x 400 mesh) silica gel from Sorbent Technologies. ^{1}H and ^{13}C NMR were recorded on Varian Inova NMR spectrometer and Bruker NMR Spectrometer. All chemical shifts were reported in δ units relative to tetramethylsilane or the corresponding deuterated solvent. High resolution mass spectra (ESI) were obtained on a JEOL AccuTOF DART spectrometer. Infrared spectra were recorded on a Varian 4100 FT-IR using KBr pellets or KBr salt plates. Absorption spectra were collected on a Thermo Scientific Evolution

600. High pressure liquid chromatography (HPLC) was performed using a Beckman Coulter System equipped with a UV-Vis detector, autosampler, Varian C18 column, and a mobile phase composed of acetonitrile and trifluoroacetic acid.

Synthetic Methods used to prepare 4-substituted-1,2,4-triazoles

General Method A: To a solution of primary alkyl, benzyl, or aryl amine (RNH_2, 1 mmol) in 4 mL of toluene was suspended N,N-dimethylformamide azine dihydrochloride (**1**, 1 mmol, 215 mg). The slurry was heated to 80 °C for 2 – 24 h with complete dissolution in most cases. Progress of the reaction was monitored by TLC. The reaction mixture was cooled to room temperature and then to -20 °C and the resulting precipitate was washed with 2 mL of cold ethanol and 5 mL of diethyl ether. Yields: 28 – 81%. In an alternate method, conventional heating was replaced with microwave irradiation at 150^{o}C for 2-6 hours. Other variables were kept constant.

General Method B: Aryl amine (RNH_2, 1.945 mmol), diformylhydrazine (**2**, 5.84mmol), and silica gel (1g) were suspended in boiling methanol. The resulting suspension was evaporated to dryness under reduced pressure. The dried silica was heated in a conventional microwave at 750W for 10 minutes. The silica gel was cooled to ambient temperature and washed three times with methanol (20 mL). The combined extracts were concentrated *in vacuo* and the crude product purified by elution from a plug of silica gel using ethyl acetate as the eluent.

4-(2-nitrophenyl)-4H-1,2,4-triazole[130] (2.1)

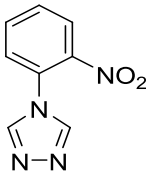

Prepared using method A and isolated as a yellow solid in 75% yield. **^{1}H NMR** (300 MHz, $CDCl_3$) δ 9.4 (s, 2H), 8.14 (d, 1H, J=7.0 Hz), 7.34 (d, 1H, J=7.0 Hz), 6.86 (d,1H, J=6.2 Hz), 6.73 (t, 1H, J=6.4 Hz). **^{13}C NMR** (75 MHz, $CDCl_3$) δ 146.1, 145.2, 130.1, 129.8, 123.1, 121.2, 120.7. **DART-MS** *m/z* observed 191.0479 ($C_8H_7N_4O_2$, $[M+H]^+$), *m/z* calculated 191.0569 ($C_8H_7N_4O_2$, $[M+H]^+$).

4-(*o*-Hydroxyphenyl)-1,2,4-triazole[131] (2.2)

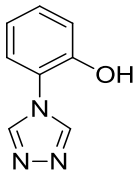

Prepared using method B and isolated as a pale yellow solid in 78% yield. **^{1}H NMR** (300 MHz, $CDCl_3$) δ 7.32-7.81 (m, 4H), 9.20 (s, 2H), 10.92 (br.s, 1H). **^{13}C NMR** (75 MHz, $CDCl_3$) δ 150.53, 143.17, 129.79, 125.63, 121.71, 119.70, 119.95. **DART-MS** *m/z* observed 162.0687 ($C_8H_8N_3O$, $[M+H]^+$), *m/z* calculated 162.0667 ($C_8H_8N_3O$, $[M+H]^+$).

Compounds **2.3** and **2.4** were purchased through commercial sources. Subsequent batches were prepared as follows. Spectral data matched with the commercial compounds.

Methyl 2-(4H-1,2,4-triazol-4-yl)benzoate (2.3)

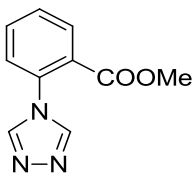

Prepared using method A and isolated as pale white solid in 81% yield. **^{1}H NMR** (300 MHz, $CDCl_3$) δ 9.4 (s, 2H), 8.1 (d, 1H, J=7.0 Hz), 7.56 (d, 1H, J=7.0 Hz)), 6.23 (d,1H, J=6.4 Hz), 6.16 (t, 1H, J=6.4 Hz), 3.82 (s, 3H), **^{13}C NMR** (75 MHz, $CDCl_3$) δ 170.5, 146.1, 130.3, 129.4, 129.1, 129.0, 125.6,

120.2, 51.2. **DART-MS** *m/z* observed 204.0699 ($C_{10}H_{10}N_3O_2$, $[M+H]^+$), *m/z* calculated 204.0773 ($C_{10}H_{10}N_3O_2$, $[M+H]^+$).

2-(4H-1,2,4-triazol-4-yl)benzoic acid (2.4)

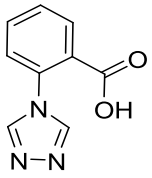

Prepared using method A and isolated as pale white solid in 88% yield. **^{1}H NMR** (300 MHz, $CDCl_3$) δ 12.3 (br.s.), 9.4 (s, 2H), 8.1 (d, 1H, J=7.0 Hz), 7.56 (d, 1H, J=7.0 Hz), 6.23 (d,1H, J=6.4 Hz), 6.16 (t, 1H, J=6.4 Hz). **^{13}C NMR** (75 MHz, $CDCl_3$) δ 170.5, 146.1, 130.3, 129.4, 129.1, 129.0, 125.6, 120.2. **DART-MS** *m/z* observed 190.0523 ($C_9H_8N_3O_2$, $[M+H]^+$), *m/z* calculated 190.0617 ($C_9H_8N_3O_2$, $[M+H]^+$).

4-(2-methoxyphenyl)-4H-1,2,4-triazole (2.5)

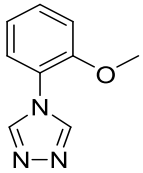

Prepared using method B and isolated as a pale yellow solid in 83% yield. **^{1}H NMR** (300 MHz, $CDCl_3$) δ 8.40 (s, 2H), 7.30-7.84 (m, 4H), 3.86 (s, 3H). **^{13}C NMR** (75 MHz, $CDCl_3$) δ 152.5, 143.1, 130.53, 125.3, 121.4, 112.6, 56.1. **DART-MS** *m/z* observed 162.0687 ($C_8H_8N_3O$, $[M+H]^+$), *m/z* calculated 162.0667 ($C_8H_8N_3O$, $[M+H]^+$).

4-(4-nitrophenyl)-4H-1,2,4-triazole[130] (2.6)

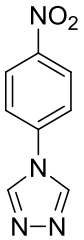

Prepared using method A and isolated as a yellow solid in 71% yield. **^{1}H NMR** (300 MHz, d_6-DMSO) δ 9.32 (s, 2H), 8.45 (d, 2H, J=9.0 Hz), 8.03 (d, 1H. J=9.0

Hz). **^{13}C NMR** (75 MHz, d_6-DMSO) δ 146.1, 141.0, 138.7, 125.4, 121.5. **DART-MS** *m/z* observed 191.0579 ($C_8H_7N_4O_2$, $[M+H]^+$), *m/z* calculated 191.0569 ($C_8H_7N_4O_2$, $[M+H]^+$).

4-(4-methoxyphenyl)-4H-1,2,4-triazole[132] (2.7)

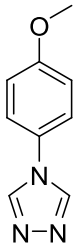

Prepared using method A and isolated as a pale yellow solid in 89% yield. **^{1}H NMR** ($CDCl_3$, 300 MHz) δ 8.46 (s, 2H), 7.26 (d, 2H, J=9 Hz), 6.98 (d, 2H, J=9 Hz), 3.81 (s, 3H). **^{13}C NMR** ($CDCl_3$, 75 MHz) δ 169.5, 165.5, 145.8, 126.1, 115.5, 56.1. **DART-MS** *m/z* observed 176.0799 ($C_9H_{10}N_3O$, $[M+H]^+$), *m/z* calculated 176.0824 ($C_9H_{10}N_3O$, $[M+H]^+$).

4-(4H-1,2,4-triazol-4-yl)phenol[131] (2.8)

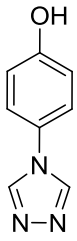

Prepared using method A and isolated as a pale yellow solid in 85% yield. **^{1}H NMR** ($CDCl_3$, 300 MHz) δ 8.46 (s, 2H), 7.26 (d, 2H, J=9 Hz), 6.99 (d, 2H, J=9 Hz), 5.3 (b. s., 1H). **^{13}C NMR** ($CDCl_3$, 7 5MHz) δ 167.5, 165.5, 145.8, 126., 115.5. **DART-MS** *m/z* observed 160.0442 ($C_8H_6N_3O$, $[M-H]^-$), *m/z* calculated 160.0516 ($C_8H_6N_3O$, $[M-H]^-$).

4-benzyl-4H-1,2,4-triazole[109] (2.9)

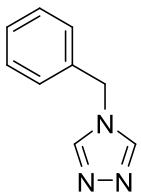

Prepared using method A and isolated as colorless crystals in 95% yield. **^{1}H NMR** (d_6-DMSO, 250 MHz) δ 3.93 (2H, s), 7.39 (3H, m), 7.53 (2H, d J=9.0 Hz), 8.55 (2H, s). **^{13}C NMR** (d_6-DMSO, 63 MHz) δ 136.2, 129.9, 129.5,

129.3, 123.8, 42.0. **DART-MS** *m/z* observed 160.1041 ($C_9H_{10}N_3$, $[M+H]^+$), *m/z* calculated 160.0875 ($C_9H_{10}N_3$, $[M+H]^+$).

2-((4H-1,2,4-triazol-4-yl)methyl)pyridine[105] (2.10)

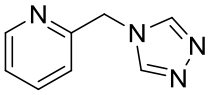

Prepared using method A and isolated as a white solid in 77% yield. **^{1}H NMR** (d_6-DMSO, 250MHz) δ 4.02 (2H, s), 7.40-7.62 (4H, m), 8.54 (2H, s). **^{13}C NMR** (d_6-DMSO, 63MHz) δ 136.1, 130.1, 129.9, 129.7, 129.2, 123.5, 44.2. **DART-MS** *m/z* observed 161.0833 ($C_8H_9N_4$, $[M+H]^+$), *m/z* calculated 161.0827 ($C_8H_9N_4$, $[M+H]^+$).

4-((4H-1,2,4-triazol-4-yl)methyl)pyridine[133] (2.11)

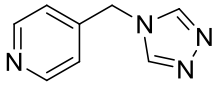

Prepared using method A and isolated as a white solid in 72% yield. **^{1}H NMR** (d_6-DMSO, 250MHz) δ 4.01 (2H, s), 7.42-7.63 (m, 4H), 8.56 (2H, s). **^{13}C NMR** (d_6-DMSO, 63MHz) δ 136.1, 130.0, 129.8, 129.5, 129.3, 123.5, 44.2. **DART-MS** *m/z* observed 161.0902 ($C_8H_9N_4$, $[M+H]^+$), *m/z* calculated 161.0827 ($C_8H_9N_4$, $[M+H]^+$).

2-(4H-1,2,4-triazol-4-yl)pyridine[134] (2.12)

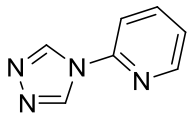

Prepared using method A and isolated as white solid in 81% yield. **^{1}H NMR** ($CDCl_3$, 250 MHz) δ 8.73–8.68 (m, 2 H), 8.5 (s, 2H), 7.77–7.82 (m,

1H), 7.47–7.52 (m, 1H). **^{13}C NMR** (62.5 MHz, $CDCl_3$) δ 153.3, 150.4, 143.4, 141.3, 130.0, 124.8. **DART-MS** *m/z* observed 147.0680 ($C_7H_7N_4$, $[M+H]^+$), *m/z* calculated 147.0671 ($C_7H_7N_4$, $[M+H]^+$)

3-(4H-1,2,4-triazol-4-yl)pyridine[105] (2.13)

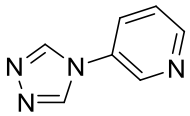

Prepared using method A and isolated as a white solid in 80% yield. **^{1}H NMR** (CDCl3, 250 MHz) δ 8.75–8.69 (m, 2 H), 8.47 (s,2 H), 7.78–7.85 (m,1 H), 7.45–7.50 (m, 1 H). **^{13}C NMR** (62.5 MHz, CDCl3) δ 153.3, 150.4, 143.4, 141.3, 130.1, 124.8. **DART-MS** *m/z* observed 147.0680 ($C_7H_7N_4$, $[M+H]^+$), *m/z* calculated 147.0671 ($C_7H_7N_4$, $[M+H]^+$)

4-phenyl-4H-1,2,4-triazole[105] (2.14)

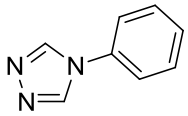

Prepared using method A and isolated as colorless needles in 98% yield. **^{1}H NMR** (d_6-DMSO, 300 MHz) δ 7.26-7.40 (2H, m), 7.46-7.56 3H, m), 8.47 (2H, s). **^{13}C NMR** (d_6-DMSO, 150 MHz) δ 141.3, 133.7, 130.2, 129.9, 122.1. **DART-MS** *m/z* observed 146.0722 ($C_8H_8N_3$, $[M+H]^+$), *m/z* calculated 146.0718 ($C_8H_8N_3$, $[M+H]^+$).

5-chloro-2-(4H-1,2,4-triazol-4-yl)pyridine (2.15)

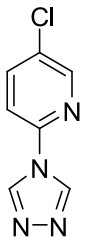

Prepared using method B and isolated as a white solid in 70% yield. **^{1}H NMR** ($CDCl_3$, 250 MHz) δ 8.88 (s, 2H), 8.48-8.47 (d, 1H, J=2.5 Hz), 7.90-7.86 (1H, dd,

J_1=2.5 Hz, J_2=8.6 Hz), 7.43-7.39 (d, 1H, J=8.6 Hz). **^{13}C NMR** ($CDCl_3$, 62.5 MHz) δ 192.4, 148.4, 139.7, 139.2, 131.4, 119.8, 113.7. **DART-MS** *m/z* observed 181.0283 ($C_7H_7ClN_4$, $[M+H]^+$), *m/z* calculated 181.0281 ($C_7H_7ClN_4$, $[M+H]^+$).

4-(naphthalen-1-yl)-4H-1,2,4-triazole (2.16)

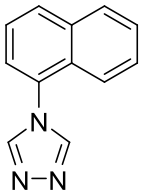

Prepared using method A and isolated as a white solid in 87% yield. **^{1}H NMR** ($CDCl_3$, 300MHz) δ 8.46 (s, 2H) 8.04 (d, 1H, J=8.5 Hz), 7.99 (d, 1H, J=8.5 Hz), 7.66-7.55 (m, 3H), 7.49-7.44 (m, 2H). **^{13}C NMR** ($CDCl_3$, 75MHz) δ 143.9, 130.7, 128.8, 128.5, 127.6, 125.3, 124.1, 121.5. **DART-MS** *m/z* observed 196.0869 ($C_{12}H_{10}N_3$, $[M+H]^+$), *m/z* calculated 196.0875 ($C_{12}H_{10}N_3$, $[M+H]^+$).

4-(naphthalen-2-yl)-4H-1,2,4-triazole (2.17)

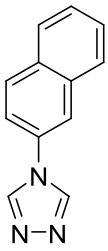

Prepared using method A and isolated as a white solid in 88% yield. **^{1}H NMR** ($CDCl_3$, 300MHz) δ 8.59 (s, 2H), 8.02 (d, 1H, J=8.5 Hz), 7.94 (d, 1H, J=5.5 Hz), 7.91 (d, 1H, J=5.2 Hz), 7.86 (d, 1H, J=2.2 Hz), 7.66-7.57 (m, 2H), 7.48 (dd, 1H, J_1 =8.5 Hz, J_2=2.5 H z). **^{13}C NMR** ($CDCl_3$, 75MHz) δ 141.8, 133.5, 133.0, 131.36, 130.9, 128.2, 128.1, 128.1, 127.6, 120.6, 120.3. **DART-MS** *m/z* observed 196.0871 ($C_{12}H_{10}N_3$, $[M+H]^+$), *m/z* calculated 196.0875 ($C_{12}H_{10}N_3$, $[M+H]^+$).

Compounds **2.18** and **2.19** were purchased through commercial sources. Subsequent batches were prepared as follows. Spectral data matched with the commercial compounds.

5-(1,2,4-triazol-1-yl)pentanoic acid (2.18)

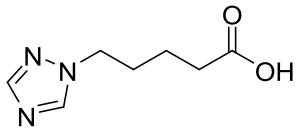

5-bromopentanoic acid (5 mmol), 1,2,4-1*H*-triazole (5.2 mmol), and freshly ground potassium carbonate (5.2 mmol) were dissolved in DMF (5 mL). The reaction mixture was subjected to microwave irradiation for 2 hours at 150 ^{o}C. The reaction was quenched with water (5.0 mL). The water was extracted with ethyl acetate 3 times. The organic layers were combined and washed with brine. The organic layer was dried over sodium sulfate, filtered and concentrated down via *in vacuo*. Isolated as white solid in 67% yield. **^{1}H NMR** ($CDCl_3$, 600 MHz) δ 12.05 (br.s.), 8.29 (s, 1H), 8.05 (s, 1H), 4.17 (t, 2H, J=6.0 Hz), 2.38 (t, 2H, J=6.0 Hz), 1.97 (m, 2H), 1.71 (m, 2H). **^{13}C NMR** ($CDCl_3$, 151 MHz) δ 185.1, 151.7, 143.1, 49.4, 36.7, 29.5, 22.4. **HRMS (ESI)** *m/z* calculated 170.0930 ($C_7H_{12}N_3O_2$, $[M+H]^+$), *m/z* observed 170.0977 ($C_7H_{12}N_3O_2$, $[M+H]^+$.

6-(1H-1,2,4-triazol-1-yl)hexanoic acid (2.19)

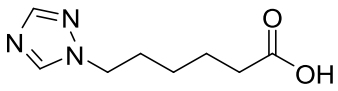

6-bromohexanoic acid (5 mmol), 1,2,4-1*H*-triazole (5.2 mmol), and freshly ground potassium carbonate (5.2 mmol) were dissolved in DMF (5 mL). The reaction mixture was subjected to microwave irradiation for 2 hours at 150^{o}C. The reaction was quenched with water (5.0 mL). The water was extracted with ethyl acetate (3 X 20 mL). The organic layers were combined and washed with brine (20 mL). The organic layer was dried over sodium sulfate, filtered and concentrated down via *in vacuo*. Isolated as white solid in 72% yield. **^{1}H NMR** ($CDCl_3$, 600 MHz) δ 12.06 (br.s.), 8.17 (s, 1H), 8.12 (s, 1H), 2.42 (t, 2H, J=12.0 Hz), 1.97 (m, 2H), 1.78 (m, 2H), 1.41 (m, 2H). **^{13}C NMR** ($CDCl_3$, 151 MHz) δ 178.6, 147.5,

138.6, 44.7, 32.60, 25.1, 21.4, 20.1. **HRMS (ESI)** *m/z* calculated 184.1086 ($C_8H_{14}N_3O_2$, $[M+H]^+$), *m/z* observed 184.1055 ($C_8H_{14}N_3O_2$, $[M+H]^+$.

5-bromo-N-phenylpentanamide[135]

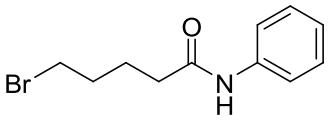

5-bromopentanoic acid (5.52 mmol) was dissolved in DCM (15.5 mL) with a catalytic amount of DMF (56.0 µL). The reaction mixture was cooled to 0 ^{o}C. A solution of 2 M oxalyl chloride (6.09 mmol) in DCM (3.04 mL) was added drop wise to the reaction with vigorous stirring over 15 minutes. The suspension was warmed to room temperature and stirred for 1 hour. The volatiles were evaporated under a stream of nitrogen. The residue was dissolved in DCM (25.6 mL) and cooled to 0 ^{o}C. The DIEA (11.60 mmol) was added drop wise. The aniline (5.52 mmol) was added drop wise over 1 hour. The reaction mixture was warmed to room temperature after the addition of the aniline and the reaction stirred for 2 hours. The reaction was quenched by adding water (5.0 mL). The solution was extracted with DCM (2 X 20 mL). The DCM layer was washed with saturated sodium bicarbonate (2 X 20 mL), water (20 mL), 1M hydrochloric acid (2 X 20 mL), and sodium chloride (20 mL). The organic layer was dried over sodium sulfate, filtered and concentrated down *in vacuo*. Isolated as a white solid in 92% yield. Product formation and purity was confirmed by DART-MS and HPLC.

N-phenyl-5-(1H-1,2,4-triazol-1-yl)pentanamide (2.20)

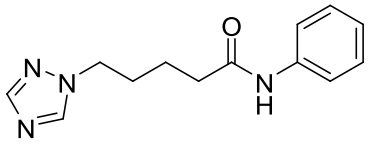

5-bromo-N-phenylpentamide (0.234 mmol), 1,2,4-1*H*-triazole (0.258 mmol), and freshly ground potassium carbonate (0.258 mmol) were dissolved in DMF (669.0 µL). The reaction mixture was subjected to microwave irradiation for 2 hours at 150 ^{o}C. The reaction was quenched with water (5.0 mL). The water was extracted with ethyl acetate (3 X 20 mL). The organic layers were combined and washed with brine (20 mL). The organic layer was dried over sodium sulfate, filtered and concentrated down via *in vacuo*. Isolated as a white solid in 72% yield. **^{1}H NMR** ($CDCl_3$, 600 MHz) δ 8.29 (s, 1H), 8.09 (s, 1H), 7.93 (s, 1H), 7.48 (d, 1H, J=6.0 Hz), 7.27 (t, 2H, J=6.0), 7.07 (t, 2H, J=6.0 Hz), 4.16 (t, 2H, J=6.0 Hz), 2.36 (t, 2H, J=6.0 Hz), 1.94 (m, 2H), 1.69 (m, 2H). **^{13}C NMR** ($CDCl_3$, 151 MHz) δ 171.09, 151.70, 138.41, 133.31, 124.48, 119.76, 115.25, 72.71, 44.83, 32.60, 24.97, 21.43. **HRMS (ESI)** *m/z* calculated 245.14024 ($C_{13}H_{17}N_4O_1$, $[M+H]^+$), *m/z* observed 245.13918 ($C_{13}H_{17}N_4O_1$, $[M+H]^+$.

6-bromo-N-phenylhexanamide[135]

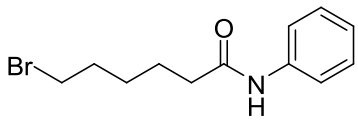

6-bromohexanoic acid (5.13 mmol) was dissolved in DCM (14.4 mL) with a catalytic amount of DMF (51.6 µL). The reaction mixture was cooled to -5 degrees. A solution of 2 M oxalyl chloride (5.64 mmol) in DCM (2.81 mL) was added drop wise to the reaction with vigorous stirring over 15 minutes. The suspension was warmed to room temperature and stirred for 1 hour. The volatiles were evaporated under a stream of nitrogen. The residue was dissolved in DCM (23.7 mL) and cooled to zero degrees. The DIEA (10.77 mmol) was added drop

wise. The aniline (5.13 mmol) was added drop wise over 1 hour. The reaction mixture was warmed to room temperature after the addition of the aniline and the reaction stirred for 2 hours. The reaction was quenched by adding water (4.62 mL). The solution was extracted with DCM (2 X 20 mL). The DCM layer was washed with saturated sodium bicarbonate (2 X 20 mL), water (20 mL), 1M hydrochloric acid (2 X 20 mL), and sodium chloride (20 mL). The organic layer was dried over sodium sulfate, filtered and concentrated down *in vacuo*. Product formation and purity was confirmed by DART-MS and HPLC. Isolated as a white solid in 88% yield.

N-phenyl-6-(1H-1,2,4-triazol-1-yl)hexanamide (2.21)

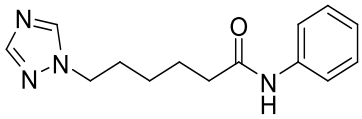

Prepared as listed above for N-phenyl-5-(1*H*-1,2,4-triazol-1-yl)pentanamide and isolated as colorless semi-solid material in 72% yield. **^{1}H NMR** ($CDCl_3$, 600 MHz) δ 8.05 (s, 1H), 7.93 1H), 7.40 (s, 1H), 7.50 (d, 2H, J=6.0 Hz), 7.29 (t, 2H, J=12.0 Hz), 7.08 (t, 1H, J=6.0 Hz), 4.17 (t, 2H, J=6.0 Hz), 2.35 (t, 2H, J=12.0 Hz), 1.94 (m, 2H), 1.76 (m, 2H), 1.36 (m, 2H). **^{13}C NMR** ($CDCl_3$, 151 MHz) δ 166.2, 147.3, 138.1, 133.3, 124.4, 119.7, 115.2, 44.8, 32.6, 24.9, 21.4, 20.1. **HRMS (ESI)** *m/z* calculated 259.15589 ($C_{14}H_{19}N_4O_1$, $[M+H]^+$), *m/z* observed 259.15473 ($C_{14}H_{19}N_4O_1$, $[M+H]^+$.

4-Amino-3,5-di(2-pyridyl) -1,2,4-triazole[101] (2.22)

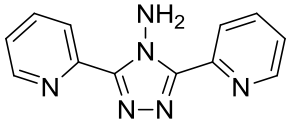

A mixture of 2-pyridinecarbonitrile (1 eq.), $N_2H_4{\cdot}HCl$ (1 eq.) and $N_2H_4{\cdot}H_2O$ (3 eq.) in ethanol was heated at 100 °C for 24 hours.

On cooling to room temperature, the reaction mixture solidified to give an almost colorless solid contaminated with some orange material. H_2O (100 mL) was added, the resulting slurry was filtered and the crude product was washed with water and dried in vacuo. Product was recrystallized from H_2O/ EtOH and isolated as a white solid in 85% yield. (1:1). **^{1}H NMR** (d_6-DMSO, 600 MHz) δ 8.65 (ddd, 2H, J=7.2 Hz), 8.49 9br. s, 2H), 8.38 (ddd, 2H, J=7.2 Hz), 7.86 (dt, 2H, J=7.2 Hz), 7.36 (ddd, 2H, J=7.2 Hz) **^{13}C NMR** (d_6-DMSO, 151 MHz) δ 148.4, 148.1, 147.8, 137.4, 124.1, 122.8. **DART-MS** *m/z* observed 239.1002 ($C_{12}H_{11}N_6$, $[M+H]^+$), *m/z* calculated 239.1045 ($C_{12}H_{11}N_6$, $[M+H]^+$).

General method for synthesis of 3,5-disubstituted-1,2,4-triazoles

Method A – From 3,5-disubstituted-4-amino-1,2,4-triazoles: To a stirred solution of 3,5-disubstituted-4-amino-1,2,4-triazole (0.01 moles) in an aqueous solution of 50 % hypophosphorous acid (30 mL), an aqueous solution of sodium nitrite (0.05 moles in 10 mL of water) was added slowly. Vigorous nitrogen evolution was observed during this addition and the mixture was stirred at room temperature for 1 hour. The reaction mixture was dried on rotovap and the obtained residue was purified by column chromatography.

Method B - From condensation of hydrazide and nitrile: substituted hydrazide (0.005 moles) and substituted nitrile (0.0055 moles) were added to a 20 mL microwave reaction vessel with 10 mL of n-Butanol. Potassium carbonate (0.0055 moles) was added and the reaction mixture was subjected to microwave irradiation at 150 ^oC for 2 hours. Precipitated triazole was filtered after cooling the reaction mixture and recrystallized from ethanol.

3,5-Di(2-pyridyl)-1,2,4-triazole[101] (2.23)

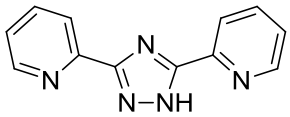

Synthesized using both general methods A and B and isolated as white amorphous solid. Method A yield – 22%, Method B yield – 79% **^{1}H NMR** (d_6-DMSO, 600 MHz) δ 7.51-7.98 (m, 4H), 8.16-8.71 (m, 4H), 9.21 (br.s., exch. 1H). **^{13}C NMR** (d_6-DMSO, 151 MHz) δ 122.8, 124.6, 137.8, 147.1, 148.9, 162.2. **DART-MS** *m/z* observed 224.0922 (C12H10N5, [M+H]+), *m/z* calculated 224.0936 ($C_{12}H_{10}N_5$, [M+H]+).

3,5-diphenyl-1H-1,2,4-triazole[101] (2.24)

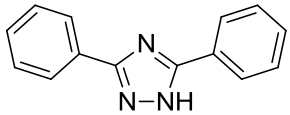

Synthesized using general method B and isolated as white amorphous solid in 85% yield. **^{1}H NMR** (d_6-DMSO, 600 MHz) δ 7.33-7.42 (m, 6H),7.82-7.99 (m, 4H), 8.6 (br.s., exch., 1H). **^{13}C NMR** (d_6-DMSO, 151 MHz) δ 126.8, 129.3, 129.7, 130.7, 159.2. **DART-MS** *m/z* observed 222.1025 ($C_{14}H_{12}N_3$, $[M+H]^+$), *m/z* calculated 222.1031 ($C_{14}H_{12}N_3$, $[M+H]^+$).

4-(5-phenyl-1H-1,2,4-triazol-3-yl)pyridine[102] (2.25)

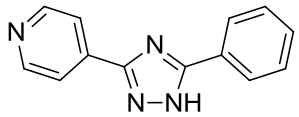

Synthesized using general method B and isolated as white amorphous solid in 81% yield. **^{1}H NMR** (d_6-DMSO, 600 MHz) δ 7.35-8.52 (m, 9H), 14.28 (s, 1H), 9.14 (br.s., exch. 1H). **^{13}C NMR** (d_6-DMSO, 151 MHz) δ 121.6, 127.55, 127.99, 129.42, 129.77, 130.65, 133.60, 135.05, 140.90, 151.92, 154.70, 158.20, 160.71. **DART-MS** *m/z* observed 223.0945 ($C_{13}H_{11}N_4$, $[M+H]^+$), *m/z* calculated 223.0984 ($C_{13}H_{11}N_4$ $[M+H]^+$).\

4,4'-(1H-1,2,4-triazole-3,5-diyl)dipyridine[101] (2.26)

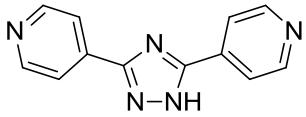

Synthesized using general method B and isolated as white amorphous solid in 77% yield. **^{1}H NMR** (d_6-DMSO, 600 MHz) δ 8.01-8.11 (m, 4H), 8.95-8.98 (m, 4H), 8.9 (br.s., exch., 1H). **^{13}C NMR** (d_6-DMSO, 151 MHz) δ 134.6, 135.8, 145.2, 156.8. **DART-MS** *m/z* observed 224.0967 ($C_{12}H_{10}N_5$, $[M+H]^+$), *m/z* calculated 224.0936 ($C_{12}H_{10}N_5$, $[M+H]^+$).

General method for synthesis of 3-amino-5-substituted-1,2,4-triazoles

In a 10 mL microwave vessel, substituted hydrazide (1 eq.) was added to a solution of s-methyl isothiourea (1.1 eq.) in n-Butanol (0.5 M). Potassium carbonate (0.1 eq.) was then added and the reaction was subjected to microwave irradiation for 12 hours at 150 ^{o}C. Reaction mixture was filtered upon cooling. Isolated solid was then recrystallized form ethanol to get analytically pure compound.

3-(pyridin-2-yl)-1H-1,2,4-triazol-5-amine[136] (2.27)

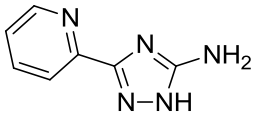

Synthesized using the general method described above and isolated as white amorphous solid in 84% yield. **^{1}H NMR** (500 MHz, d_6-DMSO): δ 6.03 (b.s, 2H), 7.24-7.88(m, 4H), 12.54 (br.s., 1H). **^{13}C NMR** (75 MHz, d_6-DMSO): δ 125.2, 128.0, 128.2, 132.3, 157.2, 158.3. **DART-MS** *m/z* observed 162.0770 ($C_7H_8N_5$, $[M+H]^+$), *m/z* calculated 162.0780 ($C_7H_8N_5$, $[M+H]^+$).

3-phenyl-1H-1,2,4-triazol-5-amine[103] (2.28)

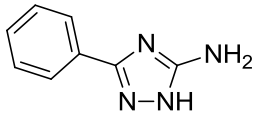

Synthesized using the general method described above and isolated as white amorphous solid in 92% yield. **^{1}H NMR** (300 MHz, d_6-DMSO): δ 6.05 (br s, 2H), 7.32 (t, 1H), 7.39 (t, 2H), 7.89 (d, 2H), 12.55 (b. s., 1H). **^{13}C NMR** (75 MHz, d_6-DMSO): δ 125.2 (2C), 128.0, 128.2(2C), 132.3, 157.2, 158.3. **DART-MS** *m/z* observed 161.0853 ($C_8H_9N_4$, $[M+H]^+$), *m/z* calculated 161.0827 ($C_8H_9N_4$, $[M+H]^+$).

3-methyl-1H-1,2,4-triazol-5-amine[103] (2.29)

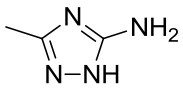

Synthesized using the general method described above and isolated as white amorphous solid in 92% yield. **^{1}H NMR** (300 MHz, d_6-DMSO): δ 2.32 (s, 3H), 5.99 (br s, 2H), 12.21 (b. s., 1H). **^{13}C NMR** (75 MHz, d_6-DMSO): δ 12.3, 155.7, 157.1. **DART-MS** *m/z* observed 99.0662 ($C_3H_7N_4$, $[M+H]^+$), *m/z* calculated 99.0671 ($C_3H_7N_4$, $[M+H]^+$).

Compounds 2.30 and 2.31 were procured from commercial sources

3,5-diazido-1H-1,2,4-triazole[137] (2.32)

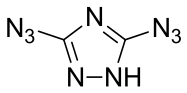

Sodium nitrite (12.5 mmol) was added to a solution of 3,5-diamino-1H-1,2,4-triazole 5 mmol) in 50% HCl-water (10 mL) at 0 ^{o}C over a period of 30 minutes. The reaction mixture was stirred at room temperature for 30 minutes and then cooled down to 0 ^{o}C. Sodium Azide (12.5 mmol) was added and the reaction mixture was stirred for another 30 minutes at room temperature. The precipitated

product was filtered and washed well with water and diethyl ether and dried in vacuo to give colorless crystals in 88% yield. **^{1}H NMR** ($CDCl_3$, 500 MHz): δ 8.90 (s, 1H). **^{13}C NMR** ($CDCl_3$, 125 MHz): δ 154.2. **DART-MS** *m/z* observed 152.0457 ($C_2H_2N_9$, $[M+H]^+$), *m/z* calculated 152.0433 ($C_2H_2N_9$, $[M+H]^+$).

3,4,5-tri-p-tolyl-4H-1,2,4-triazole (2.33)

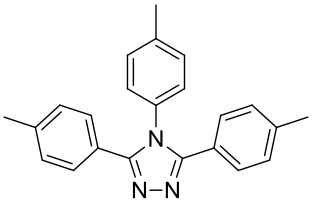

A mixture of 4-methylbenzoic acid (10 mmol), 5 mL of polyphosphoric acid (PPA), and hydrazine hydrate (50 mmol) was stirred for 12 hours at 120 °C. The mixture was poured into ice water and then brought to pH 7 by addition of sodium carbonate causing formation of a white precipitate. The precipitate was isolated by filtration, washed with a 0.1 M aqueous solution sodium carbonate, and then with deionized water. The precipitate was dried and isolated in 81% yield (based upon the carboxylic acid). The intermediate 1,2-bis(4-methylbenzoyl)-hydrazine intermediate was of sufficient purity to be used in the next step and spectral data match literature results. To a stirred suspension of 4-methylaniline (4 mmol) in 5 mL of xylenes cooled in an ice-water bath was added $POCl_3$ (1 mmol) drop wise over the course of 5 minutes. The mixture was stirred at 0 °C for an additional 25 minutes. To the reaction mixture was then added 1,2-bis(4-methylbenzoyl)-hydrazine (1 mmol) and the reaction flask was fitted with a reflux condenser and was then heated to 140 °C for 3.5 hours and allowed to cool to rt. The precipitate was collected by filtration, washed with additional xylenes, and then with diethyl ether, and was then recrystallized from hot ethanol to give off-white feathery crystals in 91% yield. **^{1}H NMR** (d_6-DMSO, 500 MHz) δ 7.84 (d, 4H, J = 10 Hz), 7.64 (d,

1H, J = 10 Hz), 7.38 (d, 1H, J = 10 Hz), 7.33 (d, 4H, J = 9 Hz), 7.22 (d, 1H, J = 9 Hz) 7.13 (d, 1H, J = 9 Hz), 2.38 (s, 6H), 2.29 (s, 3H). **^{13}C NMR** (d_6-DMSO,, 126 MHz) δ 166.2, 142.2, 131.1, 130.4, 130.2, 129.4, 129.3,127.8, 21.5, 21.0. **HRMS (ESI)** *m/z* calculated 340.1814 ($C_{23}H_{22}N_3$, $[M+H]^+$), *m/z* observed 340.1815 ($C_{23}H_{22}N_3$, $[M+H]^+$).

quinoxaline-2,3(1H,4H)-dione[138]

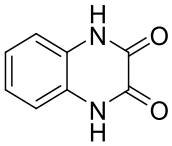

A solution of oxalic acid (0.0215 moles) in 4N aqueous HCl (5 mL) was added to a solution of 1,2-diaminobenzene (0.0193 moles) in 4N HCl (15 mL), and the resulting solution was heated to reflux for 2 hours. The reaction mixture was cooled to ambient temperature, and the resulting precipitate was isolated by filtration, washed with water, and dried giving product as an off white powder in 94% yield. **^{1}H NMR** (d_6-DMSO, 500 Mhz) δ 11.90 (s, 2H), 7.13–7.04 (m, 4H); **^{13}C NMR** (d_6-DMSO, 125 Mhz): δ 155.1, 125.5, 122.9, 115.0. **DART-MS** *m/z* observed 163.0497 ($C_8H_7N_2O_2$, $[M+H]^+$), *m/z* calculated 163.0508 ($C_8H_7N_2o_2$, $[M+H]^+$).

2,3-dichloro-1,2-dihydroquinoxaline[138]

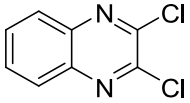

Quinoxaline-2,3(1*H*,4*H*)-dione (6.2 mmols) was dissolved in thionyl chloride (275 mmols) and 2-3 drops of DMF were added. The reaction mixture was refluxed for 2 hours. Upon completion, thionyl chloride was evaporated under reduced pressure leaving the product behind as solid residue in 97% yield. **^{1}H NMR** (300 MHz, d_6-DMSO) δ 7.9 (d, 2H, J=9.0Hz), 7.59 (d, 2H, J=9.0 Hz). **^{13}C NMR** (300 MHz, d_6-DMSO) δ 152.5, 139.1, 130.2, 125.7. **DART-MS** *m/z* observed 198.9901

($C_8H_5Cl_2N_2$, $[M+H]^+$), *m/z* calculated 198.9830 ($C_8H_5Cl_2N_2$, $[M+H]^+$).

General method for the synthesis of bistriazoloquinoxalines

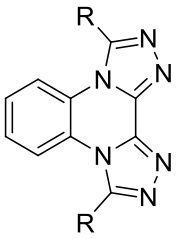

A mixture of 2,3 Dichloroquinoxaline (1 eq.) and substituted hydrazide (2.2 eq.) was dissolved in HMPA (0.25 M). The solution was stirred at 100^0C for 5 hours. The temperature was raised to 200 ^{o}C and the solution was stirred for another two hours until precipitation was observed. The solution was allowed to cool to ambient temperature followed by cooling in ice bath until no more precipitation was observed. Precipitates were filtered to yield the products as solid.

3,10-dimethylbis([1,2,4]triazolo)[4,3-a:3',4'-c]quinoxaline[115] (2.34)

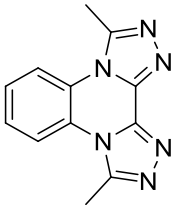

Prepared using the general method described above and isolated as a white solid in 44% yield. **^{1}H NMR** (600 MHz, d_6-DMSO) δ 8.33 (dd, 2H, J=9.0 Hz) 7.69 (dd, 2H, J=9.0 Hz), 3.04 (s, 6H). **^{13}C NMR** (600 MHz, d_6-DMSO) δ 128.2, 127.5, 115.6, 114.9, 105.7, 14.4. **DART-MS** *m/z* observed 239.0982 ($C_{12}H_{10}N_6$, $[M+H]^+$), *m/z* calculated 239.1045 ($C_{12}H_{10}N_6$, $[M+H]^+$).

3,10-diphenylbis([1,2,4]triazolo)[4,3-a:3',4'-c]quinoxaline[139] (2.35)

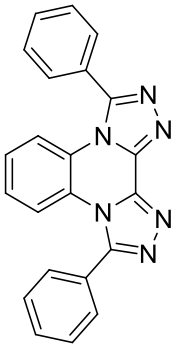

Prepared using the general method described above and isolated as a white solid in 38% yield. **^{1}H NMR** (600 MHz, d_6-DMSO) δ 7.67-7.74 (m, 10H) 7.29 (s, 4H). **^{13}C NMR** (600 MHz, d_6-DMSO) δ 131.1, 129.6, 129.5, 128.0, 127.2, 124.4, 118.2. **DART-MS** *m/z* observed 363.1282 ($C_{22}H_{14}N_6$, $[M+H]^+$), *m/z* calculated 363.1358 ($C_{22}H_{14}N_6$, $[M+H]^+$).

3,3'-(bis([1,2,4]triazolo)[4,3-a:3',4'-c]quinoxaline-3,10-diyl)dipropanoic acid[115]

(2.36)

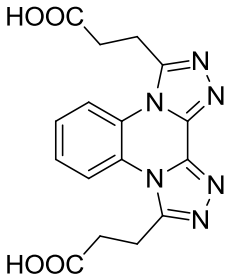

Prepared using the general method described above and Isolated as a pale yellow liquid in 32% yield. **^{1}H NMR** (300 MHz, D_2O) δ 7.36-7.31 (m, 4H) 2.64 (t, 4H, J=2.4 Hz), 2.15 (t, 4H, J=2.4 Hz). **^{13}C NMR** (300 MHz, D_2O) δ 200.1, 200.0, 132.3, 132.3, 128.9, 127.0, 33.4, 20.0. **DART-MS** *m/z* observed 353.1045 ($C_{16}H_{13}N_6O_4$, $[M-H]^+$), *m/z* calculated 353.0998($C_{16}H_{13}N_6O_4$, $[M-H]^+$).

3,10-di-p-tolylbis([1,2,4]triazolo)[4,3-a:3',4'-c]quinoxaline (2.37)

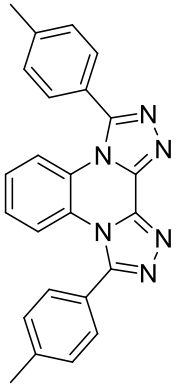

Prepared using the general method described above and isolated as a white solid in 35% yield. **^{1}H NMR** ($CDCl_3$, 500 MHz) δ 7.64-7.57 (m, 6H) 7.45-7.42 (m, 4H), 7.22-7.20 (m, 2H), 2.52 (s, 6 H). **^{13}C NMR** ($CDCl_3$, 125 MHz) 151.4, 141.9, 140.8, 130.3, 129.8, 127.5, 124.7, 124.4, 118.7, 21.8.

DART-MS *m/z* observed 391.1700 ($C_{24}H_{19}N_6$, $[M+H]^+$), *m/z* calculated 391.1671 ($C_{24}H_{19}N_6$, $[M+H]^+$).

N-5-(3-amino-1H-isoindol-1-ylidene)-1H-1,2,4-triazole-3,5-diamine (2.38)

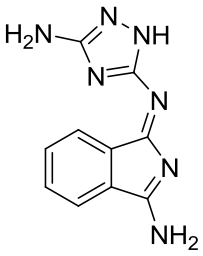

3,5-diamino-1,2,4-triazole (1 mmol) was suspended in a solution of 1,3-diiminoisoindole (1 mmol) in ethanol (5 mL) in a 10 mL microwave vessel. The resulting solution was heated to 160 °C for 12 hours in a microwave reactor. Precipitation was observed when the reaction mixture was cooled to ambient temperature. Precipitates were filtered, washed with ethanol, ether and dried in a vacuum oven. Product purity and identity was confirmed by HPLC and DART-MS. Yield – 88%

DART-MS *m/z* observed 228.1010 ($C_{10}H_{10}N_7$, $[M+H]^+$), *m/z* calculated 228.0998 ($C_{10}H_{10}N_7$, $[M+H]^+$).

N-5-(3-((3-amino-1H-1,2,4-triazol-5-yl)amino)-1H-isoindol-1-ylidene)-1H-1,2,4-triazole-3,5-diamine[140] (2.39)

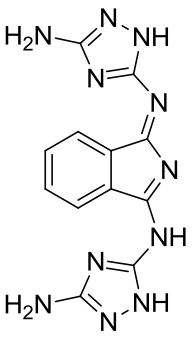

2.38 (1 mmol) was suspended in a solution of 3,5-diamino-1,2,4-triazole (1 mmol) in ethanol (5 mL) in a 10 mL microwave vessel. The resulting solution was heated to 160 °C for 12 hours in a microwave reactor. Precipitation was observed when the reaction mixture was cooled to ambient temperature. Precipitates were filtered, washed with ethanol, ether and dried in a vacuum oven. Product purity and identity was confirmed by HPLC,

NMR and DART-MS. Yield – 85%. **^{1}H NMR** (500 MHz, d_6-DMSO) δ 8.05 (br.s.), 7.87-7.94 (m, 3H), 7.76-7.79 (m, 4H). **^{13}C NMR** (500 MHz, d_6-DMSO) δ 169.6, 135.5, 133.1, 116.0, 123.3, 115.2. **DART-MS** *m/z* observed 310.1254 ($C_{12}H_{12}N_{11}$, $[M+H]^+$), *m/z* calculated 310.1227 ($C_{12}H_{12}N_{11}$, $[M+H]^+$).

N3,N3'-(quinoxaline-2,3-diyl)bis(1H-1,2,4-triazole-3,5-diamine) (2.40)

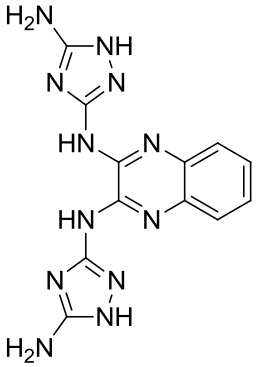

2,3-dichloroquinoxaline (1 mmol) was added to a solution of 3,5-diamino-1,2,4-triazole in ethnol (5 mL) in a 10 mL microwave vessel. The resulting solution was heated to 180^{o}C for 12 hours. A yellow precipitate was observed upon cooling the reaction mixture to ambient temperature. Precipitates were filtered, washed with ethanol, ether and dried in a vacuum oven. Product purity and identity was confirmed by HPLC and DART-MS. Yield 85%. **DART-MS** *m/z* observed 325.1402 ($C_{12}H_{13}N_{12}$, $[M+H]^+$), *m/z* calculated 325.1386 ($C_{12}H_{13}N_{12}$, $[M+H]^+$).

3-azido-1H-1,2,4-triazole[137] (2.41)

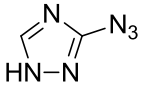

Sodium nitrite (5.5 mmol) was added to a solution of 3-amino-1H-1,2,4-triazole 5 mmol) in 50% HCl-water (10 mL) at 0 ^{o}C over a period of 30 minutes. The reaction mixture was stirred at room temperature for 30 minutes and then cooled down to 0 ^{o}C. Sodium Azide (5.5 mmol) was added and the reaction mixture was stirred for another 30 minutes at room temperature. The precipitated product was filtered and washed well with water and diethyl ether and dried in vacuo to give

colorless crystals in 94% yield. **^{1}H NMR** ($CDCl_3$, 500 MHz): δ 8.90 (s, 1H), 8.35 (b.s). **^{13}C NMR** ($CDCl_3$, 125 MHz): δ 155.1, 149.4. **DART-MS** *m/z* observed 111.0399 ($C_2H_3N_6$, $[M+H]^+$), *m/z* calculated 111.0419 ($C_2H_3N_6$, $[M+H]^+$).

di(1H-1,2,4-triazol-3-yl)amine (2.42)

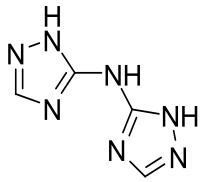

Sodium nitrite (12.5 mmol) was added to a solution of 3-amino-1H-1,2,4-triazole 5 mmol) in 50% HCl-water (10 mL) at 0 ^{o}C over a period of 30 minutes. The reaction mixture was stirred at room temperature for 30 minutes and then cooled down to 0 ^{o}C. Another equivalent of 3-amino-1H-1,2,4-triazole (5.5 mmol) was added and the reaction mixture was stirred for another 30 minutes at room temperature. Product was isolated followed by aqueous workup, column chromatography and obtained as pale yellow crystals in 85% yield. **^{1}H NMR** ($CDCl_3$, 500 MHz): δ 8.59 (s, 1H), 8.30 (br.s.). **^{13}C NMR** ($CDCl_3$, 125 MHz): δ 139.24, 146.08. **DART-MS** *m/z* observed 152.0457 ($C_4H_6N_7$, $[M+H]^+$), *m/z* calculated 152.0433 ($C_4H_6N_7$, $[M+H]^+$).

1H-1,2,4-triazole-3-carbaldehyde[141] (2.43)

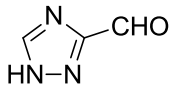

Catalytic amount of sodium methoxide was added to diethoxyacetonitrile (5 mmol) in methanol (10 mL) at room temperature and the reaction mixture was stirred for 3 h under argon atmosphere. The resulting solution was treated with formylhydrazine (5 .1 mmol) dissolved in methanol at room temperature for 12 h, depositing colorless crystals. Then, the reaction mixture was heated at reflux for 14 h. After neutralization with AcOH and removal of the solvent, a pale pink solid was

obtained. It was purified by column chromatography on silica gel and afforded a colorless crystalline 1,2,4-triazole-3-carboxaldehyde diethyl acetal (recrystallized from n-hexane-ether). The acetal was hydrolyzed to 1,2,4-triazole-3-~arboxaldehyde by treatment with 1N HCl in acetone at reflux for 3 h followed by neutralization with $NaHCO_3$, workup and chromatography on silica gel. The Aldehyde **2.43** was obtained as white crystals in 82% overall yield. **^{1}H NMR** (500 MHz, d_6-DMSO) δ 9.98 (s, 1H), 8.78 (s, 1H). **DART-MS** *m/z* observed 98.0323 ($C_4H_4N_3O$, $[M+H]^+$), *m/z* calculated 98.0354 ($C_{12}H_{12}N_{11}$, $[M+H]^+$).

3. *Solid Phase Synthesis*

3.1. Introduction

Solid phase synthesis, as the name suggests, is the synthesis of organic entities that are insoluble in any organic as well as aqueous solvents, unlike their homogeneous counterparts. One of the most notable examples of heterogeneous synthesis is the solid phase peptide synthesis pioneered by Robert Merrifield in 1963[142]. The basic idea behind this methodology was that an amino acid could be attached to a solid support, which then could undergo successive peptide coupling steps. At each coupling step, the impurities could simply be washed away by rinsing the solid supported peptide chain with organic solvents, thus greatly simplifying the purification process. At the end of the synthesis, the final peptide could then be cleaved from the solid support. This approach is different than the the classical organic synthetic approaches in which the target molecule is in the solution phase and has to be separated through phase separation or column chromatography. The advent of heterogeneous synthetic methodologies provided an alternative when the above mentioned classical purification techniques would become too cumbersome and result in highly depreciated product recoveries such as in a long multi step synthesis. A great deal of progress has been made in the last couple of decades in extending this approach towards solid phase organic synthesis[143-147].

Simplified purification is not the only advantage conferred by adoption of heterogeneous synthesis. In the context of catalysis, heterogeneous catalysts offer many other important advantages over their homogeneous counterparts. To name a

few, higher tolerance for multiple solvents, more stable active site and better steric control of reaction intermediates are just some of the advantages. Heterogeneous catalysts also have much better potential for recyclability due to the ease with which they can be separated from the reaction mixture. Metal contamination of products of catalysis reactions is a major problem when using homogeneous catalysts. This problem can be avoided by using heterogeneous catalysts. Numerous materials, including alumina[148], silica[149], zeolite[150] and polystyrene[151], have successfully been utilized as insoluble supports, each offering unique pros and cons.

This chapter details the efforts undertaken in our group towards derivatizing solid surfaces with organic molecules. Silica and polystyrene were used as solid supports. The discussion about various synthetic and analytical strategies used constitutes the core of this chapter. All the materials synthesized from silica and polystyrene contain covalently bonded organic component.

3.1.1. General synthetic strategy

The synthetic strategy for surface modification is greatly dependent on the type of functional groups present on the surface. The silica surface is decorated with hydroxyl groups whereas polystyrene resins are available in different varieties containing either hydroxyl or the amine group as the terminal moiety. Thus, a unique strategy specific to the surface being utilized has to be devised for each surface.

3.1.2. Polystyrene supported ligands

Polystyrene supports have been widely utilized for solid phase organic synthesis since the inception of the concept. There are a huge number of different polystyrene supports available for a variety of purposes although the majority of these supports are geared towards solid phase peptide synthesis. Some of the examples of widely used resins are Knorr amide resin, Rink amide resin, Wang hydroxyl resin and Merrifield resin **(Figure 3-1)**.

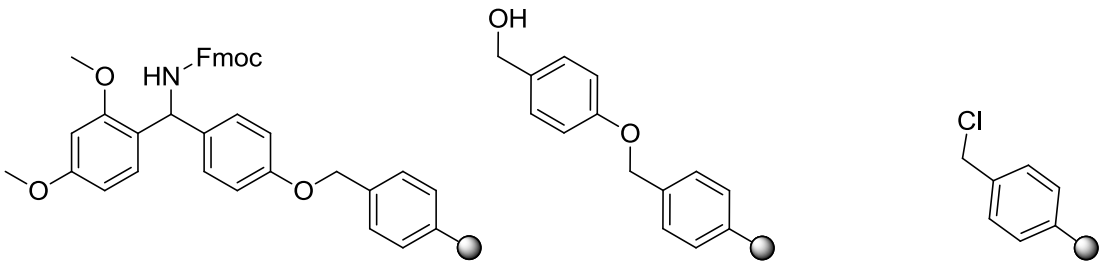

Figure 3-1 – Commercially available polystyrene resins

3,5-dipyridyl-1,2,4-triazole was found to be one of the most active ligands for Ni(II) catalyzed aziridination reaction (Chapter 6). Thus, our intention was to immobilize 3,5-dipyridyl-1,2,4-triazole on polystyrene. For this purpose we decided to adopt triazine accelerated copper catalyzed azide alkyne cycloaddition reaction (CuAAC), which was previously developed in our group. We decided to use the modified Merrifield resin as the azide component and suitably modified 1,2,4-triazole as the alkyne component. Towards this goal, we identified the para position of the phenyl ring of 3-aryl-5-pyridyl-1,2,4-triazole as a suitable point of attachment. We wanted to situate the 1,2,4-triazole core, which is responsible for the catalytic activity, pointing away from the surface. We

believed that this would result in the least interference from the surface while also giving the triazole core maximum exposure for participation in the catalytic reaction. The decision to situate the alkyne group on the phenyl group instead of the pyridine moiety was based partly on the same reason as we believed that the nitrogen atom in the pyridine ring is involved in the metal binding. Further support of this synthetic plan was based on the availability and the cost of starting materials.

The synthesis of this molecule was achieved starting with commercially available para-iodo benzoic acid which was converted to the corresponding hydrazide using the methodology described in the preceding chapter. Sonogashira reaction of the hydrazide with TMS-alkyne followed by microwave mediated condensation with 2-picolinyl nitrile resulted in the formation of the protected alkyne **3.3**. TMS-deprotection resulted in the formation of alkyne **3.4**. This alkyne was then subjected to the click reaction with azido functionalized Merrifield resin to produce the targeted surface bound compound **3.5**.

The azide component was synthesized from Merrifeld resin. Merrifeild resin contains a terminal chloride. This chloride was displaced with sodium azide to install the azido functionality on the resin. Azide loading on polystyrene was calculated with Fmoc assay[152]. In order to carry out the Fmoc assay the azide was reduced to the amine with $SnCl_2$ and subsequently protected with Fmoc protecting group. The Fmoc group was then removed and the amount of Fmoc was quantitated using UV-VIS spectroscopy. This reaction sequence is depicted in the **scheme 3-2**.

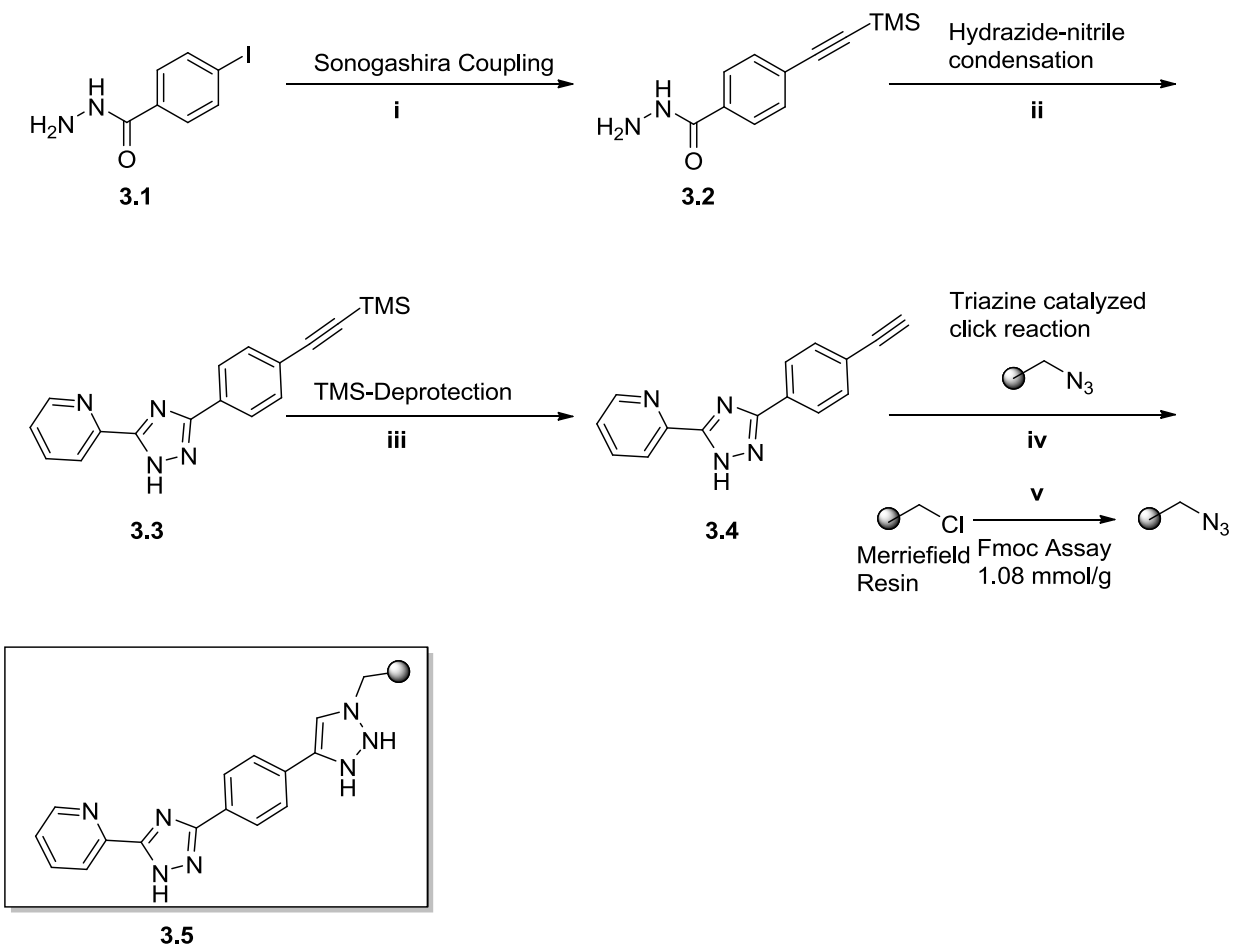

Scheme 3-2 - Immobilization of 3,5-disubstituted 1,2,4-triazole on polystyrene. i) $Pd(PPh_3)_2Cl_2$, TMS-acetylene, copper iodide, THF, ii) K_2CO_3, n-BuOH, M.W. 150 ^oC, iii) K_2CO_3, MeOH, iv) Azide (polystyrene), tetrakis(acetonitrile-N) copper (I) tetrafluoroborate, triazine catalyst, acetonitrile, v) NaN_3, tetrabutylammonium iodide, NMP, H_2O

The resultant 1,2,4-triazole modified Merrifield resin was complexed with Nickel Nitrate hexahydrate and used to catalyze aziridination reactions (stoichiometric calculations were based on azide loading as calculated by Fmoc assay). The observations from these experiments are detailed in chapter 6.

3.1.3. Silica Supported Ligands

Silica is an excellent support offering very high surface area as well as high thermal and chemical stability[153]. Silica enjoys many advantages over polystyrene supports. Silica supports are compatible with aqueous reaction condition whereas polystyrene supports are hydrophobic. This property is very useful for aqueous hydrocarbon oxidation reactions. In addition, thermal stability of silica becomes very important factor in the context of 1,2,4-triazole synthesis. The ring forming step in the 1,2,4-triazole synthesis requires high temperatures, usually 150 ^{o}C to 200 ^{o}C. Polystyrene based resins melt at high temperatures, making them unsuitable for such high temperature reactions. On the other hand silica can be heated to temperatures in excess of 600 ^{o}C without observing any degradation. Thus, the use of silica supports to immobilize triazoles was an obvious choice for heterogeneous 1,2,4-triazole based catalyst synthesis.

As discussed in previous chapter, 1,2,4-triazoles are synthesized from various precursors, e.g. substituted primary amines, hydrazides and alkyl halides. None of these functional groups are present on the surface of the silica. Thus it was necessary to install the appropriate linker on the silica surface beforehand. Amino substituted triethoxy silanes were selected as linkers to carry out this modification. Two linkers as shown in the **figure 3-3** were used. The primary reason behind using two different linkers was to judge the effect of variance in tether length on catalytic activity. **Figure 3-4** lists all silica supported 1,2,4-triazoles synthesized.

3-(triethoxysilyl)propan-1-amine **N^1-(3-(triethoxysilyl)propyl)ethane-1,2-diamine**

Figure 3-3 - Triethylsilyl linkers used for immobilized triazole synthesis

3.1.3.1. Synthesis of 4-substituted triazoles appended to silica

The first step in the synthesis was activation of silica gel with strong acids to get rid of chemical contaminants on the silica surface. This was followed by reaction of the triethoxy silane linkers with the activated silica. For the actual triazole immobilization step we decided to adopt two different strategies. The first one was the direct formation of the triazole using the primary amine already immobilized on silica. The second strategy was to use a preformed 1,2,4-triazole with an appropriate linker and immobilizing it through amide bond formation. **Scheme 3-5** illustrates the dual synthetic approach.

While the former route is shorter and gives maximum flexibility, it also has more uncertainty. The triazole ring formation reaction is the most difficult step in the synthesis. Carrying out this step on a solid surface has much less chance of success. The characterization of the solid surface is also much harder than characterizing soluble triazoles due to the fact that it is nearly impossible to cleave appended substrates from silica without decomposition. Thus, the second strategy, described above, was applied to overcome these challenges and validate the chemistry.

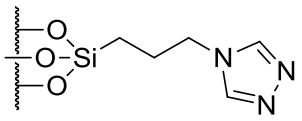

3.8

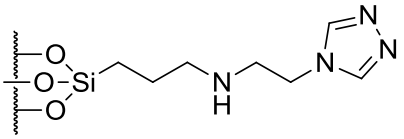

3.9

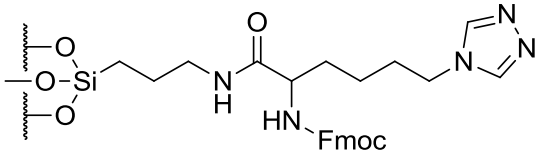

3.10

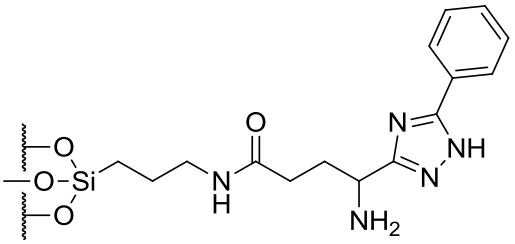

3.14

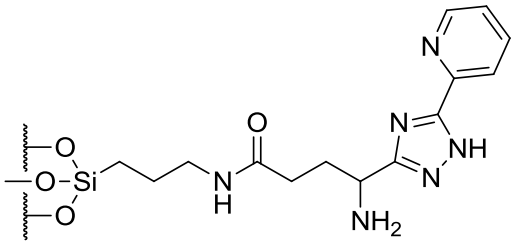

3.15

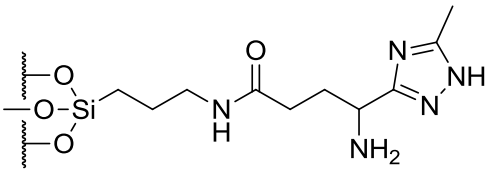

3.16

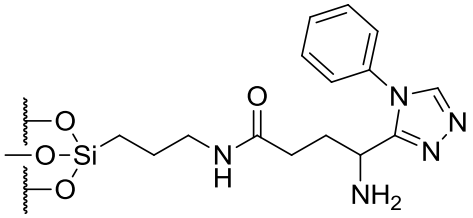

3.17

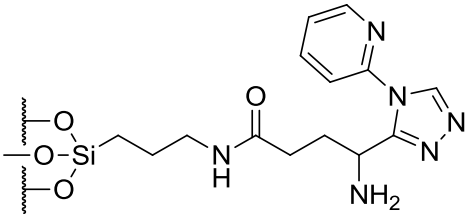

3.18

Figure 3-4 - Silica supported 1,2,4-triazole ligands

In this approach an amino acid is converted to the 1,2,4-triazole and thoroughly characterized. This modified amino acid is coupled to the surface through the amine already immobilized on the surface. Not only is the coupling step more efficient than the triazole forming step, but the loading of the amino acid can be calculated using Fmoc-assay. The amino acid best suited for the Fmoc assay was determined to be lysine due to the presence of two amino functional groups, one that can be used for triazole formation and the other one protected with Fmoc group which can be removed to calculate the loading via Fmoc assay. The resultant silica immobilized triazoles were complexed with copper and tested for catalytic activity in hydrocarbon oxidation reactions. These results are explained in chapter 4 of this dissertation.

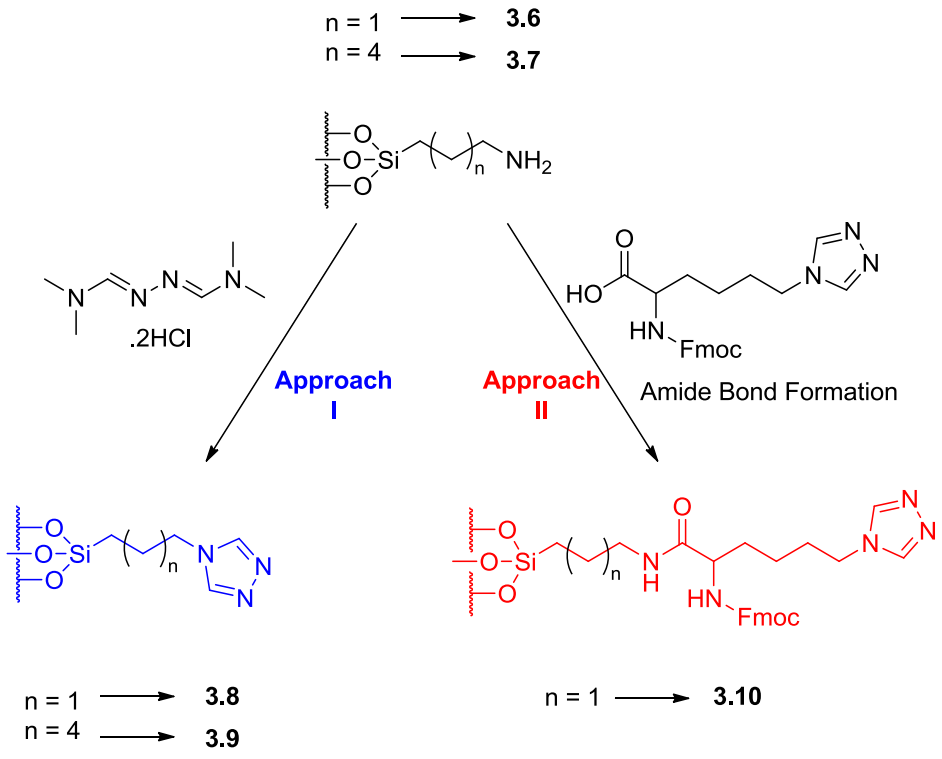

Scheme 3-5 - Dual approach towards triazole immobilization on silica. (n=4 represents the (triethoxysilyl)propyl)ethane-1,2-diamine linker)

3.1.3.2. Synthesis of 3,5-disubstituted and 3,4-disubstituted 1,2,4-triazoles appended to silica

With the successful synthesis of 4-substituted triazoles on silica, we then moved to the immobilization of 3,5- and 3,4-disubstituted triazoles. **Scheme 3-6** describes the general synthetic strategy adopted towards synthesis of disubstituted triazoles. N-Fmoc-L-glutamic acid t-butyl ester was coupled to the aminopropyl derivatized surface using standard amino acid coupling conditions. The tert-butyl ester was removed by treatment with phosphoric acid. The resulting carboxylic acid **3.12** was then treated with hydrazine hydrate to generate the hydrazide. At this point in the synthesis, two options opened up. One option was the condensation of the hydrazide with substituted nitriles to form the 3,5-disubstituted triazole. The second method involved treating the hydrazide with DMF-DMA to form the 3,4-disubstituted triazole. Having validated the synthetic steps in solution phase (chapter 2) and based on the literature precedents[154], we were confident of success of these methodologies on the solid support. In both the synthetic approaches adopted, the Fmoc protecting group was removed right after the triazole formation step. Fmoc assay was carried out to estimate the extent of functionalization. The presence of the triazole ring was confirmed by IR spectroscopy. Fmoc assay[152] was also carried out on **3.11,** in order to better estimate the stoichiometry of the reagents to be used in the following synthetic steps.

Compounds **3.14** through **3.18** were thus synthesized and complexed with metal. These complexes were screened for catalytic activity in oxidation reactions. Their catalytic activity is discussed in chapter 4.

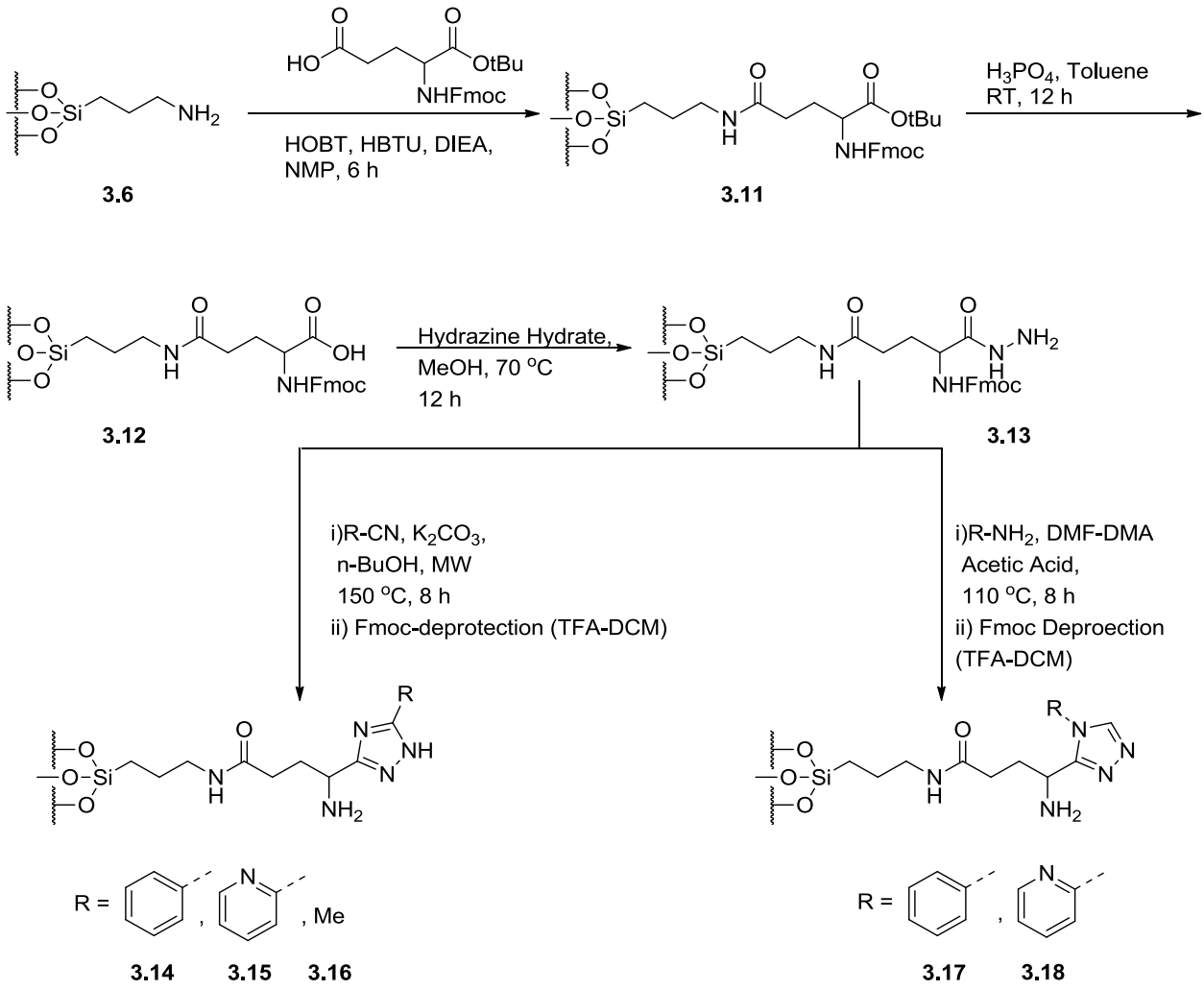

Scheme 3-6 - Synthesis of 3,5- and 3,4-disubstituted-1,2,4-triazoles immobilized on silica

3.1.4. Capping of functionalized silica surface

Given the large surface area of silica supports, it is impossible to functionalize every hydroxyl group on the silica surface. Thus, a silica surface immobilized with triazole retains a high population of free hydroxyl functional groups. In order to determine the effect of these groups on the catalytic activity, we performed an additional step to cap the free hydroxyl groups. This was achieved by reaction of silica with

trimethoxysilane under reflux conditions **(Scheme 3-7).** This process was repeated for all functionalized silica surfaces. The activity of functionalized capped silica surfaces was compared with that of uncapped functionalized silica surfaces. These results are discussed in chapter 4.

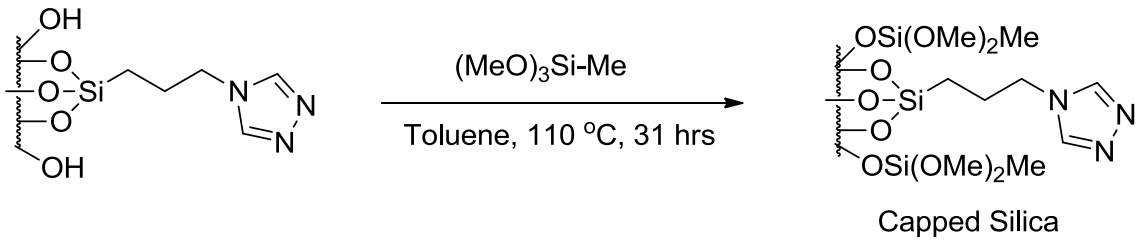

Scheme 3-7 – Capping free hydroxyl groups with trimethoxymethysilane

3.2. Analytical techniques

Silica appended organic molecules cannot be cleaved off the surface without running the risk of decomposition. Therefore techniques such as solution phase NMR and mass spectrometry were ruled out as viable analytical tools. Instead we had to rely on infrared spectroscopy to a large extent. Solid state NMR spectroscopy was also attempted, however very broad peaks, often spanning 10 ppm were observed. This ruled out the use of solid state NMR techniques for characterization purposes. Kaiser test was used to confirm the presence of primary amines at certain stages. Fmoc assays[152] were utilized to calculate the loading of the triazole or the triazole precursors on the silica surface. IR spectroscopy was used to confirm the presence of the triazole functional groups on the surface. In case of polystyrene support Infrared spectroscopy was used to qualitatively confirm substitution of the azide by the appearance of a characteristic absorption at approximately 2100 cm^{-1}

Table 3-1 lists IR frequencies corresponding to the bonds present in 1,2,4-triazole containing molecules synthesized by us. These characteristic triazole bond frequencies[155] were used to confirm the presence of triazoles on the surface. Other frequncies observed often corresponded to primary amines (3400-3500 cm^{-1}) (if present), alcohols (silica surface) (3200-3600 cm^{-1}, often broad), Si-H (2100-2360 cm^{-1}), Si-OR (1000-1120 cm^{-1}), Aromatic rings (3000-3100 cm^{-1}) (if present) and alkyl peaks (2800-2960 cm^{-1}).

Table 3-1 – Charecteristic IR frequencies observed for 1,2,4-triazoles[155]

Entry	Type of Bond	Absorption cm^{-1}	Vibrational Assignment
1	N-N	1150-1260	Stretching
2	Aromatic C=C	1500-1600	Stretching
3	C=N	1550-1500	Stretching
4	C-N	1400	Stretching
5	N-H	1180-1200	In-plane bending
6	C-H	1100	In-plane bending
7	Ring	1000	In-plane bending

3.3. Conclusions

In conclusion, 1,2,4-triazole derivatives were successfully appended to polystyrene and silica supports. Characterization of appended 1,2,4-triazoles was carried out using IR spectroscopy, Solid state NMR spectroscopy, Fmoc assay and Kaiser tests. The loading levels of the triazoles on silica were found to be lower by a factor of two when compared to commercially available polystyrene resins. Observations on the catalytic activity of polystyrene supported ligands (Aziridination) and silica supported ligands (Oxidation) are discussed in following chapters.

3.4. Experimental

Materials and methods- Reagents and solvents were purchased from various commercial sources and used without further purification unless otherwise stated. Anhydrous solvents were purified using a Grubb's solvent system. Analytical thin-layer chromatography (TLC) was performed using aluminum backed silica gel TLC plates with UV indicator from Sorbent Technologies. Microwave reactions were carried out using Biotage Initiator 2.5 microwave synthesizer. ^{1}H and ^{13}C NMR were recorded Varian Inova NMR spectrometer, Bruker NMR Spectrometer and Bruker solid state NMR spectrometer. Infrared spectra were recorded on a Varian 4100 FT-IR using KBr pellets or KBr salt plates. Absorption spectra were collected on a Thermo Scientific Evolution 600. High pressure liquid chromatography (HPLC) was performed using a Beckman Coulter System equipped with a UV-Vis detector, autosampler, Varian C18 column, and a mobile phase composed of acetonitrile and trifluoroacetic acid.

3.4.1. Polysteyrene Supports

Polystyrene-supported Azide Method. Merrifield resin (14 mmol), sodium azide (42 mmol), tetrabutylammonium iodide (14 mmol) were added to 60 mL of NMP and 10 mL of water. Reaction was heated at 80 °C overnight. After cooling to room temperature, the resin was filtered, washed with NMP, water, DCM, MeOH, and Et_2O, and air dried.

IR (KBr) ν_{max} - 3456, 2974, 2102, 1381, 1346, 1115 cm^{-1}.

2-(3-(4-ethynylphenyl)-1H-1,2,4-triazol-5-yl)pyridine (3.4).

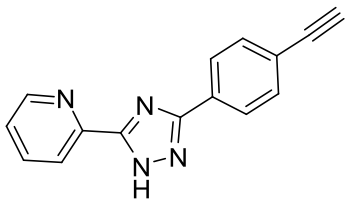

4-iodobenzohydrazide (10 mmol), dichlorobis-(triphenylphosphine) palladium(II) (0.25 mmol), and CuI (0.15 mmol) were combined in a round bottom flask and flushed with N_2. Anhydrous THF was added (12.5 mL) followed by a dropwise addition of triethylamine (15 mmol) and trimethylsilylacetylene (15 mmol) in anhydrous THF (12.5 mL). Reaction was stirred at room temperature and monitored by TLC. Upon completion, solvent was removed *in vacuo* and purified by silica gel chromatography to yield the corresponding trimethylsilyl protected alkyne. To the protected alkyne (10 mmol) in MeOH (20 mL) was added solid K_2CO_3 (1.5 mmol) and the resulting suspension stirred at room temperature, with reaction progress monitored by TLC. Upon completion, the reaction was concentrated *in vacuo*, and the residue brought up in DCM and water. The aqueous layer was extracted with DCM (20 mL X 3)). The combined organic layers were washed with water (20 mL), sat'd $NaHCO_3$ (20 mL), and

brine (20 mL). The solution was dried with sodium sulfate, concentrated *in vacuo* and purified by silica column chromatography to yield corresponding terminal alkyne.

^{1}H NMR ($CDCl_3$, 500 MHz) δ 8.95 (d, 1H, J = 4.8 Hz), 8.69 (d, 1H, J = 7.8 Hz), 8.30 (d, 2H, J = 8.4 Hz), 7.96 (dt, 1H, J = 7.8, 1.8 Hz), 7.71 (d, 2H, J = 8.4 Hz), 7.52–7.50 (m, 1H), 3.3 (s, 1H). **^{13}C NMR** ($CDCl_3$, 125 MHz) δ 155.1, 153.1, 150.7, 145.3, 137.3, 133.7, 133.2, 127.9, 126.8, 125.9, 124.4, 82.9, 80.8. **HRMS (ESI)** *m/z* calculated 247.0984 ($C_{15}H_{11}N_4$, $[M+H]^+$), *m/z* observed 247.09788 ($C_{15}H_{11}N_4$, $[M+H]^+$).

Polystyrene supported 1,2,3 triazole (3.5) –

Polystytrene supported azide (1 mmol), alkyne **3.4** (1 mmol), and triethylamine (1 mmol) were dissolved in acetonitrile (5 mL). **5,6-diphenyl-3-(pyridin-2-yl)-1,2,4-triazine** (10 μmol) and tetrakis(acetonitrile-N)copper(I) tetrafluoroborate (10 μmol) were added to the reaction solution and stirred at room temperature for 18 hours. Polystyrene resin was then filtered and washed well with ACN, DCM, methanol and ether.

IR (KBr) ν_{max} 3414, 2099, 1948, 1878, 1809, 1612, 1539, 1362, 1319, 1188, 1119, 1045 cm^{-1}.

3.4.2. Silica Support

Silica Gel Activation

Silica gel activation and pretreatment was carried out according to one of the following protocols. Silica gel from Sorbent Tech, premium R_f, 40-75 μm, 60Å was used in all the cases.

Protocol A:

10 g of silica gel was refluxed with 100 mL of 1.2N HCl for 23 hours. Suspension was then allowed to cool to room temperature and then filtered. Filtered silica gel was washed with de-ionized water until neutral pH was achieved. Silica gel was then washed successively with methanol (30mL), acetone (15mL), dichloromethane (15mL), toluene (15mL), methanol (15mL) and diethyl ether (30mL). Silica gel was then air dried overnight. Dry silica gel was spread on a petri dish and further dried in oven at 160 ^{o}C for 24 hours. Silica was then dried again under vacuum overnight.

Protocol B:

10g of silica gel was suspended in 80mL conc. H_2SO_4 and 15mL conc. HNO_3. The mixture was then heated at 110 ^{o}C for 50 hours. The suspension was then allowed to cool to room temperature and then filtered. Filtered silica gel was washed with de-ionized water until neutral pH was achieved. Silica gel was then washed successively with methanol (20mL), acetone (20mL), Dichloromethane (20mL), toluene (20mL), methanol (20mL) and diethyl ether (20mL). Silica gel was then air dried for 1 hour, followed by oven drying at 160 ^{o}C for 12 hours. Silica was then dried again under vacuum overnight.

Immobilization of 3-Aminopropyl-triethoxysilane on activated silica gel - 3.6

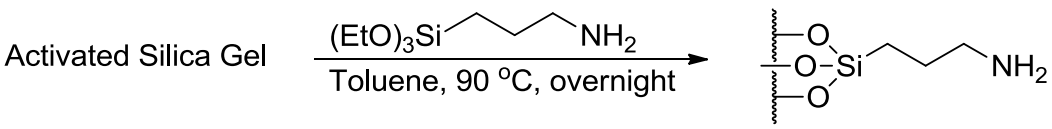

3-Aminopropyl-triethoxysilane (1 mmol) was added to a suspension of 1 g of activated silica in toluene (10mL). Reaction mixture was heated overnight at 90 ^{o}C. Reaction mixture was then allowed to cool to room temperature and filtered. Silica was washed successively with 30 mL each of methanol, de-ionized water, methanol, dichloromethane, acetone and diethyl ether and then dried overnight under vacuum.

IR (KBr) ν_{max} 3200-3600, 3400, 2870, 2930, 1600, 1320, 1200 cm^{-1}.

Kaiser test – Beads turned dark Blue confirming presence of free amine

Immobilization of N-[3-(Triethoxysilyl)propyl]-ethylenediamine on activated silica gel - 3.6

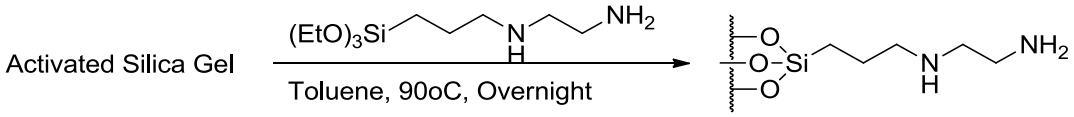

N-[3-(Triethoxysilyl)propyl]-ethylenediamine was added to a suspension of 1 g of activated silica in toluene (10 mL). Reaction mixture was heated overnight at 90^{o}C. Reaction mixture was allowed to cool to room temperature. Mixture was then filtered and silica washed successively with 30 mL each of methanol, de-ionized water, methanol, dichloromethane, acetone and diethyl ether. Silica was then dried overnight under vacuum.

IR (KBr) ν_{max} 3600-3200, 3420, 2870, 2930, 1600, 1320, 1200 cm^{-1}.

Kaiser test – Beads turned dark Blue confirming presence on free amine

General procedure for triazole formation on silica

A. from amines

Amino functionalized triethoxy silane immobilized on silica (0.7 mmols) and diazine reagent (1.4 mmols) were added to a 2:1:1 mixture of toluene, n-butanol and acetic acid. The reaction mixture was heated at 70 ^{o}C for 25 hours. Reaction mixture was then cooled to room temperature and filtered. The solid compound was washed successively with methanol (40 mL), dichloromethane (40mL), methanol (20 mL) and diethyl ether (20mL). Silica was then air dried.

B. from hydrazides

a) Silica immobilized hydrazide **(3.13)** (1 eq.) was added to a solution of Dimethyl formamide - dimethyl acetal (1eq.) and acetic acid (1 eq.) in acetonitrile. Reaction mixture was heated at 50 ^{o}C for 1 hour. Amine (1.1 eq.) was added and the reaction mixture was heated at 120 ^{o}C for additional 7 hours. Reaction mixture was then cooled to room temperature and filtered. The solid compound was washed successively with methanol (40 mL), dichloromethane (40mL), methanol (20 mL) and diethyl ether (20mL). Silica was then air dried.

b) Silica immobilized hydrazide **(3.13)** (1 eq.) was added to a solution of substituted nitrile (1.1 Eq.) in nBuOH. Reaction mixture was heated at 150 ^{o}C in microwave reactor for 4 hours. Reaction mixture was then cooled to room temperature and filtered. The solid compound was washed successively with methanol (40 mL), dichloromethane (40mL), methanol (20 mL) and diethyl ether (20mL). Silica was then air dried.

General method for immobilizing amino acids on the silica surface

Modified amino acids were coupled to amino propane triethoxysilane immobilized on silica using standard HOBT/HBTU coupling conditions. Modified amino acid (0.2 mmol) was dissolved in N-methyl pyrrolidine (2 mL) and HOBT (0.3 mmol), HBTU (0.9 mmol) and DIEA (2.8 mmol) were added. The reaction mixture was sonicated for 15 minutes until complete dissolution was observed. This solution was added to silica **3.6**. This suspension was shaken for 6 hours. The reaction mixture was filtered and filtered silica was washed successively with methanol, dimethylformamide, dichloromethane, acetone and diethyl ether.

Kaiser Test – Yellow beads – Indicating absence of free primary amine

Procedure for functionalizing hydrazide on silica support (3.13)

Silica immobilized modified amino acid **(3.12)** (1 eq.) was then added to a solution of hydrazine monohydrate (2.5 eq.) in methanol. Reaction mixture was heated at 70 ^{o}C for 12 hours. Reaction mixture was then cooled to room temperature and filtered. The solid compound was washed successively with methanol (40 mL), dichloromethane (40mL), methanol (20 mL) and diethyl ether (20mL). Silica was then air dried to give **3.13**

General procedure for complexation of silica immobilized ligands with metal

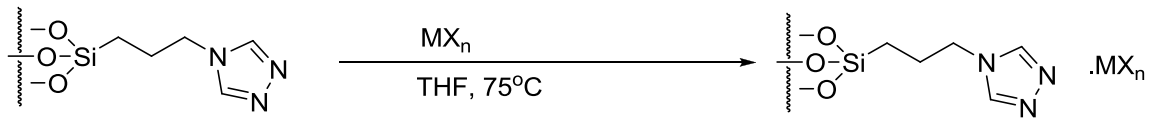

Silica immobilized triazole (1 eq.) and metal (1.1 eq.) were mixed together in tetrahydrofuran. The reaction mixture was heated at 75 ^{o}C for 2 hours. The reaction mixture was filtered and filtered silica was washed successively with methanol, acetone and diethyl ether. A color change depending on the metal used was observed.

General Procedure for capping silica surface

Trimethoxymethylsilane (10 eq.) was added to a suspension of silica immobilized triazole in toluene. Reaction mixture was heated at 110 ^{o}C for 31 hours. Reaction mixture was then cooled to room temperature and filtered. The solid compound was washed successively with methanol (40 mL), dichloromethane (40mL), methanol (20 mL) and diethyl ether (20mL). Silica was then air dried.

Fmoc Assay: Determination of the resin substitution using 2% DBU in DMF

Approximately 50 mg of resin was weighed into a graduated 100 mL flask and 20 mL of DMF is added. The suspension was stirred for 30 min and then 0.4 ml of DBU was added, affording a solution of 2% DBU/DMF (v/v). This mixture was stirred for another 30 min and diluted with ACN to 100 mL. Two mL of this solution was transferred to a graduated 25 mL flask and diluted with ACN to 25 mL. A reference solution was prepared in the same manner but without addition of the resin.

Fmoc-quantitation: 3 ml of the reference was transferred to one of a matched pair of 1 cm quartz glass cuvettes. The second cuvette was filled with 3 mL of the sample solution. A UV spectrometer was used to measure the absorbance of the solutions at

294 nm. The cuvettes were emptied and cleaned and the measurement repeated twice with fresh solutions. The loading was calculated by inserting the average value of the three readings into equation (1). The quantitation can also be performed at 304 nm and calculated using equation (2).

(1) Loading (mmol/g) 294 nm:

absorbance x 142.14/mg

(2) Loading (mmol/g) 304 nm:

absorbance x 163.96/mg.

Kaiser Test:

Kaiser reagent 1- 1:20 (w:v) Ninhydrin in Ethanol

Kaiser reagent 2- 4:1 (w:v) Phenol in Ethanol

Kaiser reagent 3- 0.02 mM (aq.) KCN in Pyridine

1 drop of each Kaiser reagent was added to 5 mg of functionalized silica in a small eppendorf tube. The tube was heated at 60 ^{o}C and the color of the silica particles was observed. Blue color indicates presence of free primary amines, clear solution indicates their absence.

Silica supported 4-propyl-4H-1,2,4-triazole (3.8)

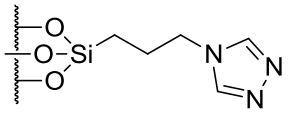

3.8 was synthesized using general procedure for triazole formation A. IR (KBr) v_{max} 3200-3600, 3100, 3180, 2870, 2930, 2100, 1640, 1600, 1580, 1550, 1320, 1200, 1000 cm^{-1}.

Silica supported N-(2-(4H-1,2,4-triazol-4-yl)ethyl)propan-1-amine (3.9)

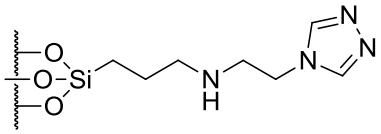

3.9 was synthesized using general procedure for triazole formation A. IR (KBr) v_{max} 3200-3600, 3100, 3180, 2870, 2930, 2100, 1640, 1600, 1580, 1550, 1320, 1200, 1000 cm^{-1}.

Silica supported (9H-fluoren-9-yl) methyl (1-oxo-1-(propylamino)-6-(4H-1,2,4-triazol-4-yl)hexan-2-yl)carbamate (3.10)

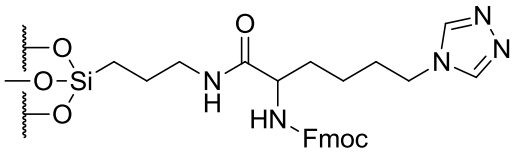

3.10 was synthesized using general method for immobilizing amino acids on the silica surface. IR (KBr) v_{max} 3600-3200, 3000, 2850, 1860, 1680, 1600, 1520, 1500, 1425, 1210, 1105, 1091 cm^{-1}. Fmoc Assay indicated loading to be 0.64 mmols/g.

Silica supported 4-amino-4-(5-phenyl-1H-1,2,4-triazol-3-yl)-N-propylbutanamide (3.14)

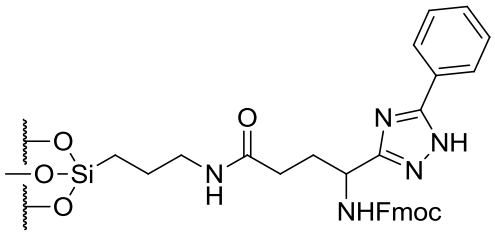

3.14 was synthesized using general procedure for triazole formation B (b). IR (KBr) v_{max} 3600-3200, 3100, 3000, 2980, 2850, 1860, 1680, 1600, 1520, 1405, 1230, 1100, 1000 cm^{-1}. Fmoc Assay indicated loading to be 0.56 mmols/g.

Silica supported 4-amino-N-propyl-4-(5-(pyridin-2-yl)-1H-1,2,4-triazol-3-yl) butanamide (3.15)

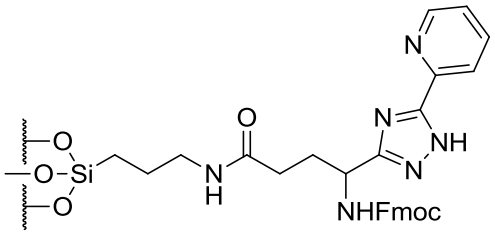

3.15 was synthesized using general procedure for triazole formation on silica B (b). IR (KBr) v_{max} 3600-3200, 3100, 3020, 2980, 2850, 1860, 1680, 1600, 1520, 1500, 1400, 1200, 1100, 1000 cm^{-1}. Fmoc Assay indicated loading to be 0.56 mmols/g.

Silica supported 4-amino-4-(5-methyl-1H-1,2,4-triazol-3-yl)-N-propylbutanamide (3.16)

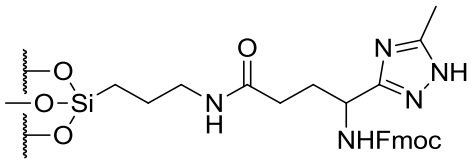

3.16 was synthesized using general procedure for triazole formation B (b). IR (KBr) v_{max} 3600-3200, 2910, 2850, 1860, 1680, 1600, 1520, 1500, 1400, 1150, 1050 cm^{-1}. Fmoc Assay indicated loading to be 0.56 mmols/g.

Silica supported 4-amino-4-(4-phenyl-4H-1,2,4-triazol-3-yl)-N-propylbutanamide (3.17)

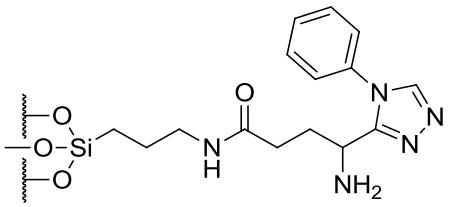

3.17 was synthesized using general procedure for triazole formation B (a). IR (KBr) v_{max} 3550-3225, 3175, 3020, 2980, 2850, 1860, 1680, 1620, 1520, 1420, 1210, 1125, 1000 cm^{-1}. Fmoc Assay indicated loading to be 0.56 mmols/g.

Silica supported 4-amino-N-propyl-4-(4-(pyridin-2-yl)-4H-1,2,4-triazol-3-yl) butanamide (3.18)

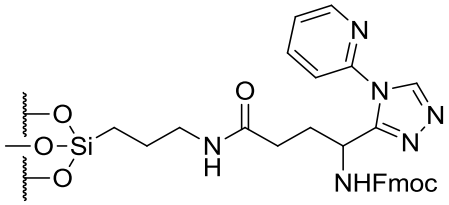

3.18 was synthesized using general procedure for triazole formation B (b). IR (KBr) v_{max} 3580-3200, 3120, 3020, 2990, 2850, 1850, 1680, 1620, 1520, 1420, 1210, 1125, 1000 cm^{-1}. Fmoc Assay indicated loading to be 0.56 mmols/g.

4. *1,2,4-Triazole ligand accelerated copper catalyzed hydrocarbon oxidation*

4.1. General investigation strategy

Preliminary studies into the catalytic activity of 1,2,4-triazoles for oxidation of hydrocarbons utilizing copper complexes of various 1,2,4-triazole derivatives were carried out. The synthesis of the ligands is described in chapter 2. Aqueous hydrogen peroxide and tert-butyl peroxide were used as the oxidants. Acetonitrile, THF and water were used as solvents. The complexes were prepared in THF at 60 ^{o}C and isolated as solids. The catalytic activity of these complexes was tested with substrates such as cyclohexane, cycloctane, cycloctene and styrene. While a moderate activity was observed for epoxidation of cycloctene, the copper-1,2,4-triazole complexes showed a greater promise for conversion of cyclohaxane to cyclohexanol and cyclohexanone, in a selective manner[156]. Cyclohexane is often used as a model for assessing the potential of a catalyst for conversion of methane to methanol[28]. Encouraged by the preliminary results, we focused our attention on the optimization of copper-1,2,4-triazole catalyzed cyclohexane oxidation reactions. Based on the preliminary studies we identified a number of promising ligands to for further study **(Figure 4-1)**. We also identified copper (II) nitrate and copper (II) chloride as the most active copper salts and acetonitrile as the optimal solvent for the oxidation reaction. This chapter describes the investigation of the catalytic activity, nature of metal binding and identity of copper complexes of ligands A-D.

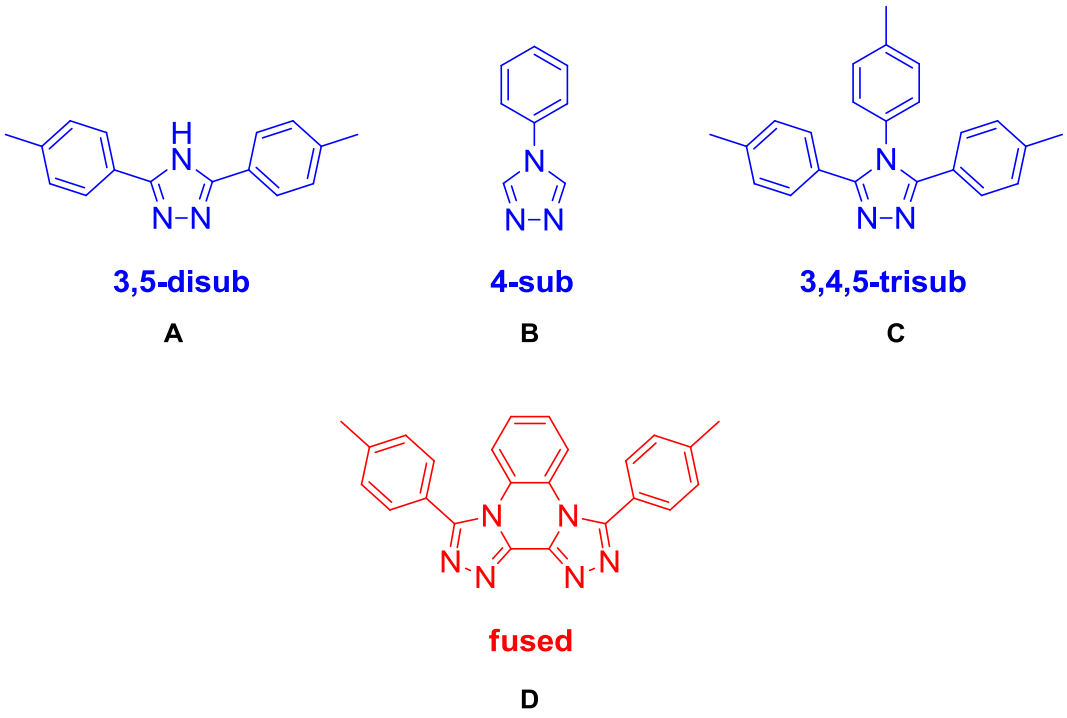

Figure 4-1 - 1,2,4-triazole-based ligands used in catalytic studies.

4.2. Observations

The catalysts reported here are based on in situ formation of a pre-catalytic species which was identified to be $Cu(NO_3)_2Lx_2$ where Lx refers to 1,2,4-triazole ligands x=A-D as denoted in **figure 4-1**. Briefly, a THF solution of $Cu(NO_3)_2 \cdot 2.5H_2O$ was added to 2.2 molar equivalents of ligand in THF and stirred at 60 °C for 12 hours. Within the first 20 minutes, a precipitate formed and after subsequent stirring at 60 °C there was complete dissolution, followed by precipitation of a complex of a different color. Such behavior has been observed in the formation of copper metal-organic frameworks (MOFs)[34-35]. In the presence of H_2O_2, the complexes undergo both spectroscopic and solubility changes. In general, the complexes are insoluble in most organic solvents and water. However, stirring suspensions of the complexes in acetonitrile in the presence of

two or more equivalents of H_2O_2 leads to homogeneous solutions within 1-10 minutes. This process was monitored by UV-Vis spectroscopy.

Table 4-1 shows experiments with copper complexes of ligand B with different stoichiometries of hydrogen peroxide. Entry 1 shows the results from the control experiment which showed 15% conversion 2 hours in presence of only copper nitrate. No selectivity between cyclohexanol and cyclohexanone was observed in this experiment. Entires 2-4 show effect of using variable amounts of hydrogen peroxide. Increasing the molar equivalence of hydrogen peroxide to 5 with respect to cyclohexane (entry 3), resulted in increased conversion to oxidation product (65%) with loss of selectivity (A:K = 1.22). Upon reducing the molar equivalence to 1, the conversion to oxidation products decreased to 22% (entry 4) but no increase in selectivity was observed compared to entry 2. Based on these observations a molar ratio of 2 [$n(H_2O_2)_2$/n(CyH)]**,** was deemed optimal. The last entry shows the effect on conversion to oxidation products when copper (II) chloride was substituted for copper (II) nitrate in the complexation reaction with ligand B (entry 5). Comparison of entries 2 and 5 clearly shows that the activity decreases almost by factor of 2 when copper (II) chloride is used. Thus, copper (II) nitrate was used in the rest of the experiments.

Table 4-1 – Effect of $n(H_2O_2)_2$/n(CyH) on catalytic activity

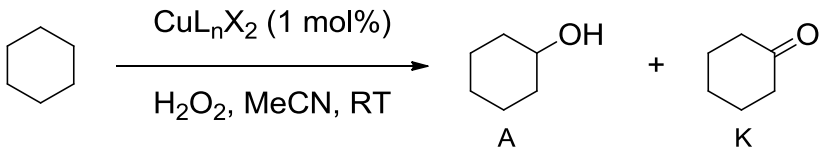

Entry[a]	Copper Salt	Ligand	*n*(H_2O_2)/ *n*(CyH)	Time (h)	Conversion (%)	Major products (%)	A:K
1	Copper (II) Nitrate	None (Control)	2	2	15	A (50), K (50)	1.00
2	Copper (II) Nitrate	B	2	2	50	A (71), K (29)	2.45
3	Copper (II) Nitrate	B	5	2	65	A (55), K (45)	1.22
4	Copper (II) Nitrate	B	1	2	22	A (60), K (40)	1.50
5	Copper (II) Chloride	B	2	2	28	A (70), K (30)	2.33

a) Data represent the averages of reactions in triplicate after quenching with PPh_3

The next series of experiments were designed the test the ligand scope. Complexes of ligands A through D with copper (II) nitrate were tested for the catalytic activity with cyclohexane. **Table 4-2** details the observations from these experiments. The highest

activity is observed for ligand C for both 1 hour and 4 hour timepoints (46% and 65% conversion, respectively), closely followed by ligand D (38% and 51%).

Table 4-2 – Ligand scope with cyclohexane

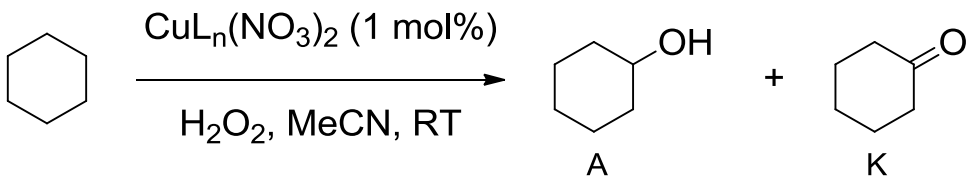

Entry [a]	Ligand[b]	*n*(H_2O_2)/ *n*(CyH)	Time (h)	Conversion (%)	Major products (%)	A:K
1	B	2	1	31	A (71), K (29)	2.45
2	A	2	1	0	Nil	Nil
3	C	2	1	46	A (89), K (11)	8.09
4	D	2	1	38	A (94), K (6)	15.67
5	B	2	4	44	A (70), K (30)	2.33
6	C	2	4	65	A (87), K (13)	6.69
7	D	2	4	51	A (92), K (8)	11.50
8	D	2	0.5	26	A (97), K (3)	32.33
9	D	5	1	42	A (89), K (11)	8.09

a) Data represent the averages of reactions in triplicate after quenching with PPh_3.

b) CyOOH formation for 4-sub complexes was significantly higher (CyOH ca. 4 times higher) than for 3,4,5-trisub (ca. 2x) and fused (ca. 1.2-1.4x) complexes.

However, much higher selectivity towards cyclohexanol formation is seen in the case of ligand D. Ligands C and D show a greater than five fold preference towards cyclohexanol formation. The selectivity factor slowly decreases over the time. The best selectivity is observed in the case of ligand D at the 0.5 hour timepoint (97% cyclohexanol). Increasing the amount of oxidant (hydrogen peroxide) also has adverse effect on the selectivity (entry 9). Finally, the ligand A does not show any activity.

Next, we extended the scope of our study to the oxidation of adamantane. Adamantane offers more insight into the selectivity afforded by each catalyst than cyclohexane as it contains multiple tertiary positions. As adamantine is a highly symmetrical molecule there are only two possible sites of oxidation, making this system much easier to study than other more complex molecules. **Table 4-3** shows the results from screening of all four ligands for adamantane oxidation. It can be seen that the regioselectivity trend follows ordering of cyclohexane selectivity, with the 1-ol product being formed in the highest quantity for all the ligands. The ligand D again shows the highest selectivity while the ligand A failed to show any activity. Ligand D also showed the highest activity slightly bucking the activity trend seen in the case of cyclohexane oxidation. The activities for ligands C and D are intermediate between tBuO· and some metalloenzymes (e.g. cytochrome P450). Non-selective oxidants such as HO· typically give 3°/2° ratios of 2, whereas milder oxidants such as tBuO· values of 10 are commonly observed. Metalloenzymes such as cytochrome P450 are highly regioselective, with ratios close to 50[157].

Table 4-3 – Ligand scope with adamantane

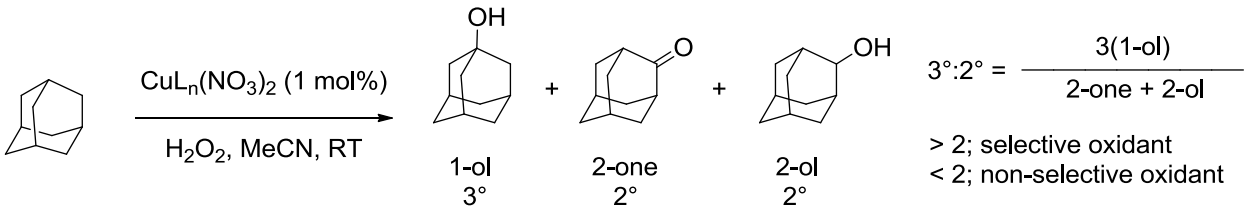

Entry	Ligand	1-ol (%)	2-one (%)	2-ol (%)	3°:2°
1	B	11	5	3	4.1
2	A	--	--	--	--
3	C	13	2	2	9.8
4	D	16	1	2	16

a) Data represent the averages of reactions in triplicate after quenching with PPh_3.

Finally we tested the silica supported 1,2,4-triazole ligands to explore the possibility of extending the practicality of this catalytic system. **Table 4-4** lists the results from experiments with silica supported complexes (synthesized as described in chapter 3). As can be seen from the table, silica supported triazoles show considerably lower activity than their homogeneous counterparts. 3,5-substitution fails to show any activity (3.15-3.16). This is consistent with the results seen for ligand A. The length of the linker does not seem to impact the activity (entries 1 and 2). Overall selectivity factors observed were equal or lower than 2 for all silica supported ligands. We attributed the lack of activity in the silica supported catalysts to lower loading of the triazole ligands. Use of more uniform silica, such as mesoporous silica may allow for higher loading of

catalyst and in turn lead to higher activities as well as more pronounced effect of ligand structure on selectivity.

One more important observation from these experiments was that the capped silica complexes (chapter 3) did not show any activity in oxidation when used as catalysts. This suggeste that the oxygen groups present on the silica surface are necessary for the formation of optimal catalytic complex.

Table 4-4 – Screening of silica supported triazoles

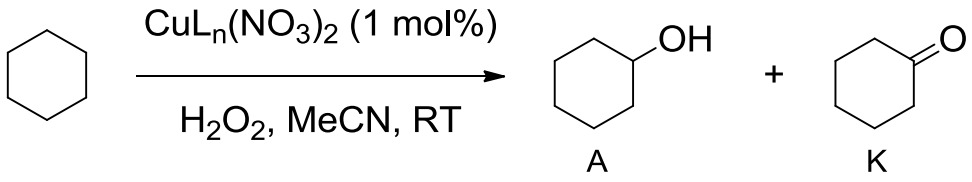

Entry [a]	Ligand[b]	*n*(H_2O_2)/ *n*(CyH)	Time (h)	Conversion (%)	A:K
1	3.8	2	1	28	2.1
2	3.9	2	1	27	1.9
3	3.10	2	1	29	2.2
4	3.14	2	1	Nil	Nil
5	3.15	2	1	Nil	Nil
6	3.16	2	1	Nil	Nil
7	3.17	2	1	24	1.7
8	3.18	2	1	29	1.9

a) Data represent the averages of reactions in triplicate after quenching with PPh_3.

4.3. ESI-MS studies on copper-1,2,4-triazole complexes

Approximately 1 mg of the in situ generated copper complex was added to 1 mL of acetonitrile and the vial was sonicated for 15 minutes. The supernatant was then transferred to a 2 mL Eppendorf tube that was centrifuged at 3300 rpm for 5 minutes. A sample of each copper complex was then injected into the Applied Biosystems QSTAR XL Hybrid LC/MS/MS hybrid quadrupole time of flight (QTOF) mass spectrometer using acetonitrile as the mobile phase. ESI-MS data suggest that for ligands A, B, and C the following species were present in solution: $[CuL_2]^+$, $[CuL_2]^{2+}$ and $[CuL]^+$ consistent with related literature examples **(Table 4-5)**[158].

Table 4-5 - ESI-MS data and some physical characteristics of the copper complexes.

Complex	**Cu-A**	**Cu-B**	**Cu-C**
Observed masses (*m/z*)	381.1, 222.8, 190.6	562.2, 312.7, 280.3	741.21, 402.17
Colour	pale blue	emerald green	lime green

4.4. Radical trap studies

Radical traps can be used in the oxidation reaction to better elucidate the possible mechanisms operating in the reaction[159-160]. Based on the prior reports, we employed three different radical traps and tested them for the ligands B,C and D. $CBrCl_3$ which is a carbon centered radical trap was used to probe intermediacy of cyclohexyl radical. Additionally, oxygen centered radical trap, $HNPh_2$ was used to assess the extent of HO· in oxidation. BHT which is both a carbon- and oxygen-centered radical trap was also

used. **Table 4-6** shows the extent of suppression of cyclohexane oxidation products in presence of each radical trap.

Table 4-6 - Radical trap experiments on cyclohexane oxidation reaction

Ligand	No trap (%)[a]	$CBrCl_3$ (%)[a,b]	$HNPh_2$ (%)[a,c]	BHT (%)[a,d]
B	31	<1	4	3
C	46	<1	7	4
D	38	3	24	11

a) total conversion of cyclohexane to oxidation products (cyclohexanol and cyclohexanone) b) $CBrCl_3$ was 5 eq. w.r.t. to substrate) c) $HNPh_2$ was 3 eq. w.r.t. to substrate d) BHT was 2.5 eq. w.r.t. to substrate

Products formation is suppressed to a large extent in presence of all three radical traps for complexes formed with ligands B and C. On the other hand complexes formed from fused-type ligand do not exhibit significant suppression in the presence of oxygen-centered radical trap; however their activity is suppressed in the presence of $CBrCl_3$. This is a possible evidence that a mixed mechanism of HO· (radical) and metal-based oxidant is operating in case of complexes formed from ligand D.

4.5. UV-Vis Experiments

Ligand field spectroscopy was carried out on the complexes to better understand the nature of the intermediates formed during catalysis of oxidation reactions. **Figure 4-2** shows the reprentative example UV-Vis studies on complexation reactions between copper and 1,2,4-triazoles.

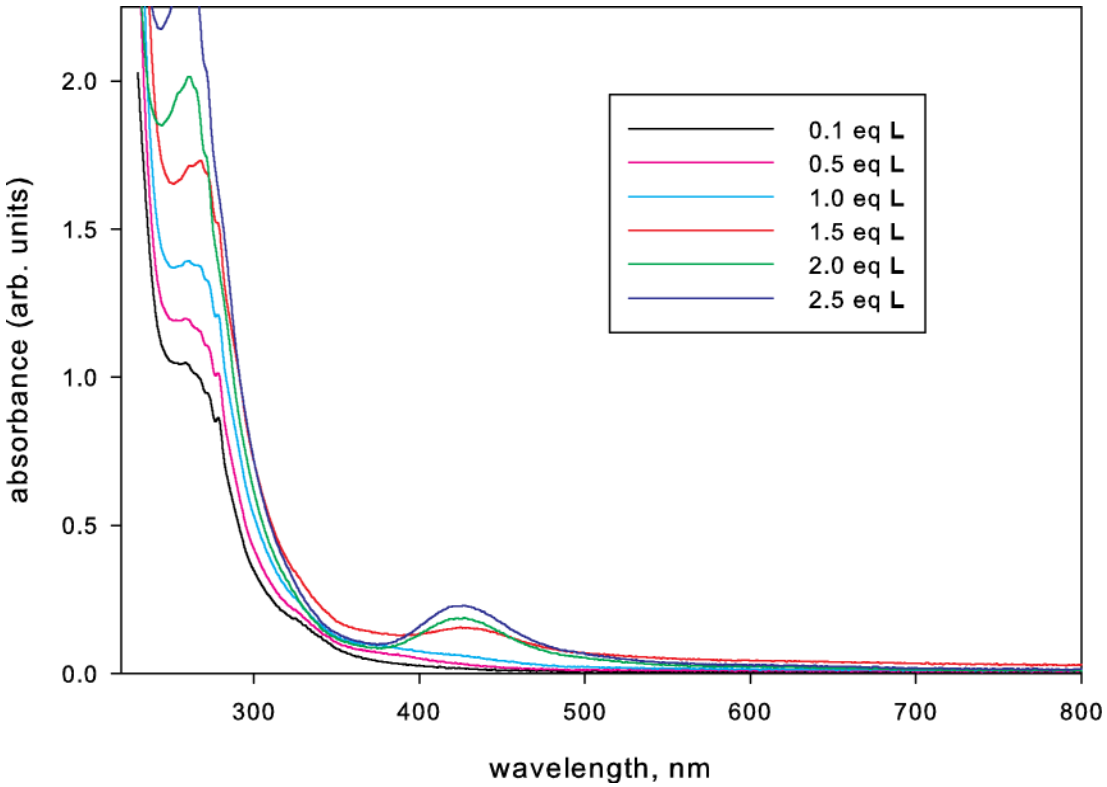

Figure 4-2 - UV-Vis titration of $Cu(NO_3)_2 \cdot 2.5H_2O$ complexed with ligand B.

Similar results were observed for the complexes with other ligands. Overall, the results from UV-Vis studies suggest that both 1:1 and 1:2 complexes (metal:ligand) are formed.

UV-Vis titrations of the reaction of an isolated complex of $Cu(NO_3)_2 \cdot 2.5H_2O$ and ligand **C** with H_2O_2 and then subsequently with cyclohexane were carried out . This experiment was performed in order to understand the effect of the oxidant as well as the substrate on the catalyst. Molar equivalents were determined by assuming an empirical formula of $Cu\mathbf{C}_2(NO_3)_2$ and each UV-Vis spectrum was recorded after a period of 15 minutes. **Figure 4-3** shows the UV-Vis spectra for titration of H_2O_2 with complex $Cu\text{-}\mathbf{C}_2(NO_3)_2$ in acetonitrile. As can be seen from the figure, a new absorption band around

410 nm can be seen with the incremental addition of hydrogen peroxide, indicating formation of new catalytic species.

Figure 4-4 shows UV-Vis spectra for subsequent titration of cyclohexane with complex Cu-$\mathbf{C}_2(NO_3)_2$ in acetonitrile.

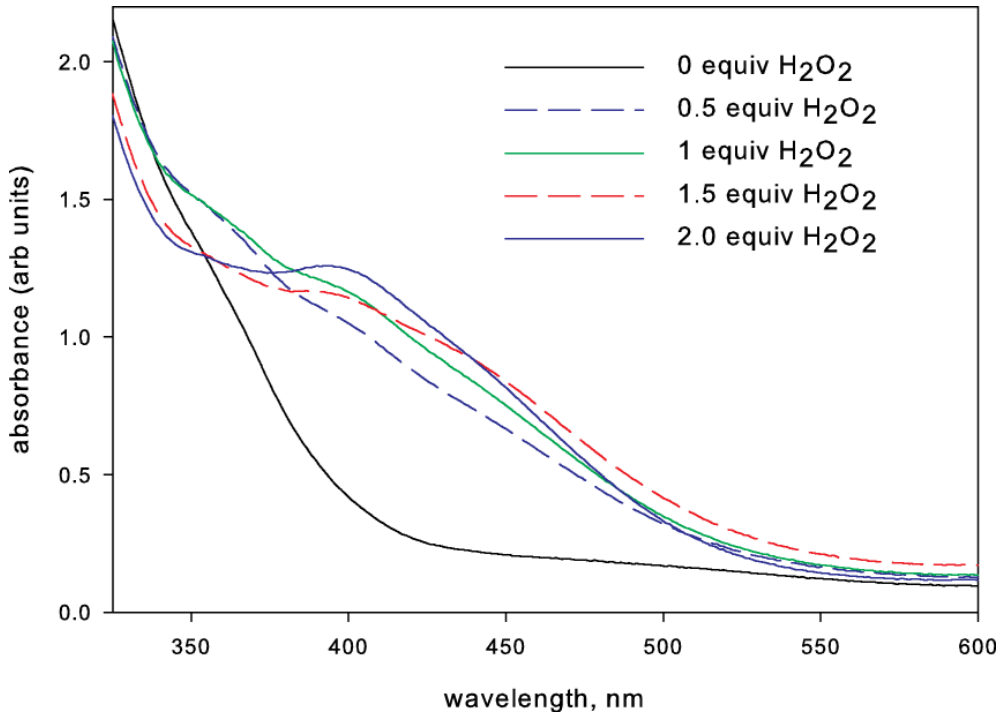

Figure 4-3 - Room temperature UV-Vis spectra for titration of H_2O_2 with complex Cu-$C_2(NO_3)_2$ in acetonitrile. The number of equivalents of H_2O_2 is with respect to copper.

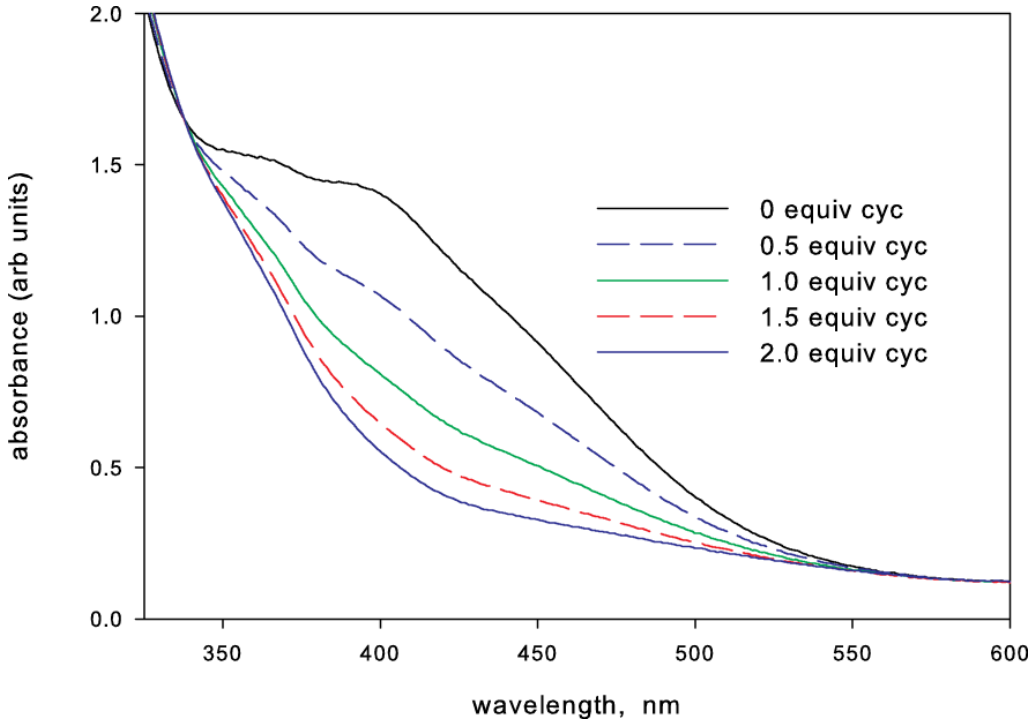

Figure 4-4 - Room temperature UV-Vis spectra for titration of cyclohexane with complex Cu-$C_2(NO_3)_2$ in acetonitrile. Equivalents of cyclohexane are with respect to copper.

As can be seen from the spectra, the absorption band at 410 nm begins to disappear after incremental addition of cyclohexane. The band completely disappears after addition of 2 equivalents of cyclohexane, indicating the regeneration of the original catalyst, i.e. before the addition of hydrogen peroxide.

The results from these UV-Vis studies point to the formation of new catalytic species coordinated with hydrogen peroxide, which in turn catalyzes the oxidation of cylcohexane and is regenerated in the process.

It is possible that there exist competitive non-radical pathways and two likely mechanisms that may be operational. The first is an electrophilic attack by a metal peroxo or oxo species to an alkane C-H followed by heterolytic cleavage of the C-H

bond to give an organocopper intermediate. Hydrogen atom abstraction from the substrate by the oxo group and subsequent oxygen rebound between the generated intermediates and cyclohexyl radical in a solvent cage gives a (μ-OH) (μ-OR)dicopper(II) intermediate, from which the alcohol product is released and bis(μ-oxo)dicopper(III) intermediate is regenerated by the reaction with another molecule of H_2O_2, completing the catalytic cycle. Alternatively, a concerted mechanism involving a direct insertion of an activated electrophilic oxygen atom, for example, a bridging oxygen atom, into an alkane C-H bond or through a pairwise process with C-H addition to two oxygen-atoms, as suggested for biological alkane hydroxylation by pMMO. These mechanisms are summarized in **figure 4-5**.

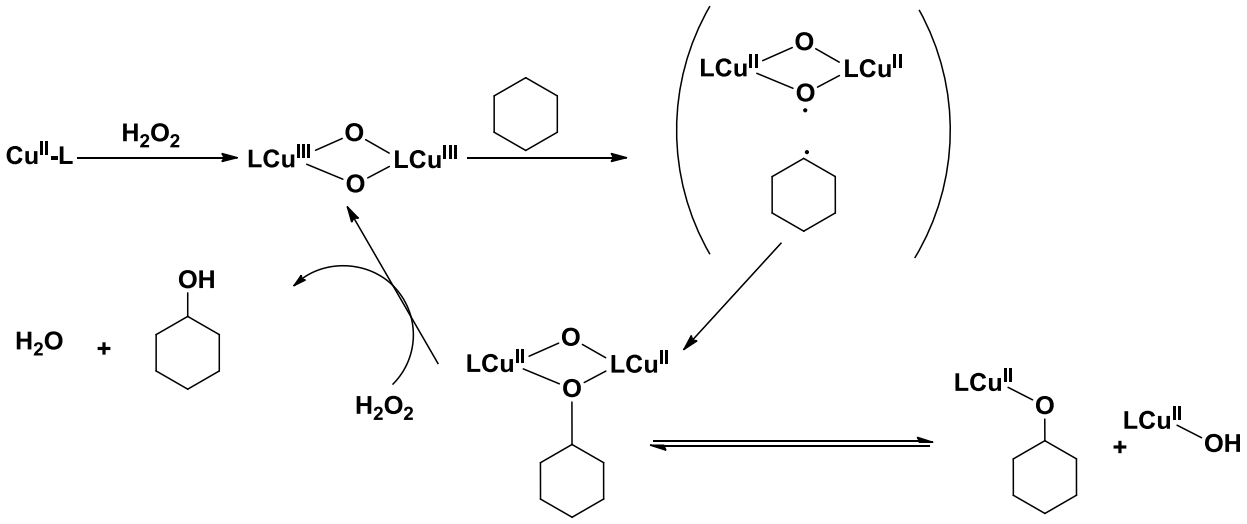

Figure 4-5 – Possible mechanism for copper-1,2,4-triazole catalyzed oxidation reaction

4.6. Conclusions

This chapter reports an efficient Copper-1,2,4-triazole based catalytic system. This system shows excellent activity along with remarkable selectivity towards the

oxidation of hydrocarbons. The results from screening reaction carried out on the model systems (adamantane and cyclohexane) show the potential of these catalysts for methane oxidation. Among the different 1,2,4-triazole ligands studied, 3,4,5-trisubstituted ligands were found to have most activity while the fused type ligands showed the highest selectivity. Silica supported 1,2,4-triazole complexes were also tested but failed to show comparable activity. Their activity could potentially be improved through use of mesoporous silica. ESI-MS characterization of complexes pointed to the possibility of presence of metal organic framework (MOF).

Finally, radical trap studies coupled with UV-Vis studies on active catalytic species provided important clues on the possible mechanism of the oxidation reaction.

4.7. Experimental

Materials and General Information

Reagents and solvents were purchased from various commercial sources and used without further purification unless otherwise stated. Analytical thin-layer chromatography (TLC) was performed using aluminum backed silica gel TLC plates with UV indicator from Sorbent Technologies. Flash column chromatography was performed using 40-63 μm (230 x 400 mesh) silica gel from Sorbent Technologies. ^{1}H and ^{13}C NMR were recorded at 500 MHz and 126 MHz, respectfully, on a Varian Inova spectrometer. All chemical shifts were reported in δ units relative to tetramethylsilane for the corresponding deuterated solvent. High-resolution mass spectra (ESI) were obtained on a JEOL AccuTOF DART spectrometer. Liquid chromatography mass spectra were

obtained on a QSTAR XL Hybrid LC/MS/MS equipped with a Vydac C18 column and a mobile phase composed of acetonitrile. Infrared spectra were recorded on a Varian 4100 FT-IR using KBr pellets or KBr salt plates. Absorption spectra were collected on a Thermo Scientific Evolution 600. Gas chromatography-mass spectrometry (GC-MS) data were collected on an HP/Agilent 6890GC/5973MSD spectrometer equipped with a HP-5ms (5%-Phenyl)-methylpoly-siloxane column. GC-MS methods and retention times have been provided below.

Synthesis and Characterization

Synthesis of Ligands

Ligands A through D were synthesized as described in Chapter 2.

Synthesis of In Situ Generated Copper Complexes

Procedure A

The same procedure was used to prepare copper complexes of ligands 1-3. 20 μmol of ligand was added to 150 μL of tetrahydrofuran in a 7 mL scintillation vial and the suspension was stirred at 60 °C. A 0.200 M solution of $Cu(NO_3)_2 \cdot 2.5H_2O$ in tetrahydrofuran (10 μmol, 50 μL) was then added to the mixture. The vial was sealed and the mixture was allowed to stir for 12 hours at 60 °C. The tetrahydrofuran was removed in vacuo and the remaining solid was used without further purification in the catalytic screening reactions.

Procedure B

The same procedure was used to prepare copper complexes of ligands 1-3. 20 μmol of ligand was added to 150 μL of acetonitrile in a 7 mL scintillation vial and the suspension was stirred at 60 °C. A 0.200 M solution of $Cu(NO_3)_2 \cdot 2.5H_2O$ in acetonitrile (10 μmol, 50 μL) was then added to the mixture. The vial was sealed and the mixture was allowed to stir for 12 hours at 60 °C. The reaction mixture was allowed to cool to room temperature and was diluted with additional acetonitrile as prescribed below.

Catalytic Screening

Cyclohexane Oxidation

The reaction of the in situ generated catalyst and methane was conducted in a 7 mL scintillation vial equipped with a Teflon coated stir bar. The catalysts used in the cyclohexane oxidation studies were prepared by Procedure B from above. To the solid that remained after in vacuo removal of tetrahydrofuran was added 2.50 mL of acetonitrile followed by addition of a 0.23 mL – 1.13 mL (2 mmol – 5 mmol) of a 30% (v/v) solution of H_2O_2. A gas-tight microsyringe was then used to add cyclohexane (54 μL, 0.50 mmol) to the reaction mixture and a poly-sealed lined vial cap was affixed to the reaction assembly. Unless otherwise noted, after 2 hours the reaction mixture was then transferred to a 15 mL Falcon™ conical tube containing 63 mg (0.50 mmol) of cyclooctanone (internal standard), diluted to a total volume of 10 mL by addition of diethyl ether, and centrifuged at 3300 rpm for 10 minutes. A 1 mL aliquot of the reaction mixture was removed and added to a 7 mL scintillation vial equipped with a Teflon coated stir bar from which a 1 μL was extracted using a gas-tight microsyringe, which was then injected into the GC-MS. To the vial containing ~10% of the original reaction

mixture was added excess (13.2 mg, 0.25 mmol) triphenylphosphine (PPh_3) and that solution was allowed to stir at room temperature for 20 minutes. After that time, 1 µL was extracted using a gas-tight microsyringe that was then injected into the GC-MS. PPh_3 acts to reduce any cyclohexyl hydroperoxide to cyclohexanol. The conversions to cyclohexanol shown in Table 2 correspond to GC-MS analysis after reduction by PPh_3. The integrated areas of the cyclohexanol and cyclohexanone peaks were then used to determine the % conversions from the catalyst screening reaction by comparison to a calibration curve generated by GC-MS analysis of 1 µL aliquots of ethereal solutions of varying concentrations of cyclohexanol and cyclohexanone and comparisons to ratios of integrated areas of the internal standard (cyclooctanone) as shown below. Experiments were repeated in triplicate and the values shown in Table 2 correspond to those averages. Method: 2 minutes at 40 °C, ramp at 15 °C/min to 150 °C, ramp at 35 °C/min to 250 °C with a 5 minute hold. In the table below, A represents the integrated area of the peak.

Table S1. GC-MS parameters for the cyclohexane oxidation studies. The concentration multiplicative factors were derived from the calibration curves shown in Figures S1-S4

	cyclohexane	**cyclohexanol**	**cyclohexanone**	**cyclooctanone**
t_R (minutes)	2.91	5.79	5.94	8.70
R^2	0.9985	0.9830	0.9905	0.9979
concentration, mM	$2.642 \times 10^{-8} \times A$	$1.869 \times 10^{-8} \times A$	$1.726 \times 10^{-8} \times A$	$1.703 \times 10^{-8} \times A$

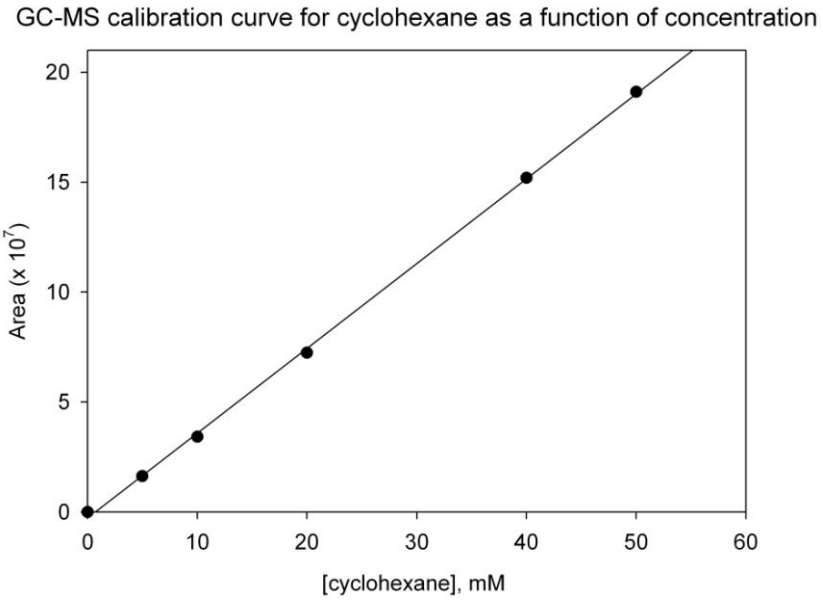

Figure S1. GC-MS calibration curve for peak area versus cyclohexane concentration.

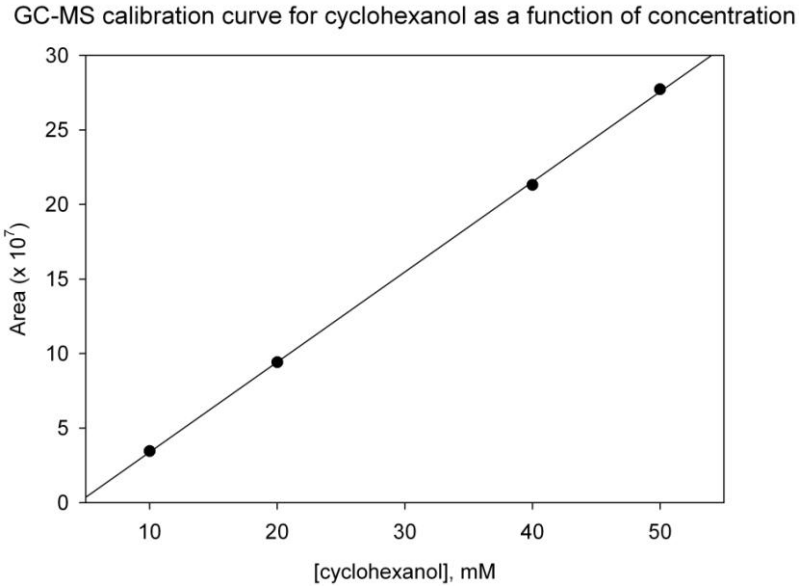

Figure S2. GC-MS calibration curve for peak area versus cyclohexanol concentration.

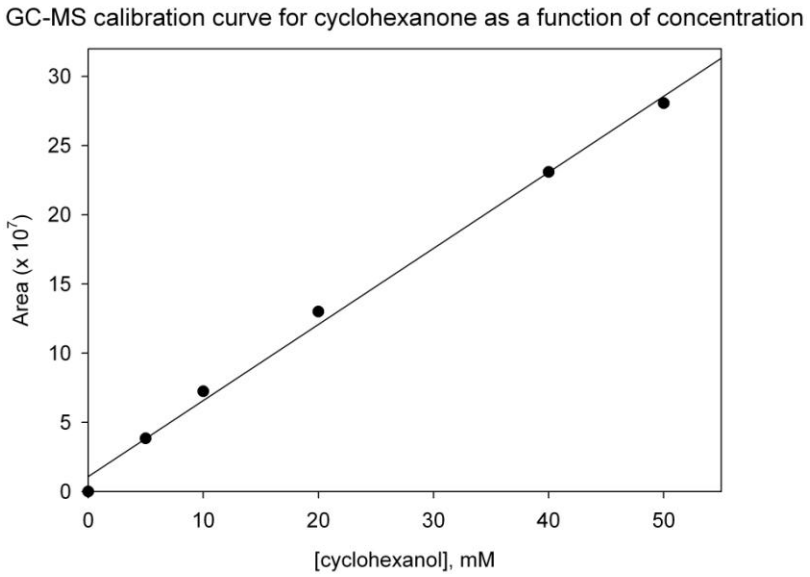

Figure S3. GC-MS calibration curve for peak area versus cyclohexanone concentration.

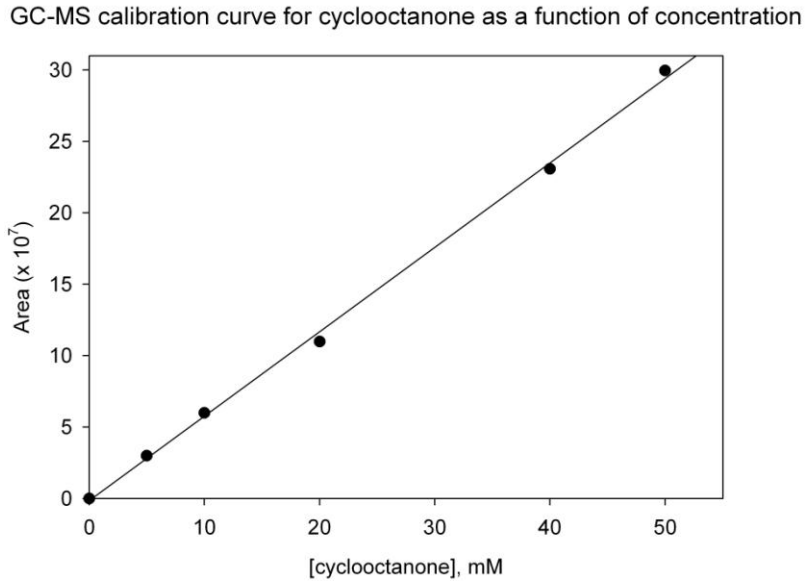

Figure S4. GC-MS calibration curve for peak area versus cyclooctanone concentration.

Adamantane Oxidation

The reaction of the in situ generated catalyst and adamantane was conducted in a 7 mL scintillation vial equipped with a Teflon coated stir bar. To the solid that remained after in vacuo removal of tetrahydrofuran was added 2.50 mL of acetonitrile followed by addition of 0.23 mL (2 mmol) of a 30% (v/v) solution of H_2O_2. Adamantane (27 mg, 0.20 mmol) was added to the reaction mixture and a poly-sealed lined vial cap was affixed to the reaction assembly. The reaction mixture was stirred for 2 hours and was then transferred to a 15 mL Falcon^{TM} conical tube, diluted to a total volume of 10 mL by addition of diethyl ether, and centrifuged at 3300 rpm for 10 minutes. A 1 mL aliquot of the reaction mixture was removed and added to a 7 mL scintillation vial equipped with a teflon coated stir bar and 8 mg of PPh_3. This mixture was stirred for 20 minutes after which a 1 µL aliquot was extracted using a gas-tight microsyringe, which was then injected into the GC-MS. The same GC-MS method used for cyclohexane was used for the adamantane studies. Values reported correspond to the ratio of the weighted sum of 3° oxidation products formed (1-adamantanol) to the 2° oxidation products formed (2-adamantanol + 2-adamantanone), i.e. 3(area of 1-adamantanol)/(area of 2-adamantanol + area of 2-adamantanone).

Table S2. GC-MS parameters for the adamantane oxidation studies.

	adamantane	**1-adamantanol**	**2-adamantanol**	**2-adamantone**
t_R (minutes)	9.73	10.65	11.48	11.73

Radical Trapping Experiments

The procedure for the radical trapping experiments is based upon a previous studies[159-160]. The reaction of the in situ generated catalyst and methane was conducted in a 7 mL scintillation vial equipped with a Teflon coated stir bar. The catalysts used in the studying the effect of radical traps on cyclohexane oxidation were prepared by Procedure A from above. To the solid that remained after in vacuo removal of tetrahydrofuran was added 2.50 mL of acetonitrile followed by addition of 0.29 mL (2.5 mmol) of a 30% (v/v) solution of H_2O_2. For each of the following: $CBrCl_3$, (2,2,6,6-tetramethylpiperidin-1-yl) oxyl (TEMPO), and diphenylamine ($HNPh_2$) 2.5 molar equivalents with respect to cyclohexane was then added to the reaction mixture. A gas-tight microsyringe was then used to add cyclohexane (54 µL, 0.50 mmol) to the reaction mixture and a poly-sealed lined vial cap was affixed to the reaction assembly. After 2 hours the reaction mixture was then transferred to a 15 mL Falcon™ conical tube containing 63 mg (0.50 mmol) of cyclooctanone (internal standard), diluted to a total volume of 10 mL by addition of diethyl ether, and centrifuged at 3300 rpm for 10 minutes. A 1 mL aliquot of the reaction mixture was removed and added to a 7 mL scintillation vial equipped with a Teflon coated stir bar from which a 1 µL was extracted using a gas-tight microsyringe, which was then injected into the GC-MS. To the vial containing ~10% of the original reaction mixture was added excess (13.2 mg, 0.25 mmol) triphenylphosphine (PPh_3) and that solution was allowed to stir at room temperature for 20 minutes. After that time, 1 µL was extracted using a gas-tight microsyringe that was then injected into the GC-MS. The methodology developed above with the cyclohexane screening experiments was employed here.

UV-Vis Experiments

To stirred suspensions of ligand in tetrahydrofuran, aliquots of a 0.2M solution of $Cu(NO_3)_2 \cdot 2.5H_2O$ in tetrahydrofuran were added. The reaction mixtures were stirred at 60 °C for 12 hours and UV-Vis spectra were recorded.

NMR Experiments on Copper Complexes

^1H NMR spectra of the free ligand **C**, $Cu\mathbf{C}_2(NO_3)_2$, and the reaction of 10 µL (fivefold excess) of H_2O_2 with $Cu\mathbf{C}_2(NO_3)_2$ in CD_3CN and acetone-d_6 were obtained. Molar equivalents were determined by assuming an empirical formula of $CuL_2(NO_3)_2$. The corresponding tolyl protons along with analogous experiments that were conducted in DMSO-d_6 are shown below.

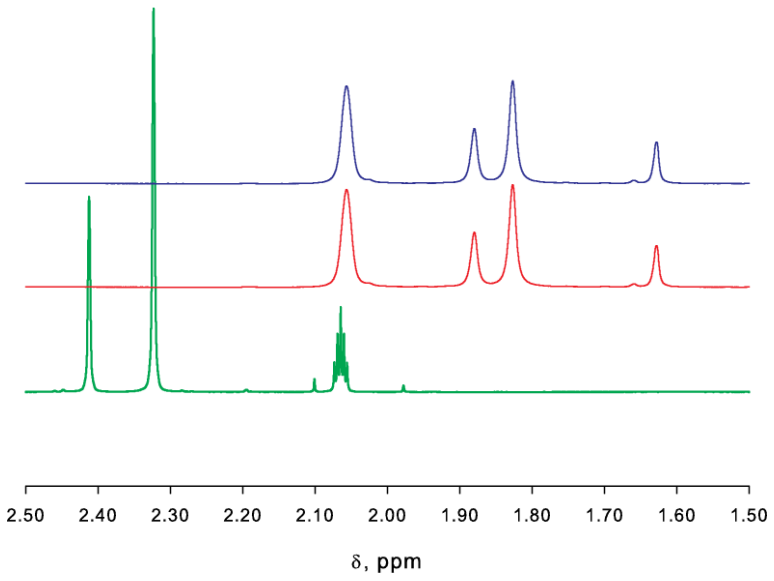

Figure S5. Zoom-in of ^1H NMR spectra of C (green), $Cu(NO_3)_2C_2$ (red), and $Cu(NO_3)_2C_2$ + 5 equivalents of H_2O_2 (blue) in acetone-d_6.

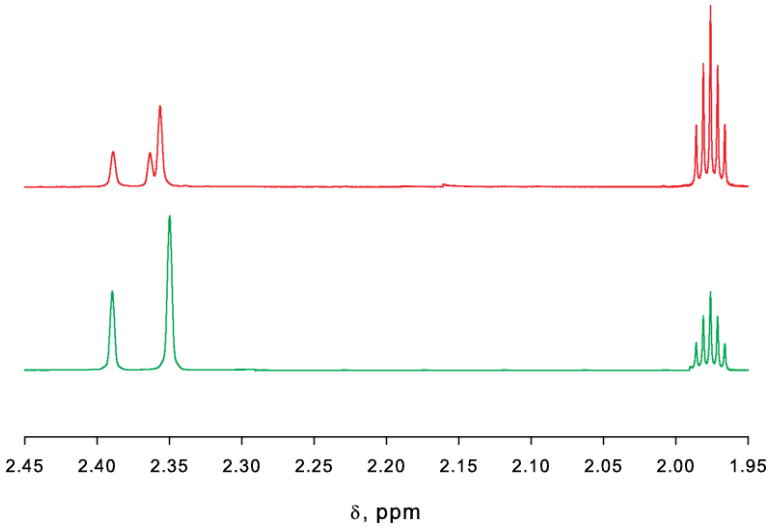

Figure S6. Zoom-in of ^{1}H NMR spectra of C (green) and $Cu(NO_3)_2C_2$ (red) in acetone-d_6. When H_2O_2 was added, the reaction mixture was NMR silent.

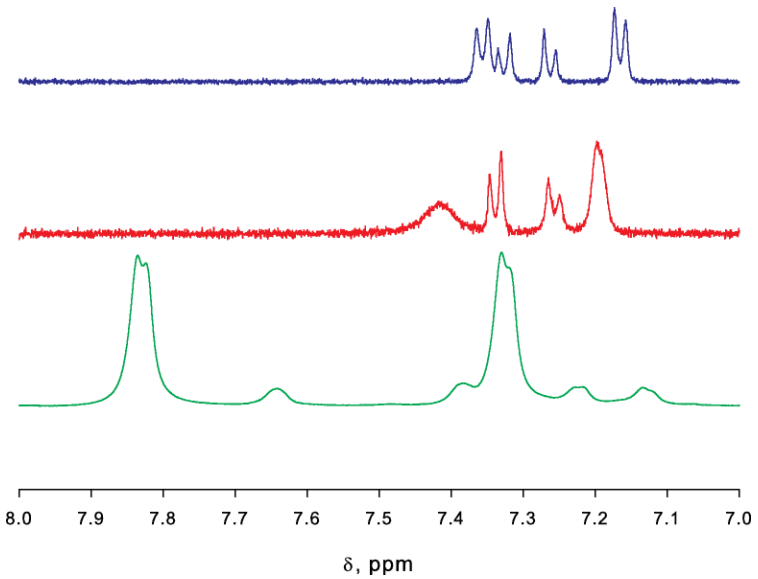

Figure S7. Zoom-in of aromatic region of ^{1}H NMR spectra of C (green), $Cu(NO_3)_2C_2$ (red), and $Cu(NO_3)_2C_2$ + 5 equivalents of H_2O_2 (blue) in DMSO-d_6.

5. *Covalent modification of carbon black surfaces and their application in ORR catalysis*

5.1. Catalysis of ORR with transition metal-1,2,4-triazole complexes attached to carbon black surfaces

This chapter describes the synthetic approaches developed for immobilization of transition metal-1,2,4-triazole complexes on carbon black supports and their application in the catalysis of ORR in fuel cells.

Catalysis of oxygen reduction reactions is an important field of research that benefits from heterogeneous synthetic techniques. Fuel cells require catalysts at both the cathode and anode to carry out electrochemical oxidation and reduction reactions efficiently. The material used for the solid support usually tends to be carbon black owing to its high surface area.

This study was divided into two parts based on the nature of catalysts used. The first part involved studies on the adsorbed 1,2,4-triazole complexes, in order to identify the optimal conditions for carbon pretreatment and adsorption protocols as well as the most active 1,2,4-triazole derivatives and copper salts. The second part of this study focused on the 1,2,4-triazoles covalently immobilized on the carbon black supports in order to impart higher stability to the catalytic system. Transition metals complexes of these triazoles, prepared using metals such as Co, Ni, Fe and Mn, were also tested during this phase of the research. Additionally, pyrolysis of the prepared materials was carried out to gauge the effects of the heat treatments. Throughout the course of this

project, constant refinements were made in order to achieve the best combination of synthetic techniques, choice of 1,2,4-triazole ligand, choice of metal and metal salts, and choice of the carbon black support. We followed the principle of 'single variable change at a time'. This helped us precisely attribute the changes in the observed activity to the corresponding variable.

The goals of this project were twofold**:** 1) - To better understand the nature of the catalytic center compared to catalysts prepared using pyrolysis. This can be achieved by extending the previous studies of transition metal 1,2,4-triazole complexes to take advantage of the presence of relatively well defined structures for insight into the influence of structure on mechanism. 2) To, utilize the insights gained from the first goal to develop catalysts that can match the performance of the PGM catalysts. The next few sections discuss the efforts made towards achieving these goals.

5.2. Carbon black supported ligands

A few important characteristics of a catalyst are its chemical composition, surface area, stability and mechanical properties. The advantage of spreading the active phase on a support is to disperse it throughout the pore system, thus making it possible to obtain a large active surface per unit weight used. Carbon black supports excel in this category. Other advantages of using carbon black as the scaffold are its resistance to acidic and basic media, as well as its thermal stability and excellent economic viability [161]. Platinum catalysts, which are traditionally used at the cathode in ORR, are supported by carbon blacks **(Figure 5-1)** [162].

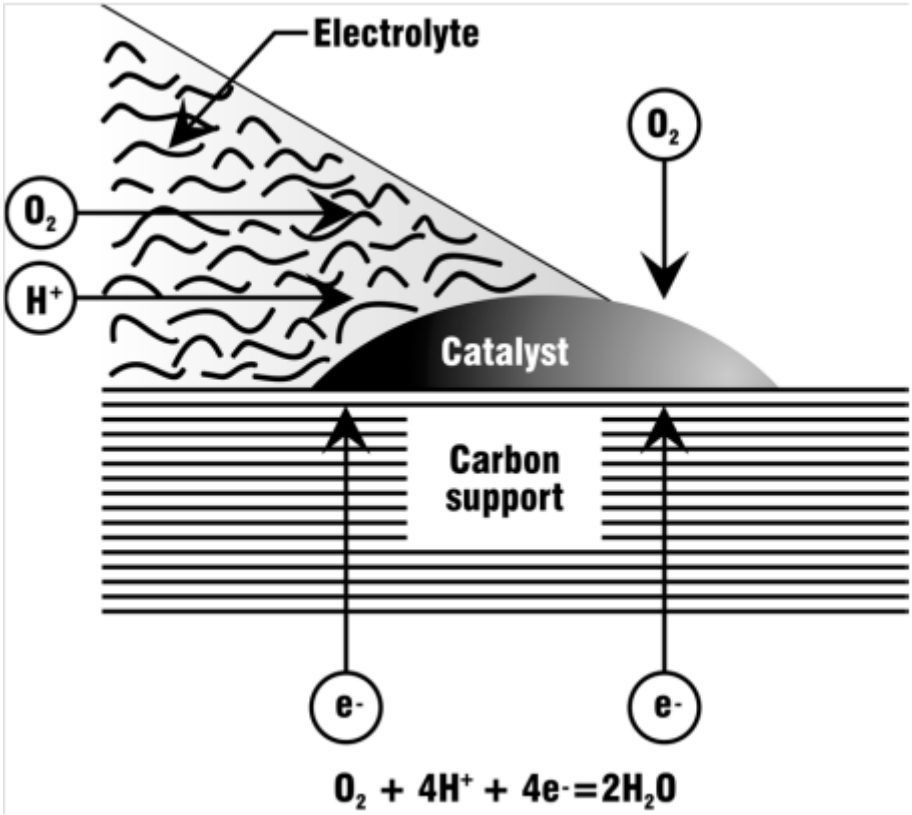

Figure 5-1 - Carbon supported Pt catalysts

Carbon black is a material produced by the incomplete combustion of heavy petroleum products such as tar, ethylene cracking tar, and a small amount from vegetable oil[163]. All carbon blacks have chemisorbed oxygen containing functional groups (i.e., carboxylic, quinonic, lactonic, phenolic and other similar functional groups) on their surfaces to varying degrees depending on the manufacturing conditions. These surface oxygen groups are collectively referred to as “volatile content”. Due to the presence of volatile content, carbon black is a non conductive material. The rest of carbon black is made up of polycondensed aromatic rings[164-166]**.** Functionalizing the surface of carbon black is a very challenging task due to the diverse nature of the functional groups present on the surface. Two kinds of problems are inherent to

functionalization of carbon black surfaces. First is the lack of selectivity in the chemical transformations due to the presence of various functional groups that have similar reactivities, but result in the formation of different products. The second problem arises from the first one; the lack of selectivity directly results in lower efficacy of the intended chemical processes. **Figure 5-2** shows the type of functional groups that populate carbon black surfaces[167-172].

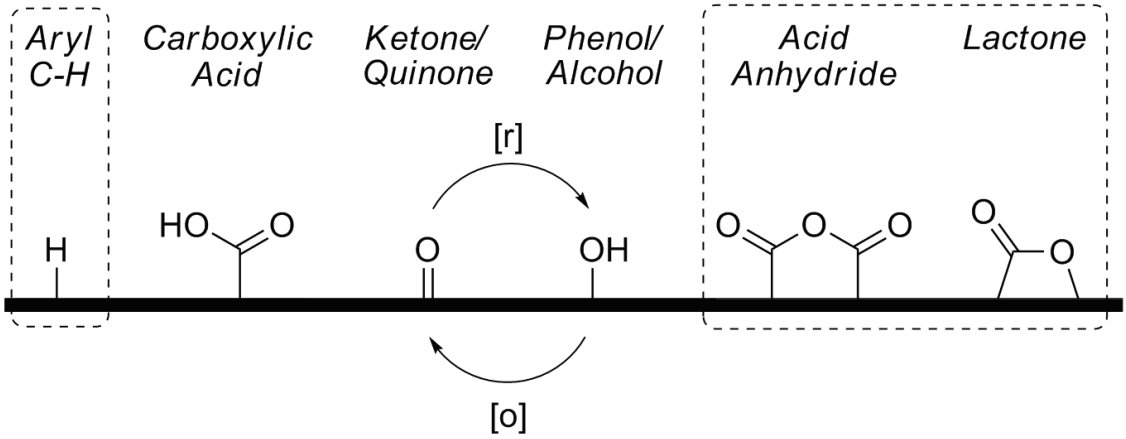

Figure 5-2 - Functional groups present on carbon black surfaces

Carbon surfaces can be functionalized utilizing two approaches, physisorption and chemisorption[164, 173-177]. Physisorption involves deposition of organic ligands on the carbon black surface through adsorption. This process does not involve formation of any kinds of covalent or ionic bonds. The organic ligands interact with the surface by the application of Van der Waal's forces. However Van der Waal's interactions are significantly weaker than the covalent interactions, thus often leading to stability issues. Covalent immobilization of organic ligands through chemisorption provides an answer to the stability problem **(Figure 5-3)**. Although chemical modification involves multiple

synthetic transformations, the payoff in the form of highly stable covalently functionalized carbon surfaces is worth the effort. Covalent attachment of ligands also allows complexation of metals in a separate step using a broader range of conditions as well as use of different metal salts. Preparation of complexes can be carried out without dependence of solubility for deposition when using chemisorption.

Two distinct approaches can be utilized for covalent immobilization of ligands; stepwise synthesis of ligands on carbon black or attachment of intact ligands onto functionalized carbon black **(Figure 5-4)**. The stepwise synthetic approach gives higher flexibility with the possibility of diversification at a later stage. Intact ligand immobilization approach on the other hand has more reliability since the target ligand can be pre-characterized in the solution phase.

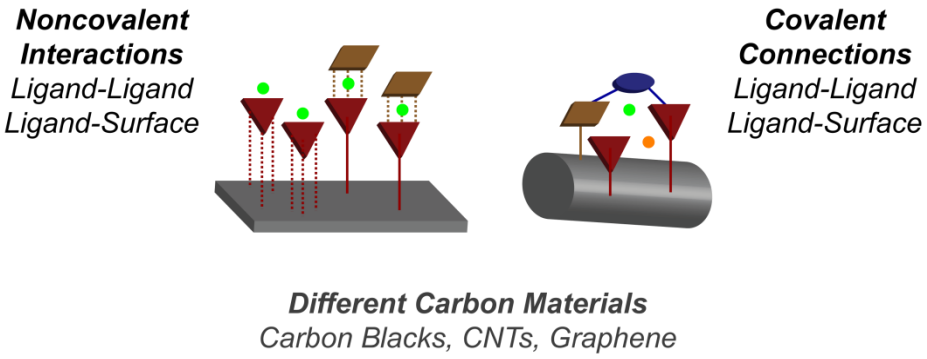

Figure 5-3 – Possible ligand interactions with carbon black surfaces (CNT – carbon nanotubes)

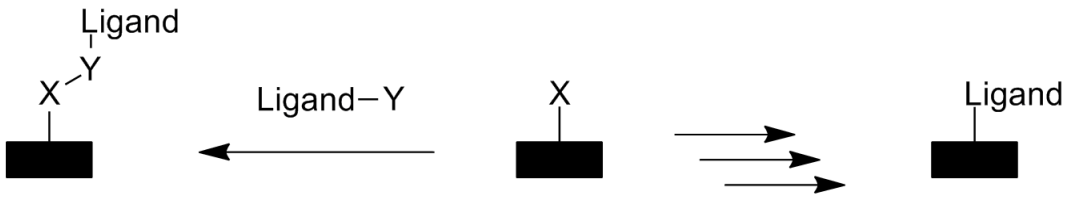

Figure 5-4 - Ligand immobilization approaches

Based on these theories, we decided to utilize both the adsorption and covalent approaches in a systematic manner. Physisorption would be first used to quickly test the ORR catalytic activity of the surface. The most active ligands from these studies would then be immobilized on the carbon surface via covalent bonding to increase the overall stability of the surface. Two types of commercially available carbon black surfaces were used throughout this study, Vulcan XC-72 and Black Pearls 2000 (BP-2K).

5.3. Electrochemical studies on copper-1,2,4-triazole complexes adsorbed on carbon black

Recent studies on adsorbed copper-3,5-diamino-1,2,4-triazole[178] and copper-phenanthroline[179] complexes have shown the potential of these materials as ORR catalysts for PEMFCs. Brushett et al[178] used rotating ring disk electrode (RRDE) experiments to characterize copper-3,5-diamino-1,2,4-triazole in a range of pHs from 2 to 13, finding the ORR catalytic activity substantially increases with the pH value. Based on this we synthesized 3,5-diamino-1,2,4-triazole, adsorbed on a carbon support for preliminary studies. These materials were characterized using rotating disk electrode (RDE) and RRDE experiments to determine onset potential, number of electrons transferred and some mechanistic aspects. Onset potential is defined as the the highest potential at which the catalyst starts displaying activity (marked by the rightmost point at

which the slope of the RDE curve changes to a non-zero value). Current density is defined as the highest absolute value for the RDE curve on the Y-axis (measured in mA/cm^2). The slope of the RDE curve indicates the kinetics of the ORR reaction. Higher slopes are observed for catalysts with better kinetics.

5.3.1. Electrochemical activity measurements

RDE and RRDE experiments: The RDE and RRDE experiments were carried out to determine the ORR activity and electron transfer mechanism of the Cu-based catalysts. To simulate the acidic environment of a PEMFC the samples were tested using 0.5 M sulfuric acid (H_2SO_4) electrolyte. A gold (Au) wire was used as the counter electrode, and Hg/Hg_2SO_4 reference electrode saturated with 0.5 M H_2SO_4. The working electrode was the glassy carbon (GC) disk of either a single piece RDE electrode AFE2M050GC or the RRDE with a Pt ring electrode AFE7R9GCPT from Pine Instruments. The potential of the reference electrode vs. RHE was measured experimentally saturating the electrolyte with hydrogen for at least 30 minutes and measuring the open circuit potential using the Pt ring on the RRDE electrode as the working electrode, and it was determined to be 0.696 V vs. RHE. All the potentials reported here are corrected to this value. The disk and ring working electrodes potentials were controlled using a two-channel VSP potentiostat from Bio-Logic Science Instruments. The rotation speed of the working electrode was controlled with an AFMSRCE Pine Modulated Speed Rotator (MSR). Inks were prepared using 5 wt% Nafion® solution (Sigma-Aldrich) in a 40/60 ionomer to catalyst ratio, with methanol as the solvent. The GC disk is polished with 0.05 µm size alumina powder. Approximately 15 µL of the sample is pipetted onto the GC electrode and the equivalent weight is determined by indirectly measuring the

weight of the same volume of ink. For these experiments we used catalyst loadings of 600 μg/cm^2. The electrolyte is initially saturated with ultrahigh purity nitrogen gas for at least 30 minutes and cyclic voltammograms are collected with the electrode static and rotating at 1600 rpm. The experiment is repeated with the electrolyte saturated in ultrahigh purity oxygen. Polarization curves are background corrected by subtracting the curves obtained under nitrogen. All experiments were done at room temperature.

5.4. Preliminary results

Figure 5-5 shows the preliminary cathodic scan RDE polarization curves obtained for adsorbed Cu-3,5-diamino-1,2,4-triazole complex. This sample exhibits an onset potential of approximately 0.4 V (compared to 0.9 V for commercial Pt/C electrode) and current density decays 10% after only three cycles. The number of electrons transferred was calculated keeping the ring electrode at a constant potential of 1.2 V during the RRDE experiment. The calculated values are in the 3.2 electrons range for potentials between -0.3 V to 0.4 V. To gain a better understanding of the behavior of the samples and to improve their performance, we designed a series of synthetic experiments.

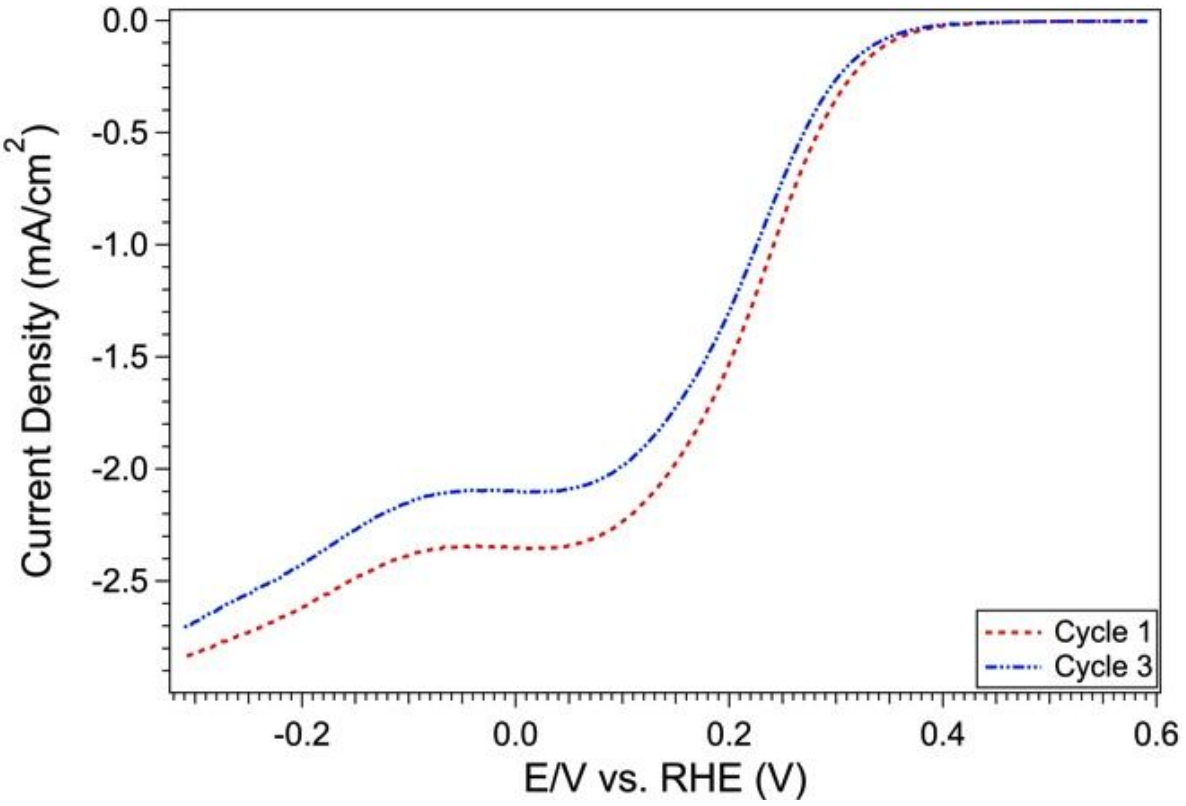

Figure 5-5 - RDE curves for adsorbed Cu-3,5-diamino-1,2,4-triazole complex.

5.5. Synthetic Toolbox for modification of carbon black surfaces

Based on the preliminary results, it was deemed necessary to carry out modifications of the surface in order to either increase the population of the reactive handles already present on the surface or to install new reactive handles. We designated this preliminary set of modifications as 'Primary Pool of Chemical Transformations'. We hoped that by carrying out these transformations we could at least partly overcome the selectivity issue. Another advantage offered by these transformations was ability to modify the surface in multiple diverging ways starting from a single carbon black support.

Depending on the chemistry utilized, it is possible to convert the carbon black surface into either an electrophile or a nucleophile. Oxidative treatments using strong acids or bases can lead to the increase in population of carbonyls and carboxylic acids on the surface making the surface much more electrophilic.[180] A similar effect can also be achieved via bromination of the surface. Nitration followed by reduction can lead to the installation of amine functional groups on the surface, making the surface nucleophilic[181-182]. A distinct approach can be adopted using diazonium chemistry. The aromatic groups on the surface are expected to be sufficiently nucleophilic to participate in a nucleophilic substitution reaction with diazonium species generated from substituted amines. A successful reaction of this kind would result in direct installation of the N-substituted group onto the carbon surface[179]. A reverse strategy can also be applied by diazotizing the amino modified surface and using it as the electrophilic component with a suitable nucleophile **(Figure 5-6)**.

Once the surface is appropriately conditioned, a secondary pool of chemical transformations can then be applied to generate a number of different 1,2,4-triazole ligands /complexes on the carbon black surface. Most of the synthetic routes described in the preceding chapter for synthesis of 1,2,4-triazoles can be utilized to achieve this.

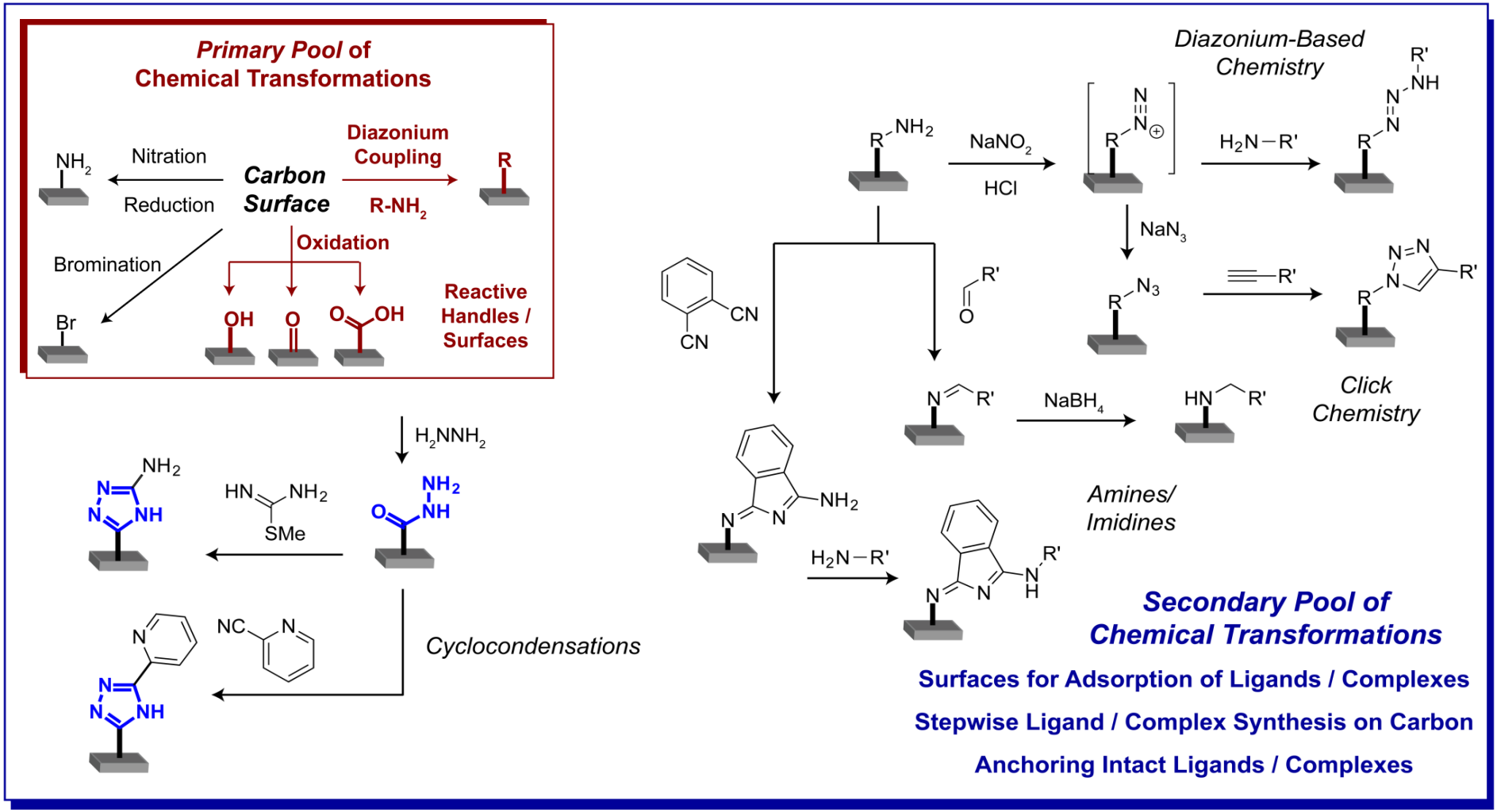

Figure 5-6 – Synthetic toolbox for modification of carbon black surfaces

5.5.1. Primary pool of chemical transformations

There are examples of 1,2,4-triazole-based MOFs containing mixed ligand sets or multiple metals[183]. In these cases, the overall macromolecular architecture created depends on the non-covalent interactions possible between different types of ligands as well as the different available modes of metal coordination. The loading levels of adsorbed complexes are controlled by non-covalent interactions between surface functional groups and ligands or complexes. In the context of 1,2,4- triazole complexes formed in the presence of carbon blacks, the chemical features of the carbon surfaces may function as co-ligands either by participation in metal coordination or by pre-organizing a network of ligands for metal binding[184]. The chemical oxidation of carbon blacks is a proven method for generating oxygen-containing functional groups and these types of surface modifications have shown promise in heterogeneous catalysts for ORR[185]. Cathodic fuel cell catalysts will experience strongly oxidizing conditions so this step also ensures that carbon surfaces are stable under RDE conditions.

For this experiment Vulcan XC-72 was oxidized using a variety of different reaction conditions. The secondary aim of this experiment was to generate a carbon surface decorated with carboxylic acid groups, which can be used as reactive handles to immobilize 1,2,4-triazoles through covalent binding. In order to estimate the extent of functionalization of carbon surface, we developed an assay using 1-napthyl amine. The idea behind this assay was to covalently attach 1-napthylamine to the surface carboxylic groups and then measure the remaining amount of 1-napthylamine in the supernatant to estimate the extent of functionalization. This approach was inspired by prior reports of FLOSS (fluorescence labeling of surface species) as a probe for chemical

composition[169]. Adsorbed copper complexes of 3,5-diamino,1,2,4-triazole were then prepared with each type of oxidized Vulcan XC-72. ICP results were obtained on the residual copper after complexation. These results are summarized in the **table 5-1**. Electrochemical experiments were carried out on the adsorbed complexes. RDE experiments on samples prepared using untreated Vulcan carbon showed that more that one mechanism could be occurring during the ORR. However, pretreatment of the carbon makes a great impact in the RDE performance, seen in **figure 5-7**. Both the onset potential and current density increases, with the oxidative carbon pretreatment **D** giving the best results, with an onset potential of 0.46 V.

Table 5-1 shows the results from loading assay, ICP experiments as well as RDE experiments. The onset potential for pretreated carbons increased across the board with the exception of entry E. The loading of the carbons also increased with the oxidative pretreatments as did the copper retention. However, while the copper retention and observed onset potential values are in good agreement with each other, the loading assay results are incongruous. The highest onset potential was observed for entry D, but the best calculated loading was observed for entry F. It must be noted that the loading assay was designed to assess the covalent binding ability of the pretreated carbons and not to identify the best surface for adsorption. Thus, carbon pretreatment D is most suitable for adsorption experiments while carbon pretreatment F is most suitable for covalent immobilization experiments.

Table 5-1 - Effects of oxidative treatments on copper retention and activity

Entry	Oxidative pre-treatment	Loading mmol/g	Copper retention % (ICP)	Onset Potential Vs. RHE (V)
-	None	2.36	33.7	0.41
A	10 mL 5M H_2SO_4, 100 °C, 17 h	4.16	36.3	0.45
B	5 mL 1M APS, 5 mL 5M H_2SO_4, 100 °C, 17 h	3.44	35.9	0.45
C	10 mL 5M HNO_3, 100 °C, 26 h	3.14	44.05	0.45
D	5 mL 30% H_2O_2, 5 mL 5M H_2SO_4, RT, 26 h	3.88	42.2	0.46
E	5 mL 5M H_2SO_4, 5 mL 5M HNO_3, 100 °C, 26 h	3.88	43.3	0.40
F	4 mL 5M H_2SO_4, 4 mL 5M $HClO_4$, 2 mL 30% H_2O_2, RT, 26 h	5.34	36.25	0.45

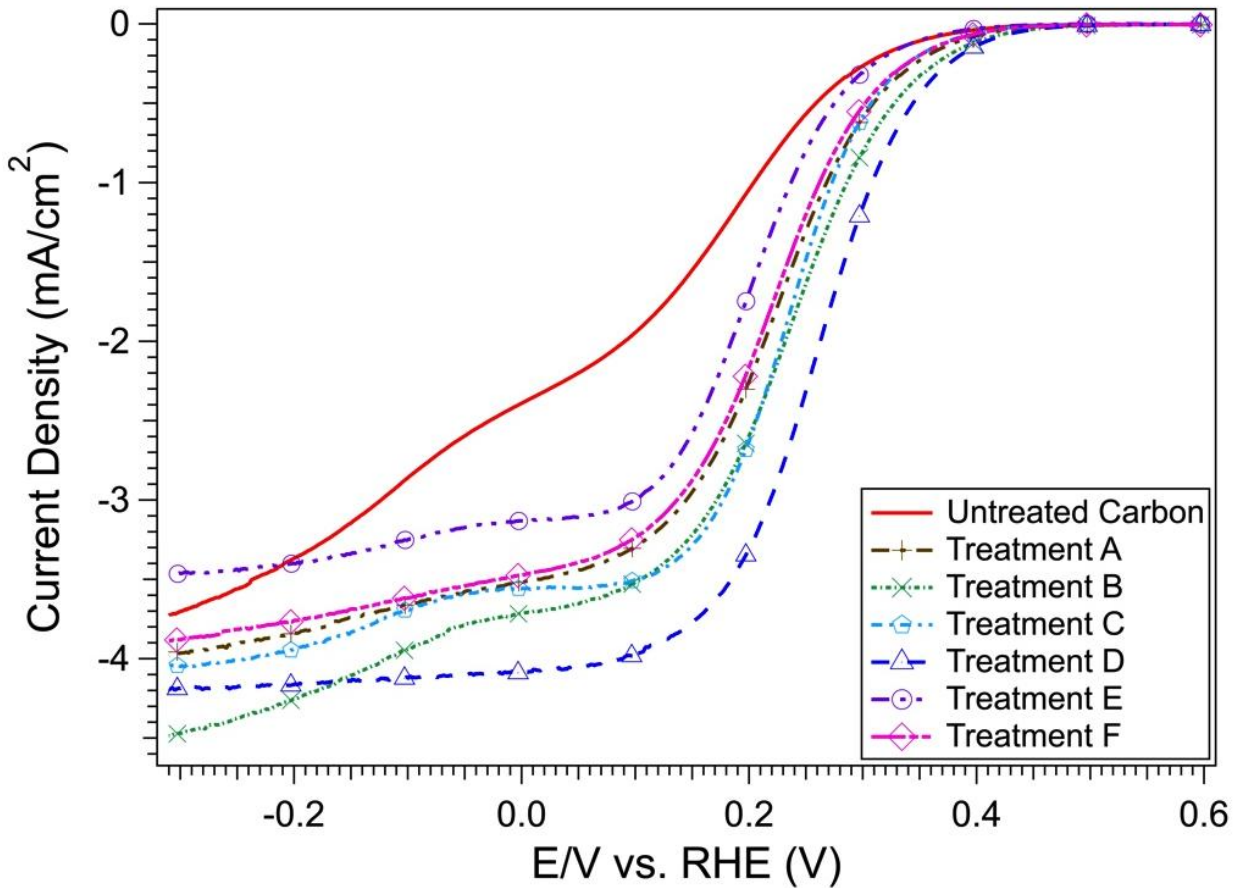

Figure 5-7 - Carbon pretreatment effects on Cu-3,5-diamino-1,2,4-triazole prepared using $Cu(ClO_4)_2$ salt.

When using pretreatment D, the number of electrons transferred was calculated holding the Pt ring electrode of the RRDE at 1.2V, and its value was 3.9 electrons in the limiting current region, (**Figure 5-8**). The durability of the adsorbed complex was also improved, the current density decreased to 10% of its initial value after 50 cycles, in comparison to the decrease in current density for untreated carbon after only 3 cycles.

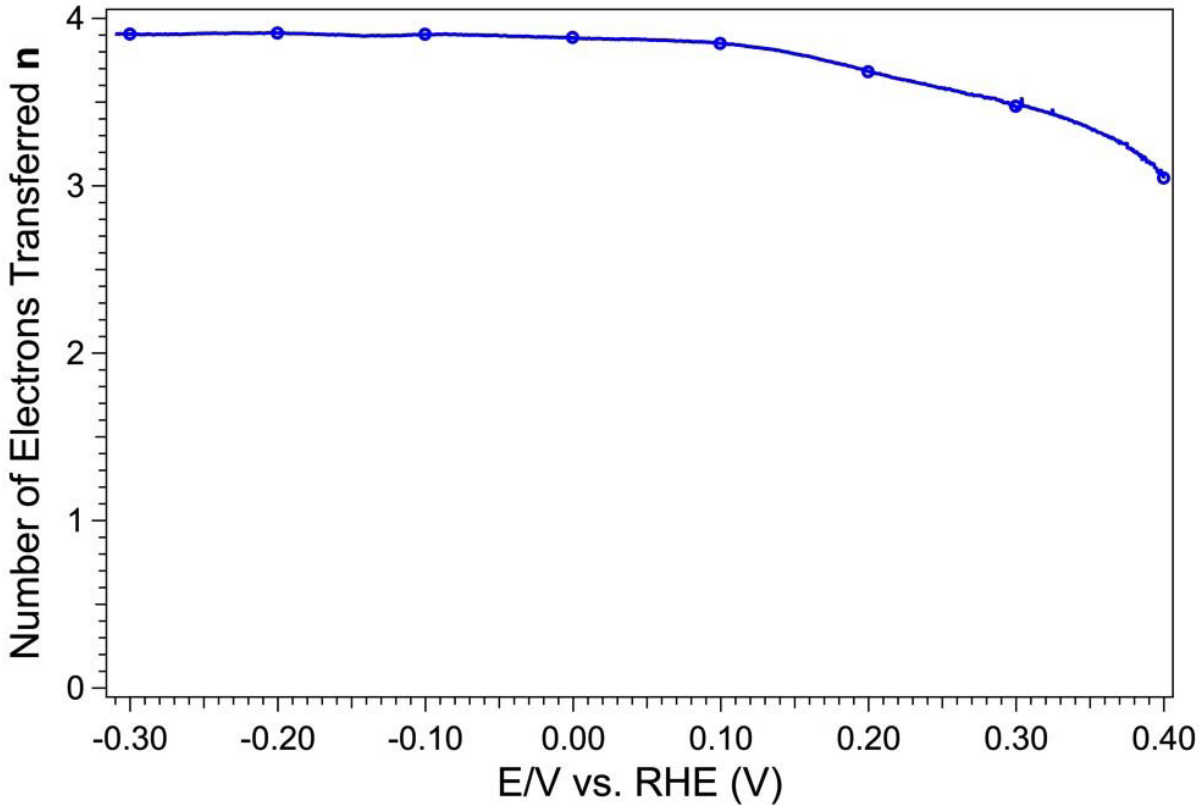

Figure 5-8 - Number of electrons transferred for Cu 3,5-diamino-1,2,4-triazole, $Cu(ClO_4)_2$ salt and oxidative carbon pretreatment D.

To analyze the behavior of the catalyst at different pH values, a Robinson-Britton buffer (pH 2 to 13) was prepared as described previously[79]. **Figure 5-9** shows that the catalytic activity of the Cu-3,5-diamino-1,2,4-triazole increases as a function of the pH. Low pH leads to the protonation of the ligand, limiting the ligand-metal coordination and the formation of catalytic centers, which is reflected in the low onset potential. As the pH is increased, the ligand is no longer protonated. This likely alters the structure of the complex, evidently leading to an increase in the ORR activity. The structures of triazole complexes are sensitive to pH value. The pH at which the ligand and metal are mixed determines which types of complexes will be formed and these likely have different stabilities/affinities for the carbon surface[186].

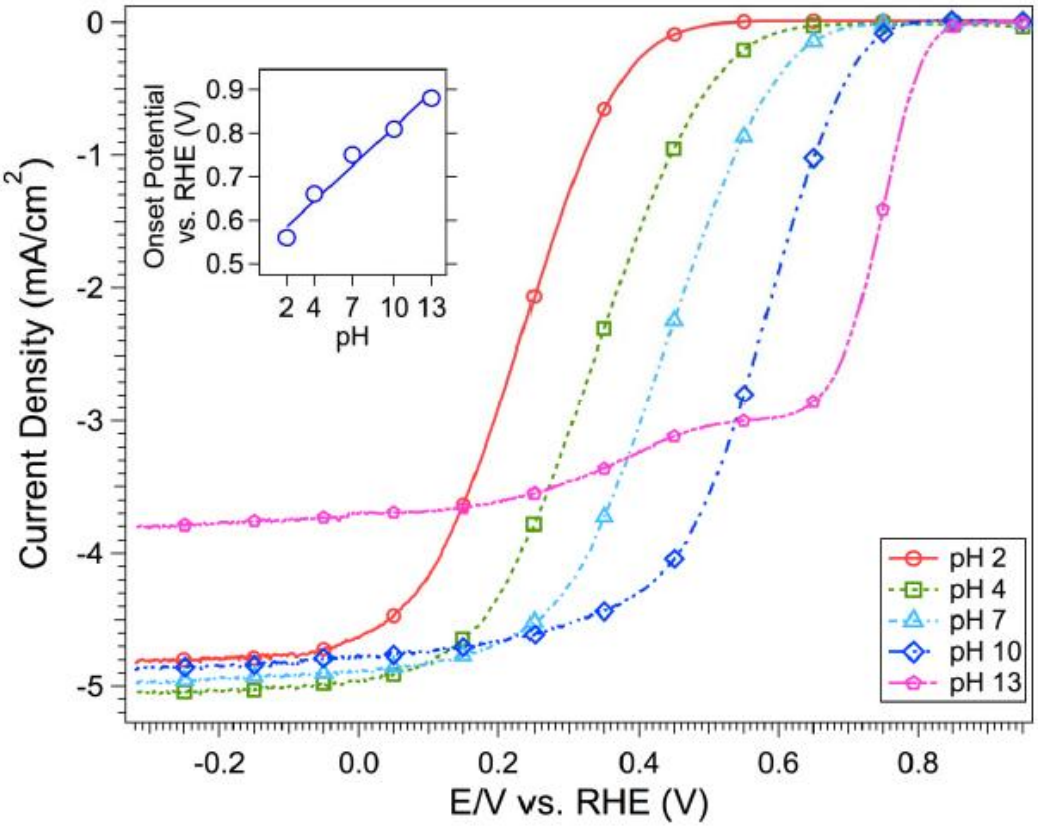

Figure 5-9 - RDE plots for Cu-3,5-diamino-1,2,4-triazole, Cu(NO3)2 salt. Robinson-Britton buffer electrolyte pH 2 to 13.

Our next target was to optimize the protocols for adsorbing 1,2,4-triazole metal complexes onto different carbon surfaces for optimal metal binding affinity. Three different experimental series were designed and experiments were carried out. ICP results were obtained on each carbon surface prepared to gauge the extent of metal binding. Multiple factors were evaluated during these experiments such as, source of heating, ligand and metal stoichiometries, reaction time and metal salts. These experiments helped identify the best experimental conditions for adsorbing ligands and metals on the carbon surface. For this particular set of experiments the ligand used throughout was 3,5-diamino-1,2,4-triazole and XC-72 carbon surface oxidized with

previously identified optimal oxidation conditions was used as the solid support. **Figures 5-10, 5-11 and 5-12** show the design of these experimental serieses.

ICP results obtained on these samples are tabulated after the figures. These ICP studies were based on the depletion model. A stock solution of copper salts was prepared and used for the adsorption studies. ICP was obtained on the solutions obtained after completion of reaction. Thus, higher amounts of copper leftover indicated lower binding to the 1,2,4-triazole adsorbed on carbon. Amount of copper retained was calculated based on difference between the copper levels in stock solution and the solutions after exposure to carbon black surfaces.

Adsorption Experimental Design Series 1
Oxidized (H_2O_2/H_2SO_4) Vulcan XC-72
Hdtrz (3,5-Diamino-1,2,4-triazole)
$Cu(NO_3)_2$

	"standard"	*2X [catalyst]*	*microwave*	*time/2*
Carbon Black	25 mg	25 mg	25 mg	25 mg
H_2O	3.875 mL	2.750 mL	3.875 mL	3.875 mL
0.2M $Cu(NO_3)_2$	0.625 mL 0.125 mmol	1.250 mL 0.250 mmol	0.625 mL 0.125 mmol	0.625 mL 0.125 mmol
0.5M Hdtrz	0.500 mL 0.250 mmol	1.00 mL 0.500 mmol	0.500 mL 0.250 mmol	0.500 mL 0.250 mmol
	80 ºC, 2 hours	80 ºC, 2 hours	120 ºC, 2 hours	80 ºC, 1 hour

order of additon A		*order of additon B*	
Carbon Black	**25 mg**	**Carbon Black**	**25 mg**
H_2O	**3.875 mL**	**H_2O**	**3.875 mL**
0.2M $Cu(NO_3)_2$	**0.625 mL 0.125 mmol 80 ºC, 2 hours**	**0.5M Hdtrz**	**0.500 mL 0.250 mmol 80 ºC, 2 hours**
0.5M Hdtrz	**0.500 mL 0.250 mmol 80 ºC, 2 hours**	**0.2M $Cu(NO_3)_2$**	**0.625 mL 0.125 mmol 80 ºC, 2 hours**

Standardized Workup:
1. Suspension centrifuged and decanted. (Supernatant was stored for analysis by ICP.)
2. Carbon was ***washed*** as follows:
   H_2O, 10 mL X 3
   MeOH, 10 mL X1
   Acetone, 10 mL X1
   Et_2O, 10 mL X1
   *(**Washed** defined as brief sonication (5 min.), centrifuge, decant.)*
3. Carbon dried in 90 °C bath overnight.
4. Carbon weighed and stored.

Figure 5-10 - Adsorption experimental design series-1

Adsorption Experimental Design Series 2
Oxidized (H_2O_2/H_2SO_4) Vulcan XC-72
Hdtrz (3,5-Diamino-1,2,4-triazole)
ASB-II-78

	Microwave 120°C, 30 min. A	*Microwave 120°C, 1 Hr. B*	*Microwave 140°C, 1 Hr. C*	*$CuBF_4$ MW, 120°C, 2Hr. D*	*$CuPF_6$ MW, 120°C, 2Hr. E*	*CuBr MW, 120°C, 2Hr. F*
Carbon Black	25 mg	25 mg	25 mg	25 mg	25 mg	25 mg
H_2O	3.875 mL	2.750 mL	3.875 mL	2.00 mL	2.00 mL	2.00 mL
Metal	0.625 mL (0.2 M) 0.125 mmol	0.625 mL (0.2 M) 0.125 mmol	0.625 mL (0.2 M) 0.125 mmol	2.5 mL (0.05 M) 0.125 mmol	2.5 mL (0.05 M) 0.125 mmol	2.5 mL (0.05 M) 0.125 mmol
0.5M Hdtrz	0.500 mL 0.250 mmol	0.500 mL 0.500 mmol	0.500 mL 0.250 mmol	0.500 mL 0.250 mmol	0.500 mL 0.250 mmol	0.500 mL 0.250 mmol
	ASB-II-78-A	**ASB-II-78-B**	**ASB-II-78-C**	**ASB-II-78-D**	**ASB-II-78-E**	**ASB-II-78-F**

Notes:-

1. Samples A,B and C use copper nitrate as metal source
2. Samples D, E and F use lower concentrations of metal solutions due to lowered solubility of Cu (I) salts in comparison to to their Cu (II) analogues

Standardized Workup:

1. Suspension centrifuged and decanted. (Supernatant was stored for analysis by ICP.)
2. Carbon was ***washed*** as follows:
   H_2O, 10 mL X 3
   MeOH, 10 mL X1
   Acetone, 10 mL X1
   Et_2O, 10 mL X1
   *(**Washed** defined as brief sonication (5 min.), centrifuge, decant.)*
3. Carbon dried in 90 °C bath overnight.
4. Carbon weighed (note mass recovery) and stored for future use.

Figure 5-11 - Adsorption experimental design series-2

Adsorption Experimental Design Series 3
Oxidized (H_2O_2/H_2SO_4) Vulcan XC-72
Hdtrz (3,5-Diamino-1,2,4-triazole)
ASB-II-79

	Microwave 140°C, 2 Hr. A	*Microwave 140°C, 4 Hr. B*	*Microwave 160°C, 2 Hr. C*	*$CuBF_4$ MW, 140°C, 1 Hr. D*	*$CuPF_6$ MW, 140°C, 1 Hr. E*	*CuBr MW, 140°C, 1 Hr. F*
Carbon Black	25 mg	25 mg	25 mg	25 mg	25 mg	25 mg
H_2O	3.875 mL	3.875 mL	3.875 mL	1.36 mL	2.16 mL	0 mL
Metal	0.625 mL (0.2 M) 0.125 mmol	0.625 mL (0.2 M) 0.125 mmol	0.625 mL (0.2 M) 0.125 mmol	3.64 mL 0.125 mmol	2.84 mL 0.125 mmol	4.5 mL 0.125 mmol
0.5M Hdtrz	0.500 mL 0.250 mmol	0.500 mL 0.500 mmol	0.500 mL 0.250 mmol	0.500 mL 0.250 mmol	0.500 mL 0.250 mmol	0.500 mL 0.250 mmol
	ASB-II-79-A	**ASB-II-79-B**	**ASB-II-79-C**	**ASB-II-79-D**	**ASB-II-79-E**	**ASB-II-79-F**

Notes:-

1. Samples A,B and C use copper nitrate as metal source
2. For samples D, E and F the actual concentration of copper (I) sources was calculated using ICP

Standardized Workup:

1. Suspension centrifuged and decanted. (Supernatant was stored for analysis by ICP.)
2. Carbon was ***washed*** as follows:
   H_2O, 10 mL X 3
   MeOH, 10 mL X1
   Acetone, 10 mL X1
   Et_2O, 10 mL X1
   *(**Washed** defined as brief sonication (5 min.), centrifuge, decant.)*
3. Carbon dried in 90 °C bath overnight.
4. Carbon weighed (note mass recovery) and stored for future use.

Figure 5-12 - Adsorption experimental design series-3

Table 5-2 details results from experimental series 1. Entries 1 and 2 reflect results from using different stoichiometries of triazole and metal salt. The standard conditions resulted in retention of about 56% of copper on the carbon surface. As can be seen from the table, using twice the amount of metal salt and the triazole did not result in additional copper retention on the carbon surface, thus suggesting that the standard conditions are optimal in this regard.

Table 5-2 - Experimental Design Series-1 ICP results

Entry	Sample	Copper Retention %
1	Standard Conditions	56.73
2	2X catalysts	55.15
3	Microwave	74.24
4	Half time – 1 Hour	49.98
5	Order of Addition - A	56.63
6	Order of Addition - B	57.42

The next entry (3) shows that when microwave heating is used for adsorption, the amount of copper retained increased by 20% over conventional heating. Stopping the reaction after only one hour under conventional heating had a negative impact on the copper retention. Lastly, entries 5 and 6 show that order of addition had little to no effect on the copper retention.

Moving on to the ICP results from the experimental series 2 (**table 5-3**), it can be seen that reducing the microwave heating time also led to the reduction in copper retention, but reducing time constant and increasing the temperature to 140 ^{o}C gave the best result thus far. Three different Cu(I) salts were also tested in this series. However,

the low solubility of these salts in water ruled out the use of ICP for copper retention studies. This phenomenon was observed again when these experiments were repeated under slightly different conditions as shown in the next table. The difficulties in handling Cu (I) salts forced us to abandon their use altogether.

Table 5-3 - Experimental design series-2 ICP results

Entry	Sample	Copper Retention %
7	A (MW – 120 – 0.5 h)	56.10
8	B (MW – 120 – 1 h)	63.63
9	C (MW – 140 – 1 h)	80.23
10	D ($CuBF_4$)	Nil*
11	E ($CuPF_6$)	Nil*
12	F (CuBr)	Nil*

*ICP results could not be obtained for these samples due to low water solubility

Lastly, fine tuning the microwave conditions led to even further increase over a short reaction time period. The corresponding ICP results are in **table 5-4**.

Table 5-4 - Experimental design series-3 ICP results

Entry	Sample	Copper Retention %
13	A (MW – 140 – 2 h)	85.01
14	B (MW – 140 – 4 h)	95.82
15	C (MW – 160 – 2 h)	97.05
16	D ($CuBF_4$)	Nil*
17	E ($CuPF_6$)	Nil*
18	F (CuBr)	Nil*

*ICP results could not be obtained for these samples due to low water solubility

RDE experiments were carried out on samples prepared using different temperatures to see if the increased copper retention would translate into higher ORR catalytic activity. However, **figure 5-13** shows that the highest onset potential is actually observed for the sample prepared at 80 ^{o}C. The sample prepared at 160 ^{o}C under microwave irradiation has the worst onset potential among all other samples, despite retaining highest amount of copper. The microwave treatment at a slightly lower temperature (140 ^{o}C) for longer duration results in superior current density, but does not show higher onset potential than the sample prepared at 80 ^{o}C. These results clearly show that while higher temperatures positively affect the copper retention, they do not necessarily lead to the formation of optimal ligand-metal complex. Additionally, it can also be seen that higher copper retention does not always correlate with the higher ORR activity. The nature and the structure of the complexes formed on the surface play a more crucial role.

Next, we tested the effect of different counter-ions on the catalytic activity. We prepared adsorbed complexes of 3,5-diamino,1,2,4-triazoles with different metal salts in presence of untreated Vulcan XC-72. **Figure 5-14** shows the curves for these experiments obtained through RDE experiment. Copper sulfate and copper nitrate show the highest onset potential as well as well defined current density, with the latter slightly edging out the former.

Having optimized the conditions for adsorption of metal-triazole complexes on the surface of carbon black, we turned our attention to the development of the covalent surface immobilization techniques.

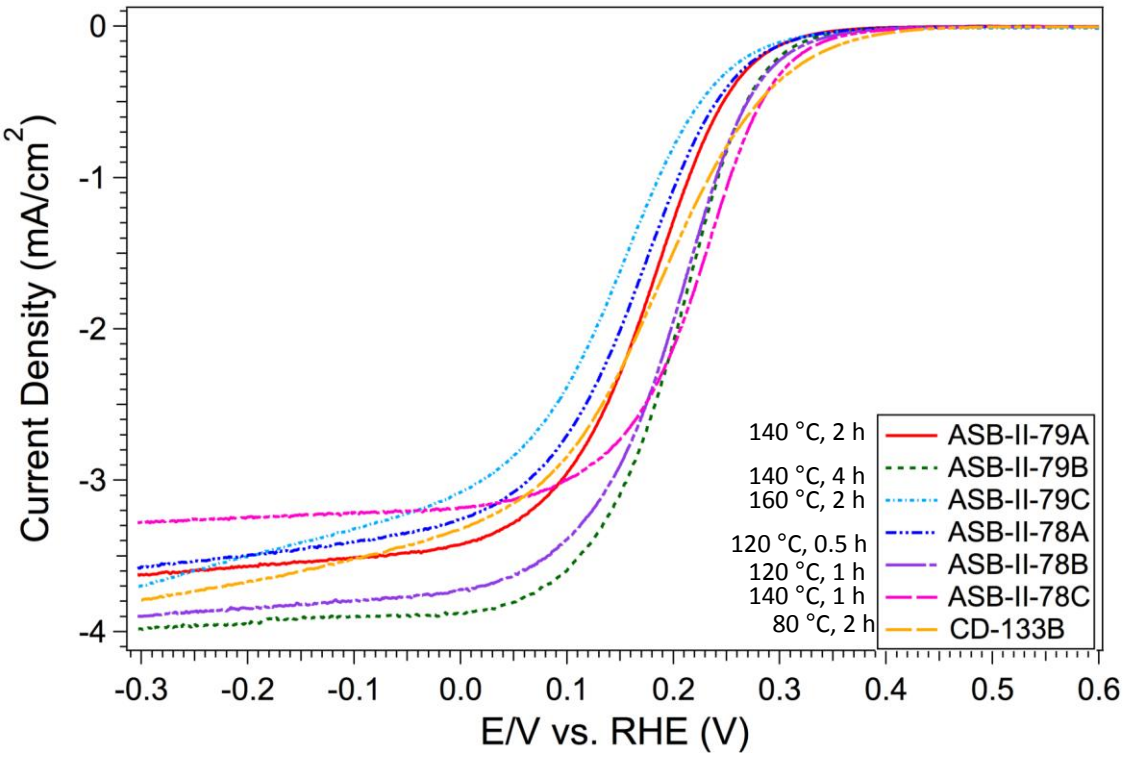

Figure 5-13 – Influence of temperature on complexation of 1,2,4-triazole ligands

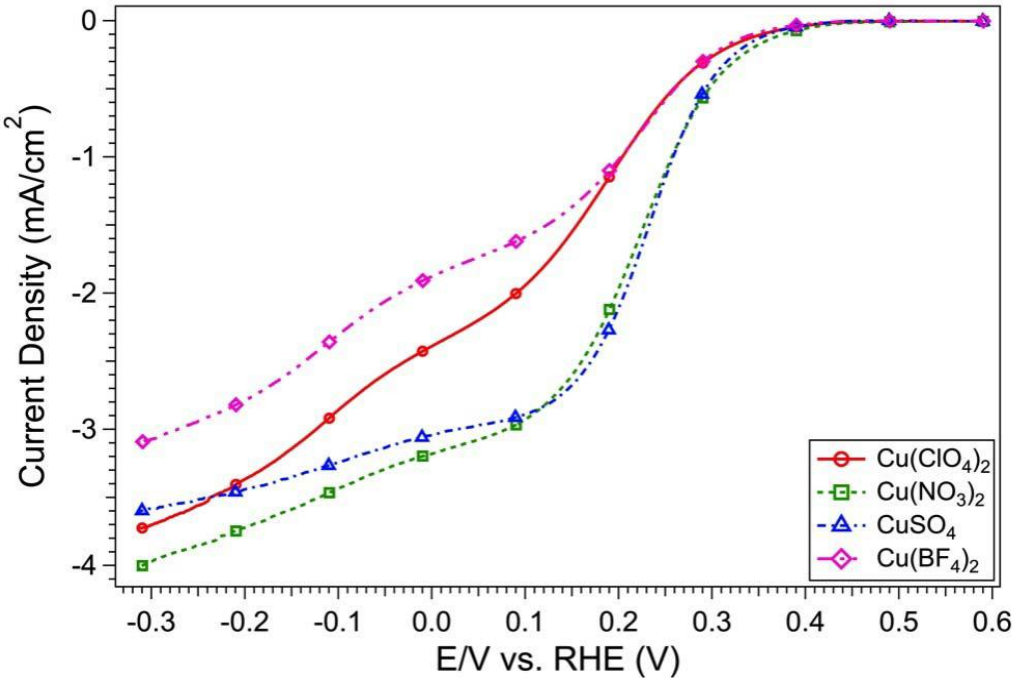

Figure 5-14 - RDE curves for adsorbed Cu-3,5-diamino-1,2,4-triazole using different copper salts.

5.5.2. Secondary pool of chemical transformations: covalent immobilization strategies

Multiple strategies were applied to covalently attach the triazoles to the carbon surfaces. As explained before we validated each synthetic step in solution before applying it to the heterogeneous synthesis, to ensure its success. Most of the covalent immobilization strategies were adopted from the existing homogeneous methods for 1,2,4-triazole synthesis. In the case of new methods the reactions were tested in the solution phase beforehand. These model reactions served as the template for heterogeneous synthesis on carbon surfaces.

The main constraint encountered when modifying these methods for heterogeneous synthesis was lack of information on the exact loading capacity of the carbon surface being utilized. Thus, we used excess of the soluble reagents whenever possible to ensure complete conversions of the surface handles. Reagents were chosen as to ensure that no cross reactivity with the carbon surface would be possible.

Scheme 5-15 shows the 1,2,4-triazole synthesis on carbon surfaces (cabot Vulcan XC-72 and cabot black pearls 2000) that have undergone oxidative pretreatment to increase the population of carboxylic acid functional groups. These surfaces were then reacted with hydrazine hydrate in the microwave synthesizer to generate hydrazides on the surface. The hydrazide modified surface was then reacted with 2-picolinyl nitrile to generate the 3-(2-pyridyl)-1,2,4-triazole on the carbon surface (**5.1**). The same hydrazide modified surface was also reacted with S-methylthiourea in a separate experiment, to form the 3-aminotriazole (**5.2)**. Table 5-5 shows the results from RDE experiments carried out on the complexes of these samples with $Cu(NO_3)_2$.

As can be seen from these results, the observed onset potentials were quite low compared to the adsorbed complexes tested earlier. This is presumably due to the lower loading of the triazoles on the surface when multiple step covalent binding approach is used. In order to increase the loading of the covalently attached triazoles on the carbon surface, we decided to try other approaches that would allow us to immobilize an intact triazole on the surface instead of forming one in a stepwise manner.

The next approach that we tried was based on existing literature[182]. This strategy was designed to exploit the polycondensed aromatic rings present on the carbon black surface. Nitration followed by tin(II) chloride reduction was carried out to functionalize the surface with aromatic amino groups. Fmoc assay was used to gauge the extent of surface modification. The results from Fmoc assay indicated the loading to be 0.089 mmols/g. Diazotization reaction was then carried out to generate the electrophilic diazo species on the surface. This surface was then exposed to 3,5-diamino-1,2,4-triazole in situ. This was expected to link the intact triazole to the surface though a triazene linkage in a single step[187] **(Scheme 5-16)**.

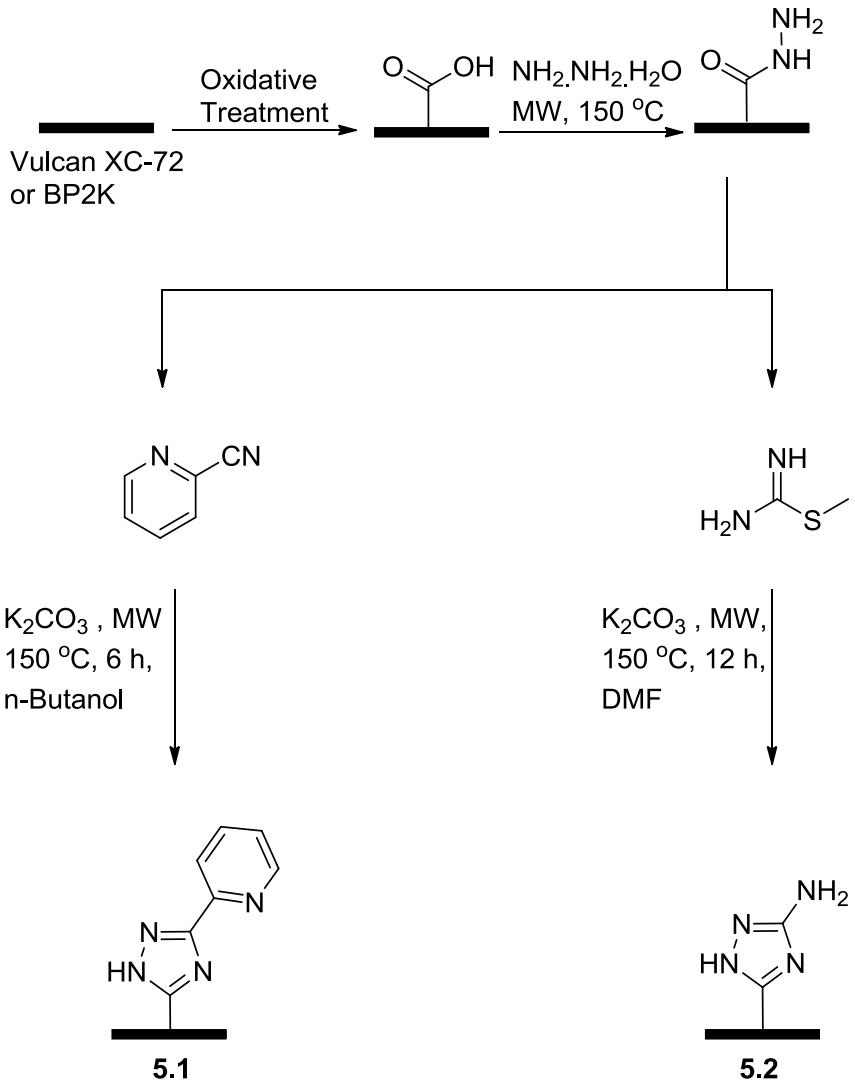

Scheme 5-15 – Covalent attachment of 1,2,4-triazoles to the carbon surfaces in a stepwise manner

Table 5-5 – Onset potentials observed for covalently attached triazoles

Entry	Sample	Onset Potential Vs. RHE (V)
1	5.1	0.28
2	5.2	0.17

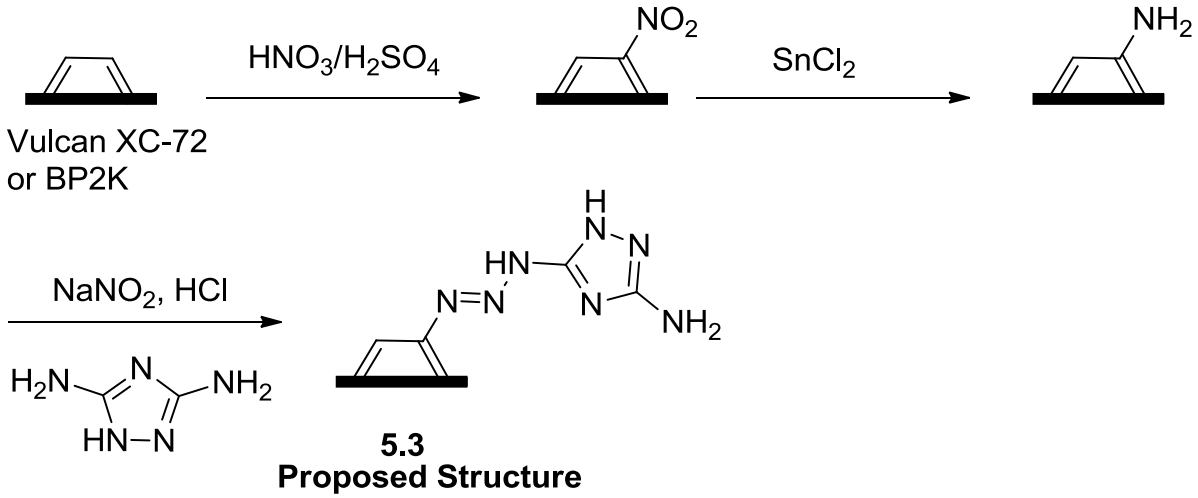

Scheme 5-16 - Nitration of polycondensed aromatic rings of carbon black surface

However, when we attempted the triazene synthesis in the solution phase using the same conditions, we got remarkably different results. We observed that, contrary to the literature reports[187], the diazo group gets displaced by the incoming nucleophile instead of participating in the triazene formation. This led to formation of multiple different products as shown in the **scheme 5-17**. The major product was the benzene ring coupled to the triazole through a secondary amine. Two more minor products generated through self coupling were also observed. By increasing the time between addition of sodium nitrite and the amino triazole the amount of major product could be further increased so as to yield the desired product exclusively. Similar results were obtained with direct use of benzene as the nucleophile. However, the side products do not matter in the context of heterogeneous synthesis since the self coupling is not possible for surface immobilized amine functional groups and the product from self coupling of soluble component can be washed away using organic solvents.

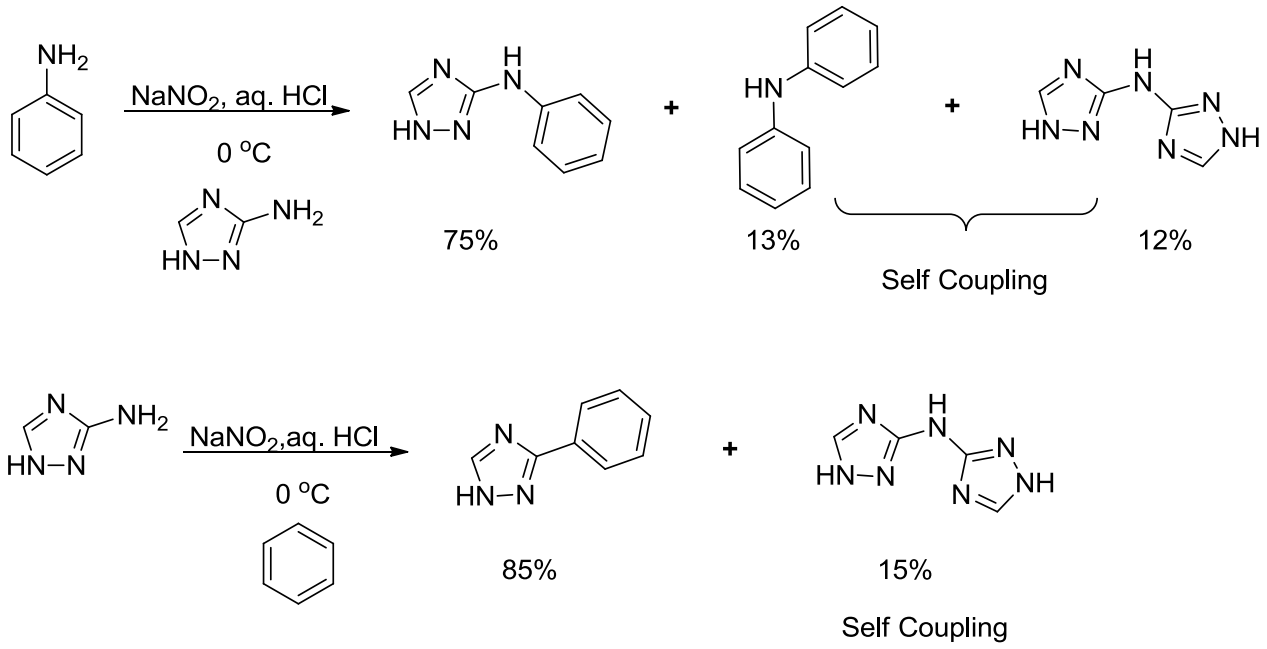

Scheme 5-17 – Solution phase investigation of the diazotization chemistry

Based on these experiments we revised the probable structure of the product formed in **scheme 5-15** to the one shown in **figure 5-18**.

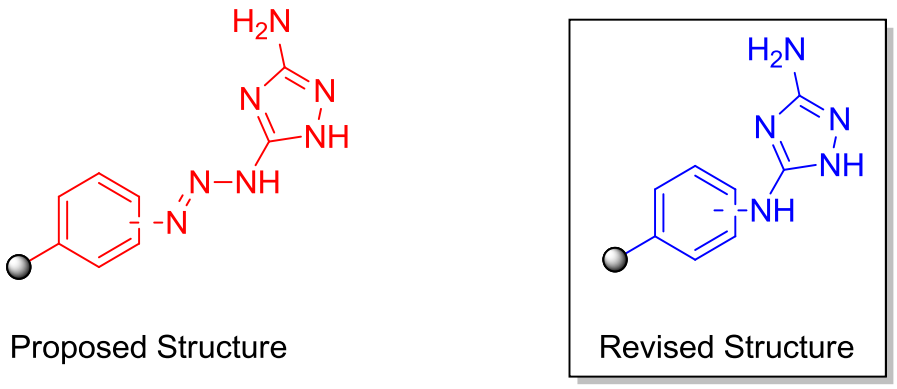

Figure 5-18 - Revised structure of product formed after coupling of diazotized 3,5-diamino-1,2,4-triazole with aromatic groups

This discovery spurred our interest in the diazotization chemistry even further. We developed a new synthetic plan that would let us take advantage of diazotization chemistry to immobilize amino substituted 1,2,4-triazoles on the carbon surface without the need for any pretreatment of the carbon surfaces. **Scheme 5-19** displays this strategy.

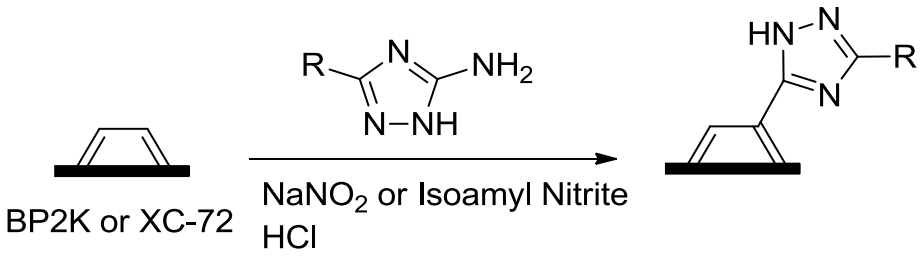

Scheme 5-19 - Covalent attachment of intact 1,2,4-triazoles to the carbon surfaces via diazotization strategy

This strategy is essentially the exact opposite of the strategy described in **scheme 5-15**. Instead of modifying the surface through multiple synthetic steps, the untreated carbon black surfaces are directly used in this method. The poly-condensed aromatic rings on the surface are utilized as the nucleophiles and the diazotized 3-amino-5-sub-1,2,4-triazole is used as the soluble electrophilic component.

Multiple functionalized surfaces were prepared using this strategy. The electrochemical analysis validated the effectiveness of this chemistry. **Figure 5-20** shows various carbon surfaces prepared using diazotization chemistry. Compounds **5.5** and **5.8** are essentially the same as compounds **5.1** and **5.2**, respectively, with difference being that the **5.5** and **5.8** were prepared using diazotization chemistry as opposed to the stepwise synthesis of the others. **Table 5-6** shows the onset potentials observed for the complexes prepared from these samples with $Cu(NO_3)_2$. At least a two

fold increase in the onset potential was observed across the board relative to the values obtained for modified surfaces prepared through stepwise synthesis. This indicates more efficient functionalization of the surface when diazotization chemistry is used. At the time of writing of this thesis, the diazotization method remains our preferred route of carbon surface modification.

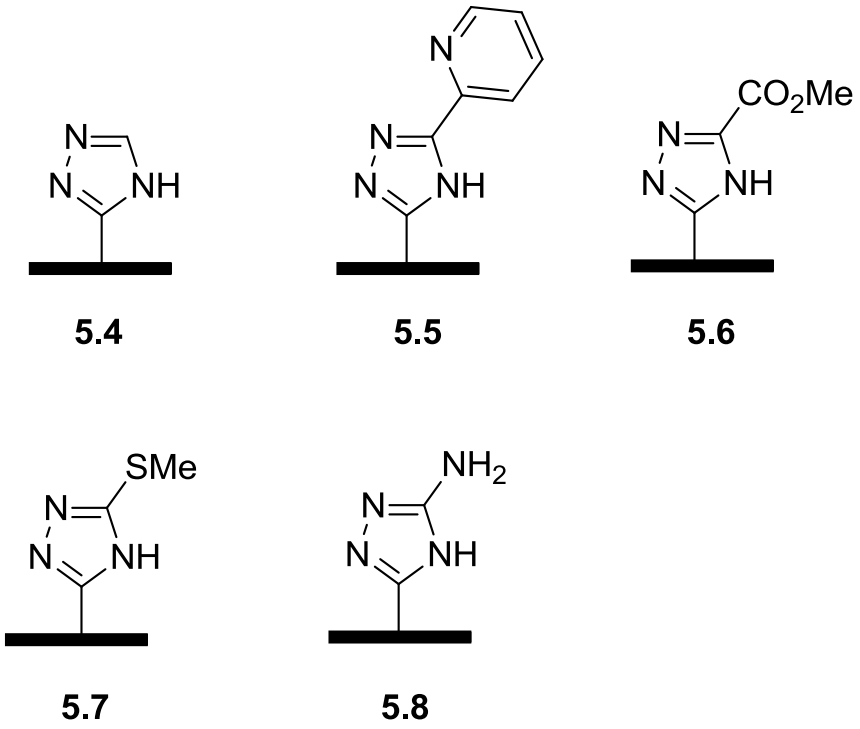

5.4 **5.5** **5.6**

5.7 **5.8**

Figure 5-20 – 1,2,4-triazole modified surfaces prepared using diazotization chemistry

Table 5-6 – Onset potentials observed for samples prepared via diazotization chemistry

Entry	Sample	Onset Potential Vs. RHE (V)
1	**5.4**	0.38
2	**5.5**	0.42
3	**5.6**	0.41
4	**5.7**	0.48
5	**5.8**	0.42

RDE results for the diazotized samples also showed that the use of oxidatively pretreated carbon surfaces results in lower onset potential. The choice of carbon black surface also seemed to impact the performance of the prepared surfaces. we designed a set of experiments to better understand the effects of oxidative pretreatment on covalent binding of 1,2,4-triazoles through diazotization. **Figure 5-20** shows a schematic representation of this experiment set. RDE curves obtained from samples prepared following the experimental design are shown in **figure 5-21.** Two important observations can be made based on these results. First, the samples prepared using the BP-2K carbon black surface consistently show much higher onset potential than the samples prepared using the Vulcan XC-72 surface. Second, the samples prepared from the oxidized surfaces show lower activity than the samples prepared from carbon surfaces without any pretreatment. However, if the oxidative treatment is carried out after the immobilization of the triazole through diazotization, then the activity increases.

Our theory behind these observations is that oxidative treatment of the carbon surface before carrying out diazotization reaction leads to increase in the oxygenated functional groups on the carbon black surface. This effectively block the access to the polycondensed aromatic rings on the surface, which are acting as nucleophilic anchoring groups in the diazotization reaction, in turn leading to the decreased population of the immobilized 1,2,4-triazoles. When untreated carbon surfaces are used this phenomenon is avoided, leading to better results. However, our earlier experiments along with literature reports indicate that the oxygenated surface groups play a vital role in the metal complexation. Thus, oxidative treatment after the immobilization of 1,2,4-triazoles leads to an increase in the population of oxygenated functional groups on the carbon black surface without negatively impacting the 1,2,4-triazole population. This arrangement is optimal in regards to the catalytic activity. This is reflected in the increased onset potential observed for these samples. **(Figure 5-22)**.

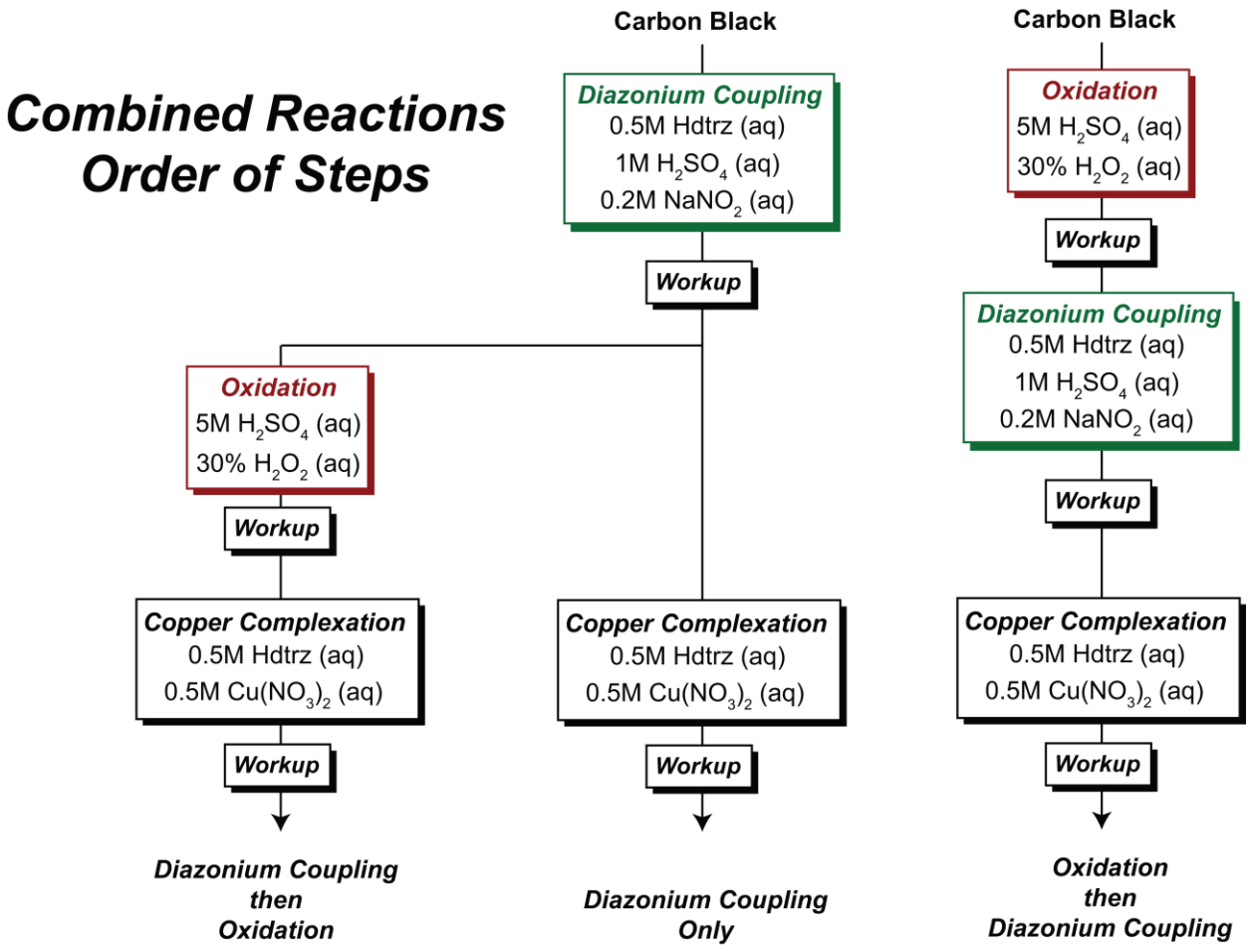

Figure 5-21 – Experimental series designed to assess the effect of oxidative treatments and the choice of carbon black surface on the activity.

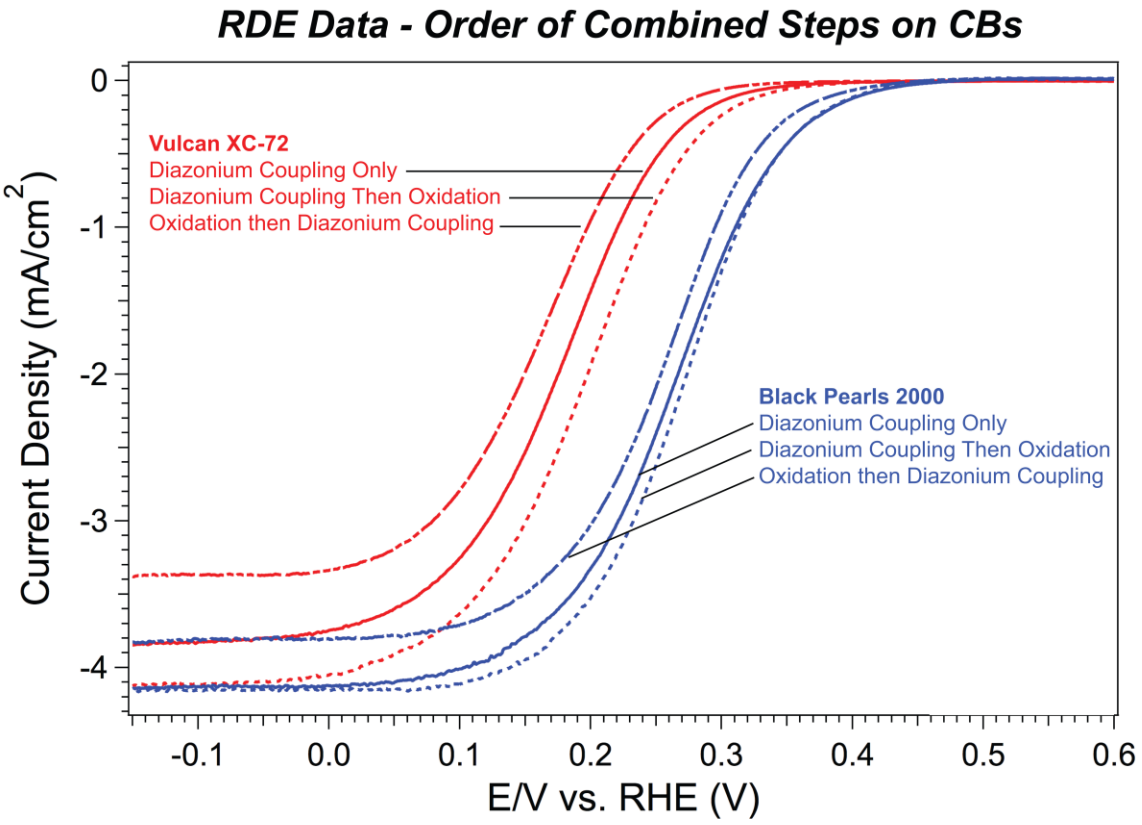

Figure 5-22 – RDE curves for samples prepared following different order of steps experiments (3,5-diamino-1,2,4-triazole - $Cu(NO_3)_2$)

Another observation from these experiments was that the performance of the standalone immobilized complexes can be improved if an auxiliary ligand, with similar structural features to that of the original triazole, was used during the complexation. According to the data best ORR activity is observed when triazoles act as bridging ligands between metal centers **(Figure 5-23)**. Our previous observations from studies on copper complexes of 1,2,4-triazoles also indicated that the preferred triazole-metal binding ratio was two to one (chapter 4).

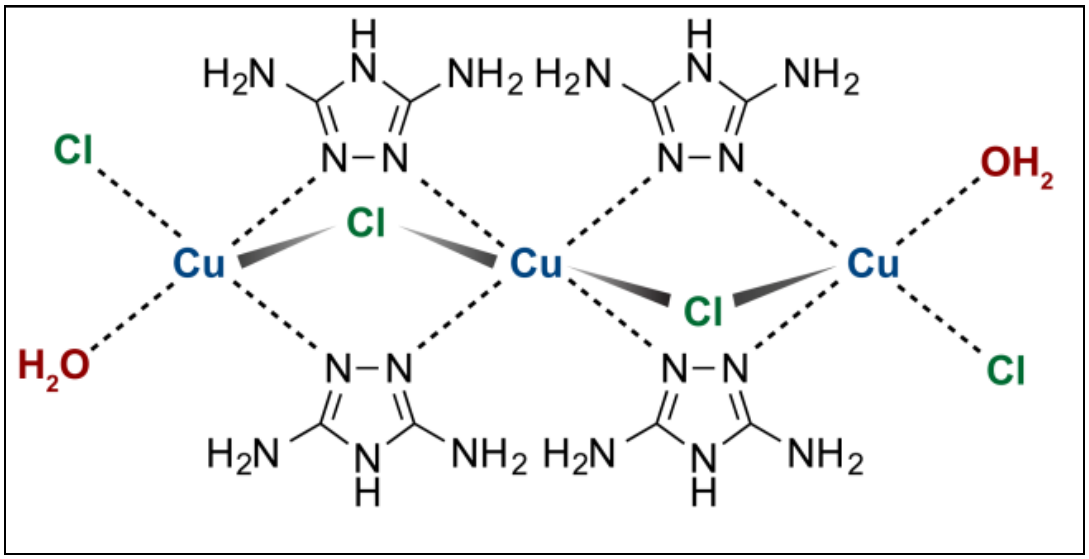

Figure 5-23 - 3,5-diamino-1,2,4-triazole as bridging ligand

Thus, if the there are large gaps between the 1,2,4-triazole functionalities on the carbon surface, they may not be able to fully carry out their function as bridging ligands, leading to lower activity. This is compounded by the fact that covalently immobilized triazoles are conformationally more restricted than their adsorbed counterparts.

Auxiliary ligands can ameliorate this issue by filling out these gaps. This theory was validated when higher onset potentials were observed in the RDE experiments for complexes prepared with the auxiliary ligands as seen in **figure 5-24**. The sample that sees the most improvement in the activity, upon addition of the auxiliary ligand, is **5.8**. In fact, the values for the onset potential and the current density observed for this sample were highest for any sample we had synthesized up to this point. 5.6 and 5.7 displayed same onset potential but worse current densities when auxiliary ligands were used during complexation, while **5.4** displayed the same trend as **5.8**.

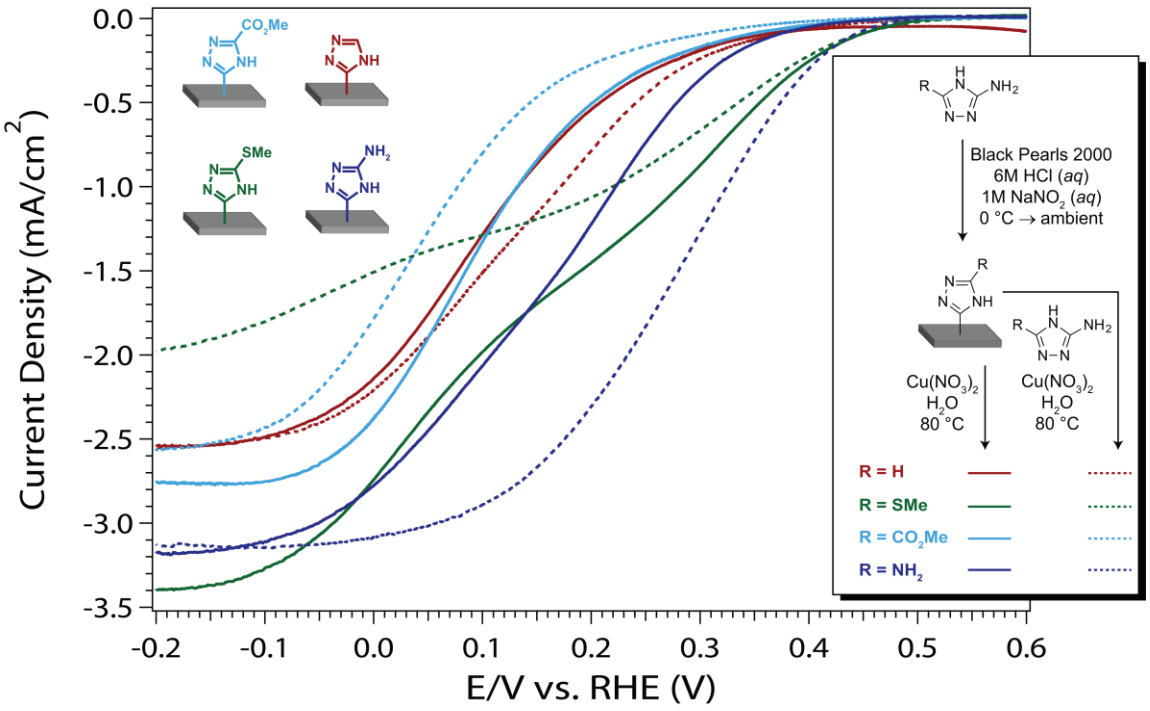

Figure 5-24 - RDE curves for samples prepared with and without auxiliary ligands

5.4→R = H, **5.7**→R = SMe, **5.6**→R = CO_2Me, **5.8**→R = NH_2

Although these results were encouraging from the point of view of activity, the core problem associated with the adsorbed complexes, viz. stability, resurfaced with the use of auxiliary ligands. Auxiliary ligands are not attached to the carbon surface through covalent binding and thus behave as adsorbed ligands. This was reflected in the RDE experiments carried out to test the stability of complexes prepared with auxiliary ligands. **Figure 5-25** shows the RDE curves obtained from the stability study. The onset potential as well as the current density decreases steadily as the catalyst is exposed to progressively higher number of cycles. At the end of 200th cycle the activity of the catalyst decreases to the level of the complex prepared from **5.8** without the auxiliary ligand. This indicates that the auxiliary ligand dissociates from the complex over time. In order to overcome this issue of stability we decided to reassess the necessity of use of

auxiliary ligands. We realized that denser functionalization of the carbon surfaces with 1,2,4-triazoles could potentially eliminate the need to use auxiliary ligands.

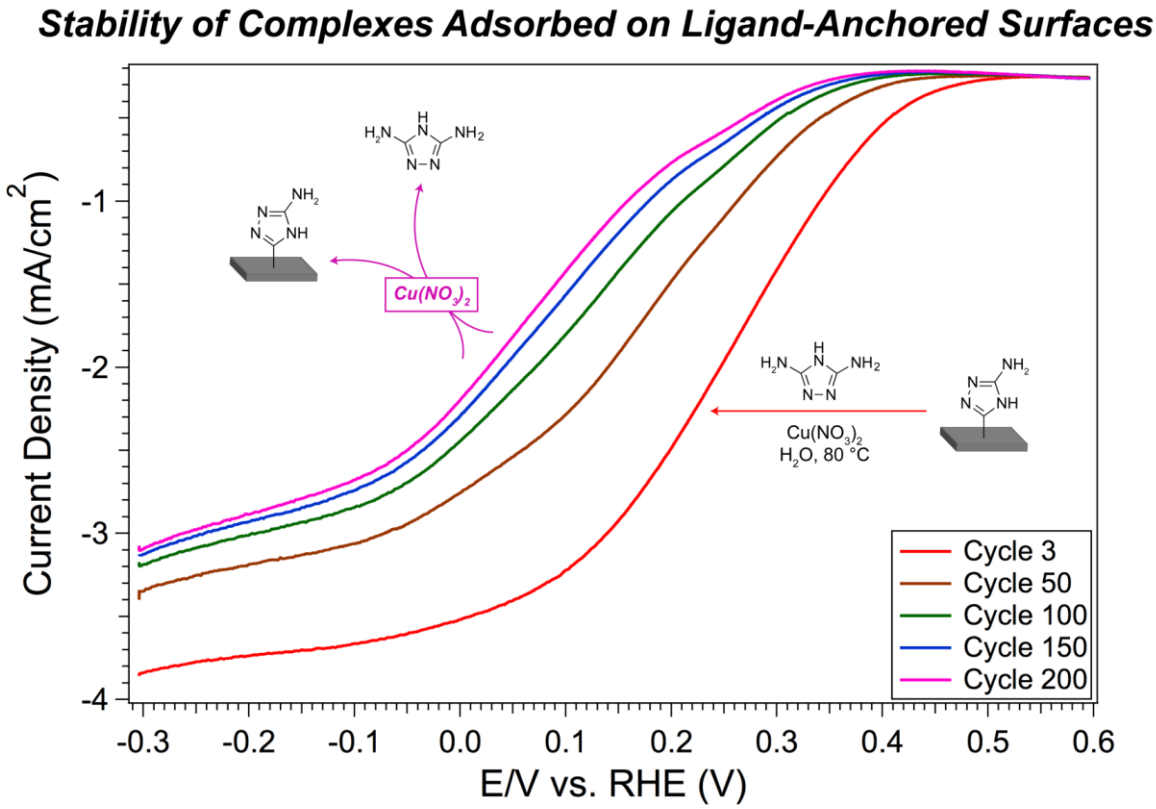

Figure 5-25 – Decrease in activity over time due to dissociation of auxiliary ligand

In order to achieve higher density, we decided to functionalize the free amine group already present in sample **5.8**. This opportunity was utilized to synthesize hemiphtalocyanine-like molecules on the carbon surfaces as shown in the **scheme 5-26**. This modification was carried out in order to increase the population of amino triazoles on the carbon surface. This was expected to not only increase the density but also decrease the conformational constraints, thus allowing the 1,2,4-triazoles to act as bridging ligands without the need of an auxiliary ligand. The synthetic route for this is same as the one discussed in the chapter 2.

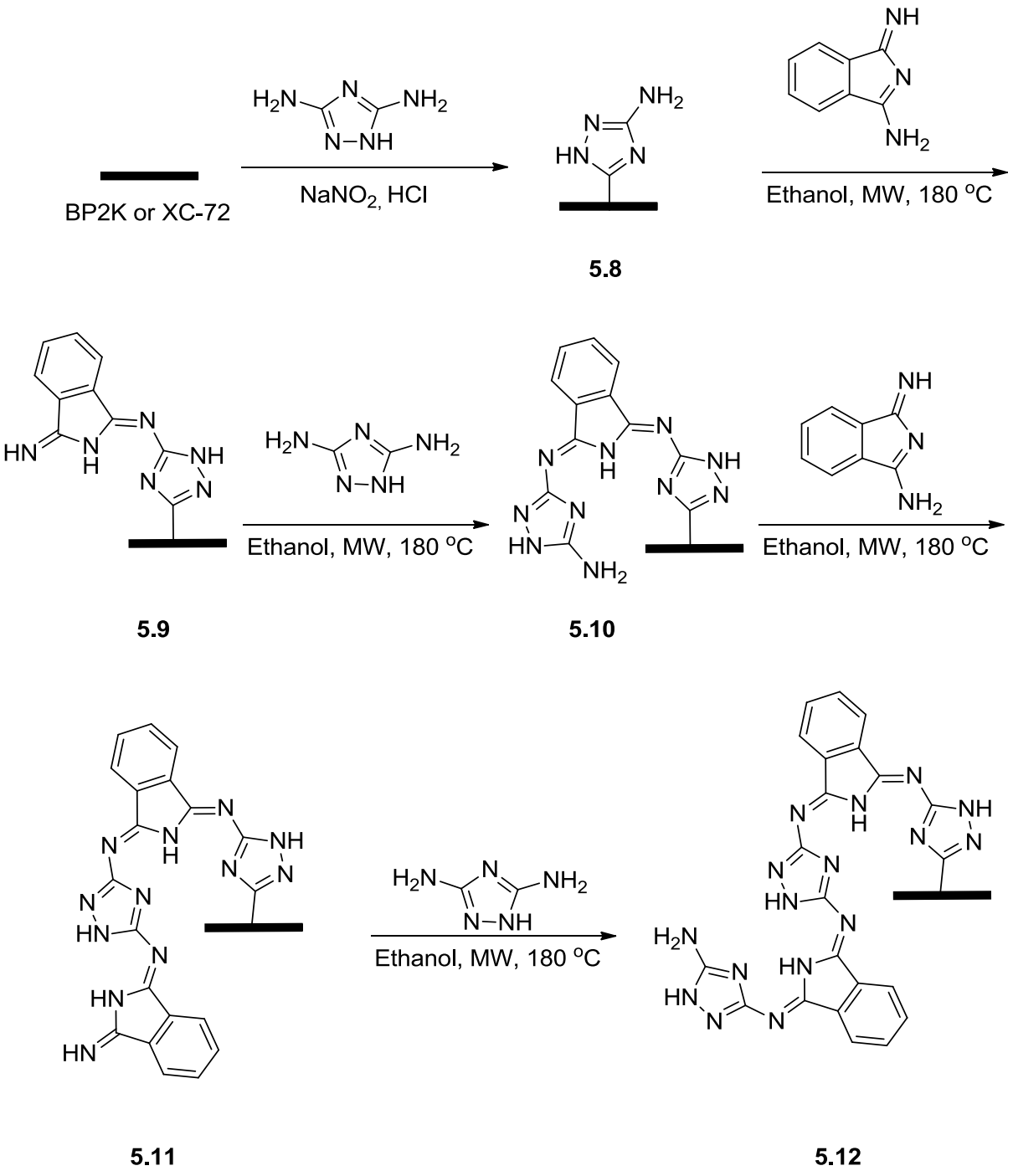

Scheme 5-26 – Syntheis of triazolo-hemiphthalocyanine on carbon surface in stepwise manner

Samples **5.10** and **5.12** were complexed with $Cu(NO_3)_2$ in the presence as well as absence of auxiliary ligands. Curves obtained from RDE experiments carried out on

these samples are shown in **figure 5-27**. This figure also includes the curves previously obtained for **5.8** for reference**.** To our delight, we observed that as the number of amino triazoles in the sample increased, the dependence of activity on the presence of auxiliary ligand decreased. For samples prepared from **5.12**, there is virtually no difference between the onset potential as well as the current density in samples with and without auxiliary ligands added. The value of onset potential was 0.55 V, which was slightly higher than the previously observed highest activity. This experiment validated our approach of increasing the density of 1,2,4-triazoles on the carbon surface in order to increase the activity and eliminate the need for auxiliary ligands. **Table 5-7** shows the results from ICP experiments carried out on these samples. The metal retention increases with the increase in number of 1,2,4-triazoles. The complex prepared from **5.10** with the auxiliary ligand holds slightly more copper than the one without the auxiliary ligand. However, this trend in not observed with the samples prepared from **5.12.** The complex prepared without the auxiliary ligand shows highest copper retention.

In summary, observed values of the onset potentials up to 0.55V vs. RHE and current densities up to 5 mA/cm^2, are high values among the non-pyrolyzed copper catalysts reported at pH 1[188]. In addition, these catalysts showed very low hydrogen peroxide production (less than 5%).

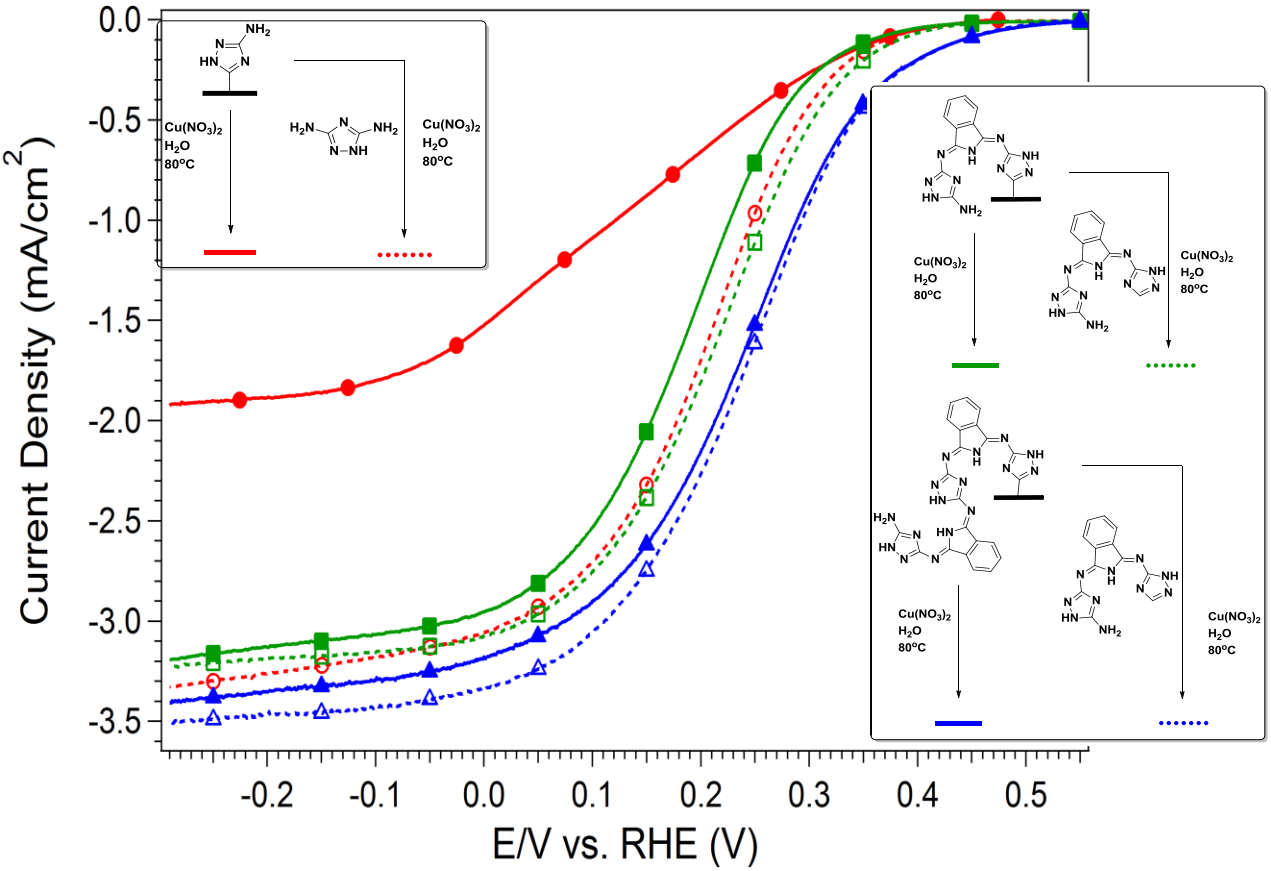

Figure 5-27 – RDE curves for triazolo-hemiphthalocyanins 5.10 and 5.12, dashed line indicates complex prepared with auxiliary ligand, solid line indicates absence of auxiliary ligand

Table 5-7 – Copper retention values observed for samples 5.10 and 5.12

Entry	Sample	Copper Retention %
1	5.10 – No Aux. lig.	62.33
2	5.10 – Aux. lig.	65.21
3	5.12 – No Aux. lig.	73.25
4	5.12- Aux. lig.	72.89

5.6. Pyrolysis

Despite the success in increasing the catalytic activity of 1,2,4-triazole/Cu/carbon complexes, the highest onset potential observed (0.55 V) was still lower than the onset potential usually observed for commercial Pt/C catalysts (0.9 V)[189]. Thus, much improvement was still needed in order for our catalysts to be commercially viable.

One of the methods used to increase the activity that is commonly employed by electrochemists, is known as pyrolysis. Pyrolysis or heat treatment is performed in 1 inch tubular furnace from ATS systems that can reach temperatures up to 1100 ^{0}C. Typically, 30 mg of the sample is placed in a coors boat, carefully spreading the sample along the length of the boat. The sample is introduced into a quartz tube at the center for the furnace, and air sealed. Nitrogen gas is passed through the tube for 30 minutes before starting to increase the temperature to the desired value. Samples are pyrolyzed for one hour at the desired temperature. The yield after heat treatment ranges from 70-50% depending on the pyrolysis temperature. It is reported that the performance of the ORR catalysts improves by several orders of magnitude after they are pyrolysed[76]. Additionally the material resulting from the heat treatment is known to favor a four-electron reduction process as opposed to a two-electron reduction process[190].

Before attempting pyrolysis, we decided to slightly alter the synthetic strategy for triazole-hemiphthalocyanines. The intent behind this change was to swap the groups that anchor triazoles to the carbon surface, as well as to test different non precious metal complexes. The anchor group in compounds **5.10** and **5.12** is the triazole. We believed that by changing the anchor group to the aromatic ring, we could introduce an extra amino group as well as increase the availability of the triazole for metal

coordination. The anchor group can be switched from the triazole to the aromatic ring in isoiminoindole by applying metal templated cyclization reaction strategy. 4-amino phthalonitrile was immobilized on the carbon surface using the diazotization strategy. Metal templated reaction with 3,5-diamino-1,2,4-triazole was then carried out to generate the metal coordinated triazole-hemiphthalocyanin (Pc). Five complexes containing different metals were synthesized in this fashion.

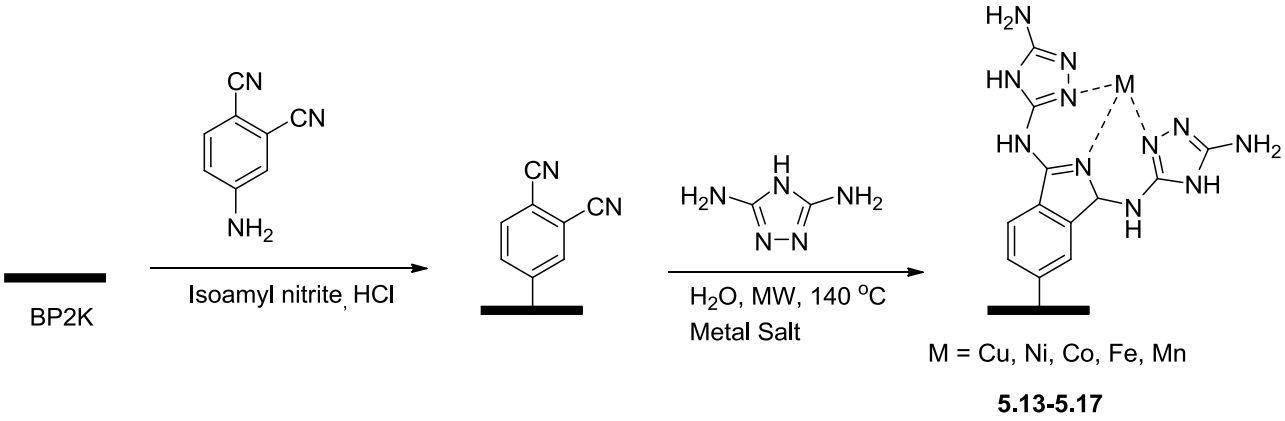

Figure 5-28 - Metal templated synthesis of triazolo-hemiphthalocyanine (Pc)

All the five hemi-phthalocyanines, Cu-Pc, Ni-Pc, Co-Pc, Fe-Pc and Mn-Pc were pyrolyzed using the conditions described earlier. As expected, substantial increase in the activity was observed across the board. **Figure 5-29** shows the RDE curves obtained for these samples. Cu-Pc and Co-Pc samples showed the best onset potential (0.84 V vs. RHE) among this set. Co-Pc had better current density than Cu-Pc. Nickel, Manganese and Iron complexes showed much lower activities both in terms of onset potential and the current densities than the copper and cobalt complexes. Cu and Fe materials showed peak activity when heat treated at 900 ^{o}C, Co and Mn materials at

700 ^{o}C and Ni at 800 ^{o}C. The number of electrons transferred during the ORR was determined via RRDE and ranges from 3.4 for Ni to 3.9 for Cu complexes **(Figure 5-30)**.

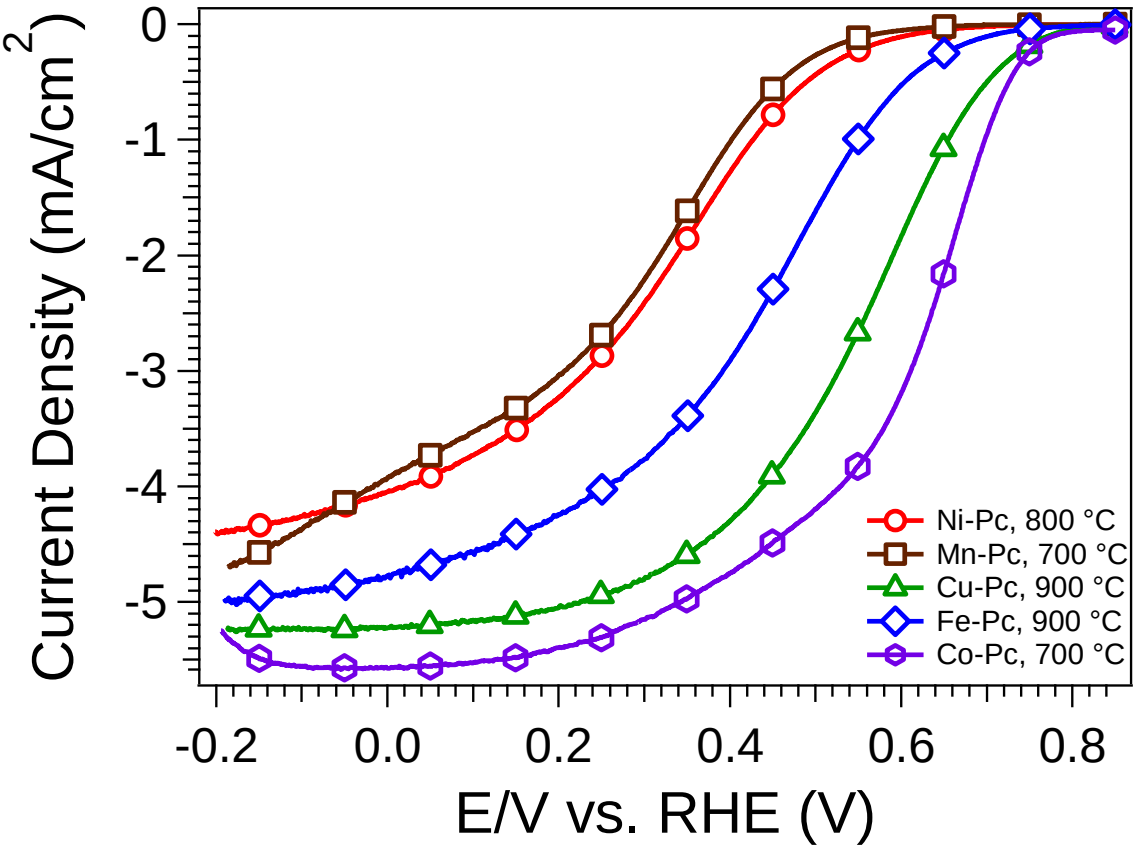

Figure 5-29 - ORR activity of pyrolyzed Metal-Pc catalysts immobilized on BP-2K

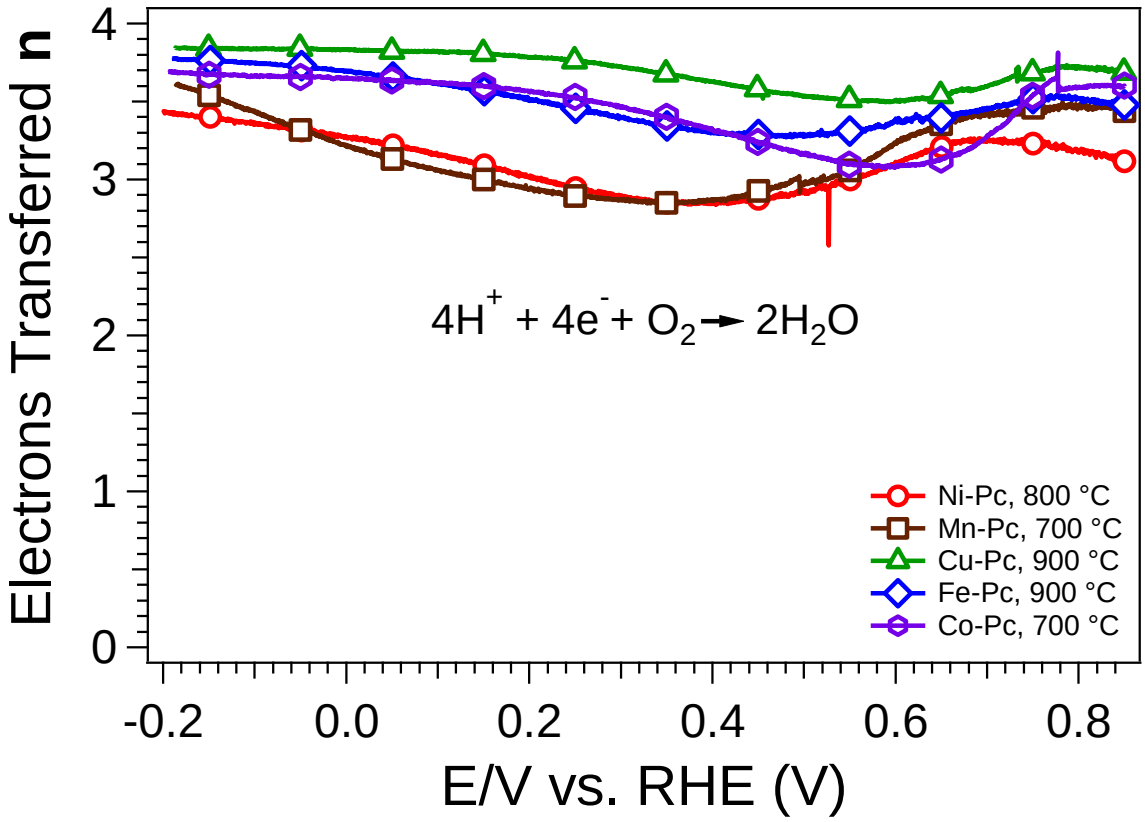

Figure 5-30 - Number of electrons transferred for M-Pc samples

Various theories have been proposed for the structure of the entity formed after pyrolysis. Yeager proposed a model for the ORR active site in which the heat-treated macrocycles are broken down to form surface nitrogen sites that coordinate transition metals remaining from the parent macrocycle, present as impurities in the carbon support, or deliberately added after pyrolysis[191-193]. Strelko et al. modeled the electron-donating properties of carbon containing hetero-atoms and found that replacing carbon with nitrogen improves the ability of the carbon black to donate electrons to O_2 or other reactants. In simplified terms, nitrogen can be viewed as an n-type dopant, such that when it replaces carbon in the matrix, the plane will contain an extra electron that is more easily donated, which in turn improves catalytic activity [194-195].

Due to the ambiguity about the nature of the material formed after the pyrolysis, it was important to confirm the effects of the methods of preparation. We investigated the catalytic activity of adsorbed and immobilized complexes as a function of the preparation method and the ligand used. To illustrate this, Co complexes were used. Adsorbed samples were prepared with Co-3,5-diamino-1,2,4-triazole complexes deposited on oxidized BP-2K. Immobilized samples were prepared attaching 3,5-diamino-1,2,4-triazole and Pc ligands to untreated BP-2K, via diazonium coupling.

The results from RDE experiments showed that the preparation method and ligand used have an effect in the pyrolysis temperature at which the samples presented peak catalytic activity as well as in the onset potential. For instance, adsorbed Co-3,5-diamino-1,2,4-triazole reaches maximum activity at 950 ^{o}C, while immobilized Co-3,5-diamino-1,2,4-triazole activity peaks at 700 ^{o}C. When Pc ligand was used instead of 3,5-diamino-1,2,4-triazole, the activity improved significantly. **Figure 5-31** compares adsorbed and immobilized Co-3,5-diamino-1,2,4-triazole samples with immobilized Co-Pc.

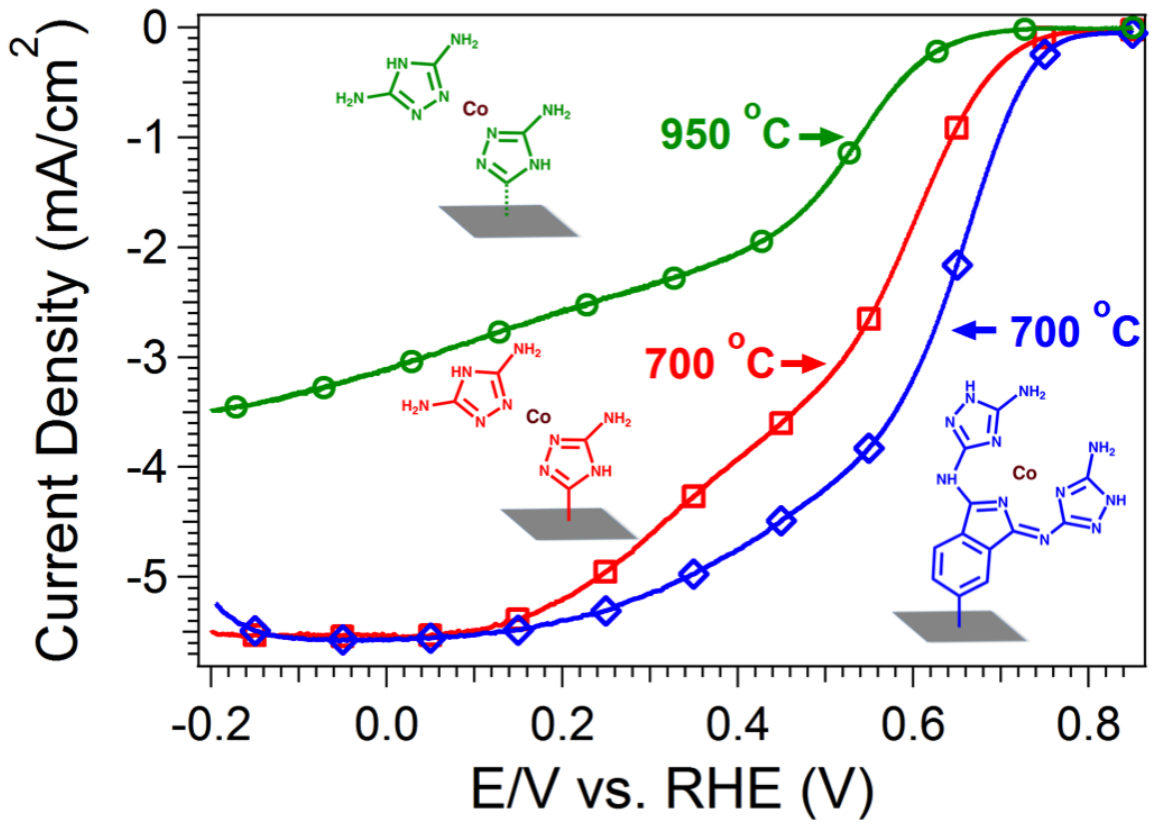

Figure 5-31 - Comparison ORR activity of pyrolyzed Co catalysts, adsorbed and immobilized on BP-2K. Adsorbed Co-3,5-diamino-1,2,4-triazole (green circles), immobilized Co-3,5-diamino-1,2,4-triazole (red squares) and immobilized Co-Pc (blue diamonds)

Comparing the activities of adsorbed and immobilized Co-3,5-diamino-1,2,4-triazole, it can be clearly seen that the preparation method has a substantial impact on the activity. In general, immobilized Pc ligands have higher density of catalytic centers resulting in higher catalytic activity. Moreover, the covalent bond between ligand and carbon in the immobilized samples increases the stability of the catalyst. No reduction in activity was observed even after 200 cycles in case of Co-Pc complexes. The Pc ligand contains more carbon and nitrogen in its aromatic rings than 3,5-diamino-1,2,4-triazole

ligand, allowing the formation of more presumed M-N catalytic centers. This process is equivalent of enriching the catalyst with a heat treatment in a reactive gas such as NH_3.

5.7. Characterization of Surface Modifications

Characterization of carbon surfaces presents unique challenges. Due to the insoluble nature as well as high degree of functional diversity[196-197], usual analytical methods such as NMR, Mass spectrometry and HPLC cannot be applied to verify identity and purity of the synthesized materials. Infrared spectroscopy can be used to perform partial validation of the synthetic steps[198]; however, problems were encountered when trying to distinguish carbon-based ligands from carbon black. High level of background noise and high opacity of sample-KBr pellets prevented routine deployment of IR spectroscopy for characterization purposes. This prompted us to explore other analytical options.

5.7.1. Estimation of loading of reactive functional groups on oxidized carbon black

Loading of amine functional groups on modified carbon surfaces was calculated using Fmoc assay. Amine functionalized carbon black surfaces were treated with standard Fmoc protection conditions (Fmoc-chloride, para-dioxane, water, sodium bicarbonate), followed by thorough washing with water, methanol, DMF and ether to ensure elimination of any leftover or adsorbed Fmoc-chloride. Fmoc groups were removed and quantitated using Fmoc assay conditions as described previously in this chapter.

A somewhat similar strategy was adopted to calculate the loading of carboxylic acids, ketones and aldehydes generated on the carbon surfaces by oxidative pre-treatments. 1-napthylamine was chosen for these experiments owing to its high UV absorbance. The oxidatively pretreated carbons were treated with thionyl chloride to convert the carboxylic acid functionalities to the corresponding acid chlorides. 1-napthylamine was then added to the reaction mixture. At the end of the reaction the supernatant solution was isolated by centrifugation and the residual amount of 1-napthylamine was measured using UV-Vis spectroscopy. The difference between this amount and the original amount used for the reaction gave the loading of oxidatively pretreated surfaces. One important drawback of this method was lack of selectivity between carboxylic acid, carbonyl and aldehyde groups. However, this method did give a general approximation of the effect of oxidative pre-treatments on the carbon surface.

5.7.2. Validation of synthetic steps

In order to validate the synthetic steps carried out on carbon surfaces we decided to employ XPS. XPS, or X-Ray photo-electron spectroscopy, is a popular quantitative spectroscopic technique[198-200] used to investigate the chemical composition of surfaces. It can be used to measure the chemical and electronic states, elemental composition and empirical formula of elements in a particular material.

Photoelectron spectroscopy utilizes photo-ionization and analysis of the kinetic energy distribution of the emitted photoelectrons to study the composition and electronic state of the surface region of a sample. The spectra are obtained by irradiating the material with a beam of X-rays (commonly Al Kα or Mg Kα) and simultaneously measuring the kinetic energy and number of electrons that escape from the top 1 to 10

nm of the material being analyzed. For each and every element, there will be a characteristic binding energy associated with each core atomic orbital. Each element will thus give rise to a characteristic set of peaks in the photoelectron spectrum at kinetic energies determined by the photon energy and the respective binding energies. Any specific element from a given sample can be identified by its peak at a particular energy. Additionally, the intensity of the peaks is related to the concentration of the element within the sampled region. This technique thus provides a quantitative analysis of the surface composition.

Because of the inability of the various other characterization methods, XPS proved to be the most valuable characterization technique for this project. Characterization of these carbons was necessary to confirm the validity of our proposed chemistry. However the problem with high background from carbon surfaces and the need to distinguish carbon based ligands from carbon surfaces still existed. We had to come up with a plan that would address these issues. To this end, we decided to use the homogeneous counterparts of the carbon immobilized ligands as XPS reference standards (model compounds). We then compared the N1s XPS data on the modified carbon surfaces with the data from reference standards. The results of the XPS experiments for modified Vulcan XC-72 as well as Black Pearls-2000 are shown below. It shows the graphs for both, the ligands alone, as well as the ligands anchored on the surface of carbon, BP-2K. It can be clearly observed that when superimposed, the curves for the ligand itself, and the ligand covalently bound onto the carbon are very similar, thereby validating the synthetic steps performed on the carbon surfaces. A curve for unmodified VulcanXC-72 and BP-2K is also shown, for the purpose of comparison.

The model compounds were synthesized in solution phase. Phenyl group was substituted in all model compounds as a substitute for carbon surface. This was done in order to mimic the polycondensed aromatic rings that populate carbon surfaces and keep the difference between model compounds and immobilized compounds to a bare minimum. **Figure 5-32** shows the model compounds prepared to validate stepwise synthetic route and the XPS data obtained. **Figure 5-33** shows the XPS data for same compounds immobilized on the Vulcan XC-72 surfaces. As can be seen from these figures the XPS curves from modified carbon surfaces match with the XPS curves from model compounds to a fair extent. However, the signal to noise ratio is very low, indicating that the extent of surface modification is limited. Similar results were obtained on all Vulcan XC-72 based materials.

Figures 5-34 and **5-35** show the XPS data on model compounds and immobilized compounds on BP-2K. These compounds were immobilized using the diazotization strategy described previously in this chapter.

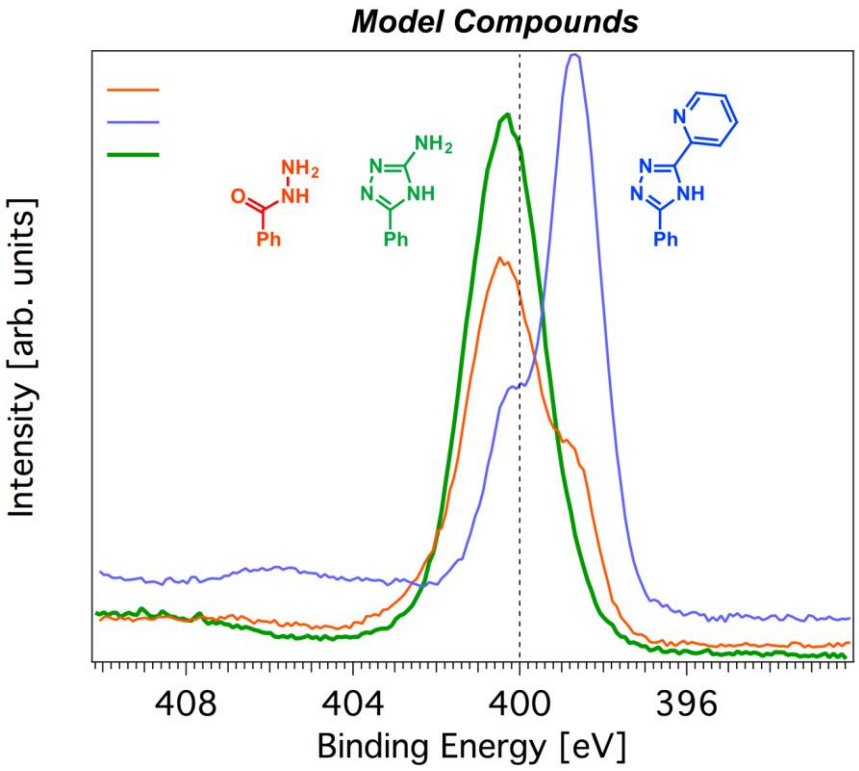

Figure 5-32 – N1s XPS on model compounds prepared to mimic the structure of compounds anchored on carbon surfaces

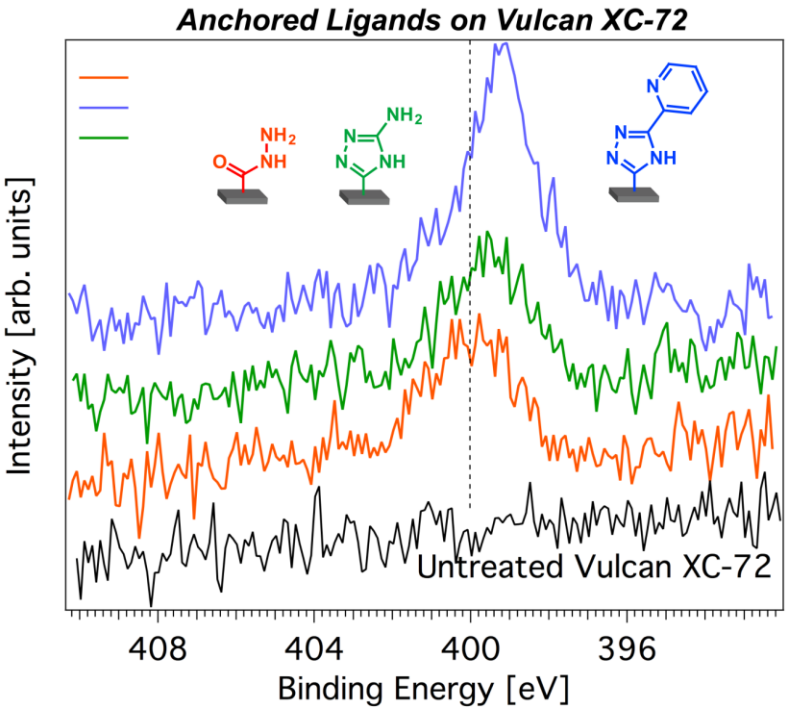

Figure 5-33 - N1s XPS on compounds anchored on vulcan XC-72

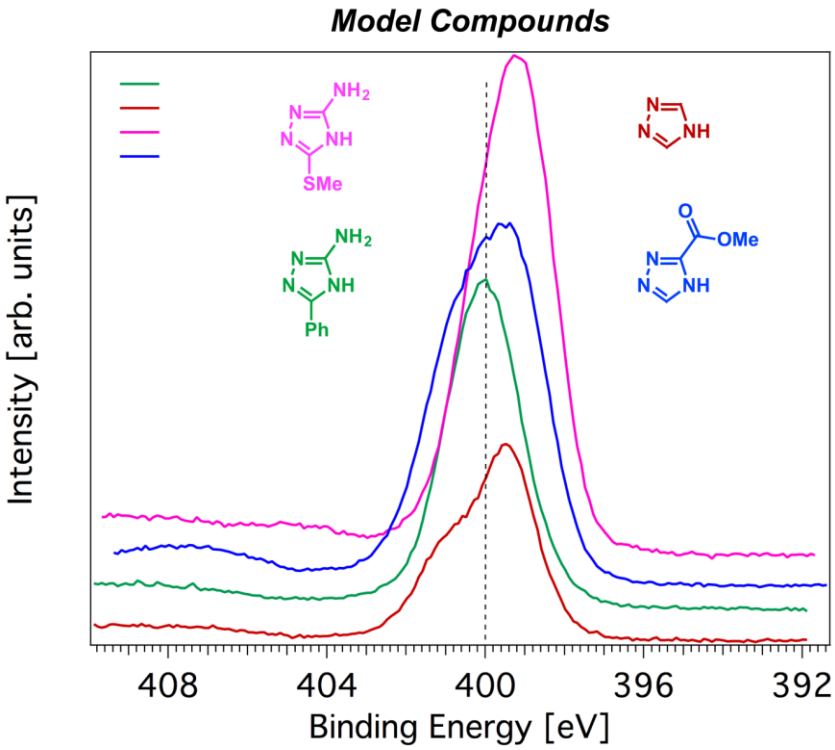

Figure 5-34 - N1s XPS on model compounds prepared to mimic the structure of compounds anchored on carbon surfaces

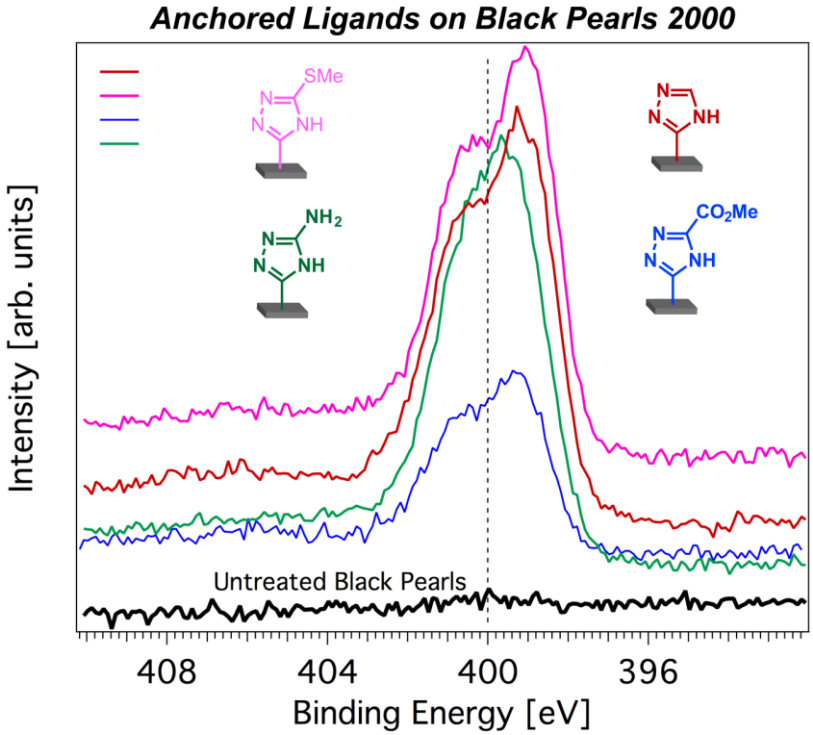

Figure 5-35 - N1s XPS on compounds anchored on BP-2K

As can be seen from the data above, the signal to noise ratio for Black Pearls-2000 is much lower as compared to the Vulcan XC-72. Based on these results we speculate the surface of Black Pearls-2000 is better suited for chemical modification as compared to Vulcan XC-72. This prompted us to abandon the use of Vulcan XC-72 as carbon support and replace it with BP-2K for all future experiments.

Finally, HATR-IR spectroscopy was used to characterize the metal complexes immobilized on the carbon surfaces. The following figures show IR spectroscopy data for 3,5-diamino,1,2,4-triazole and triazolo-hemiphthalocyanines immobilized on the carbon surfaces.

HATR-FTIR technique was utilized to confirm the immobilization of complexes on the carbon after the synthesis. Primary amine (NH_2) groups are present in both Co-3,5-diamino-1,2,4-triazole and Co-Pc complexes supported on BP-2K. These groups are believed to participate in complexation with transition metals. IR peaks corresponding to stretching of the free amine groups are usually observed in the frequency range of 3300 to 3500 cm^{-1}. **Figure 5-36** compares HATR-FTIR spectra of 3,5-diamino-1,2,4-triazole ligand and 3,5-diamino-1,2,4-triazole complex.

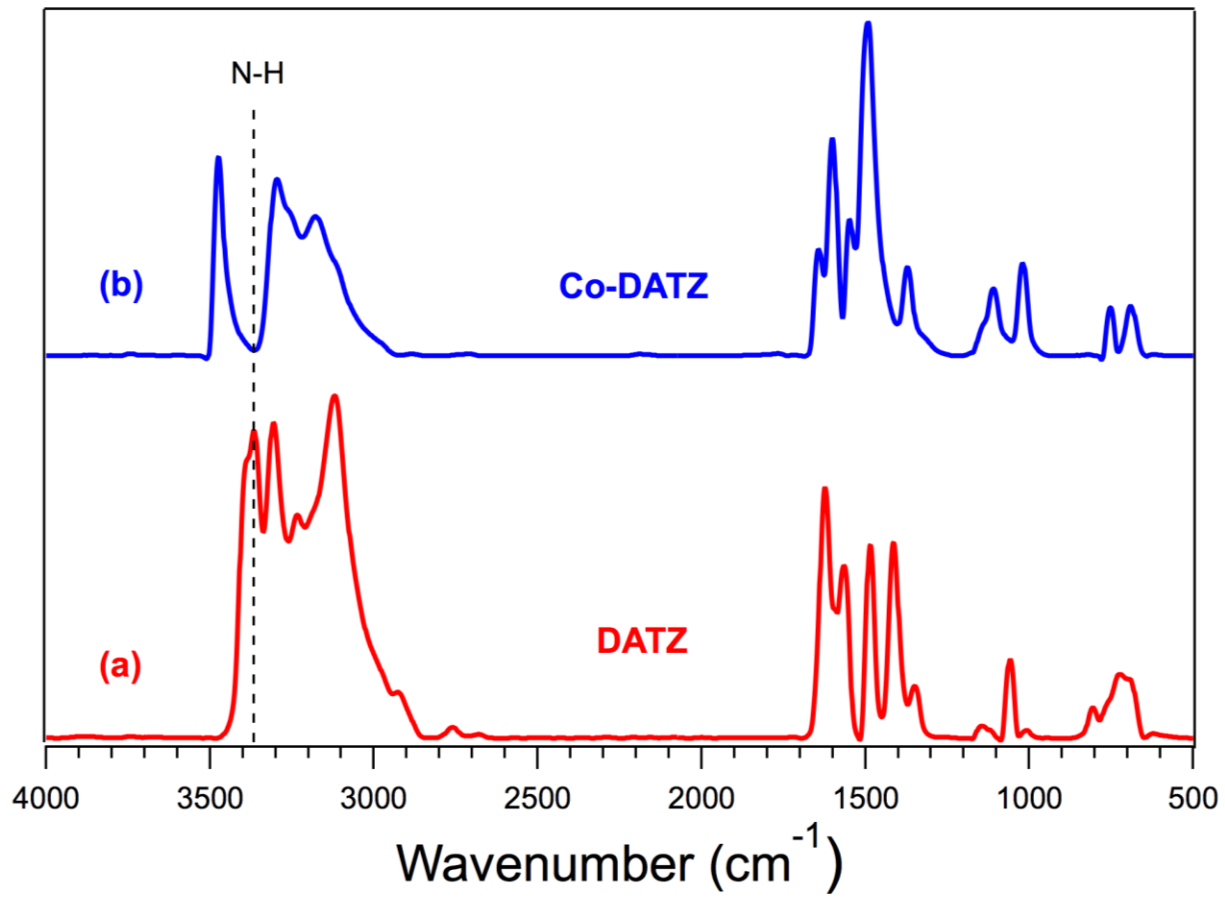

Figure 5-36 - HATR-FTIR data corresponding to (a) 3,5-diamino-1,2,4-triazole ligand (red line) and (b) Co-3,5-diamino-1,2,4-triazole complex (blue line)

As expected, free N-H peaks appear in the proximity of 3400 cm^{-1} in the 3,5-diamino-1,2,4-triazole ligand spectra. Other peaks corresponding to the N-H bend, C-N stretch and C-C stretch in the aromatic rings appear in the 1000 to 1500 cm^{-1} region, but are very difficult to differentiate. Peaks around 1000 cm^{-1} and below are related to C-H bend. It is important to notice that the N-H peak at 3400 cm^{-1} shifts to 3500 cm^{-1} when Co metal is added to form the Co-3,5-diamino-1,2,4-triazole complex. One would expect similar behavior for the complexes supported on carbon. **Figure 5-37** shows HATR-FTIR data for the BP2000 carbon support as a control, the modified carbon after

Pc ligand is attached to the surface via diazo modification, the Co-Pc complex supported on carbon and Co-Pc complex after pyrolysis at 700 ^{o}C.

As can be seen from spectra (a) and (b), the signature peak for free N-H group only appears after the Pc ligand is attached to the carbon support. In spectrum (c) the N-H peak is shifted to 3500 cm^{-1}, as it is expected after the metal is added. Spectrum (d) shows that after pyrolysis at 700 ^{o}C the N-H peak disappears, which can be an indication that a new chemical entity is formed that does not contain the metal coordinated primary amine groups.

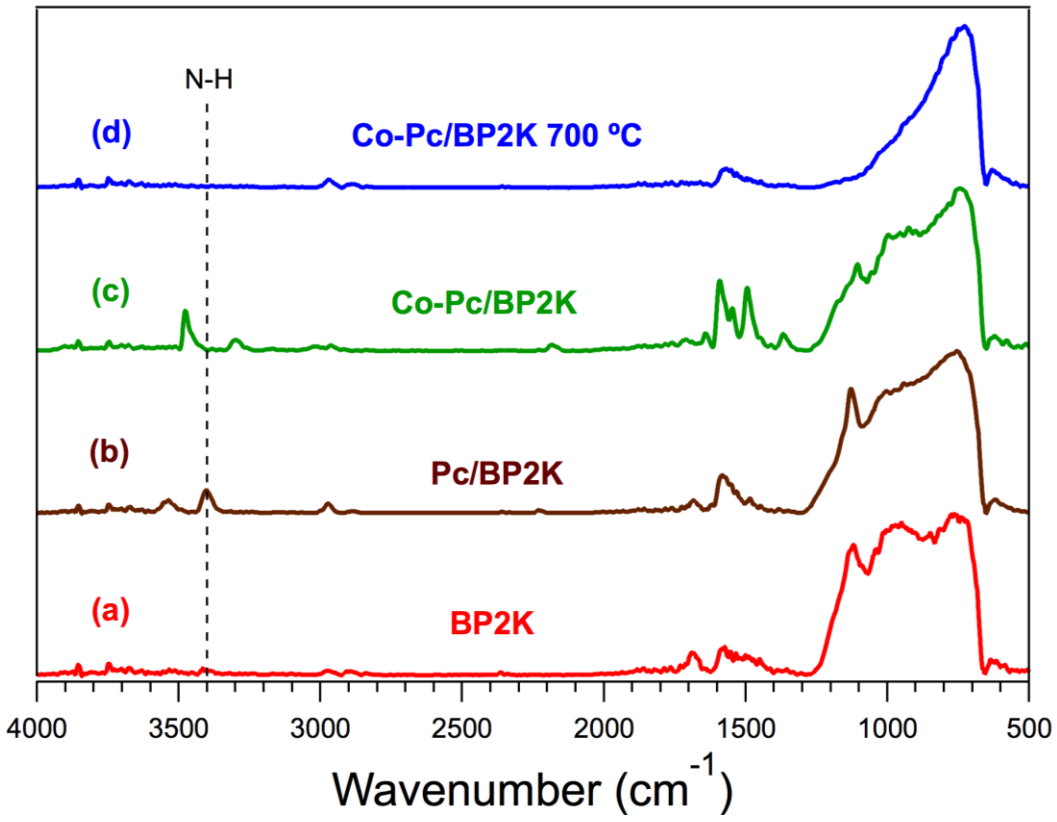

Figure 5-37 - HATR-FTIR data corresponding to (a) BP-2K carbon black (red line), (b) BP-2K diazo modified with Pc ligand (brown line), (c) Co-Pc complex added to the modified carbon (green line) and (d) Co-Pc supported on the modified BP-2Kafter heat treatment at 700 oC (blue line).

5.8. Conclusions

In this study, we developed strategies allowing 1,2,4-triazole ligands to be attached to the macromolecular surfaces in a covalent as well as in an adsorbed manner. This approach offered a means of controlling the reactivity of multifunctional ligands by spatially addressing them in a reaction medium. Techniques such as XPS, loading assays, ICP spectroscopy as well as HATR-IR spectroscopy were employed to verify the success of the synthetic steps. These modified surfaces were used to catalyze ORR in fuel cells, with the eventual goal of replacing expensive Pt/C catalysts currently in use.

A detailed study of adsorption protocols, synthetic methods, structure and activity relationships, choice of metals, choice of metal salts as well as choice of carbon surfaces, was carried out. The electrochemical activities of samples prepared using varying protocols were determined by RDE and RRDE experiments. Copper complexes of 1,2,4-triazoles covalently attached to the carbon surfaces reached onset potentials up to 0.55V vs. RHE and current densities up to 5 mA/cm^2, which are high values among the non-pyrolyzed Cu catalyst reported at acidic pH. In addition, the copper catalyst showed very low hydrogen peroxide production (less than 5%).

Further research led to the synthesis of carbon immobilized non-precious metal complexes of triazolo-hemiphthalocyanines, which when pyrolyzed displayed onset potentials as high as 0.84 V vs. RHE. These values are very close to the commercially available Pt/C catalysts.

While these catalysts show good potential for acidic fuel cells, their activity is enhanced dramatically under alkaline conditions. The application of these catalysts for the development of alkaline fuel cells is worth exploring in the future.

5.9. Experimental

Materials and methods- Reagents and solvents were purchased from various commercial sources and used without further purification unless otherwise stated. Anhydrous solvents were purified using a Grubbs solvent system. Microwave reactions were carried out using Biotage Initiator 2.5 microwave synthesizer. Infrared spectra were recorded on TENSOR Series FT-IR Spectrometer. Vulcan XC-72 (cabot corporation) and BP-2K (cabot corporation) were used as solid supports. XPS measurments were performed at Oak Ridge National Laboratory. Copper was quantified by inductively coupled plasma – optical emission spectroscopy (ICP-OES) using a Perkin Elmer Optima 2100 DV. Absorption spectra were collected on a Thermo Scientific Evolution 600.

General method of oxidative treatment of carbon black surfaces

300 mg of carbon black was added to a solution of 5 mL of 30% hydrogen peroxide and 5 mL of 5M sulfuric acid. The resultant suspension was stirred at room temperature for 26 hours. The crude suspensions were cooled to ambient temperature, centrifuged, and washed with water (10mL x 3), methanol (10 mL x 1), acetone (10 mL x 1), and diethyl ether (10 mL x 1). The carbons were then dried overnight in a vacuum oven.

General method for preparing adsorbed metal complexes of 1,2,4-triazoles on carbon black supports

25 mg of carbon black was added to a 0.5M aq. solution of 1,2,4-triazole (0.25 mmol). 3.875 ml of water was added along with a 0.2M aq. solution of metal (0.125 mmol). The suspension was stirred for 2 hours at 80 ^{o}C. The crude suspensions were cooled to ambient temperature, centrifuged, and washed with water (10mL x 3), methanol (10 mL x 1), acetone (10 mL x 1), and diethyl ether (10 mL x 1). The carbons were then dried overnight in a vacuum oven.

Synthesis of Vulcan XC-72 supported hydrazide

100 mg of oxidatively pretreated carbon black was added to 5 mL of hydrazine hydrate. The resultant suspension was heated in microwave synthesizer at 150 ^{o}C for 6 hours. The crude suspensions were cooled to ambient temperature, centrifuged, and washed with water (10mL x 3), methanol (10 mL x 1), acetone (10 mL x 1), and diethyl ether (10 mL x 1). The carbons were then dried overnight in a vacuum oven.

Synthesis of Vulcan XC-72 supported 3-(2-pyridyl)-1,2,4-triazole (5.1)

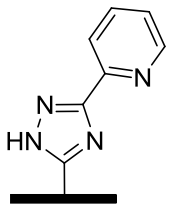

100 mg of hydrazide functionalized carbon was suspended in 10 mls of n-Butanol in a 20 ml microwave vessel. 2-cyanopyridine (2 mmols) and potassium carbonate (0.2 mmols) were added and the reaction was subjected to microwave irradiation for 12 Hrs at 150 ^{o}C. The crude suspensions were cooled to ambient temperature, centrifuged, and washed with water (10mL x 3),

methanol (10 mL x 1), acetone (10 mL x 1), and diethyl ether (10 mL x 1). The carbons were then dried overnight in a vacuum oven.

Synthesis of Vulcan XC-72 supported 3-amino-1,2,4-triazole (5.2)

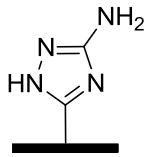

100 mg of hydrazide functionalized carbon was suspended in 10 mls of n-Butanol in a 20 ml microwave vessel. s-methyl isothiourea (2 mmols) and potassium carbonate (0.2 mmols) were added and the reaction was subjected to microwave irradiation for 12 hours at 150 ^{o}C. The crude suspensions were cooled to ambient temperature, centrifuged, and washed with water (10mL x 3), methanol (10 mL x 1), acetone (10 mL x 1), and diethyl ether (10 mL x 1). The carbons were then dried overnight in a vacuum oven.

General method for nitration of polycondensed aromatic rings of carbon black surface

2.0 g of XC-72 carbon black was added to a 500 ml round bottom flask. This was suspended in 100 mL of acetic anhydride. 20 mL of fuming nitric acid was then added, and then 5 mL of sulfuric acid was added as well. The reaction was left stirring at room temperature for 24 hours. The crude suspensions were cooled to ambient temperature, centrifuged, and washed with water (10mL x 3), methanol (10 mL x 1), acetone (10 mL x 1), and diethyl ether (10 mL x 1). The carbons were then dried overnight in a vacuum oven.

General method for reduction of nitro group immobilized on carbon black surface

1.5 g of nitrated carbon black was suspended in 50 ml of methanol and 2 g of $SnCl_2$ was added. The suspension was refluxed overnight. The crude suspensions were cooled to ambient temperature, centrifuged, and washed with water (10mL x 3), methanol (10 mL x 1), acetone (10 mL x 1), and diethyl ether (10 mL x 1). The carbons were then dried overnight in a vacuum oven. Fmoc assay was carried out on the dried material. Loading was found to be 0.089 mmol/gm.

Synthesis of vulcan XC-72 supported 3,5-diamino-1,2,4-triazole via diazotization of amino modified Vulcan XC-72 (5.3)

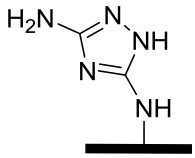

To a suspension of 100 mg of amino modified XC-72 in 5 ml of 50% aqueous hydrochloric acid was added a solution of 100 mg Sodium Nitrite dissolved in 5 ml of water. Resulting suspension was stirred for 30 minutes. Residue was isolated by centrifugation and re-suspended in 5 ml of water. 100 mg of 3,5-diamino-1,2,4 triazole and 139 mg of potassium carbonate were added to the suspension. The reaction was stirred at room temperature for 36 hours and then at 60 ^{o}C for 2 hours. The crude suspensions were cooled to ambient temperature, centrifuged, and washed with water (10mL x 3), methanol (10 mL x 1), acetone (10 mL x 1), and diethyl ether (10 mL x 1). The carbons were then dried overnight in a vacuum oven.

General method for covalently immobilizing 1,2,4-triazoles on untreated carbon black surfaces via diazotization

5 ml of 0.5M aq. amino triazole solution was added to 500 mg of carbon black. 1.083 ml of 6M HCl (6.5 mmol) was added to this suspension. The reaction mixture was placed in an ice bath and cooled to 0 ^{o}C. 2.75 ml of 1M aq. solution of sodium nitrite ($NaNO_2$) was then added slowly over 10 minutes. This suspension was allowed to stir at 0 ^{o}C for 10 minutes, after which it was warmed to room temperature and stirred for 1 hour. The crude suspension was then centrifuged, and washed with water (10mL x 3), methanol (10 mL x 1), acetone (10 mL x 1), and diethyl ether (10 mL x 1). The carbons were then dried overnight in a vacuum oven.

Synthesis of carbon black supported 1,2,4-triazole (5.4)

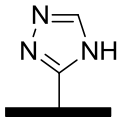

Synthesized as per general method for covalently immobilizing 1,2,4-triazoles on untreated carbon black surfaces, using 3-amino-,1,2,4-triazole. Characterized by XPS.

Synthesis of carbon black supported 3-(2-pyridyl)-1,2,4-triazole (5.5)

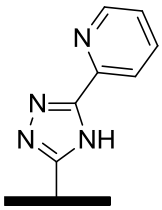

Synthesized as per general method for covalently immobilizing 1,2,4-triazoles on untreated carbon black surfaces 5.8.9, using 3-(2-pyridyl)-5-amino-1,2,4-triazole. Characterized by XPS.

Synthesis of carbon black supported methyl-1,2,4-triazole-3-carboxylate (5.6)

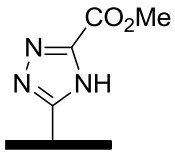

Synthesized as per general method for covalently immobilizing 1,2,4-triazoles on untreated carbon black surfaces, using methyl 5-amino-1,2,4-triazole-3-carboxylate. Characterized by XPS.

Synthesis of carbon black supported 3-methylthio-1,2,4-triazole (5.7)

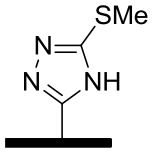

Synthesized as per general method for covalently immobilizing 1,2,4-triazoles on untreated carbon black surfaces using 3-methylthio-5-amino-1,2,4-triazole. Characterized by XPS.

Synthesis of carbon black supported 3-amino-1,2,4-triazole (5.8)

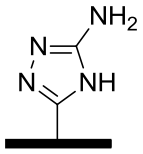

Synthesized as per general method for covalently immobilizing 1,2,4-triazoles on untreated carbon black surfaces using 3,5-diamino-1,2,4-triazole. Characterized by XPS.

Synthesis of carbon black supported triazolohemiphthalocyanine mimic [3-((1,2,4-triazol-5-yl)imino)isoindolin-1-ylidene)-1H-1,2,4-triazole-3,5-diamine] (5.10)

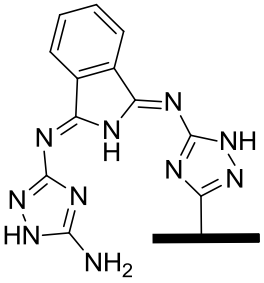

5.8 (200 mg) was suspended in a solution of 1,3-diiminoisoindole (0.8 mmol) in ethanol (5 mL) in a 10 mL microwave vessel. The resulting suspension was heated to 160 °C for 12 hours in a microwave reactor. The crude suspensions were cooled to ambient

temperature, centrifuged, and washed with water (5mL x 1), methanol (5 mL x 1), acetone (5 mL x 1), and diethyl ether (5 mL x 1). The carbons were then dried and re-suspended in a solution of 3,5-diamino-1,2,4-triazole (0.8 mmol) in ethanol (5 mL) in a 10 mL microwave vessel. The resulting suspension was heated to 160 °C for 12 hours in a microwave reactor. The crude suspensions were cooled to ambient temperature, centrifuged, and washed with water (5mL x 1), methanol (5 mL x 1), acetone (5 mL x 1), and diethyl ether (5 mL x 1). The carbons were then dried to give triazole-hemiphthalocyanine **5.10. Compound 5.12** was prepared by repeating the above steps.

General method for metal complexation of covalently modified carbon surfaces with auxillary ligands

25 mg of covalently modified carbon black was added to a 0.5M aq. solution of auxiliary ligand (0.25 mmol). 4 ml of water was added along with a 0.5 M aq. solution of metal (0.25 mmol). The suspension was stirred for 2 hours at 80 ^{o}C. The crude suspensions were cooled to ambient temperature, centrifuged, and washed with water (10mL x 3), methanol (10 mL x 1), acetone (10 mL x 1), and diethyl ether (10 mL x 1). The carbons were then dried overnight in a vacuum oven.

General method for metal complexation of covalently modified carbon surfaces without auxillary ligands

25 mg of covalently modified carbon black was added to 4.5 ml of water. 0.5 M aq. solution of metal (0.25 mmol) was then added. The suspension was stirred for 2 hours

at 80 ^{o}C. The crude suspensions were cooled to ambient temperature, centrifuged, and washed with water (10mL x 3), methanol (10 mL x 1), acetone (10 mL x 1), and diethyl ether (10 mL x 1). The carbons were then dried overnight in a vacuum oven.

Synthesis of alternate triazolo-hemiphthalocyanines (5.13-5.17)

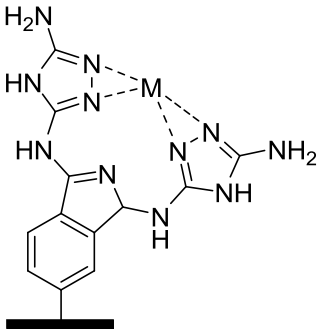

M = Cu, Ni, Co, Fe, Mn

BP2000 (2 g) was suspended in a solution of 4-aminophthalonitrile (8 mmol) in acetone (40 mL). The resulting suspension was stirred vigorously at 0 °C as isoamyl nitrite (10 mmol) and glacial acetic acid (10 mmol) was added. The carbon slurry was then stirred at 0 °C for an additional 10 minutes and for 1 hour at ambient temperature. The carbon mixture was then diluted back to a volume of 40 mL with acetone and agitated in a sonic bath at 60 °C for 10 minutes. The suspension was then centrifuged and the carbon was washed with acetone (40 mL x 3) and diethyl ether (40 mL). The carbon was then dried overnight in a vacuum oven to give 2.568 g of dry modified carbon.

Modified BP2000 (100 mg) was suspended in aqueous solutions of 3,5-diaminotriazole (1 mmol) and the desired non-precious metal (0.5 mmol). Water was then added to adjust the total reaction volume to 5 mL and the resulting suspension was heated to 140 °C for 4 hours in a microwave reactor. The crude suspensions were cooled to ambient temperature, centrifuged, and washed with water (5mL x 1), methanol (5 mL x 1), acetone (5 mL x 1), and diethyl ether (5 mL x 1). The carbons were then dried overnight in a vacuum oven.

ICP-OES Methodology. The supernatant recovered from the first centrifugation cycle after complexation reactions was diluted by a factor of 100. Samples from the initial 0.2 or 0.5 M metal stock solutions were treated in the same manner. Quantification of metals was determined using an external calibration curve ranging from 100 ppm – 1 ppm at various wavelengths.

6. *Novel Ni(II)-1,2,4-triazole complexes as catalysts for direct aziridination of alkenes with organic azides*

6.1. General Research Strategy

We began our investigation by examining the catalytic activity of 1,2,4-triazole complexes with cobalt and nickel. Our aim from the onset was to develop a practical and efficient methodology for synthesis of aziridines. We chose p-nitrophenylazide as the azide component and cis-cyclooctene as the alkene to serve as the model system[201] **(scheme 6-1)**. This choice was primarily based on prior reports where this system was shown to have high reactivity in terms of aziridine synthesis. The reactivity of cis-cyclooctene is presumably due to steric strain inherent in the 8 membered carbocycle.

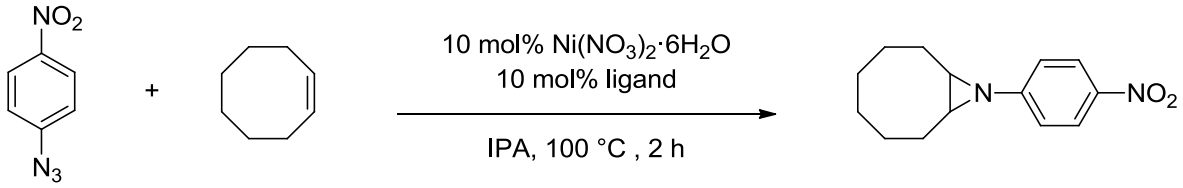

Scheme 6-1 –Model system for optimization study of Ni(II)-1,2,4-triazole catalyzed aziridination reactions

After observing high activity with the model system using nickel (II), we launched a systematic investigation to identify optimal reaction conditions by studying reaction parameters such as catalyst loading, stoichiometry, solvent effect, temperature effect,

ligand scope, metal scope and effect of addition of acid or base. All optimization reactions were performed in triplicate. These results are summarized in following tables.

6.2. Optimization of reaction conditions

Our original observations indicated that the reaction did not work efficiently at temperatures below 60 ^{o}C. Initial choice of metal was partially based on previously reported catalytically active metals and was limited to Ni(II) and Co(II) salts.[95, 99, 202]

The first parameter we chose to explore was solvent effect. As mentioned previously, many existing protocols use the alkene substrate as solvent to increase the yield of the aziridine product. We believed that this practice was disadvantageous from a practical standpoint and in terms of atom economy. Use of an appropriate solvent system was deemed a suitable course of action to overcome this challenge. The reaction was carried out using different solvents to test the effect of solvent polarity on aziridine yields. Surprisingly, yields were highest when either isopropyl alcohol (IPA) or toluene was used as solvent, with IPA being slightly more favorable. Yield depreciated considerably when acetonitrile was used. Dioxanes and water also disfavored the reaction. Other solvents like DCM and methanol were also ineffective. The inability of these two solvents to attain higher temperatures probably played a part in their ineffectiveness as suitable solvents. All further reactions were carried out with IPA at 100 ^{o}C in a closed vessel. **Table 6-1** summarizes these results.

Table 6-1 – Solvent system study

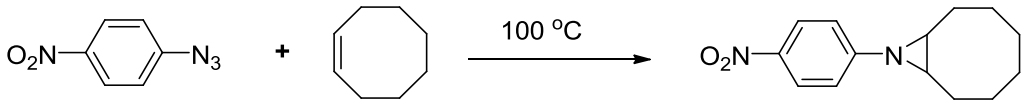

Entry[a]	Solvent	% Conversion[b]	Time
1	IPA	100	2 h
2	Toluene	95	2 h
3	Acetonitrile	35	2 h
4	Acetonitrile/Water (50%)	26	2 h
5	Dioxane	11	2 h
6	Water	5	2 h

a) Reaction conditions: p-nitrophenyl azide (1 eq.), cyclooctene (2 eq.), reaction concentration 0.25 M w.r.t. azide, Nickel Nitrate hexahydrate (10 mol%), Ligand A (10 mol%), b) Percent conversion of azide to aziridine product as observed by GCMS

Next we turned our attention to identifying the most effective metal species. Various metals have been reported to catalyze aziridination reactions including ruthenium, iron and manganese. There are also known precedents of cobalt-porphyrin complexes catalyzing aziridination.[88, 92, 95, 99, 202-203] However, to the best of our knowledge no nickel complexes have been reported to date that catalyze aziridination of organic azides. We observed, that while using the same triazole ligand the complexes made using Ni(II) salts were substantially more active than the complexes made using Co(II) salts. Over the course of the investigation we screened iron, manganese and

copper complexes in addition to cobalt and nickel. Nickel complexes consistently demonstrated better catalytic activity than all other metals tested. Metal salts in the +1 oxidation state for all of the above metals were also ineffective. Selected results are summarized in **table 6-2**.

Table 6-2 – Metal Scope

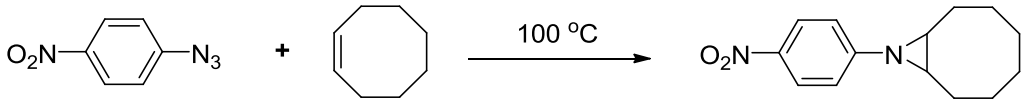

Entry[a]	Metal	% Conversion[b]	Time
1	Nickel (II) Nitrate Hexahydrate	100	2 h
2	Cobalt (II) Nitrate	77	2 h
3	Iron (II) Perchlorate	32	2 h
4	Iron (III) Nitrate	Nil	2 h
5	Manganese (II) Acetate	25	2 h
6	Copper (II) Chloride	Nil	2 h
7	No Metal	Nil	2 h
8	No Ligand (Nickel (II) Nitrate Hexahydrate)	18	2h

a) Reaction conditions: p-nitrophenyl azide (1 eq.), cyclooctene (2 eq.), reaction concentration 0.25 M w.r.t. azide, IPA used as solvent, Metal (10 mol%), Ligand A (10 mol%), b) Percent conversion of azide to aziridine product as observed by GCMS

Control experiments carried out without ligand showed minor activity whereas control experiments carried out without any metal resulted in no activity at all.

The complexes were either formed in situ or isolated and used to carry the aziridination reaction. A dark yellow – brown solid was formed after stirring the metal salt and the ligand together for approximately 15 minutes in IPA which could be isolated and used to set up a new reaction or the heterogeneous solution could be used as is. We noticed consistently higher results when using in-situ generated catalyst. The observations made during optimization studies of catalyst loading indicated that the reaction protocol worked well with catalyst loading at 1 mol%. However, the reactions times are greatly accelerated at 10 mol% catalyst loading, enhancing the practical usefulness of the reaction. **Table 6-3** lists the results from the experiments carried out to test the effect of catalyst loading. The catalyst loading was maintained at 10 mol% through the screening process until very late stage of research when we made a serendipitous discovery that led to a substantial reduction in catalyst loading while maintaining high aziridine yields and turnover rate. We were able to get these results by using the supernatant solution from the complex formation reaction. This supernatant could be evaporated to isolate the active catalytic species which proved to be far more catalytically active than the isolable solid precipitate formed during the reaction. The revised stoichiometric calculations showed that only a mole percent of active catalytic species was sufficient to catalyze aziridination reaction between p-nitrophenylazide and cyclooctene in 2 hours. **Table 6-3** reports some of the observed results with different loadings of catalyst.

Table 6-3 – Catalyst Loading

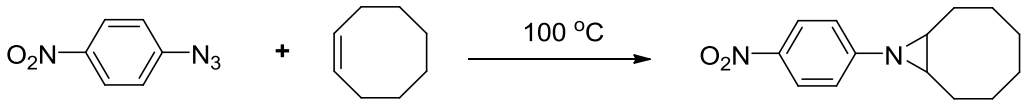

Entry[a]	Catalyst Mol %	Time Required for Complete Conversion of Azide[c]
1	10	2 h
2	5	6 h
3	1	12 h
4[b]	1	2 h
5[b]	0.1	6 h

a) Reaction conditions: p-nitrophenyl azide (1 eq.), cyclooctene (2 eq.), reaction concentration 0.25 M w.r.t. azide, IPA used as solvent, nickel nitrate hexahydrate (quantity as specified in table), Ligand A (quantity as specified in table), b) Supernatant isolated from complexation reaction used as catalyst, c) Indicated by GCMS

Next, we carried out reactions to test the effect of stoichiometry on the aziridine yields. In particular, we looked at alkene equivalency with respect to the azide. There have been a few reports of successful aziridination reactions with use of 5 to 29 equivalents of alkenes[95-96, 201, 203]. Using a large excess of alkene is a big hurdle in the synthetic practicality of these reactions. Thus, we began our screening by looking at 5, 2 and 1 equivalents of alkenes. As expected the reaction works much better with 5 eq. of alkene. However, we were able to cut down alkene equivalents to 2 and still get

respectable results. At 1 eq. of alkenes the reaction was observed to be much more sluggish. These results are summarized in **table 6-4.**

Table 6-4 – Alkene stoichiometry optimization

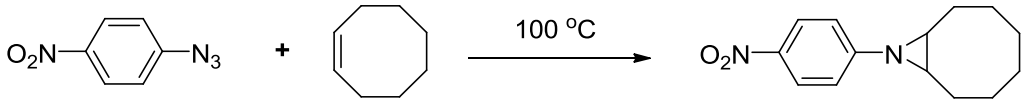

Entry[a]	Equivalents of alkene	% Conversion[b]	Time
1	5	68	1 h
2	2	48	1 h
3	1	22	1 h

a) Reaction conditions: p-nitrophenyl azide (1 eq.), cyclooctene (quantity as indicated in the table.), reaction concentration 0.25 M wrt azide, IPA used as solvent, Nickel Nitrate hexahydrate (10 mol%), Ligand A (10 mol%), b) Percent conversion of azide to aziridine product as observed by GCMS

Once we observed that triazole-metal complexes catalyzed aziridination reactions, we tested multiple analogues containing the 1,2,4-triazole moiety. Some of the notable ligands are listed in **figure 6-2**. **Table 6-5** describes observed activity of these ligands. We observed that the presence of 3,5-disubstitutions had more pronounced effect on activity as compared to triazoles with other substitution patterns. Heteroatom containing substituents such as 3,5-dipyridyl-1,2,4-triazole and 3-mercapto 5-amino triazoles were observed to be most active. It is worth noting that the activity decreased when the thiol group was replaced by thiomethyl. Replacing substituents at 3- and 5- positions with non-heterocyclic moieties reduced the activity further.

Additionally, introducing a substituent at the 4-position in addition to the existing 3- and 5- substitutions proved to have an adverse effect on activity as well. We speculate that when all three positions (3,4,5) are substituted, the number of metal binding sites are reduced, thus leading to lower catalytic activity.

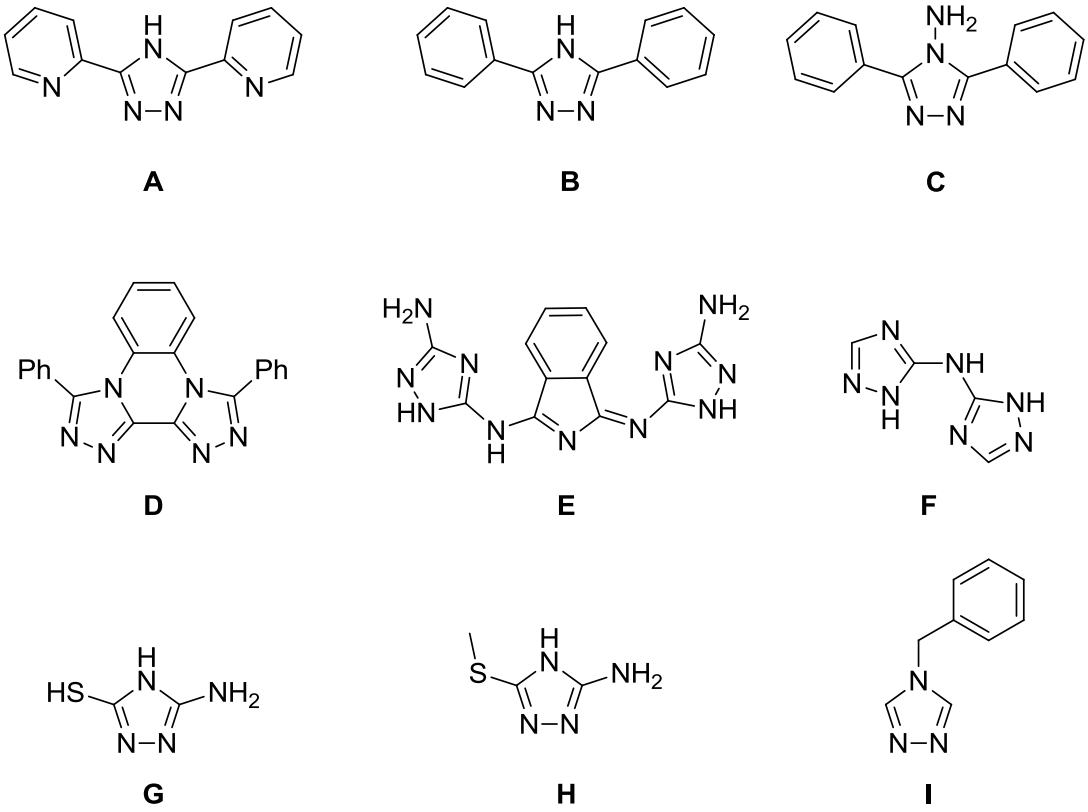

Figure 6-2 – 1,2,4-triazole ligands used in the optimization studies of Ni(II) catalyzed aziridination reaction

Table 6-5 - Ligand Study

Entry[a]	Ligand	% Conversion (cyclooctene)[b]	% Conversion (ethyl acrylate)[b]	Time
1	**A**	100	45	2 h
2	**B**	72	23	2h
3	**C**	45	Nil	2 h
4	**D**	30	Nil	2 h
5	**E**	62	22	2 h
6	**F**	35	14	2 h
7	**G**	100	62	2 h
8	**H**	67	19	2 h
9	**I**	85	35	2 h
10	**2.5**	100	35	2h

a) Reaction conditions: p-nitrophenyl azide (1 eq.), cyclooctene (2 eq.) or ethyl acrylate (2 eq.), reaction concentration 0.25 M w.r.t. azide, IPA used as solvent , nickel nitrate hexahydrate (10 mol%), Ligands as listed in the table (10 mol%), b) Percent conversion of azide to aziridine product as observed by GCMS

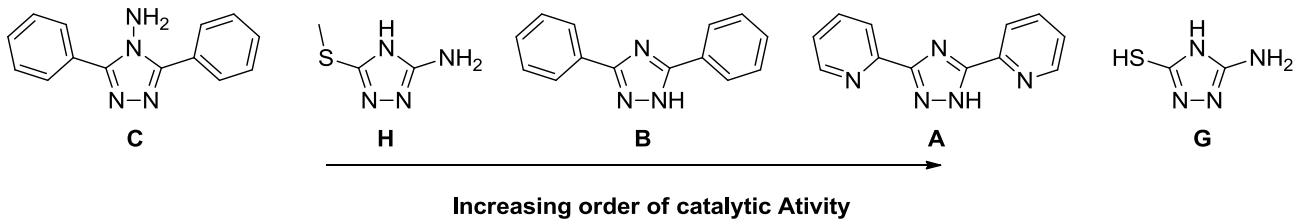

Figure 6-3 - Effect of ligand topology on the activity

We tested the effect of changing the ligand to metal ratio and those results are summarized in **table 6-6**. Reactions were carried out with various ratios of 3-mercapto 5-amino triazole ligand with Nickel (II) nitrate hexahydrate. A clear trend was observed where aziridine yields improved with lower ratios. The optimal ratio was found to be 2:1 suggesting that preferred complexation method of ligand is in bidentate fashion.

Screening reactions were carried out at temperatures ranging from 50 ^{o}C to 120 ^{o}C. At higher temperatures product decomposition was observed while at lower temperatures reaction rates were low generally requiring reaction times in excess of 12 hours. 100 ^{o}C was found to be the optimal temperature at which no product decomposition was observed and reaction completion times were low.

Table 6-6 – Ligand-metal stoichiometry study

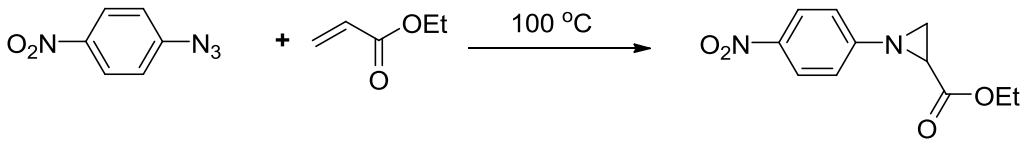

Entry[a]	Ligand to Metal Ratio	% conversion in 2 hours [b]
1	4:1	34
2	3:1	42
3	2:1	66
4	1:1	60
5	0.5:1	44

a) Reaction conditions: p-nitrophenyl azide (1 eq.), ethyl acrylate (2 eq.), reaction concentration 0.25 M wrt azide, IPA used as solvent , Nickel Nitrate hexahydrate , Ligand A, b) Percent conversion of azide to aziridine product as observed by GCMS

It was thought that use of an acid might lead to the protonation of alkene and promote the rate of aziridination. However, addition of either acid or base had adverse effect on activity leading to greatly reduced conversion rates in both cases **(table 6-7)**.

Thus having optimized major reaction parameters we turned our attention towards exploring the substrate scope of optimized reaction protocol.

Table 6-7 - Evaluation of effects of acid/base

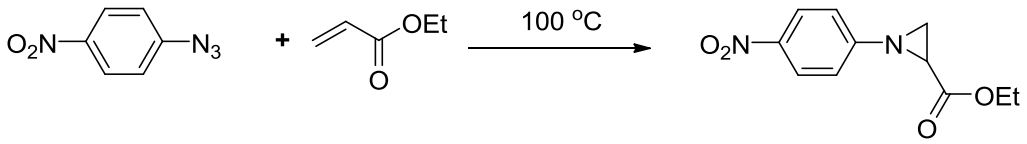

Entry[a]	Acid/Base	% Conversion[b]	Time
1	Triethylamine	12	4 h
2	Trifluoro Acetic Acid	35	4 h

a) Reaction conditions: p-nitrophenyl azide (1 eq.), ethyl acrylate (2 eq.), reaction concentration 0.25 M wrt azide, IPA used as solvent , Nickel Nitrate hexahydrate , Ligand A, b) Percent conversion of azide to aziridine product as observed by GCMS

6.3. Substrate Scope

Table 6-8 details the reactions of p-nitrophenyl azide with various alkyl alkenes. The reaction proceeds smoothly with cyclooctene, cyclopentene and ethylidene cyclohexane. Reaction with cis-octene resulted in moderate yield whereas low yield was observed with Trans-octene. The steric resistance in trans-octene presumably hinders the formation of the aziridine product. Cyclohexene on the other hand was completely unreactive and did not form any aziridine product. This result was surprising since both cyclooctene and cyclopentene were found to be compatible with this system. All products formed were determined to be cis isomers based on NMR data.

Table 6-8 – Alkene substrate scope

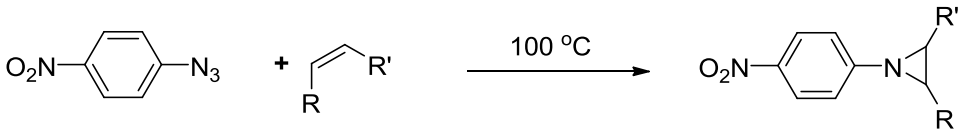

Entry[a]	Alkene	% conversion[b]	Isolated Yield	Time
1	Cyclooctene	100	95	2 h
2	Cyclopentene	70	45	12 h
3	Cyclohexene	Nil	Nil	12 h
4	Cis-octene	56	45	12 h
5	Trans-octene	13	Nil	12 h
6	Ethylidene Cyclohexane	69	60	12 h

a) Reaction conditions: p-nitrophenyl azide (1 eq.), alkene (2 eq.), reaction concentration 0.25 M w.r.t. azide, IPA used as solvent , nickel nitrate hexahydrate , Ligand A, b) Percent conversion of azide to aziridine product as observed by GCMS

Table 6-9 describes reactions of p-nitrophenyl azide with various allyl functionalities. Ethyl Acrylate was the most reactive substrate with near quantitative conversion. Allyl alcohol and acrylonitrile demonstrated moderate reactivity. Reactions carried out with acrylamide, allyl bromide and allyl amine decomposed to form tar with unidentifiable product mixtures.

Table 6-9 –Alkene substrate scope - continued

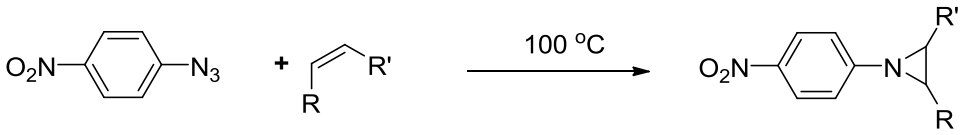

Entry[a]	Alkene	% conversion[b]	Isolated yield	Time
1	Ethyl Acrylate	95	84	4 h
2	Allyl Alcohol	45	30	12 h
3	Ally Amine	Nil	Nil	12 h
4	Allyl Bromide	Nil	Nil	12 h
5	Acrylamide	Nil	Nil	12 h
6	Acrylonitrile	45	55	12 h

a) Reaction conditions: p-nitrophenyl azide (1 eq.), alkene (2 eq.), reaction concentration 0.25 M w.r.t. azide, IPA used as solvent , nickel nitrate hexahydrate , Ligand A, b) Percent conversion of azide to aziridine product as observed by GCMS

Table 6-10 lists reactions of p-nitrophenyl azide with aromatic alkenes. The only successful reaction was with styrene while reactions with α-methyl styrene resulted in very low conversion to aziridine products. Reaction with vinyl pyridine only yielded tar. Cis-stilbene proved to be completely unreactive which can be attributed to the steric hindrance.

Table 6-10 - Alkene substrate scope - continued

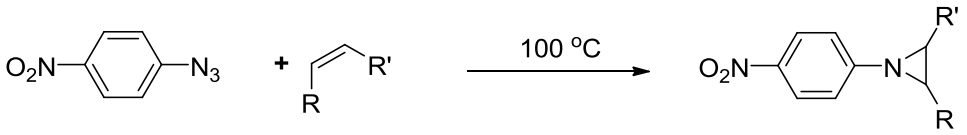

Entry[a]	Alkene	% conversion[b]	Isolated Yield	Time
1	Styrene	75	68	12 h
2	α-Methyl Styrene	22	Nil	12 h
3	4-Vinyl Pyridine	Nil	Nil	12 h
4	Cis- Stilbene	Nil	Nil	12 h

a) Reaction conditions: p-nitrophenyl azide (1 eq.), alkene (2 eq.), reaction concentration 0.25 M w.r.t. azide, IPA used as solvent , nickel nitrate hexahydrate , Ligand A, b) Percent conversion of azide to aziridine product as observed by GCMS

The scope of the reaction was also tested with various azides and **table 6-11** details the results from these experiments. p-Nitrophenyl azide was the most reactive followed by p-methoxy phenyl azide and p-methyl phenyl azide. Not surprisingly no reaction was observed with TMS-azide which is known to be a very unreactive azide. No reaction was observed PhI=NTs as well

Table 6-11 – Azide substrate scope

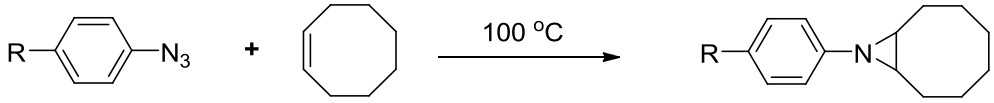

Entry[a]	R	% conversion[b]	Isolated Yield	Time
1	p-OMe	70	65	12 h
2	p-Me	62	55	12 h
3	Benzyl Azide	80	75	12 h
4	TMS-N3	0	0	12 h
5	PhI=NTs	0	0	12 h

a) Reaction conditions: azide (1 eq.), cyclooctene (2 Eq.), reaction concentration 0.25 M w.r.t. azide, IPA used as solvent , nickel nitrate hexahydrate , Ligand A, b) Percent conversion of azide to aziridine product as observed by GCMS

6.4. Active Catalytic Species

Investigations into the ligand-metal ratio **(Table 6-6)** showed that the best activity was observed when the ratio was two. At any other ratio (higher or lower) the activity decreased. This was the first clue to the possible structure of the active catalytic species. ESI mass spectrometry experiments on the in-situ formed complex between $Ni(NO_3)_2$ and 3-mercapto-5-amino-1,2,4-triazole further confirmed the mode of binding by displaying exact mass for 2:1 ligand to metal complex. No counterions were observed in the mass spectrum.

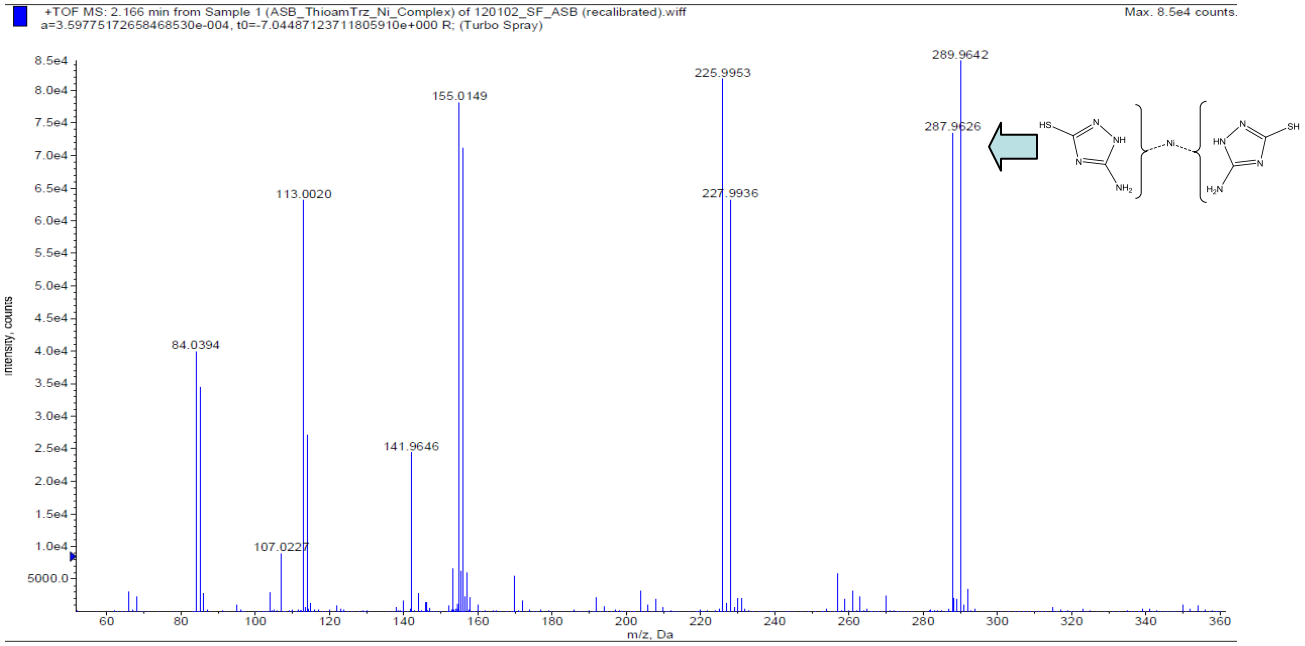

Figure 6-4 –ESI mass spectrum for Ni(II)-3-marcapto-5-amino-1,2,4-triazole complex

Similar results were obtained for other ligands. These observations are consistent with literature reports on nickel complexes of 1,2,4-triazoles. Gabryszewski reported a method of synthesis of Ni(II)-3-mercapto-5-amino-1,2,4-triazole with 2:1 ligand to metal ratio[204]. Using the method described, the complexation reaction was carried out in aqueous base and the complexes were characterized by IR spectroscopy as well as elemental analysis. We synthesized the same complex by following this method. Upon using this complex in the aziridination reaction we observed that the activity was similar to the standard complex prepared in-situ, leading us to believe that both these complexes are identical. Reports on the similar behavior by 3,5-(2-pyridyl)-1,2,4-triazole complexes with nickel salts are also available in the literature[36].

We were unable to get crystals of the aforementioned complexes. The complexes had very low solubility in organic as well as aqueous solvents indicating that

these complexes are polymeric in nature. This is consistent with the prior literature examples which assert the role of 1,2,4-triazoles as bridging ligands.

6.5. Discussion

A number of possible mechanisms have been speculated for the formation of aziridines from azides. The first metal-catalyzed nitrogen atom-transfer process was reported by Kwart and Kahn in a seminal 1967 publication[205], who demonstrated that copper powder promoted the decomposition of benzenesulfonyl azide when heated in cyclohexene. The resulting distribution of products is consistent with the intervention of nitrene (or metal nitrenoid) intermediates **(Figure 6-3)**. Possibilities of nitrene formation are strengthened when the the nitrene sources are precursors such as nosyl- or tosyl-substituted [*N*-(phenylsulfonyl)imino]phenyliodinane and chloramine/bromamine-T.

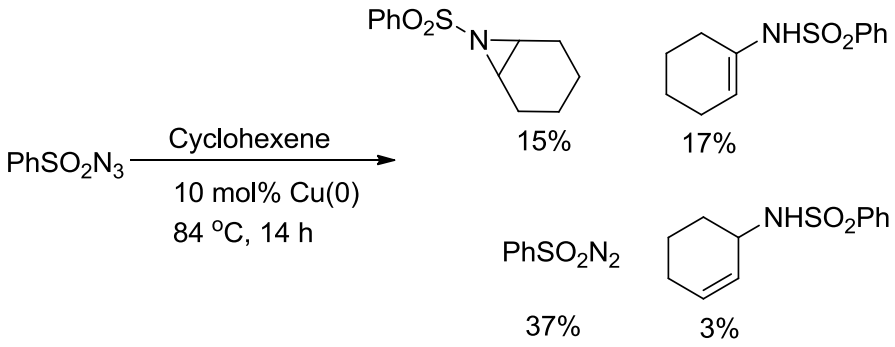

Figure 6-5 – Decomposition of benzenesulfonyl azide with cyclohexene

Bruin and coworkers have postulated a nitrene based mechanism based on computational studies carried out on a porphyrin-Co(II) catalyzed aziridination of olefins with benzenesulfonyl azide[202]. According to their hypothesis the reaction proceeds *via* a

two-step radical addition-substitution pathway. The Co^{II}(por) catalyst reacts with the azide $PhSO_2N_3$ to form a transient adduct, which loses dinitrogen to form the 'nitrene' intermediate. The electronic structure of the 'nitrene radical' is described as a cobalt(III) species with a one-electron reduced nitrene ligand, or alternatively a triplet nitrene interacting covalently with the doublet cobalt(II) centre. The radical addition of the 'nitrene radical' to the C=C double bond of styrene yields a metastable γ-alkyl radical intermediate. This species (in its doublet spin state) readily collapses in an almost barrierless ring closure reaction to form the aziridine.

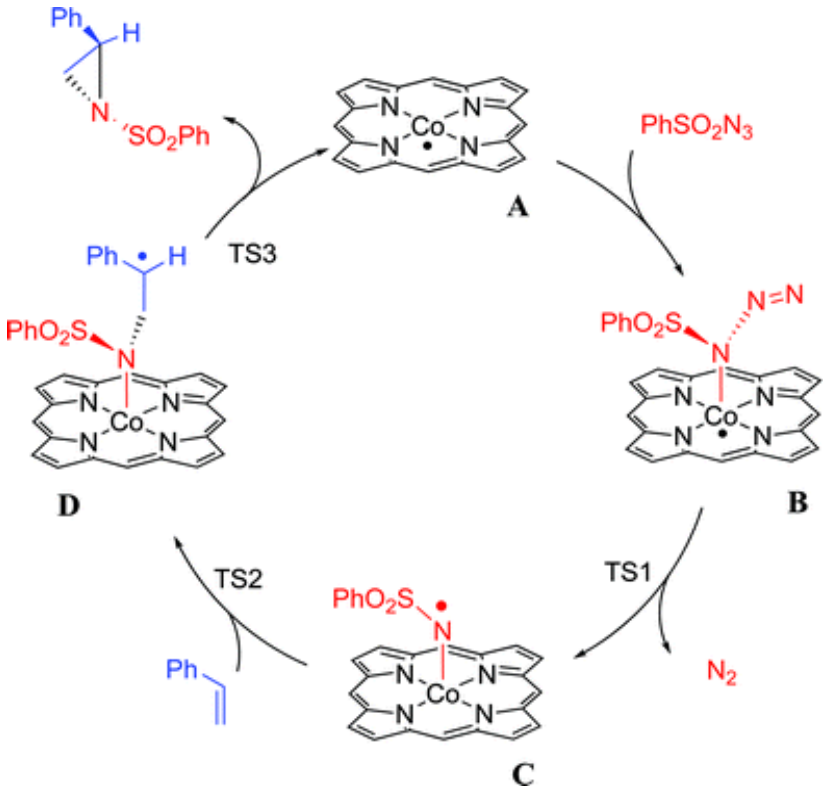

Figure 6-6 – Catalytic cycle for nitrene mediated aziridination reaction[202]

There have been reports of thermal decomposition of organic azides to form nitrene intermediates.[95] During our investigations we carried out reactions of p-nitrophenyl azide with the Ni(II) complex without the addition of alkene and did not see

decomposition of azide even after prolonged heating. However, as noted before we did observe minor amounts of aniline side product formation in presence of both alkene and azide in the reaction. This could be generated from decomposition of unreacted nitrene intermediates.

Another possible mechanism can take place through the formation of 5-membered 1,2,3-triazole ring via therma fusion of alkene and azide[201] **(Figure 6-7).** This intermediate can then undergo rearrangement in the presence of catalyst to give the aziridine product. However the thermal fusion reaction is reported to be very slow. We did not observe this intermediate during any of our studies, possibly ruling out this mechanism

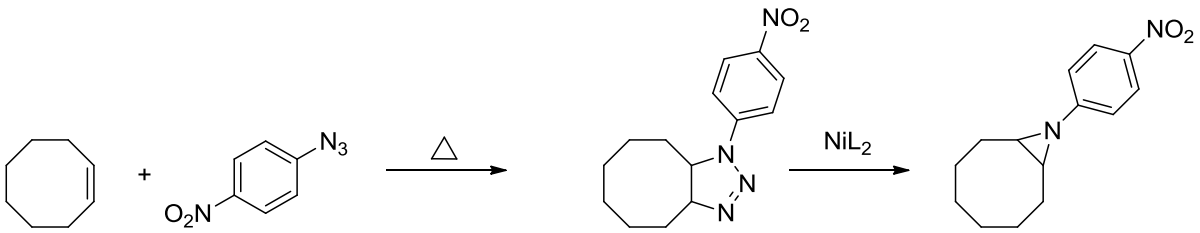

Figure 6-7 – Possible mechanism for formation of aziridine via 1,2,3-triazole intermediate

Thus, based on preceding literature and our observations, we propose that the reaction takes place via metal-nitride intermediate which then leads to the nitrene transfer to alkene to generate aziridine.

6.6. Conclusions

In conclusion, we have described an efficient and practical method towards synthesis of n-aryl aziridines from aryl and benzyl azides under ambient conditions. This reaction is catalyzed by nickel-1,2,4 triazoles complexes which can be prepared in situ. Reaction conditions were optimized via systematic study and a broad substrate scope was observed.

Very few reports on the azirionation of the organic azides exist[96, 203]. Not only are these methodologies lacking in practicality but are also limited in the substrate scope. The novel Ni(II)-1,2,4-triazole catalysts reported herein show excellent tolerance to various alkenes as well as aromatic azides without forming any amination byproducts. This compatibility is very beneficial for their practical application. Additionally, these catalysts do not require huge excess of any reagent as opposed to previously reported methods, while operating efficiently at loadings as low as 1 mol%. Studies towards the reaction mechanism are currently in progress.

6.7. Experimental

Materials and General Methods

Reagents and solvents were purchased from various commercial sources and used without further purification unless otherwise stated. Analytical thin-layer chromatography (TLC) was performed using aluminum backed silica gel TLC plates with UV indicator from Sorbent Technologies. Flash column chromatography was performed using 40-63 μm (230 x 400 mesh) silica gel from Sorbent Technologies. ^{1}H and ^{13}C NMR were recorded at 500 MHz and 126 MHz or at 600 MHz or 151 MHz, respectfully, on a Varian Inova spectrometer. All chemical shifts were reported in δ units relative to tetramethylsilane or the corresponding deuterated solvent. High resolution mass spectra (ESI) were obtained on a JEOL AccuTOF DART spectrometer. Gas chromatography mass spectra were obtained on a HP/Agilent 6890GC/5973MSD spectrometer. Infrared spectra were recorded on a Varian 4100 FT-IR using KBr pellets or KBr salt plates

WARNING: Low molecular weight azides are potentially explosive. Appropriate safety measures should always be taken when handling these compounds.

Ligands

Ligands A, B, C, D, E, F and I were prepared according to procedures described in chapter 2. Ligands G and H were procured from commercial sources. Spectroscopic characterizations were consistent with previously reported data.

Azides

General Azide Method A: Aromatic Azides

The aniline derivative (approx 2 g, 16.24 mmol) was dissolved in 80 mL of EtOAc. 40 mL of 1.5 M HCl was added and the solution cooled to 0 °C in an ice bath. Sodium nitrite (1.68 g, 24.36 mmol) was dissolved in 20 mL water and added dropwise to the reaction solution while stirring at 0°C. After 15 min, sodium azide (3.17 g, 48.72 mmol) was dissolved in 20 mL water and added dropwise to the reaction solution while stirring at 0°C. After slowly warming to room temperature, the reaction was monitored by TLC. Upon completion, the reaction was extracted with EtOAc (x3) and washed with 1 M HCl, water, and brine. The solution was then dried with sodium sulfate and concentrated *in vacuo* to yield the corresponding aromatic azide. Yields: 80 – 94%

General Azide Method B: Aliphatic/Benzylic Azides

The bromine derivative (approx 2 g, 11.17 mmol) was dissolved in 25 mL of dimethylformamide. Sodium azide (799 mg, 12.28 mmol) was added and the reaction was stirred overnight at room temperature. Progress of the reaction was monitored by TLC and GC-MS. Upon completion, the reaction was quenched with 50 mL of water (exothermic) and stirred until reaching room temperature. The solution was then extracted with diethyl ether and washed with water and brine. The solution was then dried with sodium sulfate and concentrated *in vacuo* to yield the corresponding aliphatic azide. Yields: 79 – 98%.

(azidomethyl)benzene

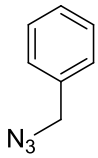

Prepared using general azide method B and isolated as a colorless oil. ^{1}H NMR ($CDCl_3$, 600 MHz) δ 7.40-7.37 (m, 2H), 7.35-7.31 (m, 3H), 4.33 (s, 2H). ^{13}C NMR ($CDCl_3$, 151 MHz) δ 135.5, 129.0, 128.44, 128.35, 54.9. IR (film) v_{max} 2099 cm^{-1}. MS (ESI) *m/z* calculated 106.066 (C_7H_8N, $[M-N_2+H]^+$), *m/z* observed 106.064 (C_7H_8N, $[M-N_2+H]^+$).

1-azido-4-methylbenzene

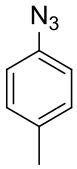

Prepared using general azide method A and isolated as a brown oil. ^{1}H NMR ($CDCl_3$, 600 MHz) δ 7.35 (t, 2H, J = 7.8 Hz), 7.14 (t, 1H, J = 7.8 Hz), 7.03 (d, 2H, J = 7.8 Hz). 2.17 (s, 3H). ^{13}C NMR ($CDCl_3$, 151 MHz) δ 140.0, 129.8, 124.9, 119.1, 18.5. IR (film) v_{max} 2129 cm^{-1}. MS (ESI) *m/z* calculated 106.0657 (C_7H_8N, $[M-N_2+H]^+$), *m/z* observed 106.0651 (C_7H_8N, $[M-N_2+H]^+$).

1-azido-4-methoxybenzene

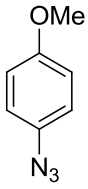

Prepared using general azide method A and isolated as a brown solid. ^{1}H NMR ($CDCl_3$, 600 MHz) δ 6.95 (d, 2H, J = 9 Hz), 6.89 (d, 2H, J = 9 Hz). ^{13}C NMR ($CDCl_3$, 151 MHz) δ 157.0, 132.3, 120.0, 115.1, 55.6. IR (film) v_{max} 2110 cm^{-1}. MS (ESI) *m/z* calculated 122.061 (C_7H_8NO, $[M-N_2+H]^+$), *m/z* observed 122.060 (C_7H_8NO, $[M-N_2+H]^+$).

1-azido-4-nitrobenzene

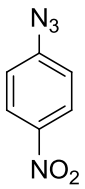

Prepared using general azide method A and isolated as a yellow solid. ^{1}H NMR ($CDCl_3$, 600 MHz) δ 8.64 (d, 2H, J = 9 Hz), 8.05 (d, 2H, J = 9 Hz). ^{13}C NMR ($CDCl_3$, 151 MHz) δ 166.4, 144.9, 131.6, 126.8, 119.0, 52.3 IR (film) ν_{max} 2125 cm^{-1}. MS (ESI) *m/z* calculated 137.0351 ($C_6H_5N_2O_2$, $[M-N_2+H]^+$), *m/z* observed 137.0377 ($C_6H_5N_2O_2$, $[M-N_2+H]^+$).

General catalysis protocols for synthesis of aziridines

General method for complexation of ligands with metals

Ligand (1 eq) and metal salt (1.1 Eq) were dissolved in acetonitrile to make a 0.2 M solution. The mixture was stirred at room temperature until all the ligand was consumed (by TLC). Resultant precipitate was filtered and washed with acetonitrile. Note: 2 equivalents of ligand were used in case of ligand D.

General method for screening with pre-complexed catalyst

Azide (1 eq) was added to a solution of catalyst (0.1 eq) in isopropyl alcohol. Alkene (2 eq) was added and the reaction mixture was stirred at 100 ^{o}C in a closed vessel. The reaction molarity was 0.2 M with respect to azide. Reaction progress was monitored via GCMS.

General method for screening with in situ generated catalyst

Azide (1 eq) was added to a solution of metal (0.1 eq) and ligand (0.1 eq) in isopropyl alcohol. Alkene (2 eq) was added and the reaction mixture was stirred at 100^{o}C in a

closed vessel. The reaction molarity was maintained at 0.2M with respect to azide. Reaction progress was monitored via GCMS.

Aziridines

9-(4-nitrophenyl)-9-azabicyclo[6.1.0]nonane (6.1)

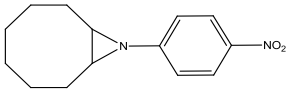

^{1}H NMR ($CDCl_3$, 500 MHz) δ 8.11 (2H, d, J = 9.0Hz), 7.00 (2H, d, J =9.0 Hz), 2.34 (2H, m), 2.23 (2H,m), range 1.73-1.4 (10H,m)

^{13}C NMR ($CDCl_3$, 125 MHz) δ 160.62, 141.10, 123.98, 119.03, 43.13, 25.81, 25.67, 25.22. **IR** (cm^{-1}) – 3050-2920, 1601, 1540, 1350. **HRMS (ESI)** – *m/z* calculated 247.1447 ($C_{14}H_{18}N_2O_2$, $[M+H]^+$), observed 247.1441)

ethyl 1-(4-nitrophenyl)aziridine-2-carboxylate (6.2)

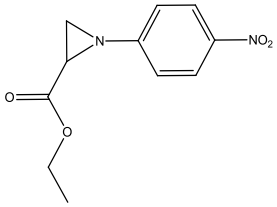

^{1}H NMR ($CDCl_3$, 500 MHz) δ 8.32 (1H, d, J=9.5 Hz), 8.17 (1H, d, J=9.5 Hz) 7.6 (1H, d, J=9.1 Hz), 7.10 (1H, d, J=9.1 Hz), 4.28 (2H, q, J=3.53), 2.95 (1H, m), 2.78 (1H, m), 2.44 (1H, dd, J=1.54, J=4.71), 1.33 (3H, J=7.19). **^{13}C NMR** ($CDCl_3$, 125 MHz) δ 164.02, 153.21, 120.72, 120.41, 115.98, 57.15, 32.88, 28.89, 9.37. **IR** (cm^{-1}) – 3050-2910, 1730, 1545, 1345. **HRMS (ESI)** – *m/z* calculated 237.0875 ($C_{11}H_{13}N_2O_4$, $[M+H]^+$), observed 237.0875)

(1-(4-nitrophenyl)aziridin-2-yl)methanol (6.3)

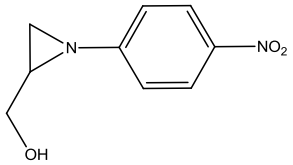

^{1}H NMR ($CDCl_3$, 500 MHz) δ 8.15 (2H, d, J=9.0 Hz), 7.10 (2H, d, J = 9.0 Hz), 4.07 (1H, m), 3.68 (1H, m), 2.54 (1H, m), 2.48 (1H, d, J=3.5 Hz), 2.2 (1H, d, J=6.2 Hz), 1.9 (1H, t, J=5.2 Hz). **^{13}C NMR** ($CDCl_3$, 125 MHz) δ 155.49, 138.21, 120.40, 116.05, 57.86, 36.26, 26.65. **IR** (cm^{-1}) – 3500-3400, 3050-2920, 1550, 1345. **HRMS (ESI)** – *m/z* calculated 195.0770 ($C_9H_{11}N_2O_3$, $[M+H]^+$), observed 195.0761)

9-(p-tolyl)-9-azabicyclo[6.1.0]nonane (6.4)

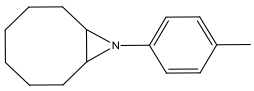

^{1}H NMR ($CDCl_3$, 500 MHz) δ 7.00 (2H, d, J=7.9 Hz), 6.89 (2H, d, J=7.9 Hz), 2.3 (2H, m), 2.28 (3H, S), 2.05 (2H, m), range 1.67-1.40 (10H, m). **^{13}C NMR** ($CDCl_3$, 125 MHz) δ 153.01, 131.09, 129.34, 120.09, 43.66, 27.28, 27.11, 26.50, 20.71. **IR** (cm^{-1}) – 3050-2920, 1612, 1463. **HRMS** (ESI) – *m/z* calculated 216.1752 ($C_{15}H_{22}N$, $[M+H]^+$), observed 216.1756)

9-(4-methoxyphenyl)-9-azabicyclo[6.1.0]nonane (6.5)

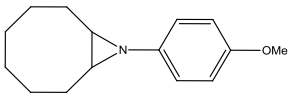

^{1}H NMR ($CDCl_3$, 500 MHz) δ 6.9 (2H, d, J=9.0 Hz), 6.77 (2H, d, J=9.0 Hz), 3.76 (3H, S), 2.28 (2H, m), 2.03 (2H, m), range 1.66-1.44 (10H, m). **^{13}C NMR** ($CDCl_3$, 125 MHz) δ 154.69, 148.81, 121.00, 114.10, 55.52, 43.85, 27.22, 27.09, 26.49. **IR** (cm^{-1}) 3050-2920, 1612, 1250. **HRMS (ESI)** – *m/z* calculated 232.1701 ($C_{15}H_{22}NO$, $[M+H]^+$), observed 232.1698)

2-methyl-1-(4-nitrophenyl)-1-azaspiro[2.5]octane (6.6)

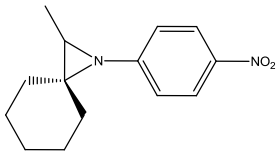

^{1}H NMR ($CDCl_3$, 500 MHz) δ 8.06 (2H, d, J=9.0 Hz), 6.50 (2H, d, J=9.0 Hz), 5.70 (1H, s), 4.47 (1H, s), 3.89 (1H, s), 2.03-1.91 (5H, m), 1.62-1.58 (3H, m), 1.37 (3H, d, J=6.5 Hz). **^{13}C NMR** ($CDCl_3$, 125 MHz) δ 152.79, 137.88, 126.26, 122.93, 11.53, 54.67, 24.93, 24.29, 22.62, 22.44, 20.90. **IR** (cm^{-1}) – 3050-2920, 1550, 1345. **HRMS (ESI)** – *m/z* calculated 247.14 ($C_{14}H_{19}N_2O_2$, $[M+H]^+$), observed 247.139)

ethyl 1-benzylaziridine-2-carboxylate (6.7)

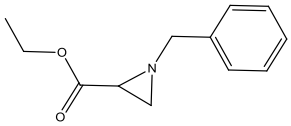

^{1}H NMR ($CDCl_3$, 500 MHz) δ 7.46-7.39 (5H, m), 4.22 (2H, s), 4.15 (1H, dd, J=13 Hz), 3.27 (2H, t, J=6.5 Hz), 2.78 (2H, t, J=6.5 Hz), 1.25 (3H, t, J=7.1). **^{13}C NMR** ($CDCl_3$, 125 MHz) δ 170.68, 130.29, 129.70, 129,64, 129.33, 61.51, 51.85, 42.56, 30.31, 14.01. **IR** (cm^{-1}) – 3050-2910, 1725, 1545, 1345. **HRMS (ESI)** – *m/z* calculated 206.1181 ($C_{12}H_{16}NO_2$, $[M+H]^+$), observed 206.1183)

1-(4-nitrophenyl)-2-phenylaziridine (6.8)

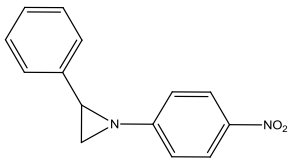

^{1}H NMR ($CDCl_3$, 500 MHz) δ 8.15 (2H, d, J=9.0 Hz), 7.41-7.30 (5H, m), 7.11 (2H, d, J=9.0 Hz), 3.25 (1H, dd, J=5.0 Hz), 2.57 (2H, m). **^{13}C NMR** ($CDCl_3$, 125 MHz) δ 160.44, 137.82, 128.56, 126.10, 125.21, 120.57, 41.96, 37.85. **IR** (cm^{-1}) – 3050-2920, , 1535, 1360. **HRMS (ESI)** – *m/z* calculated 241.0977 ($C_{14}H_{13}N_2O_2$, $[M+H]^+$), observed 241.0978)

1-(4-nitrophenyl)-2,3-dipropylaziridine[96] (6.9)

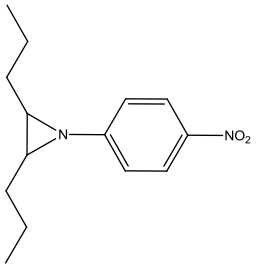

^{1}H NMR ($CDCl_3$, 500 MHz) δ 8.15 (2H, d, J=9.0 Hz), 7.10 (2H, d, J=9.0 Hz), 2.03 (2H, t, J=5.6 Hz), 1.62 (2H, m), 1.53 (4H, m), 1.10 (2H, m), 0.96 (6H, t, J=7.0 Hz). **^{13}C NMR** ($CDCl_3$, 125 MHz) δ 160.320, 137.55, 128.22, 120.95, 44.99, 33.29, 21.11, 20.80, 14.18. **IR** (cm^{-1}) – 3050-2920, , 1550, 1340 **HRMS (*ESI*):** *m/z* calculated 248.1525 ($C_{14}H_{20}N_2O_2$, $[M+H]^+$), observed 248.1523)

1-(4-nitrophenyl)aziridine-2-carbonitrile (6.10)

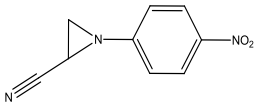

^{1}H NMR ($CDCl_3$, 500 MHz) δ 8.20 (2H, d, J=9.0 Hz), 7.14 (2H, d, J=9.0 Hz), 2.96 (1H, dd, J=3.1 Hz, 2.8 Hz), 2.8 (1H, d, J=3.7 Hz), 2.6 (1H, d J=6.3 Hz) . **^{13}C NMR** ($CDCl_3$, 125 MHz) δ 155.60, 144.16, 125.35, 120.92, 116.30, 33.66, 24.29. **IR** (cm^{-1}) – 3050-2920, 2250, 1550, 1340. **HRMS (ESI)**: *m/z* calculated 190.0617 ($C_9H_7N_3O_2$, $[M+H]^+$), observed 190.0618)

7. Conclusions

This dissertation describes the the synthesis of 1,2,4-triazoles ligands and their complexes with several transition metals. The application of these complexes towards catalysis of oxidative processes such as hydrocarbon oxidation, oxygen reduction reaction and aziridination is explored. Detailed SAR and optimization studies were carried out in order to identify the optimal ligand structure, metal and reaction conditions for each process. A remarkable phenomenon was observed during these studies. The nature of the triazole as well as the metal was found to have a profound effect on the type of process catalyzed. The most active ligands for hydrocarbon oxidation were 3,4,5-substituted triazole complexes with Cu(II). On the other hand Co(II) complexes of triazolo-hemiphthalocyanines and 3,5-diamino-1,2,4-triazole were identified as the optimal catalysts for ORR. Finally, Ni(II) complexes of 3,5-substituted triazoles showed excellent activity towards catalyzing aziridination reactions of organic azides.

Chapters 2 and 3 detail syntheses of different classes of 1,2,4-triazoles that were necessary for SAR studies. Chapter 3 in particular, describes the heterogenous approach towards immobilizing 1,2,4-triaozle ligands on solid supports such as polystyrene and silica. A number of improvements in the synthetic approaches were achieved during this research. The use of microwave synthesizer considerably improved the reaction parameters. A novel C-N bond formation method was discovered which utilizes diazonium chemistry. This method was extended towards immobilization of 1,2,4-triazoles on heterogeneous surfaces such as carbon black.

Chapter 4 presents selected observations on the catalytic activity of Cu(II)-1,2,4-triazoles in the hydrocarbon oxidation reactions. 3,4,5-trisubstituted triazoles were found to be potent ligands for this process. These catalysts are also highly selective as demonstrated by the product distribution in cyclohexane and adamantane oxidation reactions. This catalytic system can be further explored to assess its potential for methane to methanol conversion.

Chapter 5 of this dissertation is focused on studies towards immobilization of 1,2,4-triazole metal complexes on the carbon surfaces for their application in fuel cells. Extensive studies were carried out to assess the effects of surface modifications utilizing a range of synthetic tools. Covalently immobilized 1,2,4-triazole complexes showed potential for catalysis of ORR. These complexes not only demonstrated increased overall stability but also showed activity comparable to the commercially used platinum based catalysts. These catalysts show great promise as inexpensive alternatives for current platinum based catalysts and have wide ranging applications in alternate energy research.

Finally, chapter 6 presents a novel Ni(II)-1,2,4-triazole based catalytic system for aziridnation of aromatic azides. This system works under relatively mild reaction parameters while displaying a broad substrate scope. A thorough optimization of reaction parameters such as solvent systems, stoichiometry, catalyst loading as well as ligand scope was performed. The catalyst was found to work at loadings as low as 1 mol%. 3-mercapto-5-amino-1,2,4-triazole and 3,5-di(2-pyridyl)-1,2,4-triazole were identified as the most active ligands. This system provides a very practical alternative to the currently used catalytic systems.

Figure 7-1 summarizes the activity profile of 1,2,4-triazole metal complexes. In conclusion a number of ligands belonging to 1,2,4-triazole family that catalyze various oxidative processes have been identified and optimized for further applications.

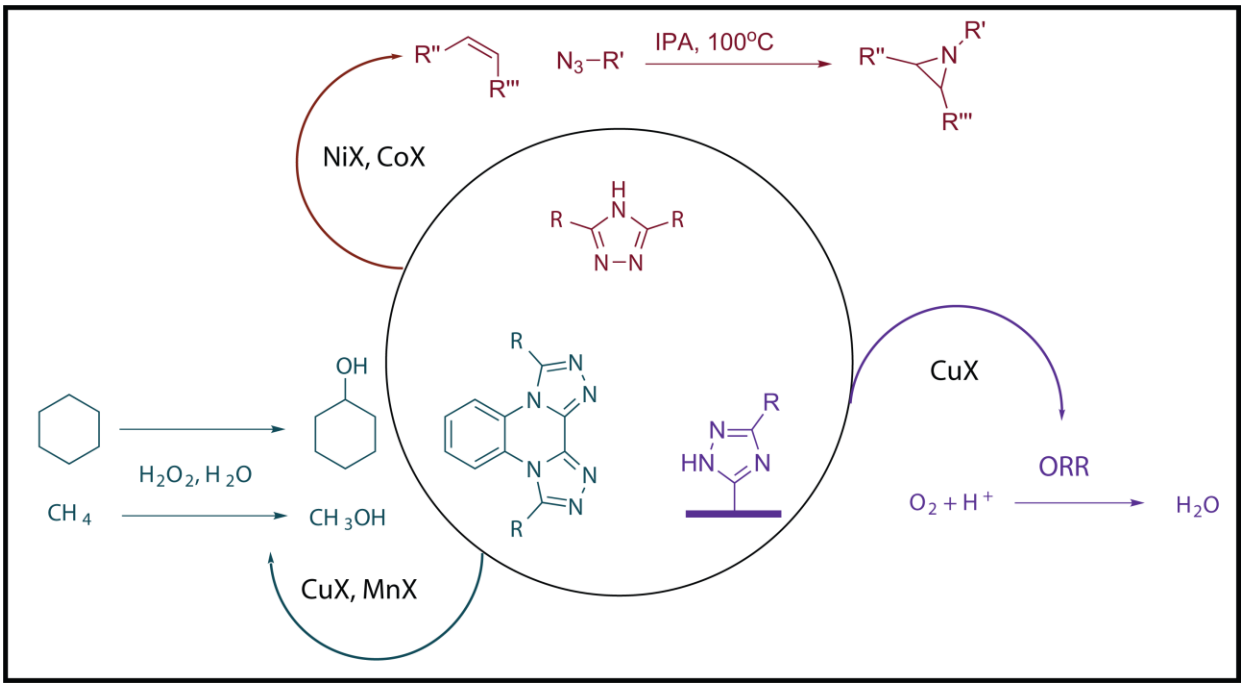

Figure 7-1 – Summary of processes catalyzed by 1,2,4-triazoles

References

1. Schoen, D., Learning from polar ice core research. *Environ Sci Technol* 1999, *33* (7), 160a-163a.

2. Arakawa, H.; Aresta, M.; Armor, J. N.; Barteau, M. A.; Beckman, E. J.; Bell, A. T.; Bercaw, J. E.; Creutz, C.; Dinjus, E.; Dixon, D. A.; Domen, K.; DuBois, D. L.; Eckert, J.; Fujita, E.; Gibson, D. H.; Goddard, W. A.; Goodman, D. W.; Keller, J.; Kubas, G. J.; Kung, H. H.; Lyons, J. E.; Manzer, L. E.; Marks, T. J.; Morokuma, K.; Nicholas, K. M.; Periana, R.; Que, L.; Rostrup-Nielson, J.; Sachtler, W. M. H.; Schmidt, L. D.; Sen, A.; Somorjai, G. A.; Stair, P. C.; Stults, B. R.; Tumas, W., Catalysis research of relevance to carbon management: Progress, challenges, and opportunities. *Chem Rev* 2001, *101* (4), 953-996.

3. Ayala, M.; Torres, E., Enzymatic activation of alkanes: constraints and prospective. *Appl Catal a-Gen* 2004, *272* (1-2), 1-13.

4. Elliott, S. J.; Zhu, M.; Tso, L.; Nguyen, H. H. T.; Yip, J. H. K.; Chan, S. I., Regio- and stereoselectivity of particulate methane monooxygenase from Methylococcus capsulatus (Bath). *Journal of the American Chemical Society* 1997, *119* (42), 9949-9955.

5. Lieberman, R. L.; Rosenzweig, A. C., Crystal structure of a membrane-bound metalloenzyme that catalyses the biological oxidation of methane. *Nature* 2005, *434* (7030), 177-182.

6. Tolman, W. B., *Activation of small molecules : organometallic and bioinorganic perspectives*. Wiley-VCH: Weinheim, 2006; p xvii, 363 p.

7. Otsuka, K.; Wang, Y., Direct conversion of methane into oxygenates. *Appl Catal a-Gen* 2001, *222* (1-2), 145-161.

8. Shu, L. J.; Nesheim, J. C.; Kauffmann, K.; Munck, E.; Lipscomb, J. D.; Que, L., An (Fe2O2)-O-IV diamond core structure for the key intermediate Q of methane monooxygenase. *Science* 1997, *275* (5299), 515-518.

9. Karlsson, A.; Parales, J. V.; Parales, R. E.; Gibson, D. T.; Eklund, H.; Ramaswamy, S., Crystal structure of naphthalene dioxygenase: Side-on binding of dioxygen to iron. *Science* 2003, *299* (5609), 1039-1042.

10. Krebs, C.; Fujimori, D. G.; Walsh, C. T.; Bollinger, J. M., Non-heme Fe(IV)-oxo intermediates. *Accounts Chem Res* 2007, *40* (7), 484-492.

11. Mahadevan, V.; Gebbink, R. J. M. K.; Stack, T. D. P., Biomimetic modeling of copper oxidase reactivity. *Curr Opin Chem Biol* 2000, *4* (2), 228-234.

12. Comba, P.; Wadepohl, H.; Wunderlich, S., Oxidation versus Dioxygenation of Catechol: The Iron-Bispidine System. *Eur J Inorg Chem* 2011, (34), 5242-5249.

13. Que, L.; Tolman, W. B., Biologically inspired oxidation catalysis. *Nature* 2008, *455* (7211), 333-340.

14. Bertrand, T.; Jolivalt, C.; Briozzo, P.; Caminade, E.; Joly, N.; Madzak, C.; Mougin, C., Crystal structure of a four-copper laccase complexed with an arylamine: Insights into substrate recognition and correlation with kinetics. *Biochemistry* 2002, *41* (23), 7325-7333.

15. Tsukihara, T.; Aoyama, H.; Yamashita, E.; Tomizaki, T.; Yamaguchi, H.; Shinzawaitoh, K.; Nakashima, R.; Yaono, R.; Yoshikawa, S., Structures of Metal Sites of Oxidized Bovine Heart Cytochrome-C-Oxidase at 2.8 Angstrom. *Science* 1995, *269* (5227), 1069-1074.

16. Marko, I. E.; Gautier, A.; Dumeunier, R. L.; Doda, K.; Philippart, F.; Brown, S. M.; Urch, C. J., Efficient, copper-catalyzed, aerobic oxidation of primary alcohols. *Angew Chem Int Edit* 2004, *43* (12), 1588-1591.

17. Marko, I. E.; Giles, P. R.; Tsukazaki, M.; Chelle-Regnaut, I.; Gautier, A.; Dumeunier, R.; Philippart, F.; Doda, K.; Mutonkole, J. L.; Brown, S. M.; Urch, C. J., Efficient, ecologically benign, aerobic oxidation of alcohols. *Adv Inorg Chem* 2004, *56*, 211-240.

18. Nam, W.; Oh, S. Y.; Sun, Y. J.; Kim, J.; Kim, W. K.; Woo, S. K.; Shin, W., Factors affecting the catalytic epoxidation of olefins by iron porphyrin complexes and H2O2 in protic solvents. *J Org Chem* 2003, *68* (20), 7903-7906.

19. Kim, C.; Chen, K.; Kim, J. H.; Que, L., Stereospecific alkane hydroxylation with H2O2 catalyzed by an iron(II)-tris(2-pyridylmethyl)amine complex. *Journal of the American Chemical Society* 1997, *119* (25), 5964-5965.

20. Sorokin, A. B.; Kudrik, E. V.; Bouchu, D., Bio-inspired oxidation of methane in water catalyzed by N-bridged diiron phthalocyanine complex. *Chem Commun* 2008, (22), 2562-2564.

21. Potts, K. T., The Chemistry of 1,2,4-Triazoles. *Chem Rev* 1961, *61* (2), 87-127.

22. Longley, N.; Muzoora, C.; Taseera, K.; Mwesigye, J.; Rwebembera, J.; Chakera, A.; Wall, E.; Andia, I.; Jaffar, S.; Harrison, T. S., Dose Response Effect of High-Dose Fluconazole for HIV-Associated Cryptococcal Meningitis in Southwestern Uganda. *Clin Infect Dis* 2008, *47* (12), 1556-1561.

23. Joung, J. K.; Ramm, E. I.; Pabo, C. O., A bacterial two-hybrid selection system for studying protein-DNA and protein-protein interactions. *P Natl Acad Sci USA* 2000, *97* (13), 7382-7387.

24. Bayer, H. O.; Cook, R. S.; Von, M. W. C. Fungicidal metal salt complexes of 4-substituted-1,2,4-triazoles. ZA7004373A, 1971.

25. Potts, K. T., 1-2-4-Triazoles .1. A Synthesis of 3-5-Disubstituted 1-2-4-Triazoles. *J Chem Soc* 1954, (Oct), 3461-3464.

26. Oziminski, W. P.; Dobrowolski, J. C.; Mazurek, A. P., DFT studies on tautomerism of C5-substituted 1,2,4-triazoles. *J Mol Struc-Theochem* 2004, *680* (1-3), 107-115.

27. Haasnoot, J. G., Mononuclear, oligonuclear and polynuclear metal coordination compounds with 1,2,4-triazole derivatives as ligands. *Coordin Chem Rev* 2000, *200*, 131-185.

28. Kirillov, A. M.; Kopylovich, M. N.; Kirillova, M. V.; Haukka, M.; da Silva, M. F. C. G.; Pombeiro, A. J. L., Multinuclear copper triethanolamine complexes as selective catalysts for the peroxidative oxidation of alkanes under mild conditions. *Angew Chem Int Edit* 2005, *44* (28), 4345-4349.

29. Alves, W. A.; de Almeida, S. A.; Santos, R. H. D.; Ferreira, A. M. D., Diimine copper(II) complexes as building blocks for microporous catalytic materials. *Inorg Chem Commun* 2003, *6* (3), 294-299.

30. Roy, P.; Manassero, M., Tetranuclear copper(II)-Schiff-base complexes as active catalysts for oxidation of cyclohexane and toluene. *Dalton T* 2010, *39* (6), 1539-1545.

31. Das, S.; Banerjee, P.; Peng, S. M.; Lee, G. H.; Kim, J.; Goswami, S., Mononuclear to polynuclear transition induced by ligand coordination: Synthesis, X-ray structure, and

properties of mono-, di-, and polynuclear copper(II) complexes of pyridyl-containing azo ligands. *Inorg Chem* 2006, *45* (2), 562-570.

32. Gruenwald, K. R.; Kirillov, A. M.; Haukka, M.; Sanchiz, J.; Pombeiro, A. J. L., Mono-, di- and polynuclear copper(II) compounds derived from N-butyldiethanolamine: structural features, magnetism and catalytic activity for the mild peroxidative oxidation of cyclohexane. *Dalton T* 2009, (12), 2109-2120.

33. Pirngruber, G. D.; Frunz, L.; Luchinger, M., The characterisation and catalytic properties of biomimetic metal-peptide complexes immobilised on mesoporous silica. *Phys Chem Chem Phys* 2009, *11* (16), 2928-2938.

34. Eubank, J. F.; Wojtas, L.; Hight, M. R.; Bousquet, T.; Kravtsov, V. C.; Eddaoudi, M., The Next Chapter in MOF Pillaring Strategies: Trigonal Heterofunctional Ligands To Access Targeted High-Connected Three Dimensional Nets, Isoreticular Platforms. *Journal of the American Chemical Society* 2011, *133* (44), 17532-17535.

35. Fang, Z. L.; Yu, R. M.; Wu, X. Y.; Huang, J. S.; Lu, C. Z., Microporous Metal-Organic Frameworks: Structures, in Situ Formation of Ligand, and Crystal-to-Crystal Transformations. *Cryst Growth Des* 2011, *11* (6), 2546-2552.

36. Klingele, M. H.; Brooker, S., The coordination chemistry of 4-substituted 3,5-di(2-pyridyl)-4H-1,2,4-triazoles and related ligands. *Coordin Chem Rev* 2003, *241* (1-2), 119-132.

37. Jarvis, J. A. J., Crystal Structure of a Complex of Cupric Chloride and 1-2-4-Triazole. *Acta Crystallogr* 1962, *15* (Oct), 964-&.

38. Reimann, C. W.; Zocchi, M., Structure of Trinuclear Cation Bis-[Mu-(Tri-1,2,4-Triazolo-N1,N2)-Triaquonickel]Nickel. *Chem Commun* 1968, (5), 272-&.

39. Reimann, C. W.; Zocchi, M., Crystal Structure of Bis-[Mu-(Tri-1,2,4-Triazolo-N1,N2)-Triaquonickel]Nickel Hexanitrate Dihydrate, $[(H_2O)_3(C_2H_3N_3)_3Ni]_2Ni(NO_3)_6(H_2O)_2$. *Acta Crystall B-Stru* 1971, *B 27* (Mar), 682-&.

40. Keij, F. S.; Degraaff, R. A. G.; Haasnoot, J. G.; Reedijk, J., Synthesis and Coordination Chemistry of a Novel Dinucleating Chelating Triazole Ligand - the Crystal-Structure of Bis-Mu-[4-Amino-3,5-Bis(Pyridin-2-yl)-1,2,4-Triazole-N',Mu-N1,Mu-N2,N'']-Bis[Aquachloronickel(Ii)] Dichloride Tetrahydrate. *J Chem Soc Dalton* 1984, (10), 2093-2097.

41. Prins, R.; Birker, P. J. M. W. L.; Verschoor, G. C., Structure of 2-[5-(2-Pyridyl)-1h-1,2,4-Triazol-3-yl]Pyridinium Perchlorate. *Acta Crystallogr B* 1982, *38* (Nov), 2934-2935.

42. Mangani, S.; Liljas, A., Crystal-Structure of the Complex between Human Carbonic Anhydrase-Ii and the Aromatic Inhibitor 1,2,4-Triazole. *J Mol Biol* 1993, *232* (1), 9-14.

43. Romanenko, G. V.; Savelieva, Z. A.; Podberezskaya, N. V.; Larionov, S. V., Structure of the Cu(II) chloride complex with 4-amino-1,2,4-triazole $Cu(C_2H_4N_4)Cl_2$. *J Struct Chem*+ 1997, *38* (1), 171-176.

44. Fokin, A. A.; Schreiner, P. R., Selective alkane transformations via radicals and radical cations: Insights into the activation step from experiment and theory. *Chem Rev* 2002, *102* (5), 1551-1593.

45. Himes, R. A.; Karlin, K. D., Copper-dioxygen complex mediated C-H bond oxygenation: relevance for particulate methane monooxygenase (pMMO). *Curr Opin Chem Biol* 2009, *13* (1), 119-131.

46. Hakemian, A. S.; Kondapalli, K. C.; Telser, J.; Hoffman, B. M.; Stemmler, T. L.; Rosenzweig, A. C., The metal centers of particulate methane monooxygenase from Methylosinus trichosporium OB3b. *Biochemistry-Us* 2008, *47* (26), 6793-6801.

47. Chen, P.; Solomon, E. I., Frontier molecular orbital analysis of Cu-n-O-2 reactivity. *J Inorg Biochem* 2002, *88* (3-4), 368-374.

48. Barton, D. H. R.; Delanghe, N. C., The selective functionalization of saturated hydrocarbons. Part 46. An investigation of Udenfriend's system under Gif conditions. *Tetrahedron* 1998, *54* (18), 4471-4476.

49. Barton, D. H. R.; Lalic, G.; Smith, J. A., The selective functionalization of saturated hydrocarbons. Part 42. Further studies in selective phenylselenation. *Tetrahedron* 1998, *54* (9), 1725-1734.

50. Barton, D. H. R.; Launay, F., The selective functionalization of saturated hydrocarbons. Part 47. Investigation of the size of the reagent involved in the Fe-II-Fe-IV manifold. *Tetrahedron* 1998, *54* (42), 12699-12706.

51. Barton, D. H. R.; Launay, F., The selective functionalization of saturated hydrocarbons. Part 44. Measurement of size of reagent by variation of steric demands of competing substrates using Gif chemistry. *Tetrahedron* 1998, *54* (14), 3379-3390.

52. Barton, D. H. R.; Li, T. S., The selective functionalization of saturated hydrocarbons. Part 43. Modified Gif oxidation in acetonitrile. *Tetrahedron* 1998, *54* (9), 1735-1744.

53. Barton, D. H. R.; Li, T. S.; Peralez, E., The selective functionalization of saturated hydrocarbons. Part 45. The effect of lower temperature on the rate and efficiency of formation of oxidized products in the Fe-III-Fe-V and Fe-II-Fe-IV manifolds. *Tetrahedron* 1998, *54* (50), 15087-15096.

54. Kirillov, A. M.; Kopylovich, M. N.; Kirillova, M. V.; Karabach, E. Y.; Haukka, M.; da Silva, M. F. C. G.; Pombeiro, A. J. L., Mild peroxidative oxidation of cyclohexane catalyzed by mono-, di-, tri-, tetra- and polynuclear copper triethanolamine complexes. *Adv Synth Catal* 2006, *348* (1-2), 159-174.

55. Nesterov, D. S.; Kokozay, V. N.; Dyakonenko, V. V.; Shishkin, O. V.; Jezierska, J.; Ozarowski, A.; Kirillov, A. M.; Kopylovich, M. N.; Pombeiro, A. J. L., An unprecedented heterotrimetallic Fe/Cu/Co core for mild and highly efficient catalytic oxidation of cycloalkanes by hydrogen peroxide. *Chem Commun* 2006, (44), 4605-4607.

56. Kirillova, M. V.; Kozlov, Y. N.; Shul'pina, L. S.; Lyakin, O. Y.; Kirillov, A. M.; Talsi, E. P.; Pombeiro, A. J. L.; Shul'pin, G. B., Remarkably fast oxidation of alkanes by hydrogen peroxide catalyzed by a tetracopper(II) triethanolaminate complex: Promoting effects of acid co-catalysts and water, kinetic and mechanistic features. *Journal of Catalysis* 2009, *268* (1), 26-38.

57. Jones, C. J.; Taube, D.; Ziatdinov, V. R.; Periana, R. A.; Nielsen, R. J.; Oxgaard, J.; Goddard, W. A., Selective oxidation of methane to methanol catalyzed, with C-H activation, by homogeneous, cationic gold. *Angew Chem Int Edit* 2004, *43* (35), 4626-4629.

58. Park, E. D.; Hwang, Y. S.; Lee, C. W.; Lee, J. S., Copper- and vanadium-catalyzed methane oxidation into oxygenates with in situ generated H2O2 over Pd/C. *Appl Catal a-Gen* 2003, *247* (2), 269-281.

59. Diaz-Requejo, M. M.; Perez, P. J., Coinage metal catalyzed C-H bond functionalization of hydrocarbons. *Chem Rev* 2008, *108* (8), 3379-3394.

60. Kim, J.; Harrison, R. G.; Kim, C.; Que, L., Fe(TPA)-catalyzed alkane hydroxylation. Metal-based oxidation vs radical chain autoxidation. *Journal of the American Chemical Society* 1996, *118* (18), 4373-4379.

61. Gozzo, F., Radical and non-radical chemistry of the Fenton-like systems in the presence of organic substrates. *J Mol Catal a-Chem* 2001, *171* (1-2), 1-22.

62. Menage, S.; Vincent, J. M.; Lambeaux, C.; Fontecave, M., Mu-Oxo-Bridged Diiron(Iii) Complexes and H2o2 - Monooxygenase-Like and Catalase-Like Activities. *J Chem Soc Dalton* 1994, (14), 2081-2084.

63. Giddey, S.; Badwal, S. P. S.; Kulkarni, A.; Munnings, C., A comprehensive review of direct carbon fuel cell technology. *Prog Energ Combust* 2012, *38* (3), 360-399.

64. Andujar, J. M.; Segura, F., Fuel cells: History and updating. A walk along two centuries. *Renew Sust Energ Rev* 2009, *13* (9), 2309-2322.

65. Morozan, A.; Jousselme, B.; Palacin, S., Low-platinum and platinum-free catalysts for the oxygen reduction reaction at fuel cell cathodes. *Energ Environ Sci* 2011, *4* (4), 1238-1254.

66. Jaouen, F.; Herranz, J.; Lefevre, M.; Dodelet, J. P.; Kramm, U. I.; Herrmann, I.; Bogdanoff, P.; Maruyama, J.; Nagaoka, T.; Garsuch, A.; Dahn, J. R.; Olson, T.; Pylypenko, S.; Atanassov, P.; Ustinov, E. A., Cross-Laboratory Experimental Study of Non-Noble-Metal Electrocatalysts for the Oxygen Reduction Reaction. *Acs Appl Mater Inter* 2009, *1* (8), 1623-1639.

67. Ding, B.; Liu, Y.-Y.; Huang, Y.-Q.; Shi, W.; Cheng, P.; Liao, D.-Z.; Yan, S.-P., Structural Variations Influenced by Ligand Conformation and Counteranions in Copper(II) Complexes with Flexible Bis-Triazole Ligand. *Cryst. Growth Des.* 2009, *9*, 593-601.

68. Bashyam, R.; Zelenay, P., A class of non-precious metal composite catalysts for fuel cells. *Nature* 2006, *443* (7107), 63-66.

69. Faubert, G.; Côté, R.; Guay, D.; Dodelet, J. P.; Dénès, G.; Bertrandc, P., Iron catalysts prepared by high-temperature pyrolysis of tetraphenylporphyrins adsorbed on carbon black for oxygen reduction in polymer electrolyte fuel cells. *Electrochimica Acta* 1998, *43* (3–4), 341-353.

70. Zhang, J.; Vukmirovic, M. B.; Xu, Y.; Mavrikakis, M.; Adzic, R. R., Controlling the Catalytic Activity of Platinum-Monolayer Electrocatalysts for Oxygen Reduction with Different Substrates. *Angewandte Chemie International Edition* 2005, *44* (14), 2132-2135.

71. Zhang, J.; Mo, Y.; Vukmirovic, M. B.; Klie, R.; Sasaki, K.; Adzic, R. R., Platinum Monolayer Electrocatalysts for O2 Reduction: Pt Monolayer on Pd(111) and on Carbon-Supported Pd Nanoparticles. *The Journal of Physical Chemistry B* 2004, *108* (30), 10955-10964.

72. Lim, B.; Jiang, M. J.; Camargo, P. H. C.; Cho, E. C.; Tao, J.; Lu, X. M.; Zhu, Y. M.; Xia, Y. N., Pd-Pt Bimetallic Nanodendrites with High Activity for Oxygen Reduction. *Science* 2009, *324* (5932), 1302-1305.

73. Peng, Z.; Yang, H., Synthesis and Oxygen Reduction Electrocatalytic Property of Pt-on-Pd Bimetallic Heteronanostructures. *Journal of the American Chemical Society* 2009, *131* (22), 7542-7543.

74. Koenigsmann, C.; Zhou, W. P.; Adzic, R. R.; Sutter, E.; Wong, S. S., Size-dependent enhancement of electrocatalytic performance in relatively defect-free, processed ultrathin platinum nanowires. *Nano Lett* 2010, *10* (8), 2806-11.

75. Fukuzumi, S.; Kotani, H.; Lucas, H. R.; Doi, K.; Suenobu, T.; Peterson, R. L.; Karlin, K. D., Mononuclear Copper Complex-Catalyzed Four-Electron Reduction of Oxygen. *Journal of the American Chemical Society* 2010, *132* (20), 6874-+.

76. Jasinski, R., New Fuel Cell Cathode Catalyst. *Nature* 1964, *201* (492), 1212-&.

77. Chen, W.; Akhigbe, J.; Bruckner, C.; Li, C. M.; Lei, Y., Electrocatalytic Four-Electron Reduction of Dioxygen by Electrochemically Deposited Poly{[meso-tetrakis(2-thienyl)porphyrinato]cobalt(II)}. *J Phys Chem C* 2010, *114* (18), 8633-8638.

78. Lee, S.-K.; George, S. D.; Antholine, W. E.; Hedman, B.; Hodgson, K. O.; Solomon, E. I., Nature of the Intermediate Formed in the Reduction of O2 to H2O at the Trinuclear Copper Cluster Active Site in Native Laccase. *Journal of the American Chemical Society* 2002, *124* (21), 6180-6193.

79. Thorum, M. S.; Yadav, J.; Gewirth, A. A., Oxygen Reduction Activity of a Copper Complex of 3,5-Diamino-1,2,4-triazole Supported on Carbon Black. *Angew Chem Int Edit* 2009, *48* (1), 165-167.

80. Aznar, E.; Ferrer, S.; Borras, J.; Lloret, F.; Liu-Gonzalez, M.; Rodriguez-Prieto, H.; Garcia-Granda, S., Coordinative versatility of guanazole [3,5-diamino-1,2,4-triazole]: synthesis, crystal structure, EPR, and magnetic properties of a dinuclear and a linear trinuclear copper(II) complex containing small bridges and triazole ligands. *Eur. J. Inorg. Chem.* 2006, (Copyright (C) 2011 American Chemical Society (ACS). All Rights Reserved.), 5115-5125.

81. Ferrer, S.; Lloret, F.; Bertomeu, I.; Alzuet, G.; Borras, J.; Garcia-Granda, S.; Liu-Gonzalez, M.; Haasnoot, J. G., Cyclic Trinuclear and Chain of Cyclic Trinuclear Copper(II) Complexes Containing a Pyramidal $Cu_3O(H)$ Core. Crystal Structures and Magnetic Properties of $[Cu_3(\mu_3\text{-}OH)(aaat)_3(H_2O)_3](NO_3)_2\cdot H_2O$ [aaat = 3-acetylamino-5-amino-1,2,4-triazolate] and $\{[Cu_3(\mu_3\text{-}OH)(aat)_3(\mu_3\text{-}SO_4)]\cdot 6H_2O\}_n$ [aat = 3-acetylamino-1,2,4-triazolate]: New Cases of Spin-Frustrated Systems. *Inorg. Chem.* 2002, *41*, 5821-5830.

82. Sweeney, J. B., Aziridines: epoxides' ugly cousins? *Chem Soc Rev* 2002, *31* (5), 247-258.

83. Yudin, A. K., *Aziridines and epoxides in organic synthesis*. Wiley: Weinheim ; Chichester, 2006; p xxi, 492 p.

84. Danshiftsoodol, N.; de Pinho, C. A.; Matoba, Y.; Kumagai, T.; Sugiyama, M., The mitomycin C (MMC)-binding protein from MMC-producing microorganisms protects from the lethal effect of bleomycin: Crystallographic analysis to elucidate the binding mode of the antibiotic to the protein. *J Mol Biol* 2006, *360* (2), 398-408.

85. Tomasz, M., Mitomycin C: Small, fast and deadly (but very selective), *Chem Biol* 1995, *2* (12), 865-865.

86. Dauban, P.; Dodd, R. H., Iminoiodanes and C-N bond formation in organic synthesis. *Synlett* 2003, (11), 1571-1586.

87. Klotz, K. L.; Slominski, L. M.; Riemer, M. E.; Phillips, J. A.; Halfen, J. A., Mechanism of the Iron-Mediated Alkene Aziridination Reaction: Experimental and Computational Investigations. *Inorg Chem* 2009, *48* (3), 801-803.

88. Mahy, J. P.; Battioni, P.; Mansuy, D., Formation of an Iron(Iii) Porphyrin Complex with a Nitrene Moiety Inserted into a Fe-N Bond during Alkene Aziridination by [(Tosylimido)Iodo]Benzene Catalyzed by Iron(Iii) Porphyrins. *Journal of the American Chemical Society* 1986, *108* (5), 1079-1080.

89. Simonato, J. P.; Pecaut, J.; Scheidt, W. R.; Marchon, J. C., Antagonistic metal-directed inductions in catalytic asymmetric aziridination by manganese and iron tetramethylchiroporphyrins. *Chem Commun* 1999, (11), 989-990.

90. Vedernikov, A. N.; Caulton, K. G., Angular ligand constraint yields an improved olefin aziridination catalyst. *Org Lett* 2003, *5* (15), 2591-2594.

91. Chanda, B. M.; Vyas, R.; Bedekar, A. V., Investigations in the transition metal catalyzed aziridination of olefins, amination, and other insertion reactions with Bromamine-T as the source of nitrene. *J Org Chem* 2001, *66* (1), 30-34.

92. Mairena, M. A.; Diaz-Requejo, M. M.; Belderrain, T. R.; Nicasio, M. C.; Trofimenko, S.; Perez, P. J., Copper-homoscorpionate complexes as very active catalysts for the olefin aziridination reaction. *Organometallics* 2004, *23* (2), 253-256.

93. Li, Z.; Quan, R. W.; Jacobsen, E. N., Mechanism of the (Diimine)Copper-Catalyzed Asymmetric Aziridination of Alkenes - Nitrene Transfer Via Ligand-Accelerated Catalysis. *Journal of the American Chemical Society* 1995, *117* (21), 5889-5890.

94. Omura, K.; Uchida, T.; Irie, R.; Katsuki, T., Design of a robust Ru(salen) complex: aziridination with improved turnover number using N-arylsulfonyl azides as precursors. *Chem Commun* 2004, (18), 2060-2061.

95. Caselli, A.; Gallo, E.; Fantauzzi, S.; Morlacchi, S.; Ragaini, F.; Cenini, S., Allylic amination and aziridination of olefins by aryl azides catalyzed by Co (II)(tpp): A synthetic and mechanistic study. *Eur J Inorg Chem* 2008, (19), 3009-3019.

96. Cramer, S. A.; Jenkins, D. M., Synthesis of Aziridines from Alkenes and Aryl Azides with a Reusable Macrocyclic Tetracarbene Iron Catalyst. *Journal of the American Chemical Society* 2011, *133* (48), 19342-19345.

97. Evans, D. A.; Faul, M. M.; Bilodeau, M. T., Copper-Catalyzed Aziridination of Olefins by (N-(Para-Toluenesulfonyl)Imino)Phenyliodinane. *J Org Chem* 1991, *56* (24), 6744-6746.

98. Evans, D. A.; Faul, M. M.; Bilodeau, M. T., Development of the Copper-Catalyzed Olefin Aziridination Reaction. *Journal of the American Chemical Society* 1994, *116* (7), 2742-2753.

99. Subbarayan, V.; Ruppel, J. V.; Zhu, S.; Perman, J. A.; Zhang, X. P., Highly asymmetric cobalt-catalyzed aziridination of alkenes with trichloroethoxysulfonyl azide (TcesN(3)). *Chem Commun* 2009, (28), 4266-4268.

100. Holm, S. C.; Straub, B. F., Synthesis of N-Substituted 1,2,4-Triazoles. A Review. *Org Prep Proced Int* 2011, *43* (4), 319-347.

101. Bentiss, F.; Lagrenee, M.; Vezin, H.; Bouanis, M.; Mernari, B., An improved procedure for the deamination of symmetrical 3,5-disubstituted 4-amino-1,2,4-triazoles. *J Heterocyclic Chem* 2002, *39* (1), 93-96.

102. Yeung, K. S.; Farkas, M. E.; Kadow, J. F.; Meanwell, N. A., A base-catalyzed, direct synthesis of 3,5-disubstituted 1,2,4-triazoles from nitriles and hydrazides. *Tetrahedron Lett* 2005, *46* (19), 3429-3432.

103. Huang, Y.; Hu, X. Q.; Shen, D. P.; Chen, Y. F.; Xu, P. F., Synthesis of 1H-imidazo[1,2-b]-1,2,4-triazol-6-amines via multicomponent reaction. *Mol Divers* 2007, *11* (2), 73-80.

104. Piccionello, A. P.; Guarcello, A.; Buscemi, S.; Vivona, N.; Pace, A., Synthesis of Amino-1,2,4-triazoles by Reductive ANRORC Rearrangements of 1,2,4-Oxadiazoles. *J Org Chem* 2010, *75* (24), 8724-8727.

105. Naik, A. D.; Marchand-Brynaert, J.; Garcia, Y., A simplified approach to N- and N,N '-linked 1,2,4-triazoles by transamination. *Synthesis-Stuttgart* 2008, (1), 149-154.

106. Bahceci, S.; Yuksek, H.; Serdar, M., Reactions of amidines with some carboxylic acid hydrazides. *Indian J Chem B* 2005, *44* (3), 568-572.

107. Stocks, M. J.; Cheshire, D. R.; Reynolds, R., Efficient and regiospecific one-pot synthesis of substituted 1,2,4-triazoles. *Org Lett* 2004, *6* (17), 2969-2971.

108. Dallacker, F.; Minn, K., Derivatives of 1h-1,2,4-Triazoles .2. Synthesis of 1-Substituted 1h-1,2,4-Triazole-5-Carbaldehydes and 1h-1,2,4-Triazole-3,5-Dicarboxylic Acids. *Chem Ztg* 1986, *110* (7-8), 275-281.

109. Horvath, A., Michael Adducts in the Regioselective Synthesis of N-Substituted Azoles. *Synthesis-Stuttgart* 1995, (9), 1183-&.

110. Haasnoot, J. G.; Groeneveld, W. L., Complexes of 1,2,4-Triazoles .7. Preparation and Vibrational-Spectra of 4,4'-Bi-1,2,4-Triazole and Some of Its Complexes with Transition Metal(Ii) Thiocyanates. *Z Naturforsch B* 1979, *34* (11), 1500-1506.

111. Bartlett, R. K.; Humphrey, I. R., Transaminations of Nn-Dimethylformamide Azine. *J Chem Soc C* 1967, (17), 1664-&.

112. Mirzaei, Y. R.; Twamley, B.; Shreeve, J. M., Syntheses of 1-alkyl-1,2,4-triazoles and the formation of quaternary 1-alkyl-4-polyfluoroalkyl-1,2,4-triazolium salts leading to ionic liquids. *J Org Chem* 2002, *67* (26), 9340-9345.

113. Dolzhenko, A. V.; Pastorin, G.; Dolzhenko, A. V.; Chui, W. K., An aqueous medium synthesis and tautomerism study of 3(5)-amino-1,2,4-triazoles. *Tetrahedron Lett* 2009, *50* (18), 2124-2128.

114. Qian, Y.; Lu, Z. F.; Lu, C. G.; Chen, Z. M.; Cui, Y. P., Synthesis and two-photon absorption properties of 2,5-bis[4-(2-arylvinyl)phenyl]-1,3,4-oxadiazoles. *Dyes Pigments* 2007, *75* (3), 641-646.

115. Sastry, C. V. R.; Krishnan, V. S. H.; Narayan, G. K. A. S. S.; Vemana, K.; Vairamani, M., Reaction of 2,3-Dichloroquinoxaline with Acid Hydrazides - a Convenient Synthesis of 1,6-Disubstituted[1,2,4]Ditriazolo[4,3-a-3',4'-C]-Quinoxalines and 2-Aryl Heteroaryl[1,3,4]Oxadiazino[5,6-B]Quinoxalines. *Indian J Chem B* 1991, *30* (10), 936-940.

116. Biyiklioglu, Z.; Kantekin, H., Synthesis and spectroscopic properties of a series of octacationic water-soluble phthalocyanines. *Synth. Met.* 2011, *161*, 943-948.

117. Yang, L.; Yuan, H.-y.; Xiao, D., Synthesis of cobalt phthalocyanine under microwave irradiation and determination of bovine albumin. *Chongqing Daxue Xuebao, Ziran Kexueban* 2008, *31* (Copyright (C) 2011 American Chemical Society (ACS). All Rights Reserved.), 707-710.

118. Liu, Q.; Zhao, F.-Q.; Zhang, X.-F.; Cao, W.-L.; Zhang, F.-S., Synthesis and spectral study of novel para-hydroxyphenoxy phthalocyanines. *Beijing Huagong Daxue Xuebao, Ziran Kexueban* 2008, *35*, 24-28.

119. Galanin, N. E.; Kudrik, E. V.; Shaposhnikov, G. P., Synthesis and spectral characteristics of phthalocyanines of unsymmetrical structure containing fragments of 3,6-didecyloxyphthalonitrile and 2-methyl-5,6-dicyanobenzimidazole. *Russ. J. Org. Chem.* 2008, *44*, 225-230.

120. Tolbin, A. Y.; Tomilova, L. G.; Zefirov, N. S., Non-symmetrically substituted phthalocyanines: synthesis and structure modification. *Russ. Chem. Rev.* 2007, *76*, 681-692.

121. Oezil, M.; Agar, E.; Sasmaz, S.; Kahveci, B.; Akdemir, N.; Guemruekcueoglu, I. E., Microwave-assisted synthesis and characterization of the monomeric phthalocyanines containing naphthalene-amide group moieties and the polymeric phthalocyanines containing oxa-aza bridge. *Dyes Pigm.* 2007, *75*, 732-740.

122. Wang, J.; Khanamiryan, A. K.; Leznoff, C. C., Multisubstituted phthalonitriles for phthalocyanine synthesis. *J. Porphyrins Phthalocyanines* 2004, *8*, 1293-1299.

123. He, X.-m.; Lu, J.-b.; Lu, J.-m.; Zhu, X.-l., Synthesis of copper phthalocyanine under microwave irradiation. *Hecheng Huaxue* 2002, *10*, 87-90.

124. Krasnokutskaya, E. A.; Semenischeva, N. I.; Filimonov, V. D.; Knochel, P., A new, one-step, effective protocol for the iodination of aromatic and heterocyclic compounds via aprotic diazotization of amines. *Synthesis-Stuttgart* 2007, (1), 81-84.

125. Moumne, R.; Lavielle, S.; Karoyan, P., Efficient synthesis of beta(2)-amino acid by homologation of alpha-amino acids involving the Reformatsky reaction and Mannich-type imminium electrophile. *J Org Chem* 2006, *71* (8), 3332-3334.

126. Barral, K.; Moorhouse, A. D.; Moses, J. E., Efficient conversion of aromatic amines into azides: A one-pot synthesis of triazole linkages. *Org Lett* 2007, *9* (9), 1809-1811.

127. Marinescu, L.; Thinggaard, J.; Thomsen, I. B.; Bols, M., Radical azidonation of aldehydes. *J Org Chem* 2003, *68* (24), 9453-9455.

128. Cadogan, J. I. G., A Convenient New Method of Aromatic Arylation. *J Chem Soc* 1962, (10), 4257-&.

129. Friedman, L.; Bayless, J. H., Aprotic Diazotization of Aliphatic Amines . Hydrocarbon Products and Reaction Parameters. *Journal of the American Chemical Society* 1969, *91* (7), 1790-&.

130. Holm, S. C.; Siegle, A. F.; Loos, C.; Rominger, F.; Straub, B. F., Preparation and N-Alkylation of 4-Aryl-1,2,4-triazoles. *Synthesis-Stuttgart* 2010, (13), 2278-2286.

131. Elokhina, V. N.; Nakhmanovich, A. S.; Yaroshenko, T. I.; Stepanova, Z. V.; Larina, L. I., Synthesis of 4-(hydroxyphenyl)-1,2,4-triazoles. *Russ J Gen Chem+* 2006, *76* (1), 158-160.

132. Tubaro, C.; Biffis, A.; Scattolin, E.; Basato, M., Efficient catalysis of Ullmann-type arylation reactions by a novel trinuclear copper(I) complex with a chelating tricarbene ligand. *Tetrahedron* 2008, *64* (19), 4187-4195.

133. Tahli, A.; Maclaren, J. K.; Boldog, I.; Janiak, C., Synthesis and crystal structure determination of 0D-, 1D-and 3D-metal compounds of 4-(pyrid-4-yl)-1,2,4-triazole with zinc(II) and cadmium(II). *Inorg Chim Acta* 2011, *374* (1), 506-513.

134. Ding, B.; Yi, L. N.; Cheng, P. N.; Song, H. B.; Wang, H. G., Synthesis and characterization of a novel Mn complex with 4-(pyridyl-2)-1,2,4-triazole. *J Coord Chem* 2004, *57* (9), 771-776.

135. Srinivasan, R.; Uttamchandani, M.; Yao, S. Q., Rapid assembly and in situ screening of bidentate inhibitors of protein tyrosine phosphatases. *Org Lett* 2006, *8* (4), 713-716.

136. Ferrer, S.; Ballesteros, R.; Sambartolome, A.; Gonzalez, M.; Alzuet, G.; Borras, J.; Liu, M. V., Syntheses, crystal structures, and oxidative DNA cleavage of some Cu(II) complexes of 5-amino-3-pyridin-2-yl-1, 2,4-triazole. *J Inorg Biochem* 2004, *98* (8), 1436-1446.

137. Xue, H.; Gao, Y.; Twamley, B.; Shreeve, J. M., New energetic salts based on nitrogen-containing heterocycles. *Chem Mater* 2005, *17* (1), 191-198.

138. Romer, D. R., Synthesis of 2,3-Dichloroquinoxalines via Vilsmeier Reagent Chlorination. *J Heterocyclic Chem* 2009, *46* (2), 317-319.

139. Aggarwal, R.; Sumran, G.; Yadav, M.; Anju, Facile and Efficient Synthesis of 3,10-Disubstituted-Bis-1,2,4-Triazolo[4,3-a][3 ',4 '-C]Quinoxalines Using Copper Dichloride as an Oxidant. *Synthetic Commun* 2012, *42* (3), 350-357.

140. Vollmann, H.; Leister, H. 1,3-Bis(heterocycloimino)isoindolines. GB1116176, 1968.

141. Murakami, T.; Otsuka, M.; Kobayashi, S.; Ohno, M., Efficient Synthesis of 3-Formyl-1,2,4-Triazole Nucleoside Using Diethoxyacetonitrile as a Synthon. *Heterocycles* 1981, *16* (1), 187-187.

142. Merrifield, R. B., Solid Phase Peptide Synthesis. I. The Synthesis of a Tetrapeptide. *Journal of the American Chemical Society* 1963, *85* (14), 2149-2154.

143. Backes, B. J.; Ellman, J. A., Carbon-Carbon Bond-Forming Methods on Solid Support - Utilization of Kenner Safety-Catch Linker. *Journal of the American Chemical Society* 1994, *116* (24), 11171-11172.

144. Gennari, C.; Nestler, H. P.; Salom, B.; Still, W. C., Solid-Phase Synthesis of Vinylogous Sulfonyl Peptides. *Angewandte Chemie-International Edition in English* 1995, *34* (16), 1763-1765.

145. Goff, D. A.; Zuckermann, R. N., Solid-Phase Synthesis of Highly Substituted Peptoid 1(2h)-Isoquinolinones. *J Org Chem* 1995, *60* (18), 5748-5749.

146. Hutchins, S. M.; Chapman, K. T., A General-Method for the Solid-Phase Synthesis of Ureas. *Tetrahedron Lett* 1994, *35* (24), 4055-4058.

147. Kick, E. K.; Ellman, J. A., Expedient Method for the Solid-Phase Synthesis of Aspartic-Acid Protease Inhibitors Directed toward the Generation of Libraries. *J Med Chem* 1995, *38* (9), 1427-1430.

148. Kantam, M. L.; Jaya, V. S.; Sreedhar, B.; Rao, M. M.; Choudary, B. M., Preparation of alumina supported copper nanoparticles and their application in the synthesis of 1,2,3-triazoles. *J. Mol. Catal. A: Chem.* 2006, *256* (1-2), 273-277.

149. Miao, T.; Wang, L., *Synthesis* 2008, *3*, 363-368.

150. Chassaing, S.; Kumarraja, M.; Sido, A. S. S.; Pale, P.; Sommer, J., Click Chemistry in Cul-zeolites: The Huisgen [3 + 2]-Cycloaddition. *Org. Lett.* 2007, *9* (5), 883-886.

151. Coelho, A.; Diz, P.; Caamano, O.; Sotelo, E., *Adv. Synth. Catal.* 2010, *352*, 1179-1192.

152. Gude, M.; Ryf, J.; White, P. D., An accurate method for the quantitation of Fmoc-derivatized solid phase supports. *Lett Pept Sci* 2002, *9* (4-5), 203-206.

153. Megia-Fernandez, A.; Ortega-Munoz, M.; Lopez-Jaramillo, J.; Hernandez-Mateo, F.; Santoyo-Gonzalez, F., Non-Magnetic and Magnetic Supported Copper(I) Chelating Adsorbents as Efficient Heterogeneous Catalysts and Copper Scavengers for Click Chemistry. *Adv. Synth. Catal.* 2010, *352*, 3306-3320.

154. Li, D.; Bao, H.; You, T., Microwave-assisted and efficient one-pot synthesis of substituted 1,2,4-triazoles. *Heterocycles* 2005, *65*, 1957-1962.

155. Krishnakumar, V.; Xavier, R. J., FT Raman and FT-IR spectral studies of 3-mercapto-1,2,4-triazole. *Spectrochim Acta A* 2004, *60* (3), 709-714.

156. Elgammal, R. A.; Foister, S. Triazole catalysts and methods of making and using the same. WO2011035064A2, 2011.

157. Traylor, T. G.; Hill, K. W.; Fann, W. P.; Tsuchiya, S.; Dunlap, B. E., Aliphatic Hydroxylation Catalyzed by Iron(Iii) Porphyrins. *Journal of the American Chemical Society* 1992, *114* (4), 1308-1312.

158. Klingele, M. H.; Boyd, P. D. W.; Moubaraki, B.; Murray, K. S.; Brooker, S., Probing the dinucleating behaviour of a bis-bidentate ligand: Synthesis and characterisation of some di- and mononuclear cobalt(II), nickel(II), copper(II) and zinc(II) complexes of 3,5-di(2-pyridyl)-4-(1H-pyrrol-1-yl)-4H-1,2,4-triazole. *Eur J Inorg Chem* 2006, (3), 573-589.

159. Fernandes, R. R.; Kirillova, M. V.; da Silva, J. A. L.; da Silva, J. J. R. F.; Pombeiro, A. J. L., Oxidations of cycloalkanes and benzene by hydrogen peroxide catalyzed by an {(FeN2S2)-N-III} centre. *Appl Catal a-Gen* 2009, *353* (1), 107-112.

160. Slaughter, L. M.; Collman, J. P.; Eberspacher, T. A.; Brauman, J. I., Radical autoxidation and autogenous O-2 evolution in manganese-porphyrin catalyzed alkane oxidations with chlorite. *Inorg Chem* 2004, *43* (17), 5198-5204.

161. Rodríguez-reinoso, F., The role of carbon materials in heterogeneous catalysis. *Carbon* 1998, *36* (3), 159-175.

162. Radovic, L. R., A Landmark Paper on Carbon-Supported Catalysts by Frank Derbyshire: The Real Story Revealed (or Obscured?) by the Science Citation Index*. *Energeia* 2001, *12* (3).

163. What is Carbon Black? http://www.carbon-black.org/what_is.html.

164. Duteanu, N.; Erable, B.; Senthil, K. S. M.; Ghangrekar, M. M.; Scott, K., Effect of chemically modified Vulcan XC-72R on the performance of air-breathing cathode in a single-chamber microbial fuel cell. *Bioresour. Technol.* 2010, *101*, 5250-5255.

165. Park, S.-J.; Seo, M.-K.; Nah, C., Influence of surface characteristics of carbon blacks on cure and mechanical behaviors of rubber matrix compounding. *J. Colloid Interface Sci.* 2005, *291*, 229-235.

166. Wildgoose, G. G.; Abiman, P.; Compton, R. G., Characterising chemical functionality on carbon surfaces. *J. Mater. Chem.* 2009, *19*, 4875-4886.

167. Dementev, N.; Feng, X.; Borguet, E., Fluorescence Labeling and Quantification of Oxygen-Containing Functionalities on the Surface of Single-Walled Carbon Nanotubes. *Langmuir* 2009, *25*, 7573-7577.

168. Borah, D.; Satokawa, S.; Kato, S.; Kojima, T., Characterization of chemically modified carbon black for sorption application. *Appl. Surf. Sci.* 2008, *254* (Copyright (C) 2011 American Chemical Society (ACS). All Rights Reserved.), 3049-3056.

169. Borguet, E.; Xing, Y.; Dementev, N.; Feng, X. In *Fluorescence labeling of surface species (FLOSS) as a probe of chemical composition of complex interfaces*, American Chemical Society: 2006; pp COLL-409.

170. Feng, X.; Matranga, C.; Vidic, R.; Borguet, E., A Vibrational Spectroscopic Study of the Fate of Oxygen-Containing Functional Groups and Trapped CO2 in Single-Walled Carbon Nanotubes During Thermal Treatment. *J. Phys. Chem. B* 2004, *108*. All Rights Reserved.), 19949-19954.

171. Domingo-Garcia, M.; Lopez, G. F. J.; Perez-Mendoza, M. J., On the Characterization of Chemical Surface Groups of Carbon Materials. *J. Colloid Interface Sci.* 2002, *248*, 116-122.

172. Burakiewicz-Mortka, W.; Jaroniec, M.; Choma, J., Studies of surface properties of carbonaceous adsorbents by means of infrared spectroscopy and thermogravimetry. *Biul. Wojsk. Akad. Tech.* 2000, *49*, 5-17.

173. Song, W.; Li, Y.; Guo, X.; Li, J.; Shen, W., Surface-functionalized carbon black as catalyst for the direct production of hydrogen peroxide by the oxidation of hydroxylamine. *Chin. J. Chem.* 2010, *28*, 693-698.

174. Lopez, d. l. T. M. D.; Melguizo, G. M., Covalent Bonds on Activated Carbon. *Eur. J. Org. Chem.* 2010, , 5147-5154.

175. Sini, N. K.; Choudhury, A.; Sarkhel, G., Chemically modified carbon black filled ethylene-propylene-diene rubber composites: mechanical and dynamic mechanical study. *Prog. Rubber, Plast. Recycl. Technol.* 2009, *25*, 29-44.

176. Huang, J.; Shen, F.; Li, X.; Zhou, X.; Li, B.; Xu, R.; Wu, C., Chemical modification of carbon black by a simple non-liquid-phase approach. *J. Colloid Interface Sci.* 2008, *328*, 92-97.

177. Asakawa, T.; Ogino, K., Adsorption of phenol on surface-modified carbon black from its aqueous solution. *J. Colloid Interface Sci.* 1984, *102*. All Rights Reserved.), 348-55.

178. Brushett, F. R.; Thorum, M. S.; Lioutas, N. S.; Naughton, M. S.; Tornow, C.; Jhong, H.-R.; Gewirth, A. A.; Kenis, P. J. A., A Carbon-supported copper complex of 3,5-diamino-1,2,4-triazole as a cathode catalyst for alkaline fuel cell applications. *J. Am. Chem. Soc.* 2010, *132*. All Rights Reserved.), 12185-12187.

179. Pauric, A. D.; MacLean, B. J.; Easton, E. B., Fe-N/C Oxygen Reduction Catalysis Prepared by Covalent Attachment of 1,10-Phenanthroline to a Carbon Surface. *J. Electrochem. Soc.* 2011, *158*, B331-B336.

180. Wepasnick, K. A.; Smith, B. A.; Schrote, K. E.; Wilson, H. K.; Diegelmann, S. R.; Fairbrother, D. H., Surface and structural characterization of multi-walled carbon nanotubes following different oxidative treatments. *Carbon* 2010, *49*, 24-36.

181. Yoshikawa, S.; Tsubokawa, N., Grafting of polymers with controlled molecular weight onto 1scarbon black surface. *Polym. J. (Tokyo)* 1996, *28*, 317-22.

182. Tsubokawa, N.; Satoh, T.; Murota, M.; Sato, S.; Shimizu, H., Grafting of hyperbranched poly (amidoamine) onto carbon black surfaces using dendrimer synthesis methodology. *Polym Advan Technol* 2001, *12* (10), 596-602.

183. Yang, E.-C.; Liang, Q.-Q.; Wang, X.-G.; Zhao, X.-J., Two Novel Triazole-Based Metal-Organic Frameworks Consolidated by a Flexible Dicarboxylate Co-ligand:

Hydrothermal Synthesis, Crystal Structure, and Luminescence Properties. *Aust. J. Chem.* 2008, *61*, 813-820.

184. Welte, L.; Garcia-Couceiro, U.; Castillo, O.; Olea, D.; Polop, C.; Guijarro, A.; Luque, A.; Gomez-Rodriguez, J. M.; Gomez-Herrero, J.; Zamora, F., Organization of Coordination Polymers on Surfaces by Direct Sublimation. *Adv. Mater. (Weinheim, Ger.)* 2009, *21*, 2025-2028.

185. Gilyazetdinov, L. P.; Romanova, V. I.; Lutokhina, A. S.; Tsygankova, E. I.; Safronova, I. M., Oxidative modification of the surface of carbon blacks. *Zh. Prikl. Khim. (Leningrad)* 1976, *49*, 420-4.

186. Yamada, T.; Maruta, G.; Takeda, S., Reversible solid-state structural conversion between a three-dimensional network and a one-dimensional chain of Cu(II) triazole coordination polymers in acidic/basic-suspensions or vapors. *Chem Commun* 2011, *47* (2), 653-655.

187. Kimball, D. B.; Haley, M. M., Triazenes: A Versatile Tool in Organic Synthesis. *Angewandte Chemie International Edition* 2002, *41* (18), 3338-3351.

188. Chen, Z. W.; Higgins, D.; Yu, A. P.; Zhang, L.; Zhang, J. J., A review on non-precious metal electrocatalysts for PEM fuel cells. *Energ Environ Sci* 2011, *4* (9), 3167-3192.

189. Kaneko, K.; Furuya, K.; Hungria, A. B.; Hernandez-Garrido, J. C.; Midgley, P. A.; Onodera, T.; Kasai, H.; Yaguchi, Y.; Oikawa, H.; Nomura, Y.; Harada, H.; Ishihara, T.; Baba, N., Nanostructural characterization and catalytic analysis of hybridized platinum/phthalocyanine nanocomposites. *J Electron Microsc* 2009, *58* (5), 289-294.

190. Gojkovic, S. L.; Gupta, S.; Savinell, R. F., Heat-treated iron(III) tetramethoxyphenyl porphyrin chloride supported on high-area carbon as an electrocatalyst for oxygen reduction - Part II. Kinetics of oxygen reduction. *J Electroanal Chem* 1999, *462* (1), 63-72.

191. Yeager, E., Electrocatalysts for O2 reduction. *Electrochimica Acta* 1984, *29* (11), 1527-1537.

192. Scherson, D. A.; Yao, S. B.; Yeager, E. B.; Eldridge, J.; Kordesch, M. E.; Hoffman, R. W., In situ and ex situ Moessbauer spectroscopy studies of iron phthalocyanine adsorbed on high surface area carbon. *The Journal of Physical Chemistry* 1983, *87* (6), 932-943.

193. Yeager, E., Dioxygen electrocatalysis: mechanisms in relation to catalyst structure. *Journal of Molecular Catalysis* 1986, *38* (1–2), 5-25.

194. Strelko, V. V.; Kartel, N. T.; Dukhno, I. N.; Kuts, V. S.; Clarkson, R. B.; Odintsov, B. M., Mechanism of reductive oxygen adsorption on active carbons with various surface chemistry. *Surface Science* 2004, *548* (1–3), 281-290.

195. Strelko, V. V.; Kuts, V. S.; Thrower, P. A., On the mechanism of possible influence of heteroatoms of nitrogen, boron and phosphorus in a carbon matrix on the catalytic activity of carbons in electron transfer reactions. *Carbon* 2000, *38* (10), 1499-1503.

196. Barton, S. S.; Evans, M. J. B.; Halliop, E.; MacDonald, J. A. F., Acidic and basic sites on the surface of porous carbon. *Carbon* 1997, *35* (9), 1361-1366.

197. Papirer, E.; Lacroix, R.; Donnet, J. B., Chemical modifications and surface properties of carbon blacks. *Carbon* 1996, *34*, 1521-1529.

198. Langley, L. A.; Villanueva, D. E.; Fairbrother, D. H., Quantification of surface oxides on carbonaceous materials. *Chem Mater* 2006, *18* (1), 169-178.

199. Lee, W. H.; Kim, S. J.; Lee, W. J.; Lee, J. G.; Haddon, R. C.; Reucroft, P. J., X-ray photoelectron spectroscopic studies of surface modified single-walled carbon nanotube material. *Applied Surface Science* 2001, *181* (1–2), 121-127.

200. Darmstadt, H.; Roy, C., Surface spectroscopic study of basic sites on carbon blacks. *Carbon* 2003, *41* (13), 2662-2665.

201. Cenini, S.; Tollari, S.; Penoni, A.; Cereda, C., Catalytic amination of unsaturated hydrocarbons: reactions of p-nitrophenylazide with alkenes catalysed by metallo-porphyrins. *J Mol Catal a-Chem* 1999, *137* (1-3), 135-146.

202. Suarez, A. I. O.; Jiang, H. L.; Zhang, X. P.; de Bruin, B., The radical mechanism of cobalt(II) porphyrin-catalyzed olefin aziridination and the importance of cooperative H-bonding. *Dalton T* 2011, *40* (21), 5697-5705.

203. Piangiolino, C.; Gallo, E.; Caselli, A.; Fantauzzi, S.; Ragaini, F.; Cenini, S., The [Ru(CO)(porphyrin)]-catalyzed synthesis of N-aryl-2-vinylaziridines. *Eur J Org Chem* 2007, (5), 743-750.

204. Gabryszewski, M., Spectral and magnetic studies of the Co(II), Ni(II), Zn(II), and Cd(II) complexes with 1H-1,2,4-triazole-3-thiol and 3-amino-5-mercapto-1,2,4-triazole. *Spectrosc Lett* 2001, *34* (1), 57-63.

205. Kwart, H.; Kahn, A. A., Copper-Catalyzed Decomposition of Benzenesulfonyl Azide in Hydroxylic Media. *Journal of the American Chemical Society* 1967, *89* (8), 1950-&.

APPENDIX

^{1}H and ^{13}C NMR for selected compounds

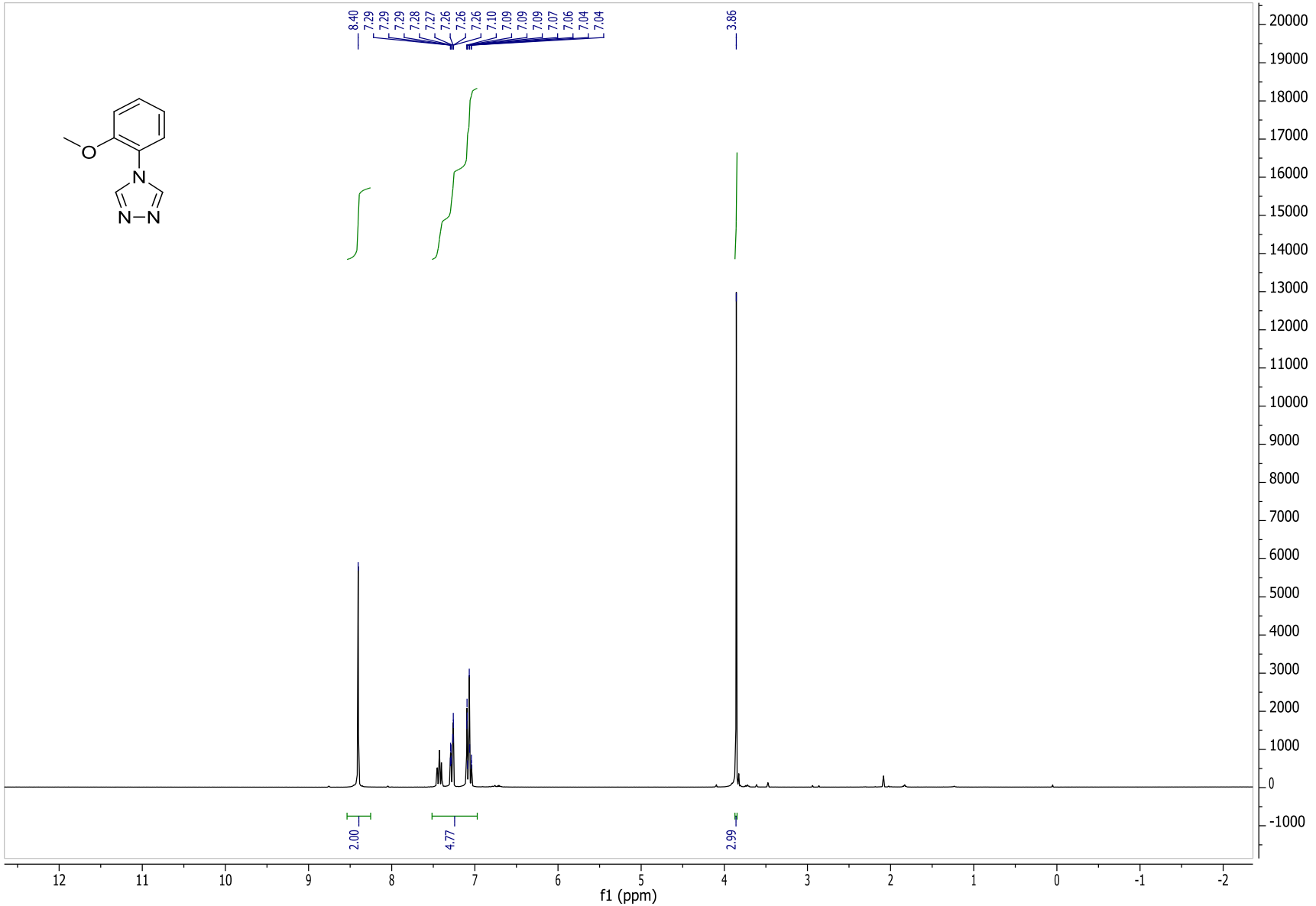

[1]H NMR spectrum of 2.5

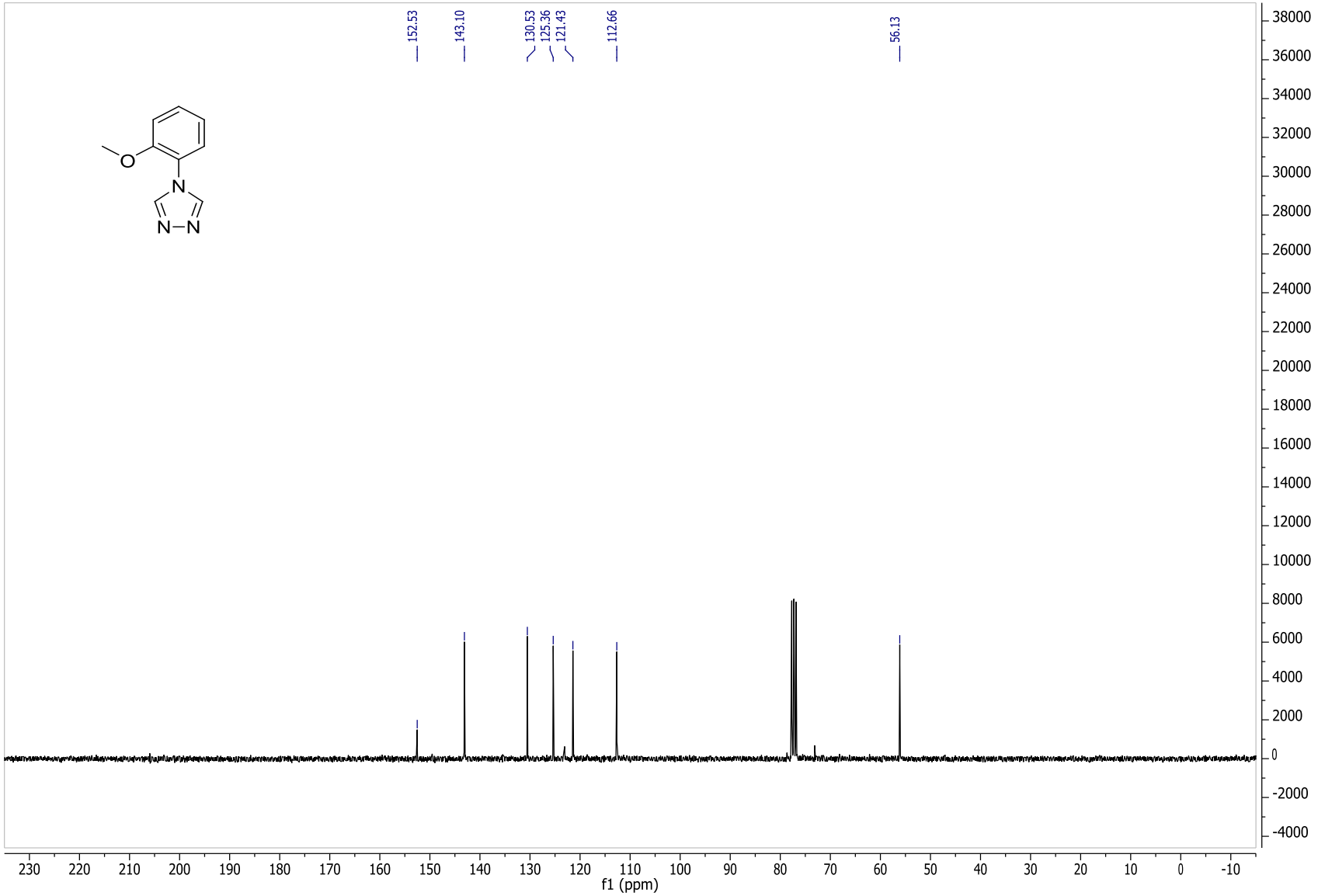

^{13}C NMR spectrum of 2.5

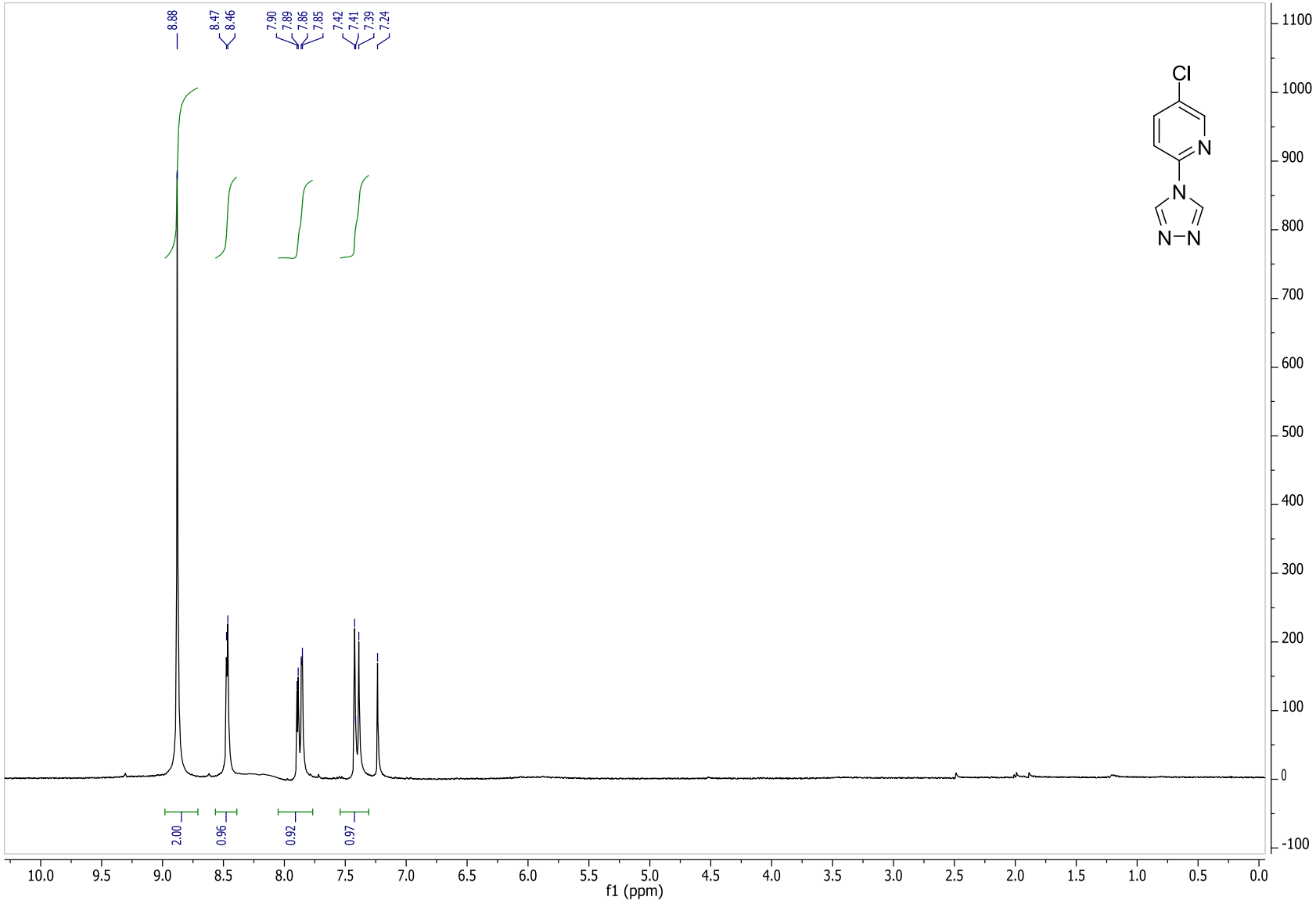

^{1}H NMR spectrum of 2.15

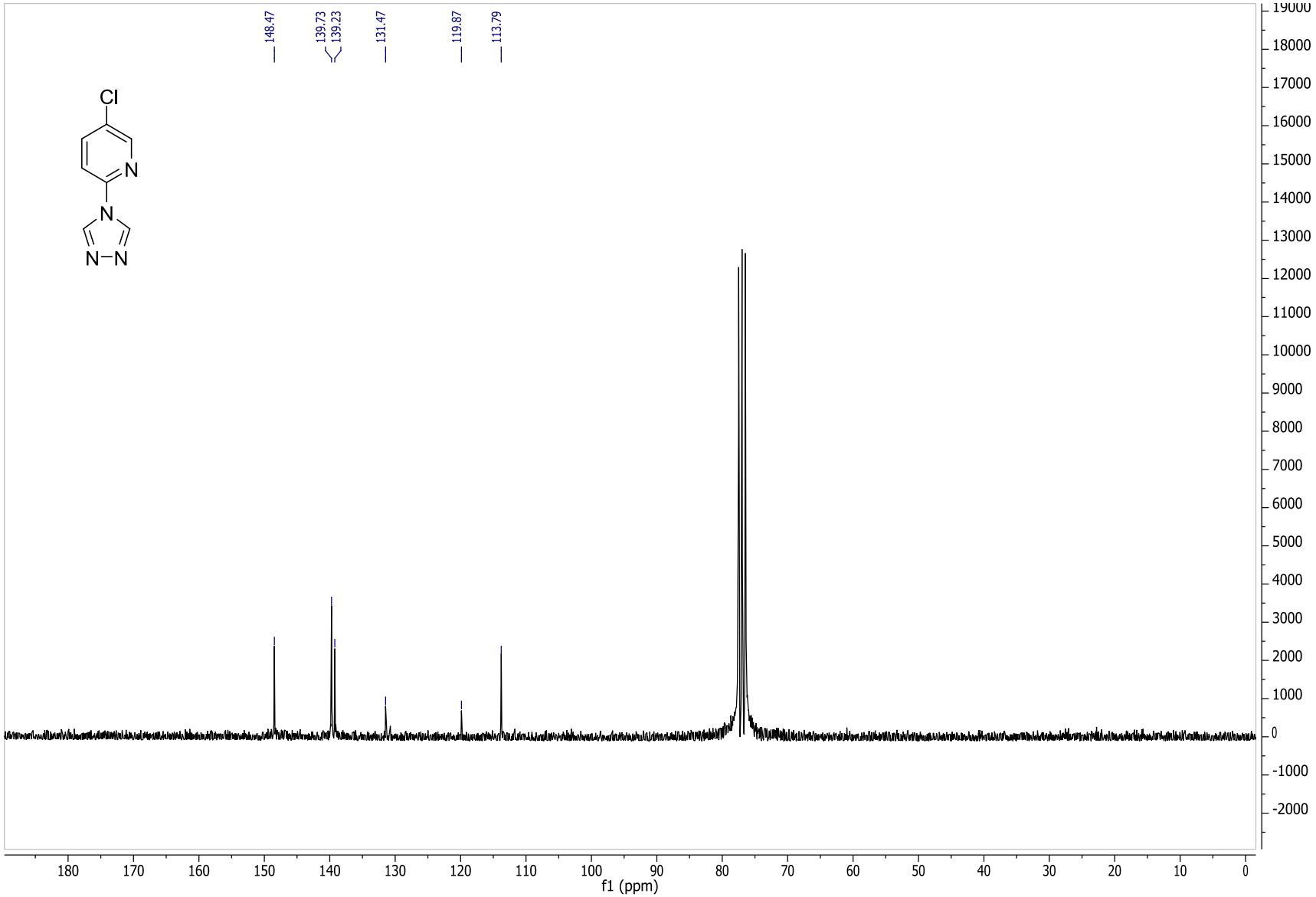

^{13}C NMR spectrum of 2.15

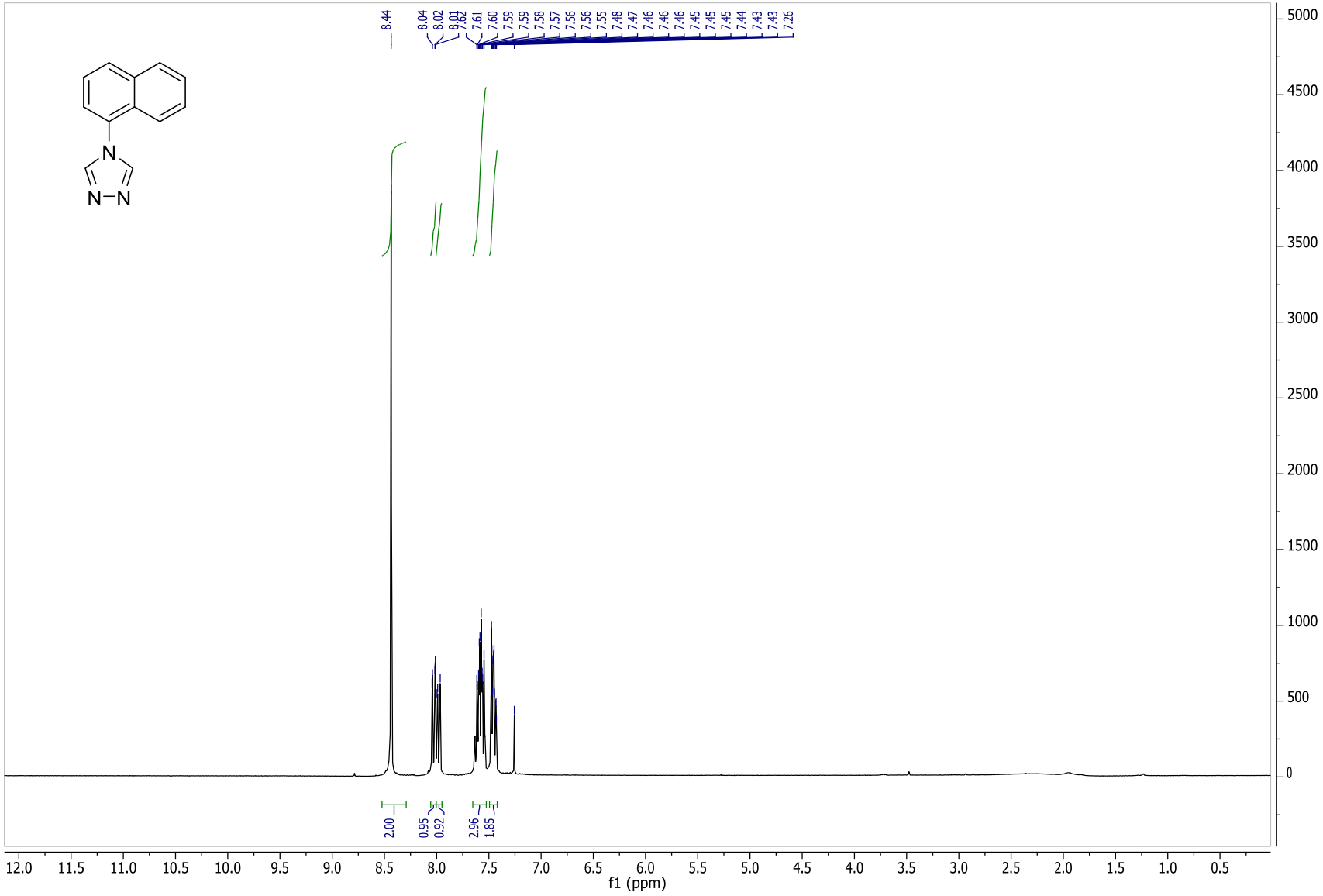

^{1}H NMR spectrum of 2.16

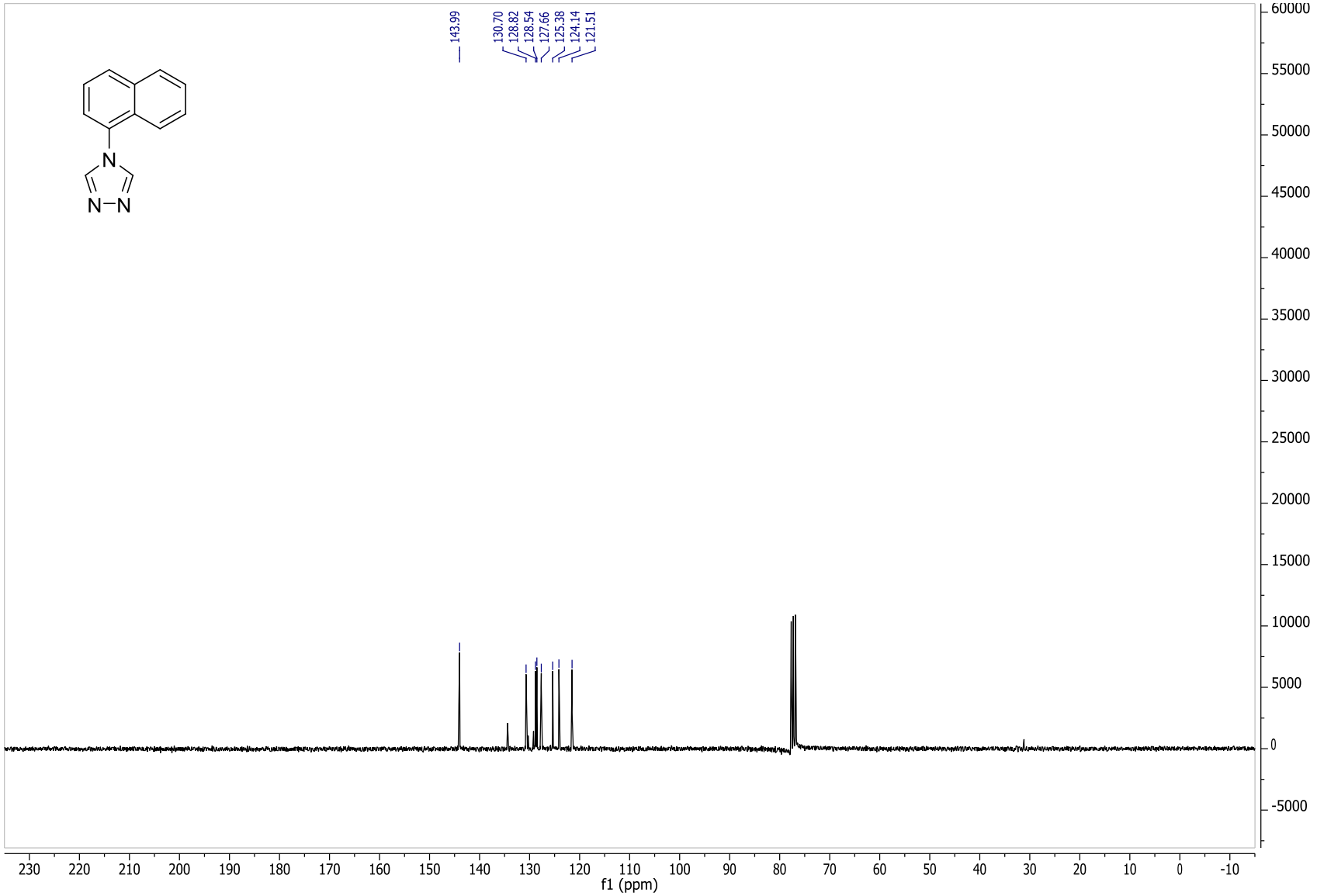

^{13}C NMR spectrum of 2.16

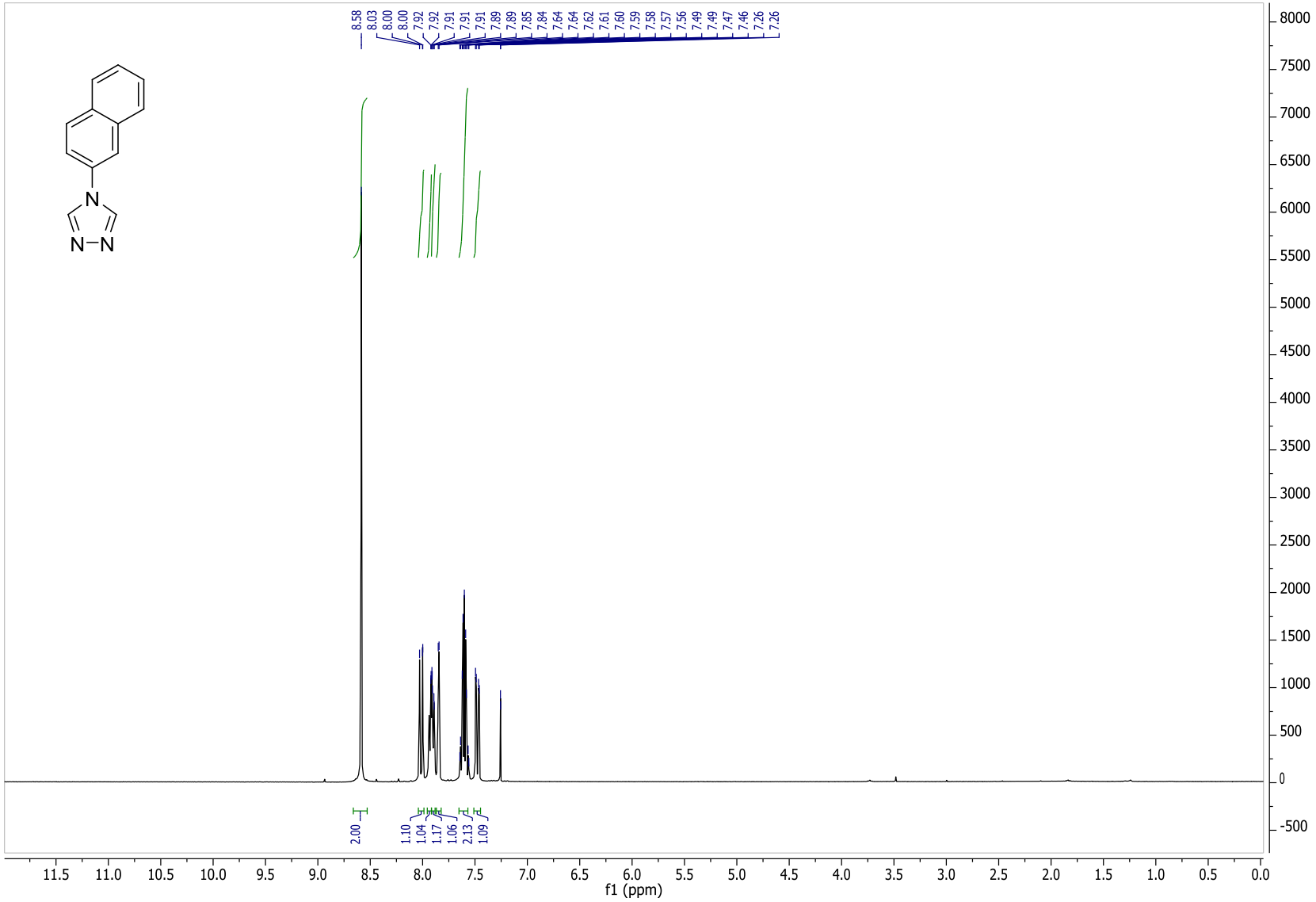

^{1}H NMR spectrum of 2.17

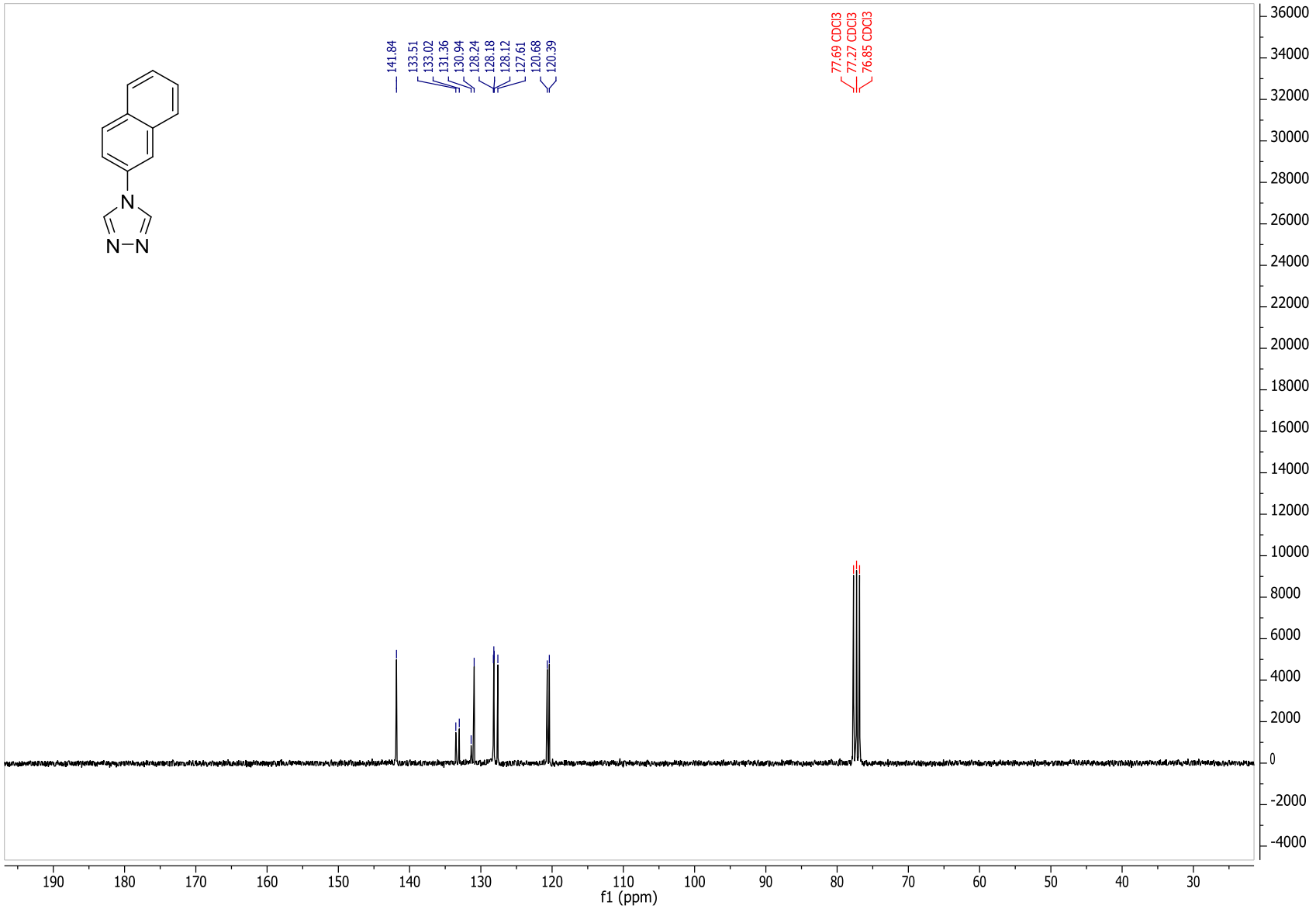

^{13}C NMR spectrum of 2.17

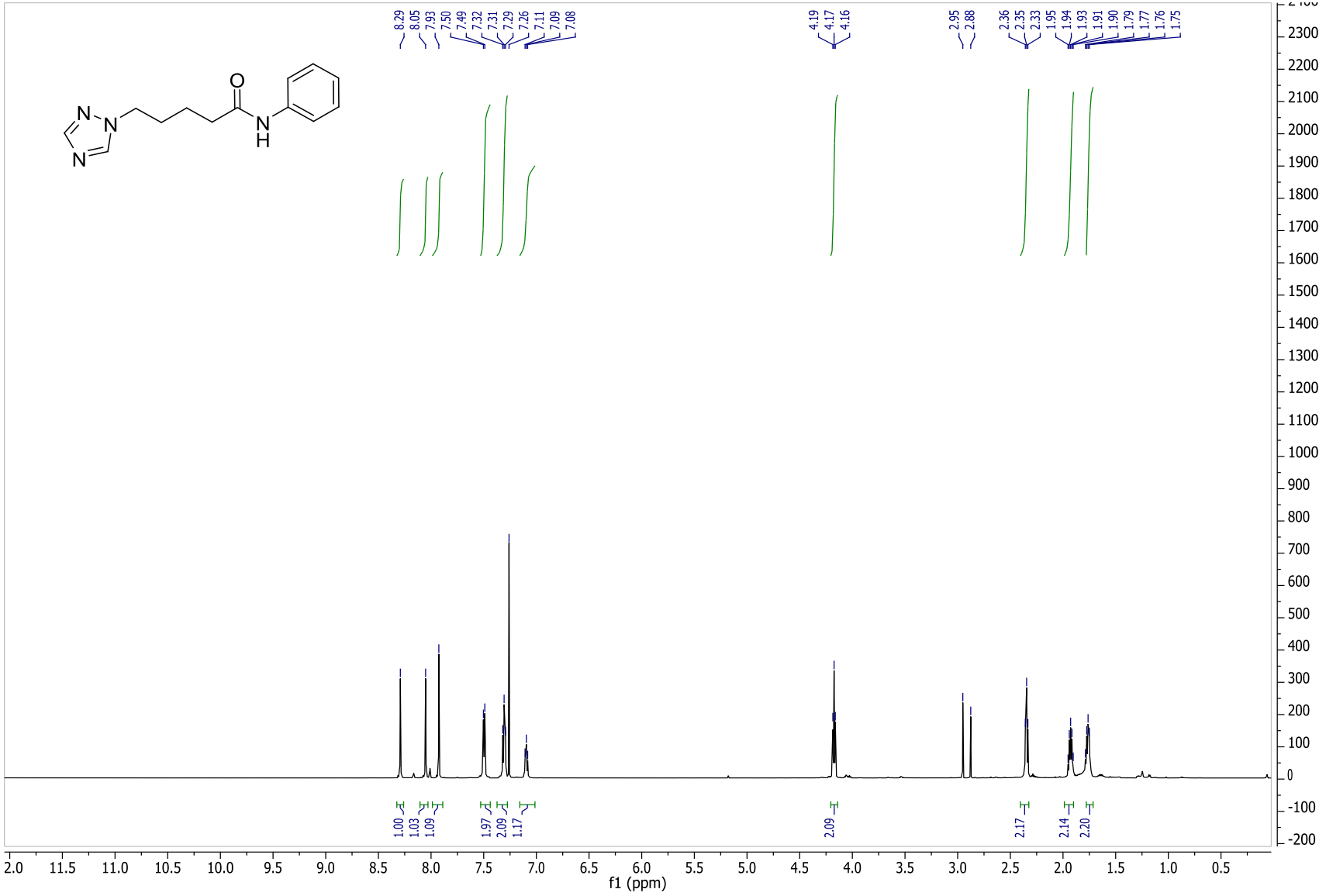

[1]H NMR spectrum of 2.20

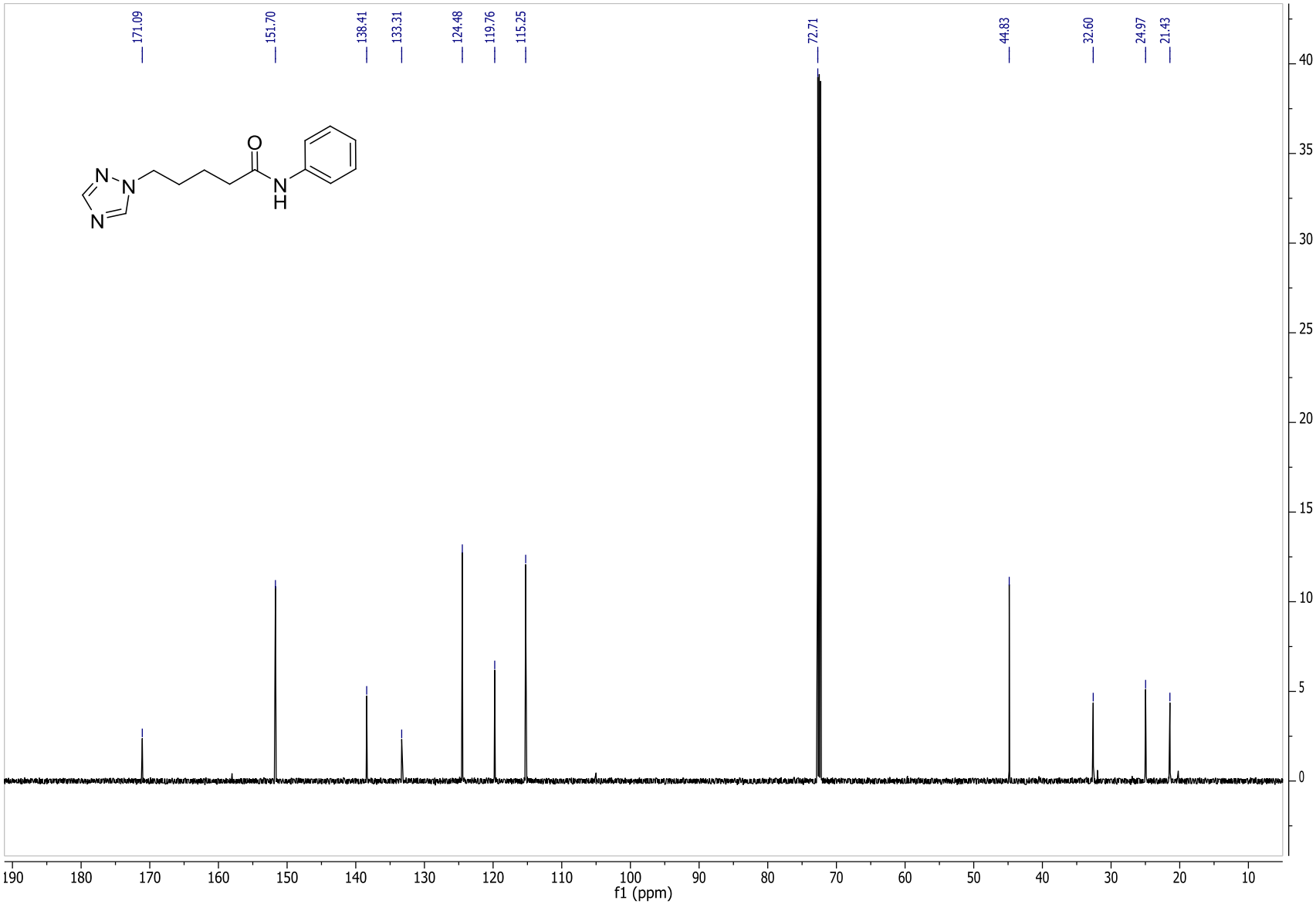

^{13}C NMR spectrum of 2.20

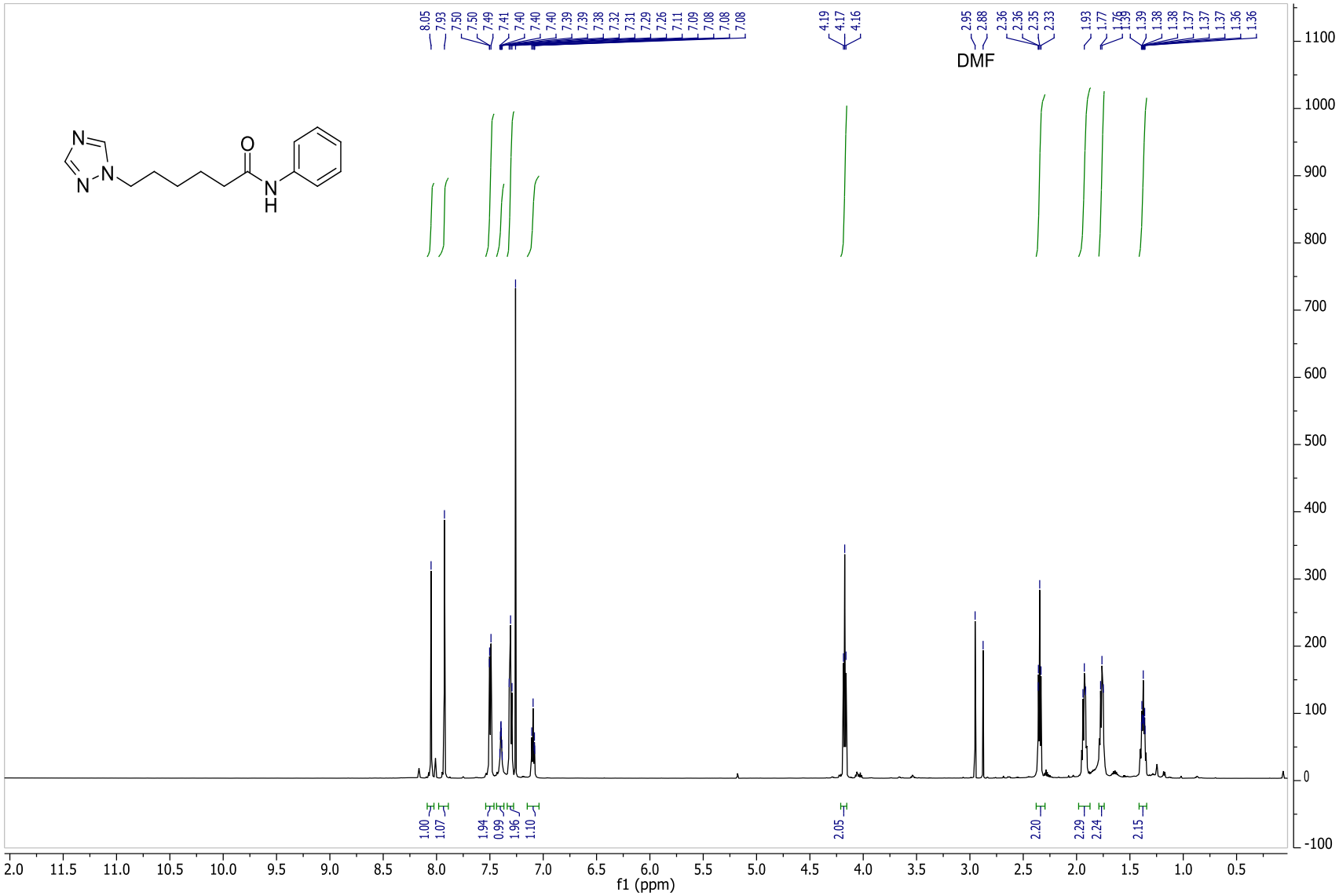

[1]H NMR spectrum of 2.21

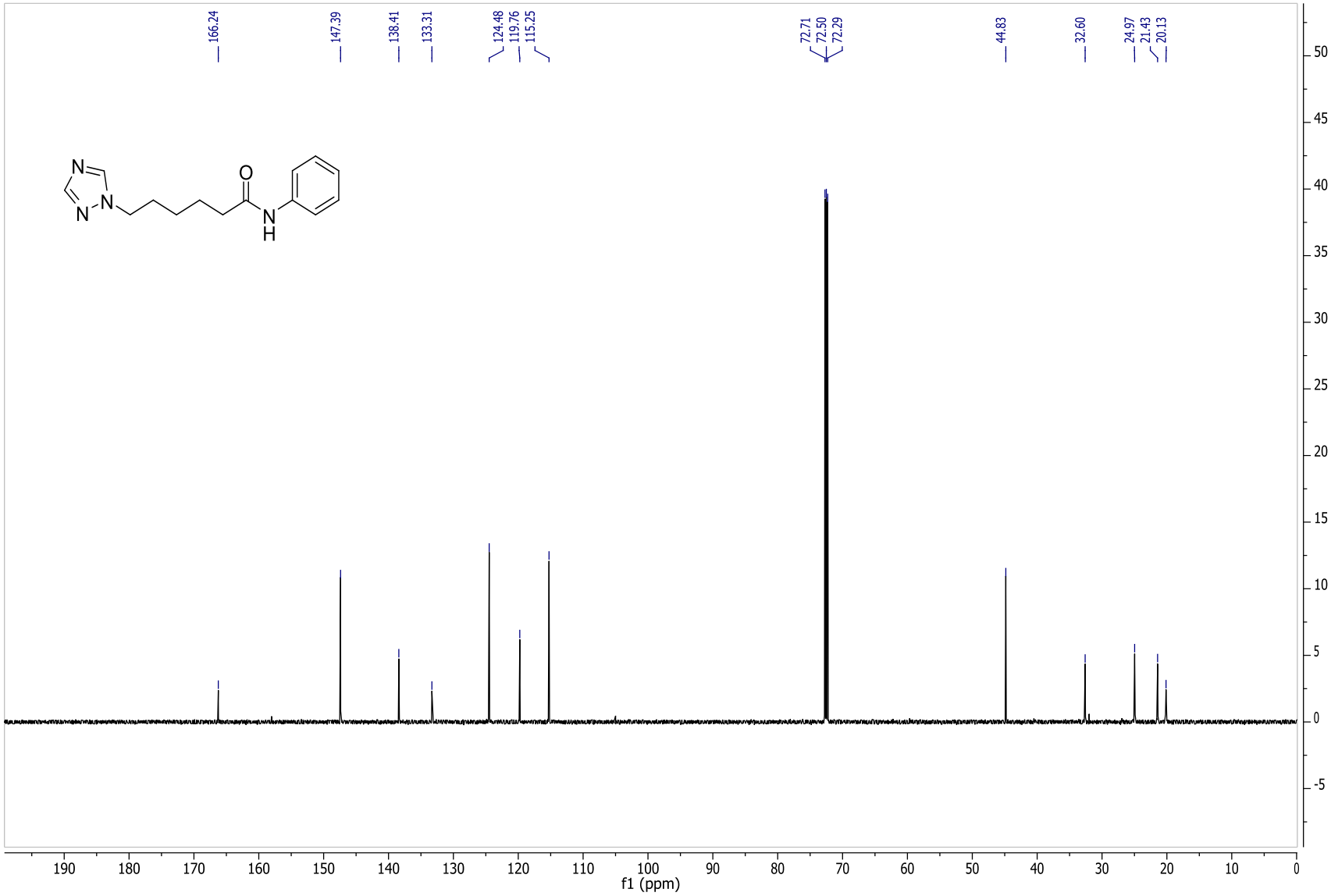

^{13}C NMR spectrum of 2.21

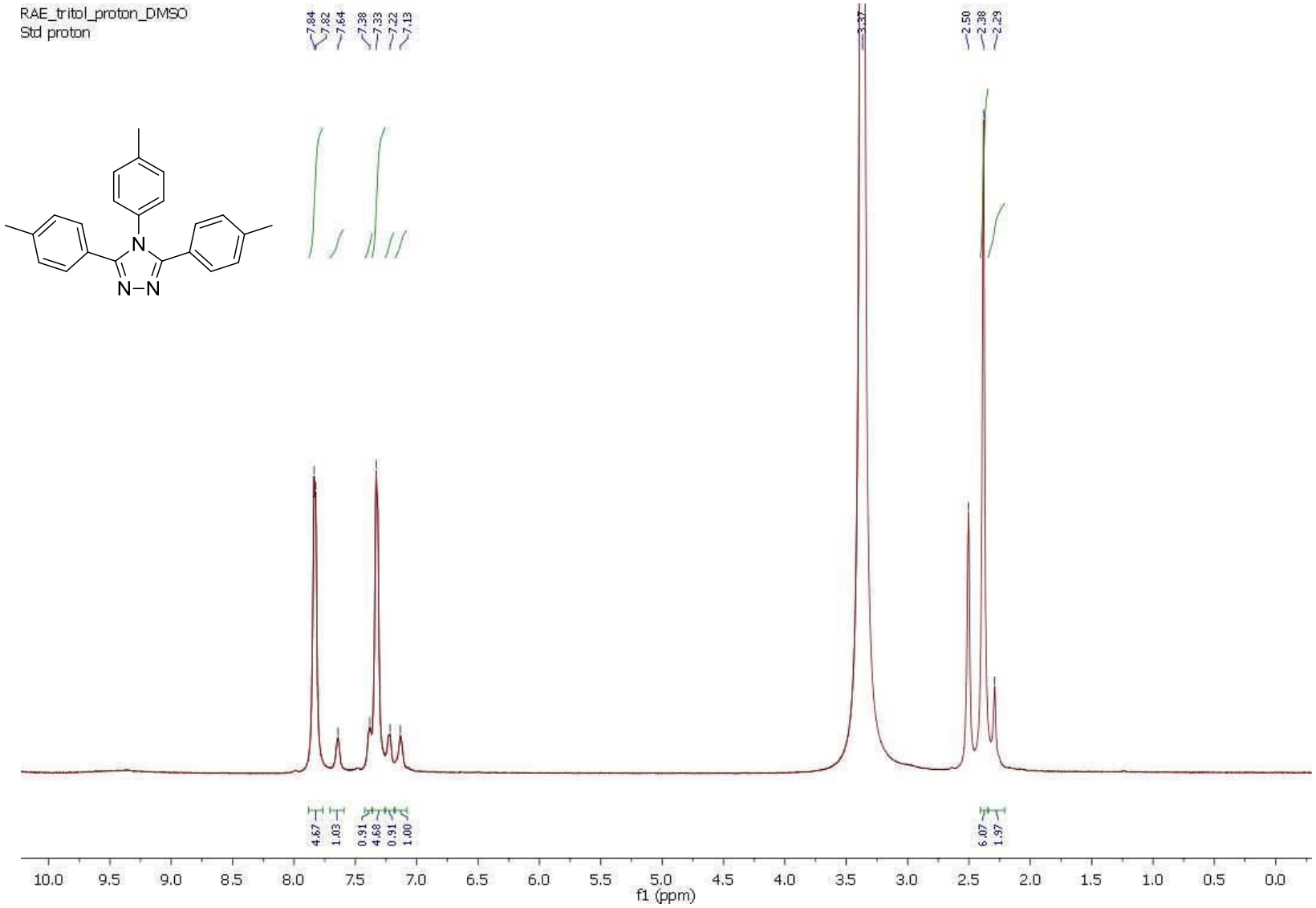

^{1}H NMR spectrum of 2.33

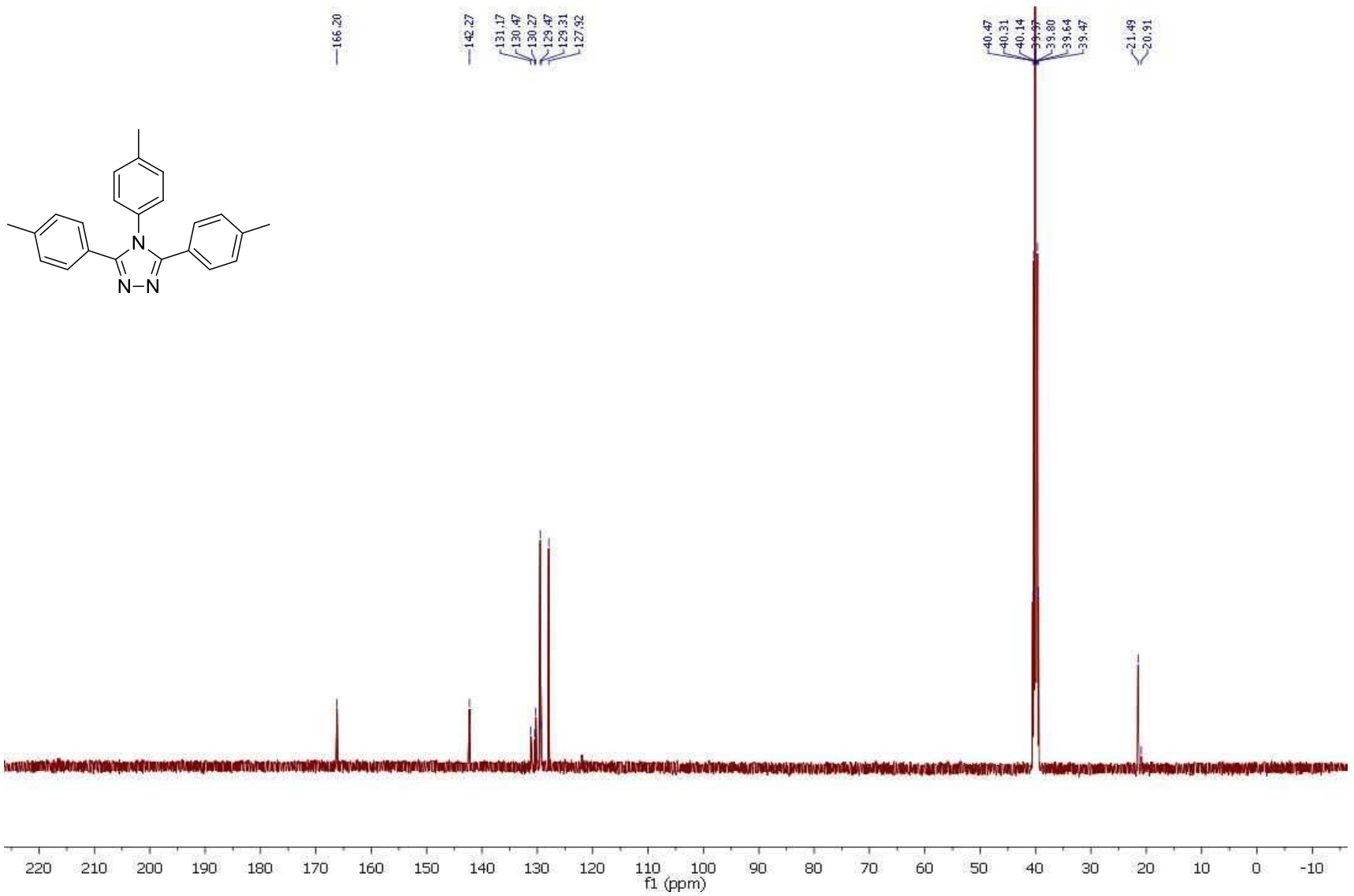

^{13}C NMR spectrum of 2.33

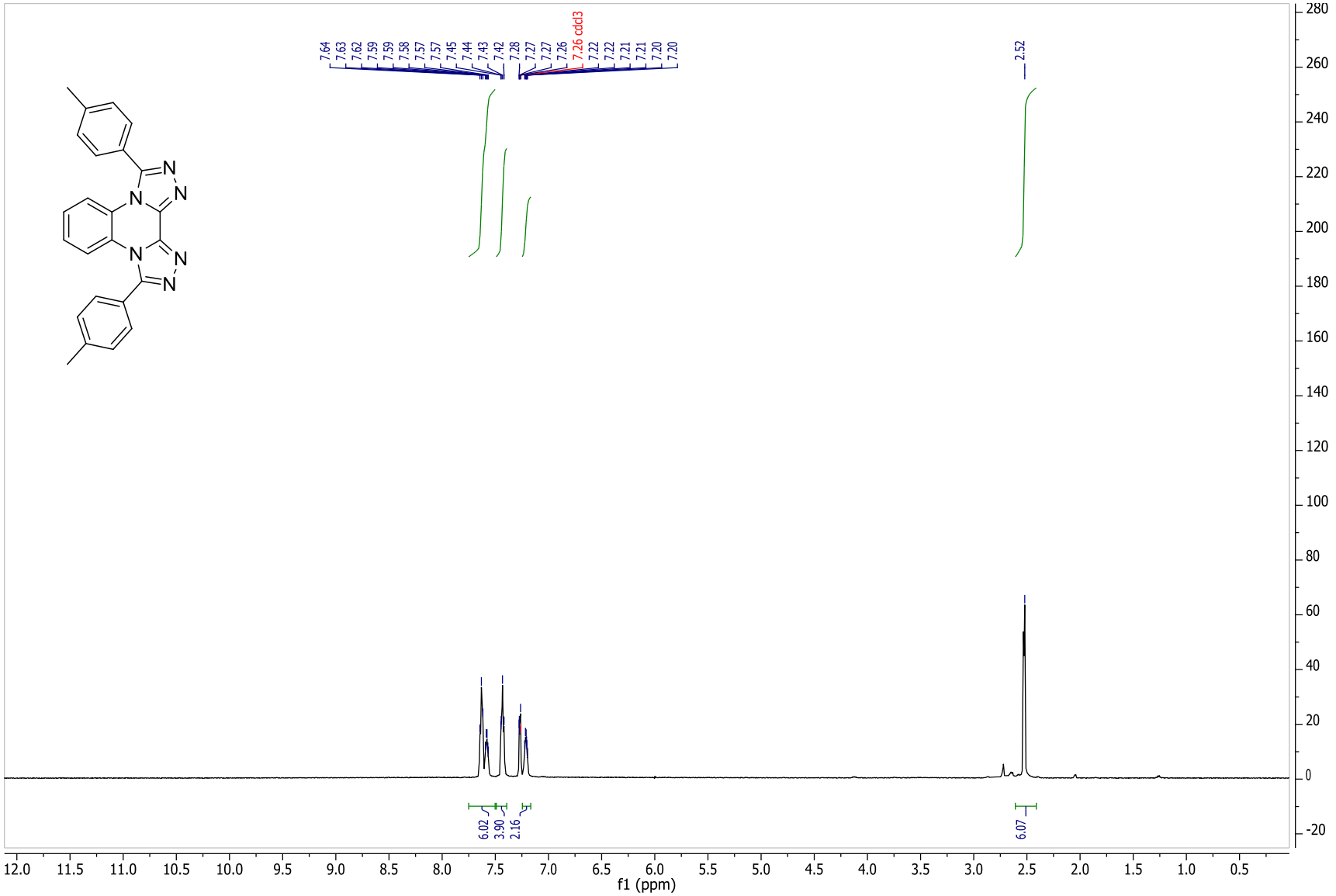

[1]H NMR spectrum of 2.37

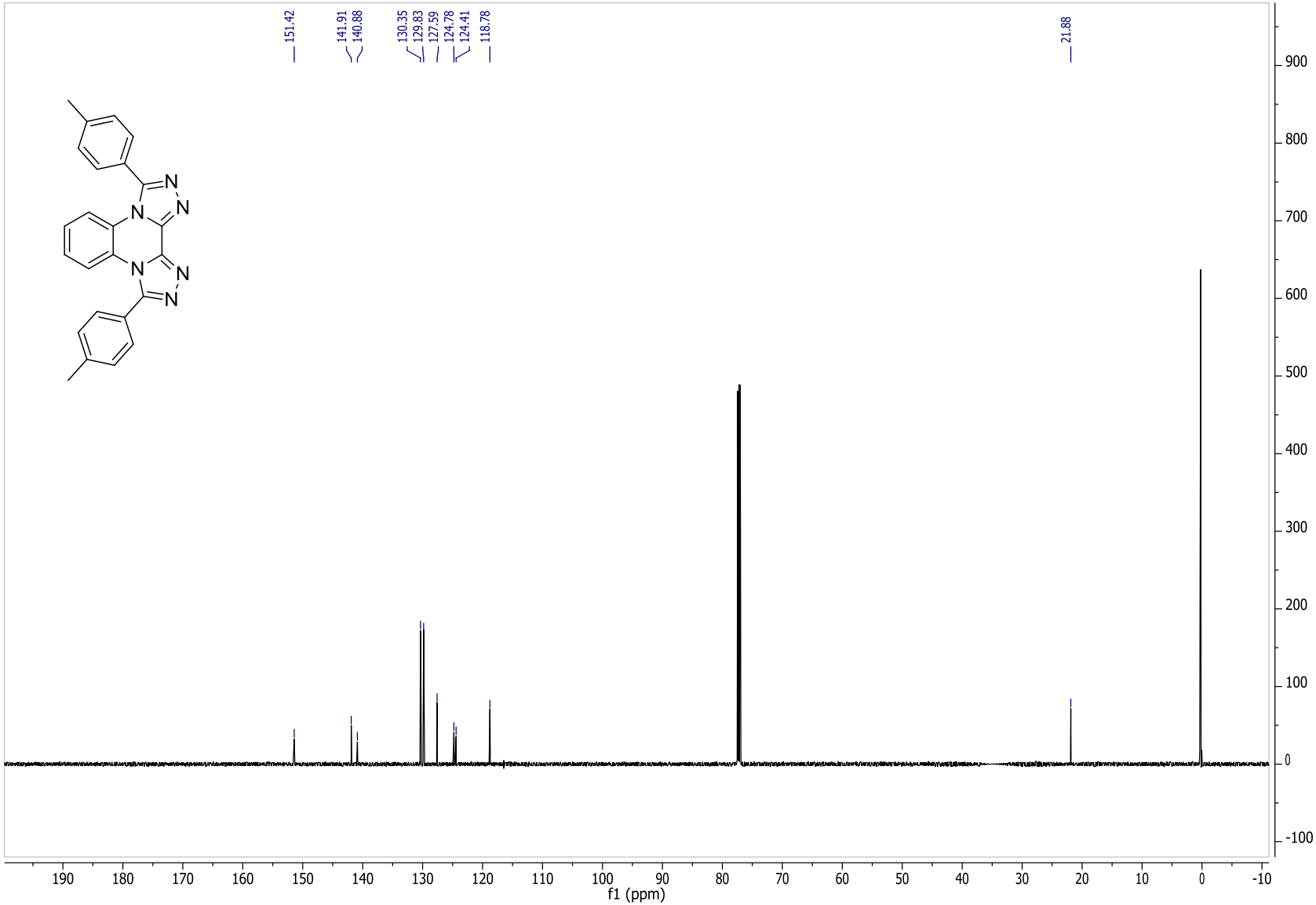

^{13}C NMR spectrum of 2.37

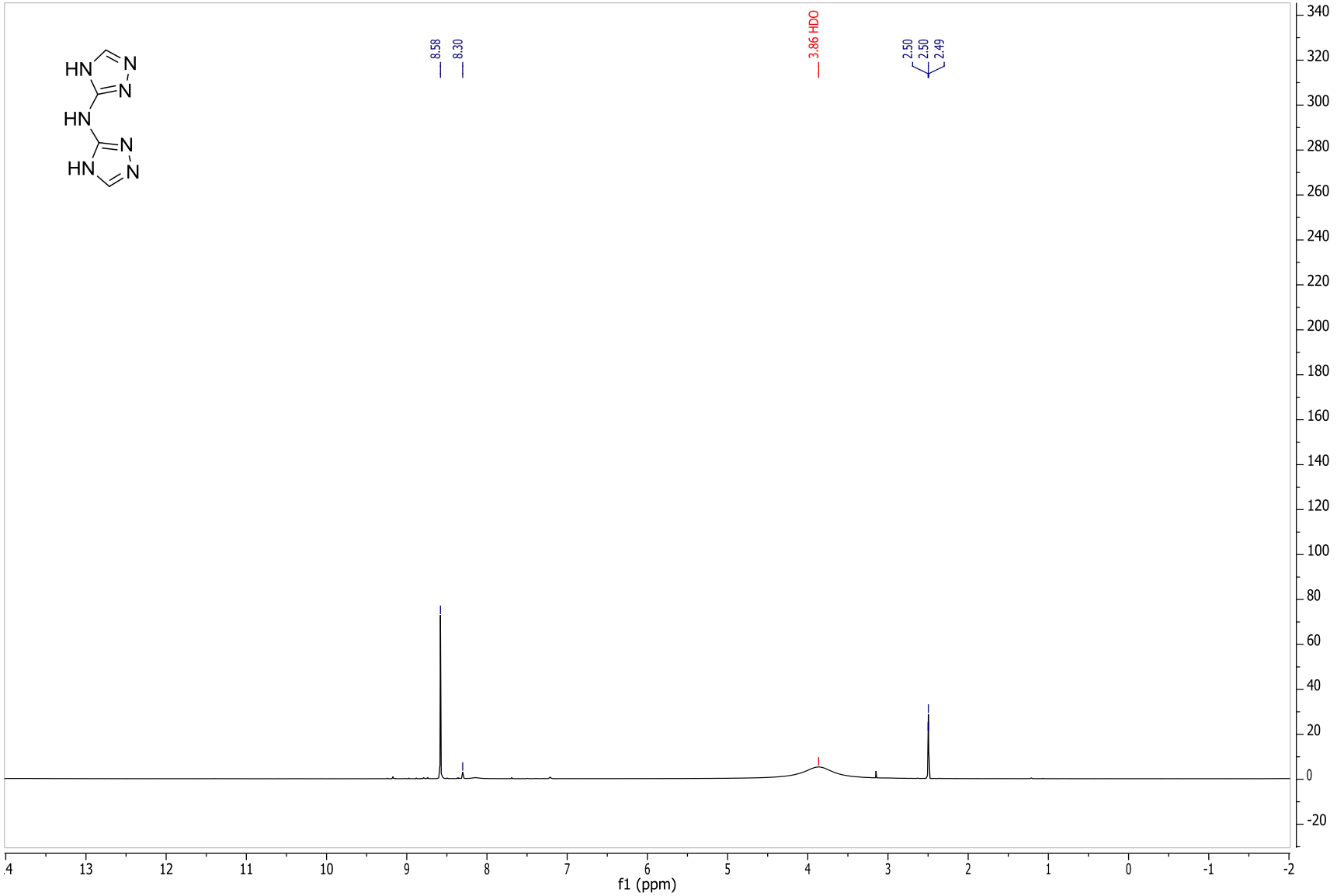

^{1}H NMR spectrum of 2.42

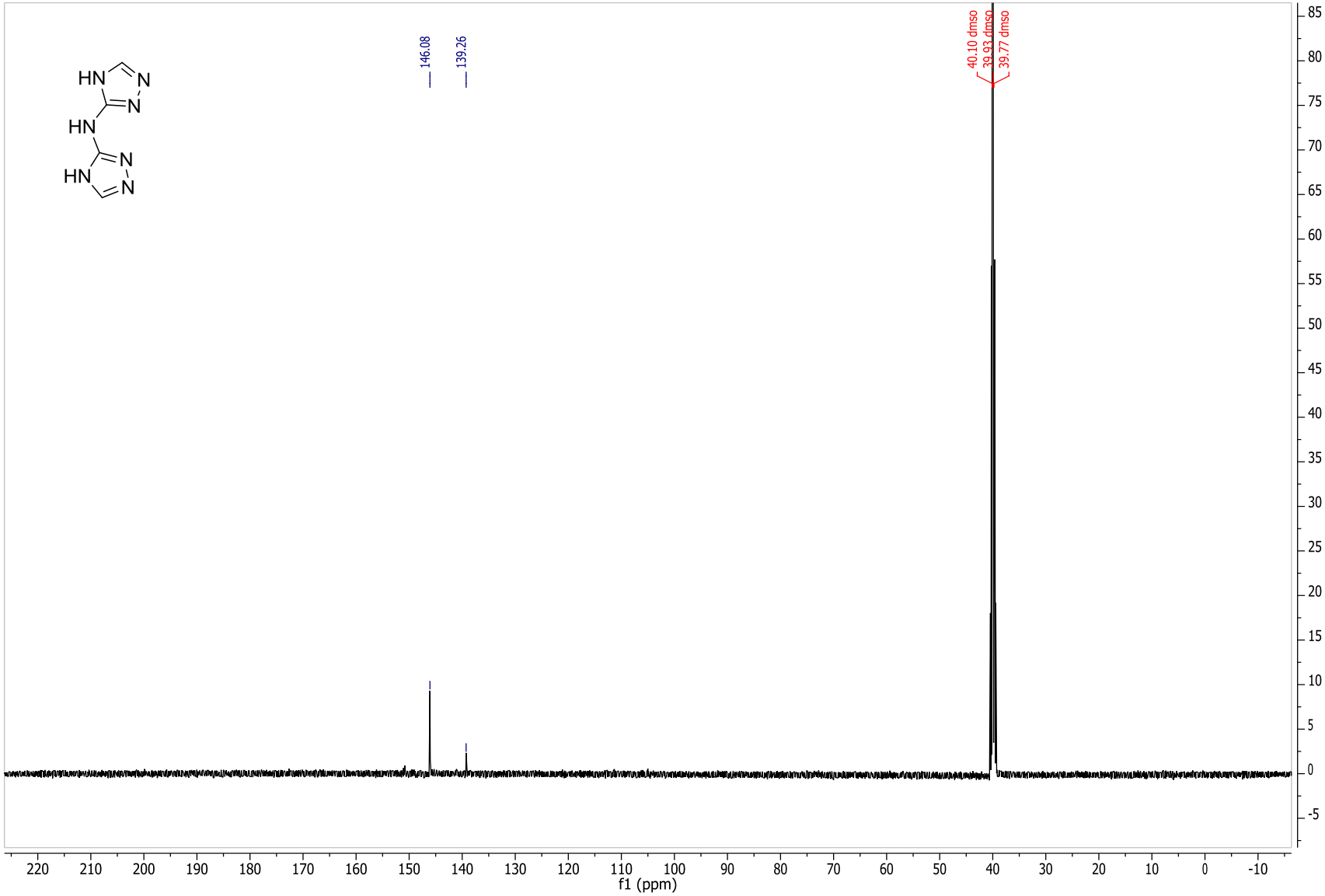

^{13}C NMR spectrum of 2.42

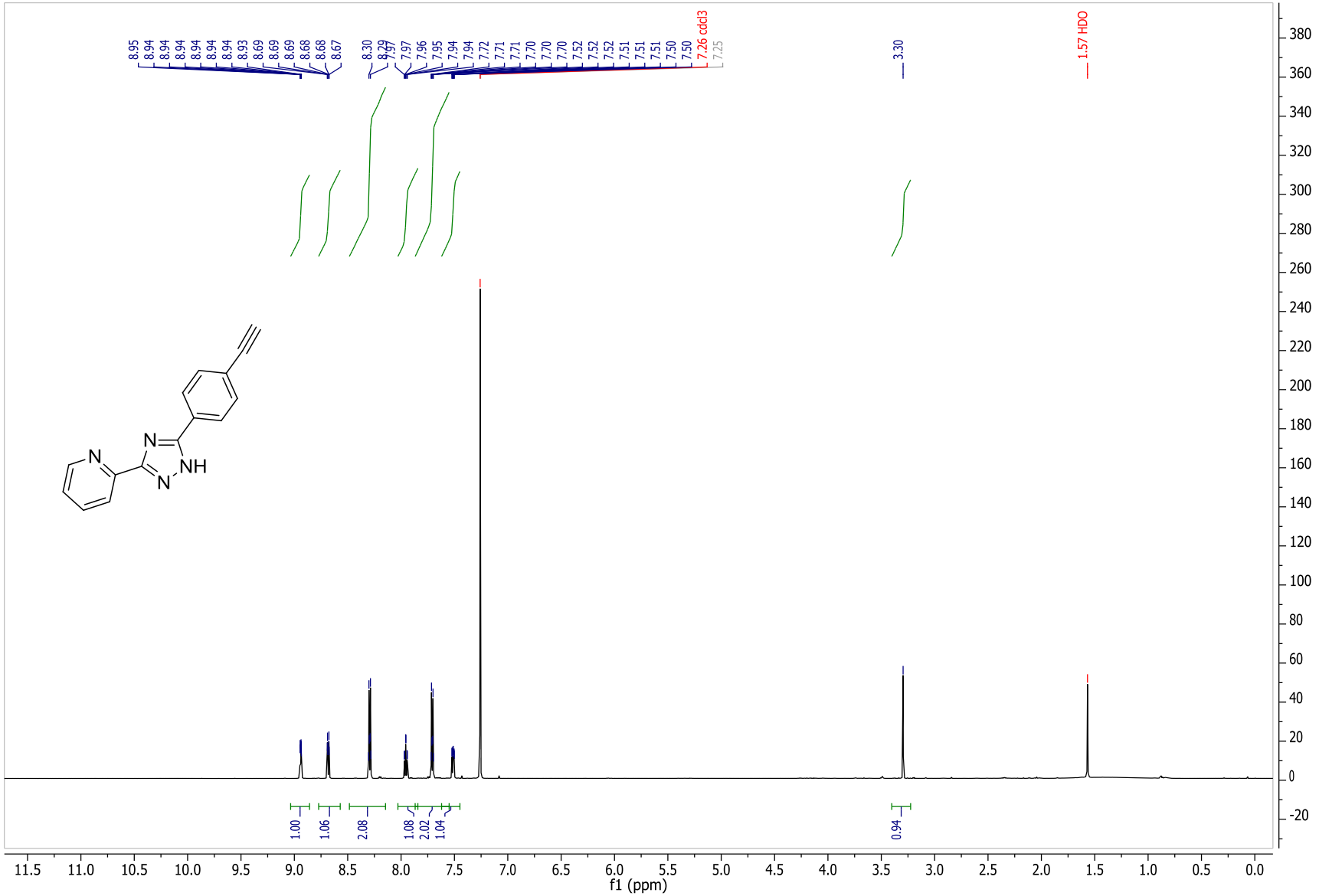

^{1}H NMR spectrum of 3.4

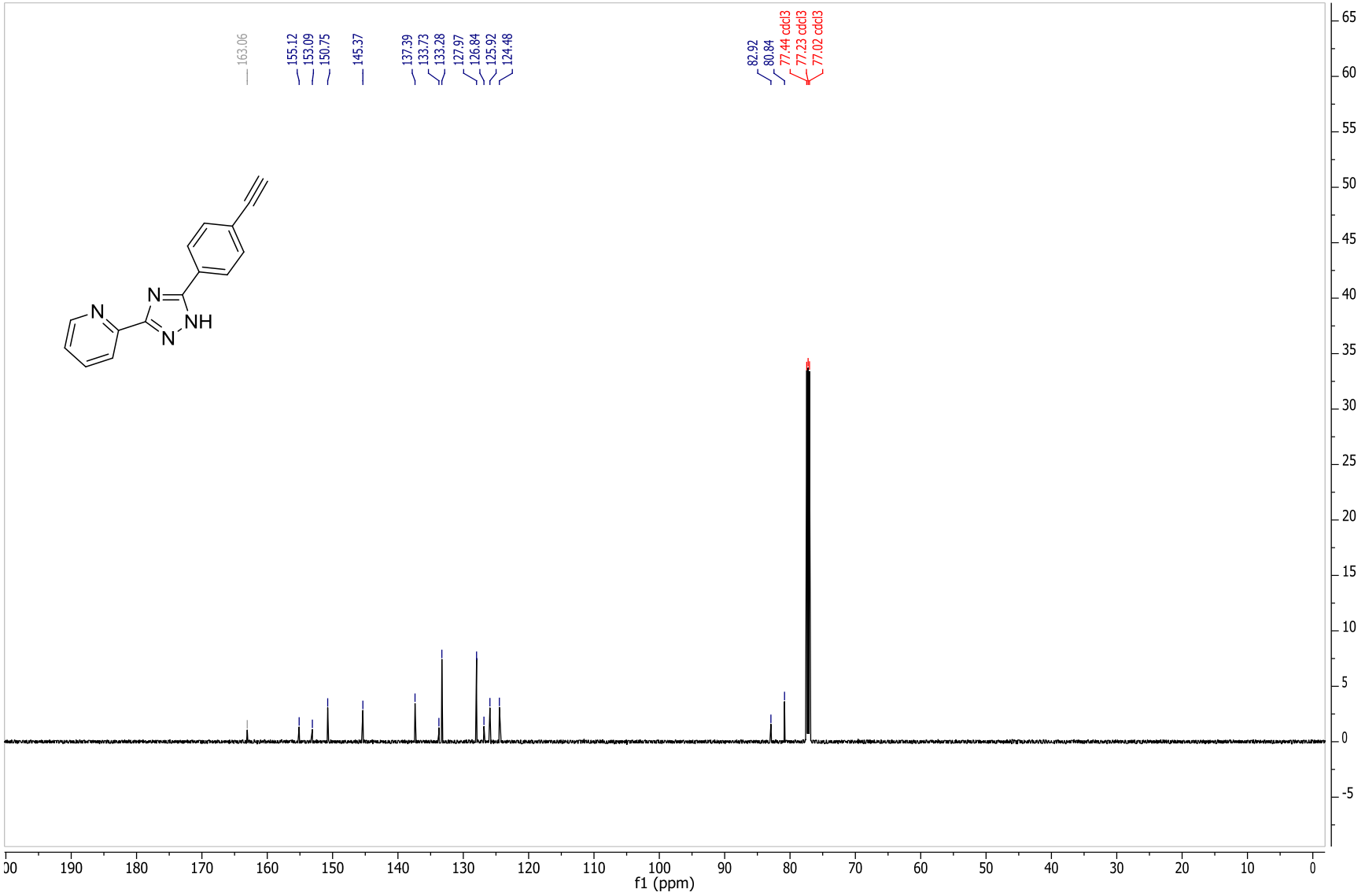

^{13}C NMR spectrum of 3.4

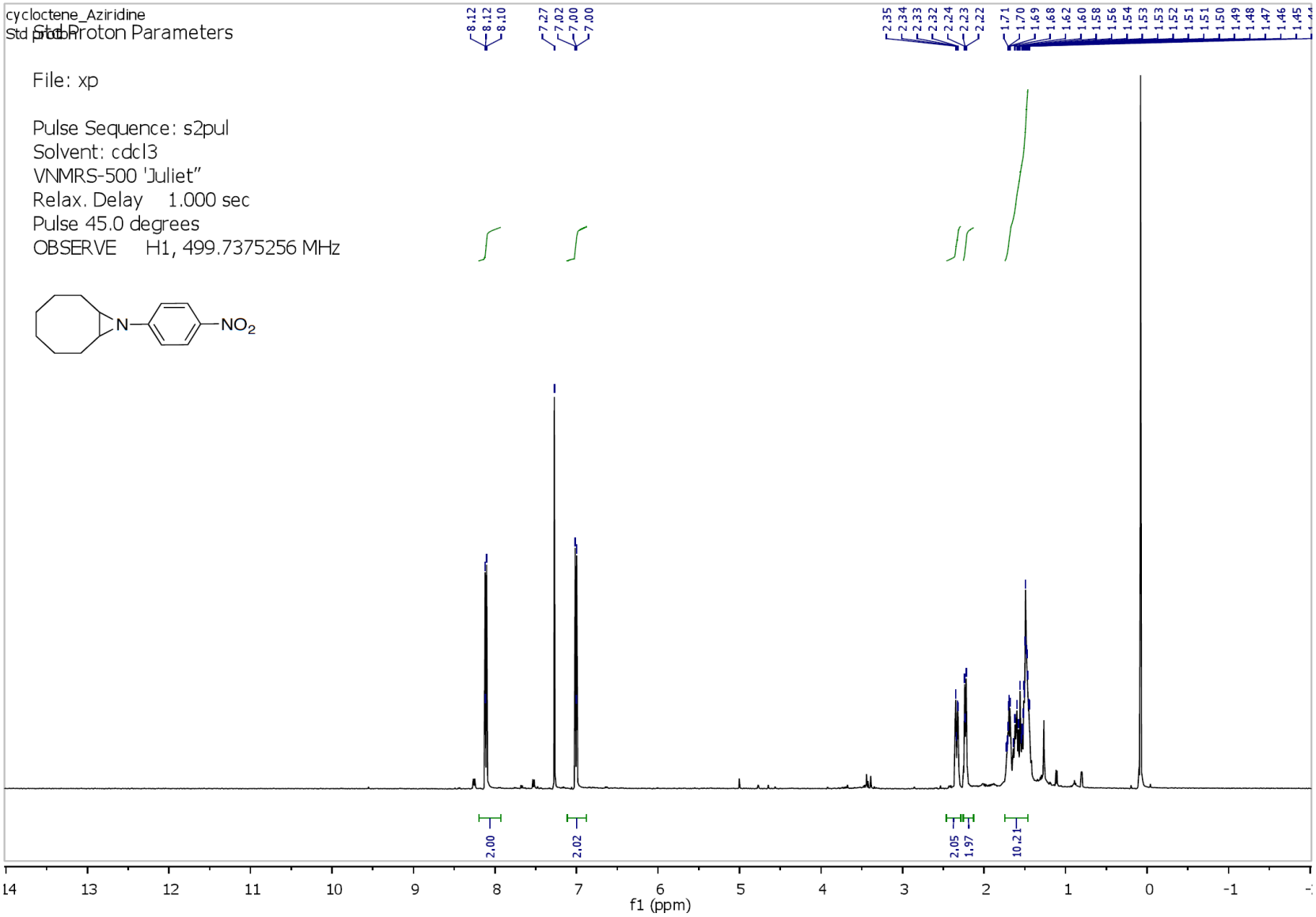

^{1}H NMR spectrum of 6.1

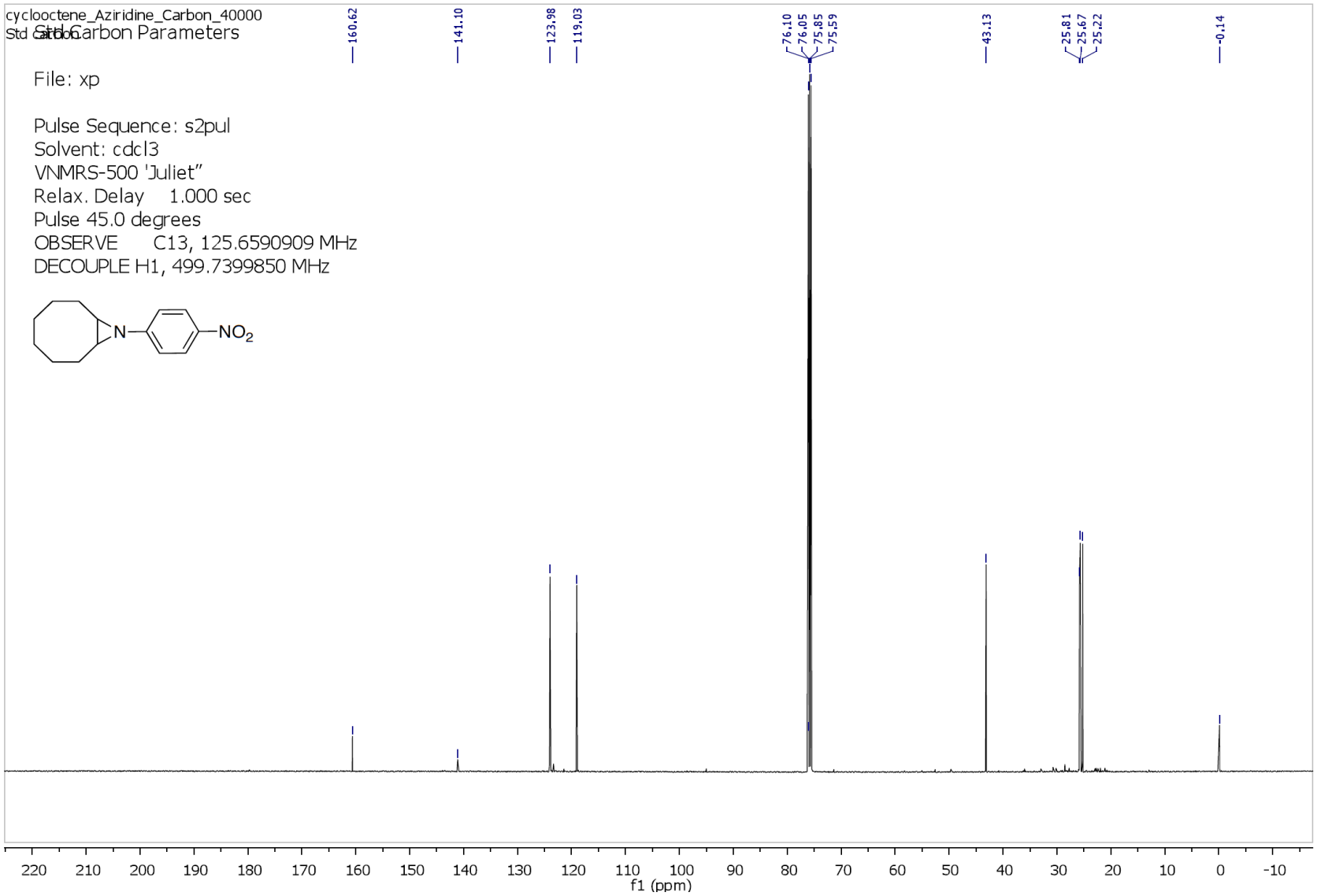

^{13}C NMR spectrum of 6.1

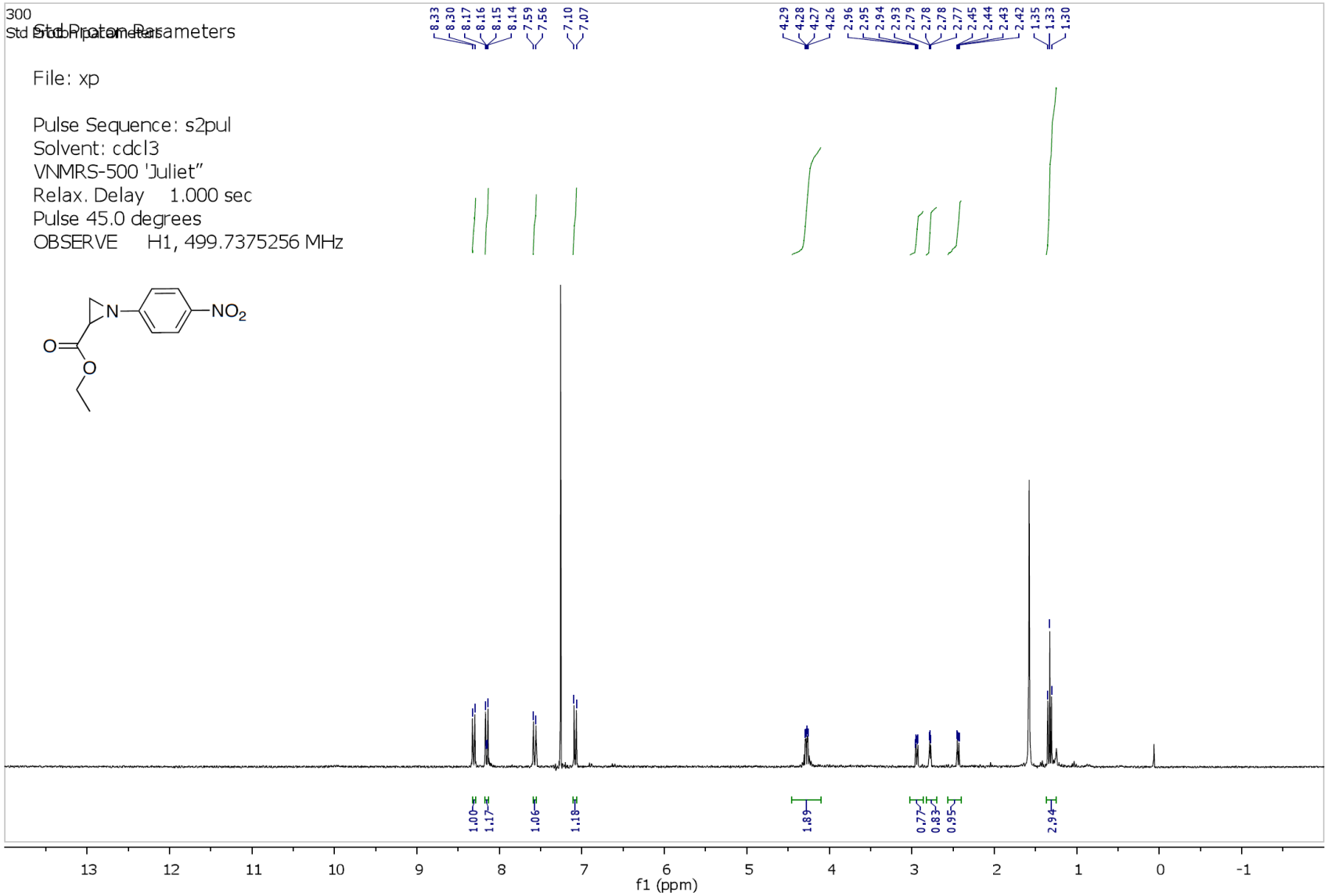

^{1}H NMR spectrum of 6.2

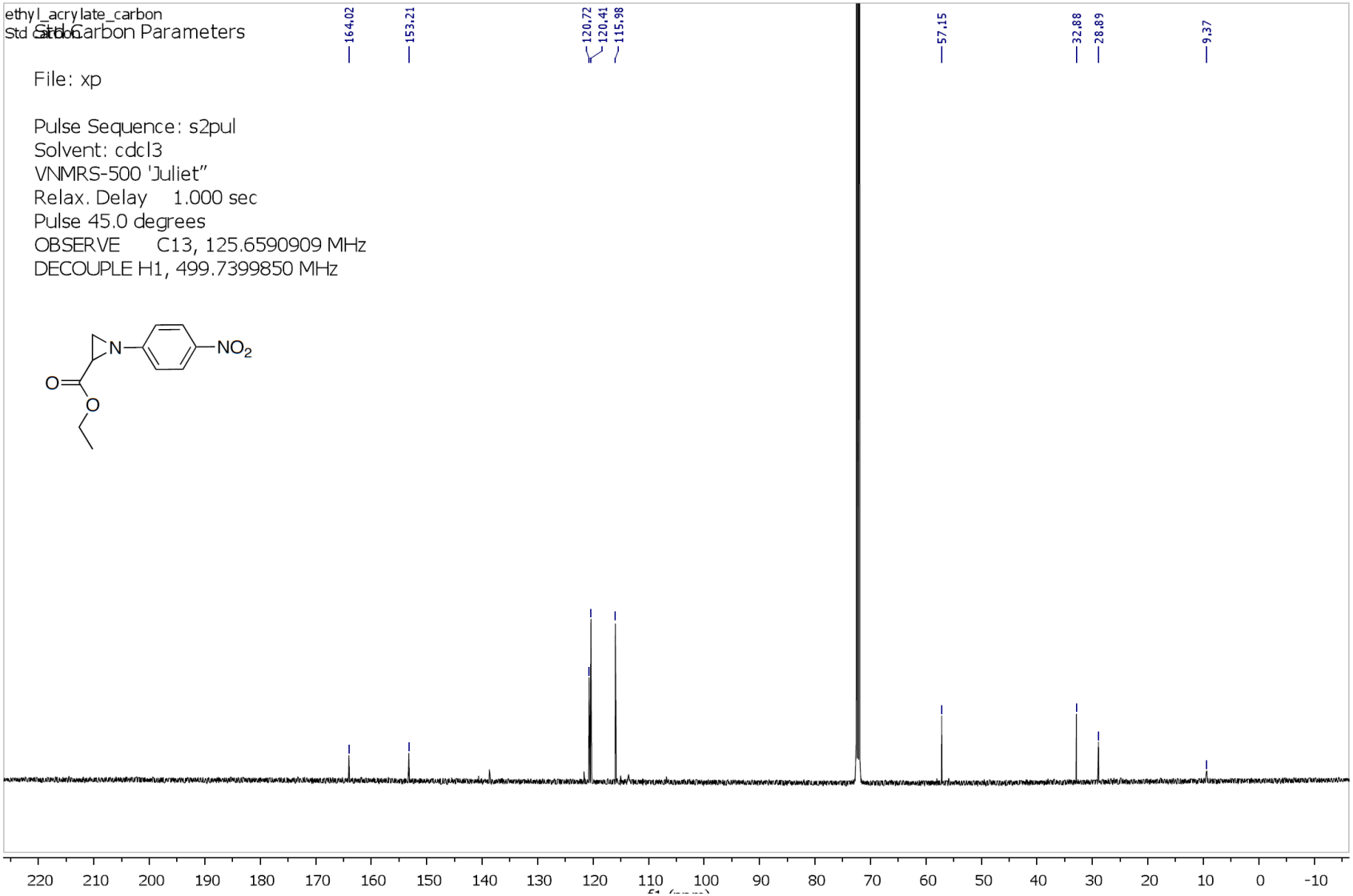

^{13}C NMR spectrum of 6.2

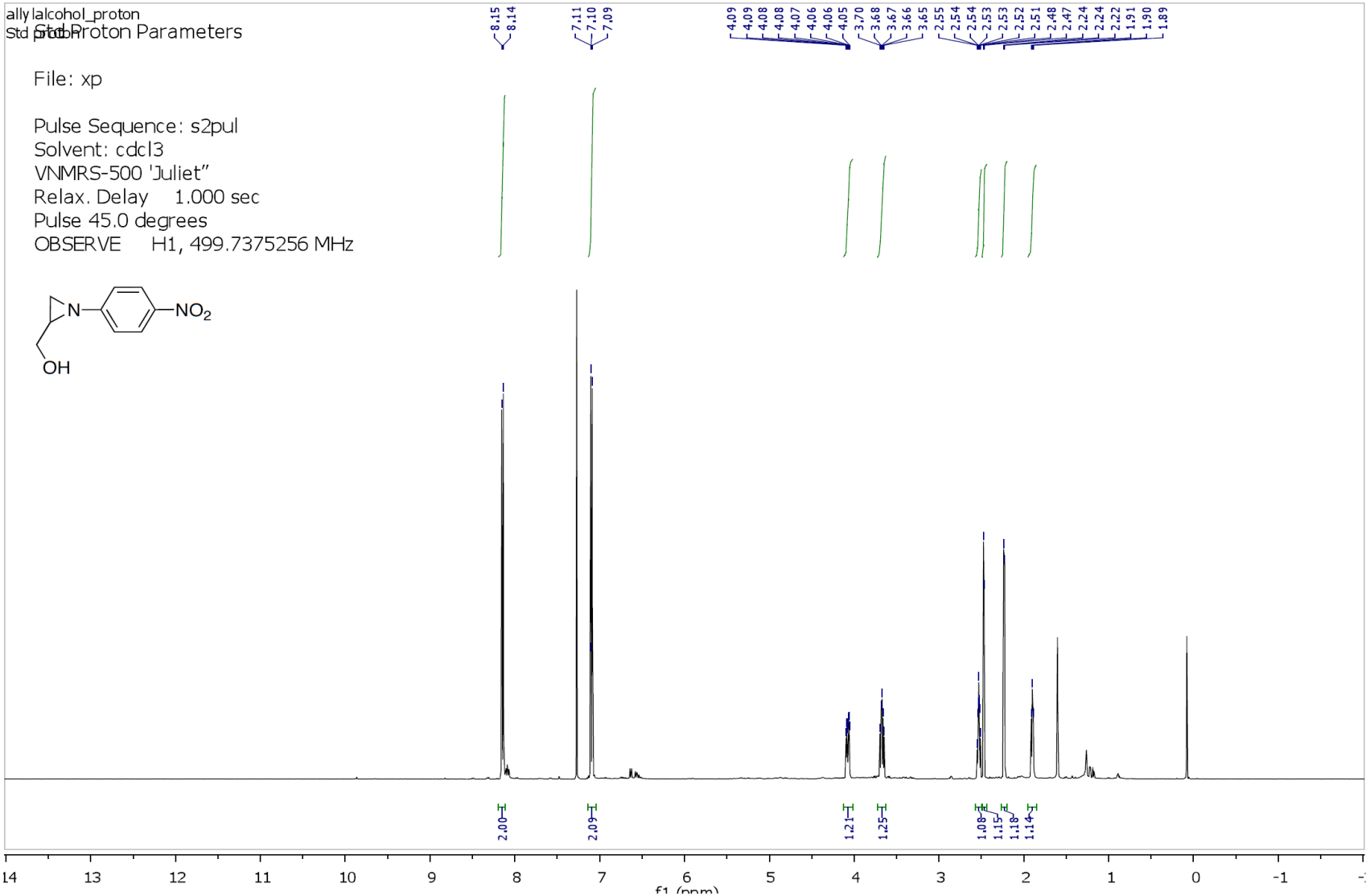

^{1}H NMR spectrum of 6.3

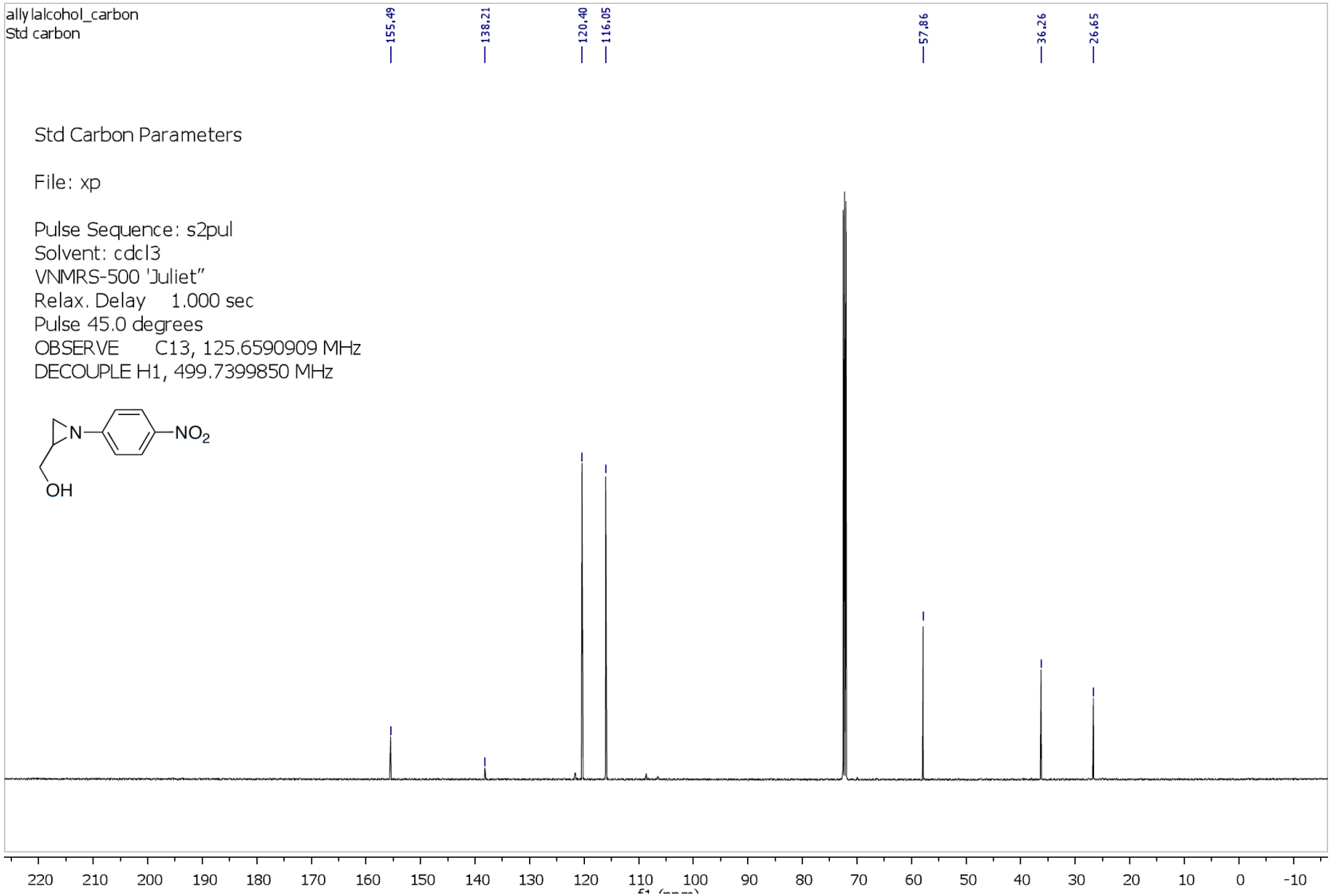

^{13}C NMR spectrum of 6.3

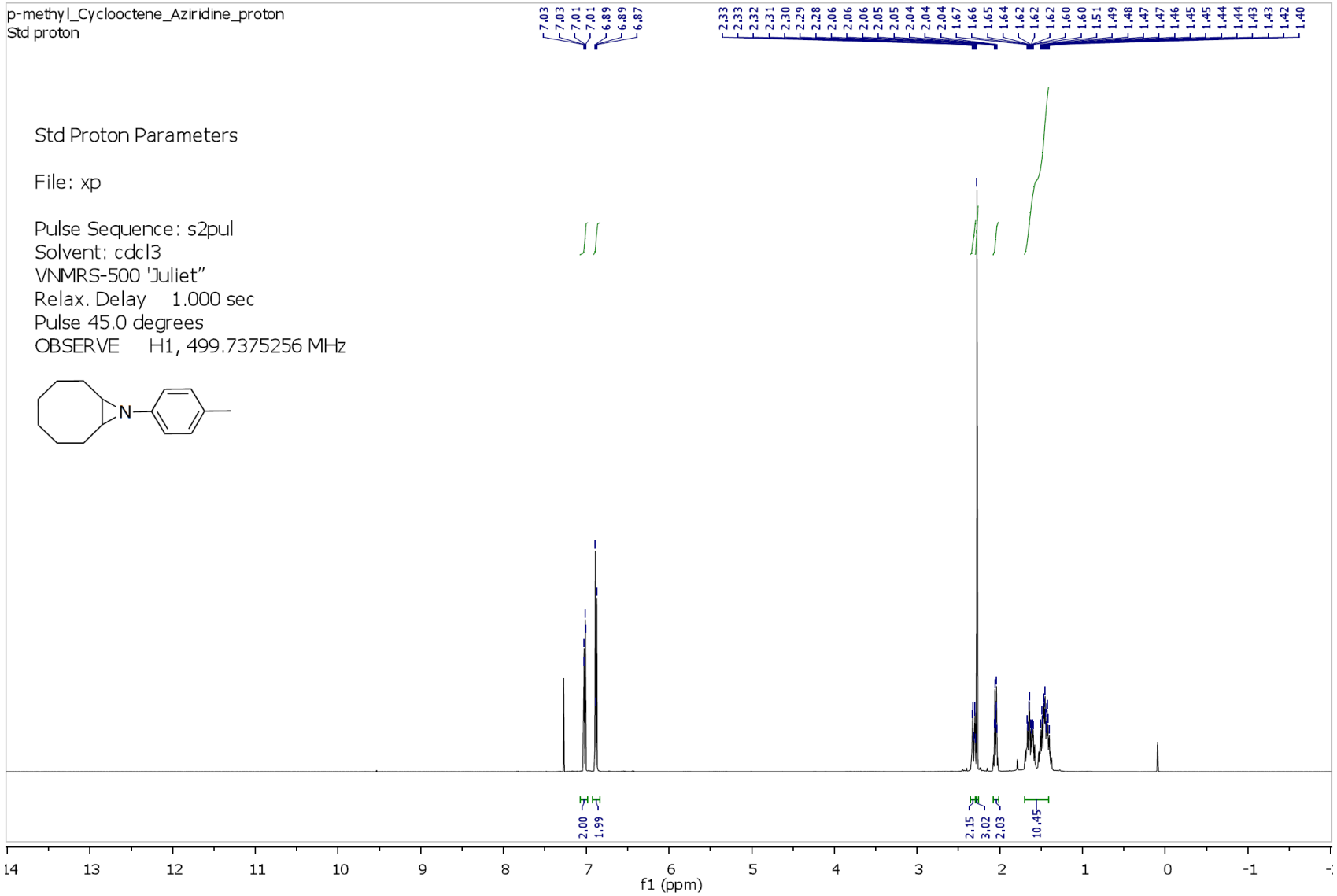

^{1}H NMR spectrum of 6.4

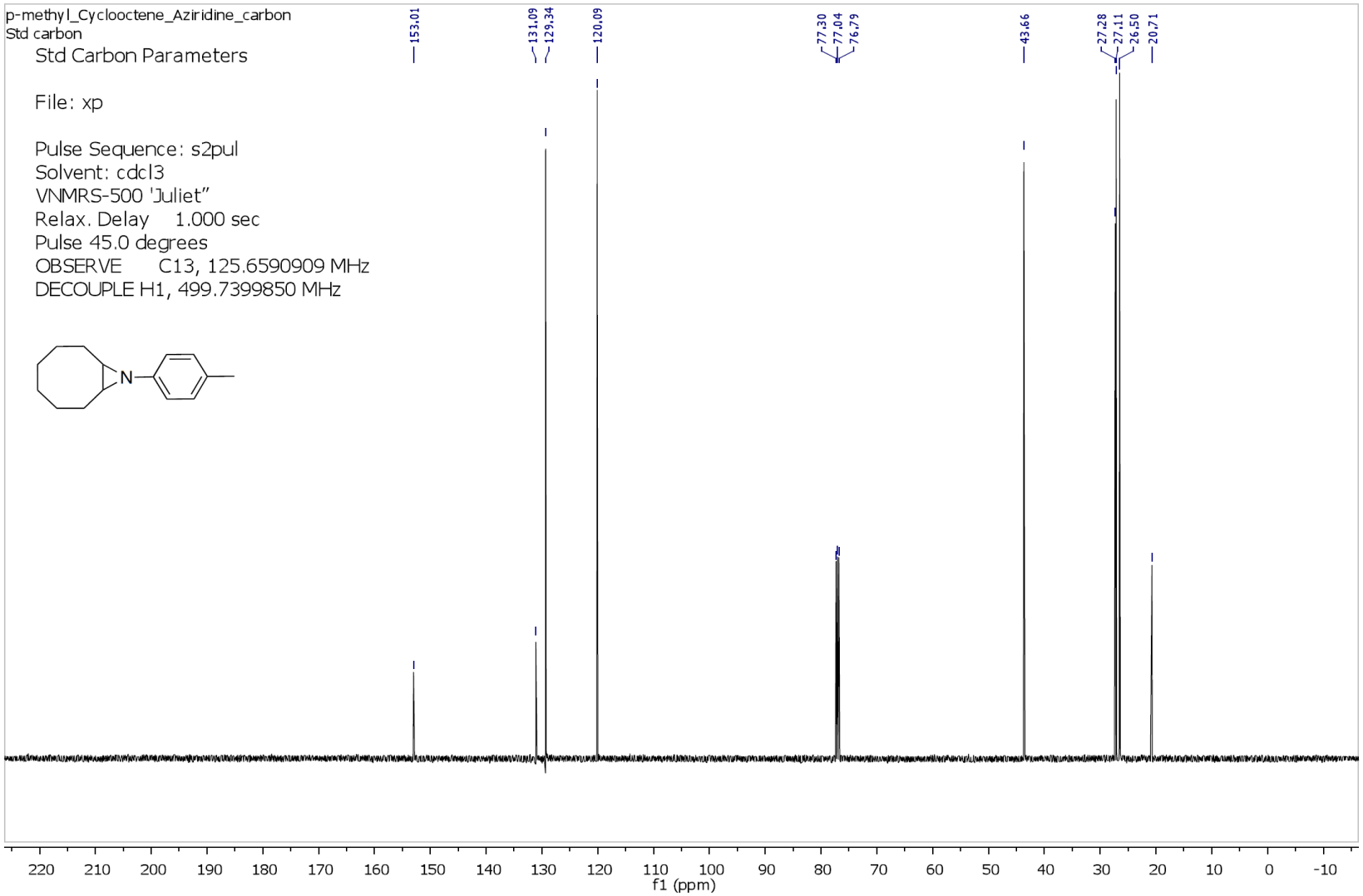

^{13}C NMR spectrum of 6.4

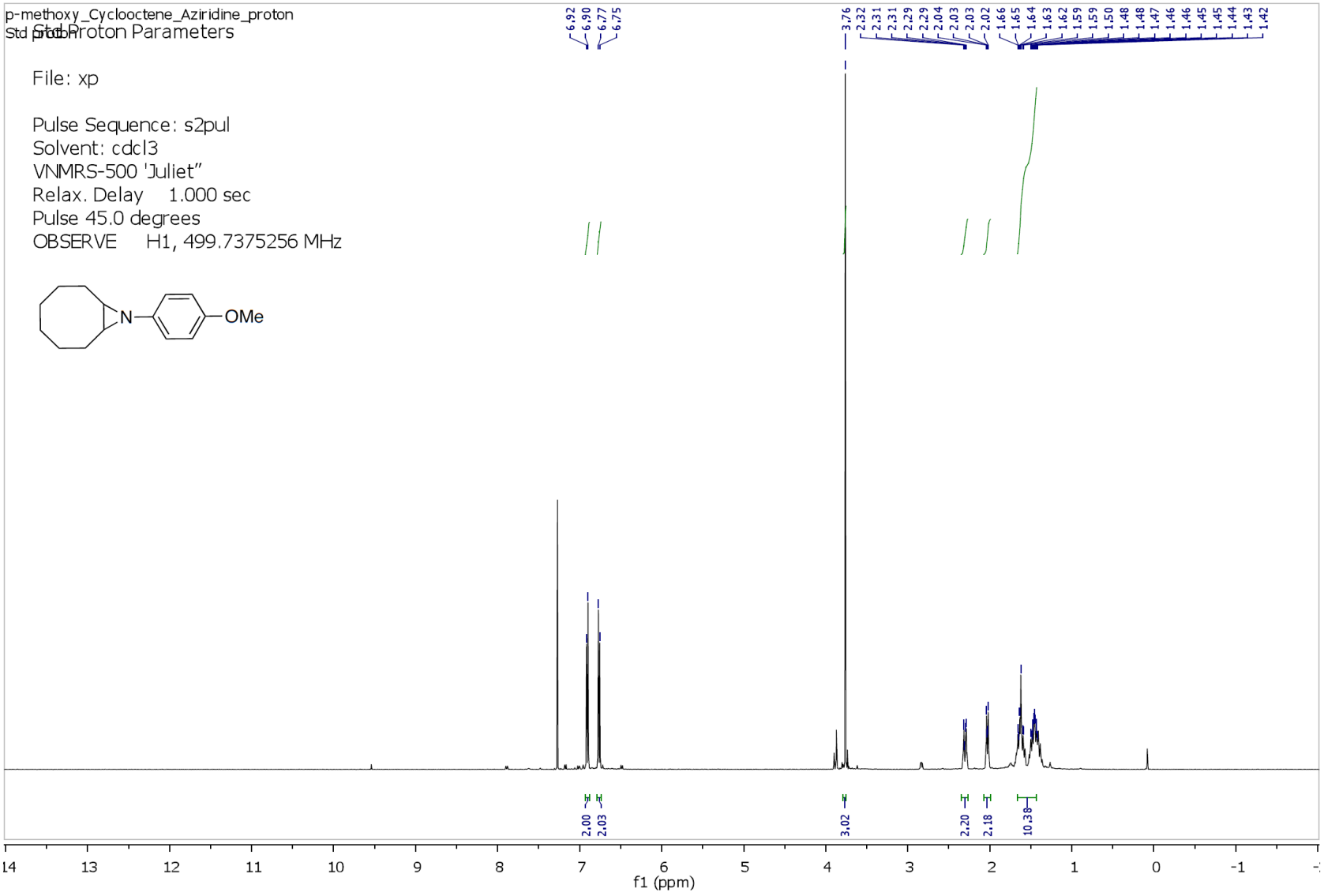

^{1}H NMR spectrum of 6.5

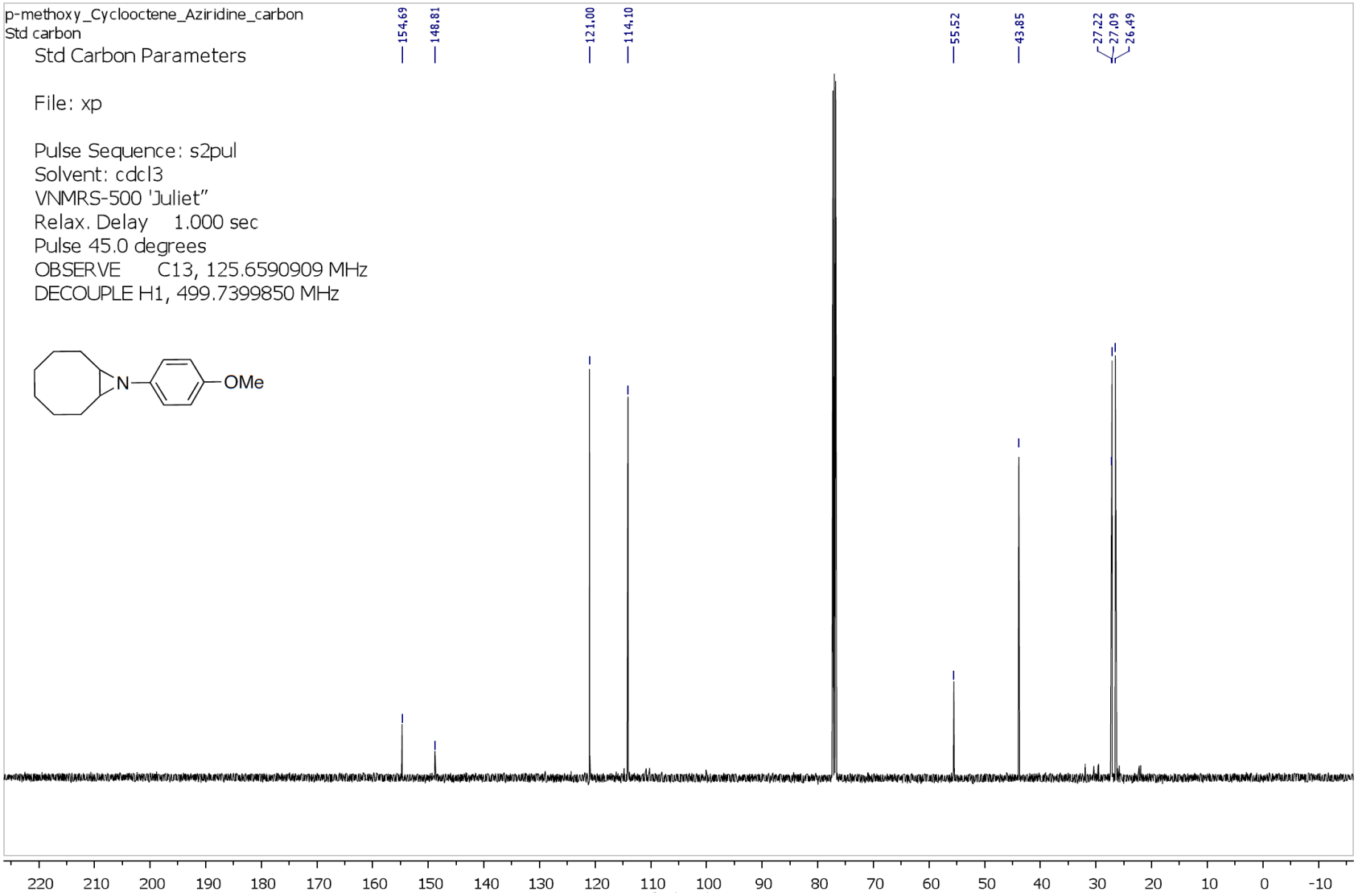

^{13}C NMR spectrum of 6.5

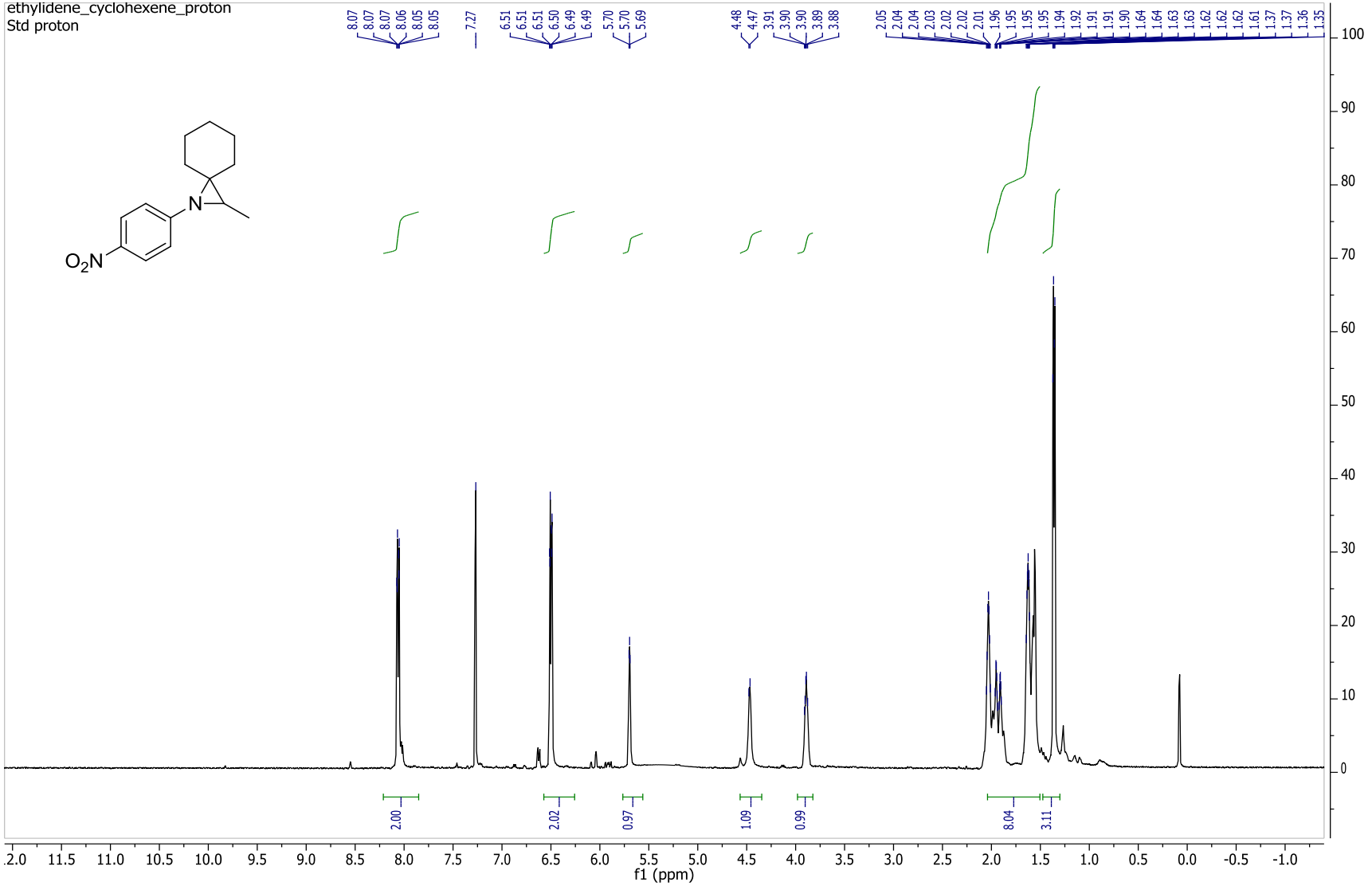

^{1}H NMR spectrum of 6.6

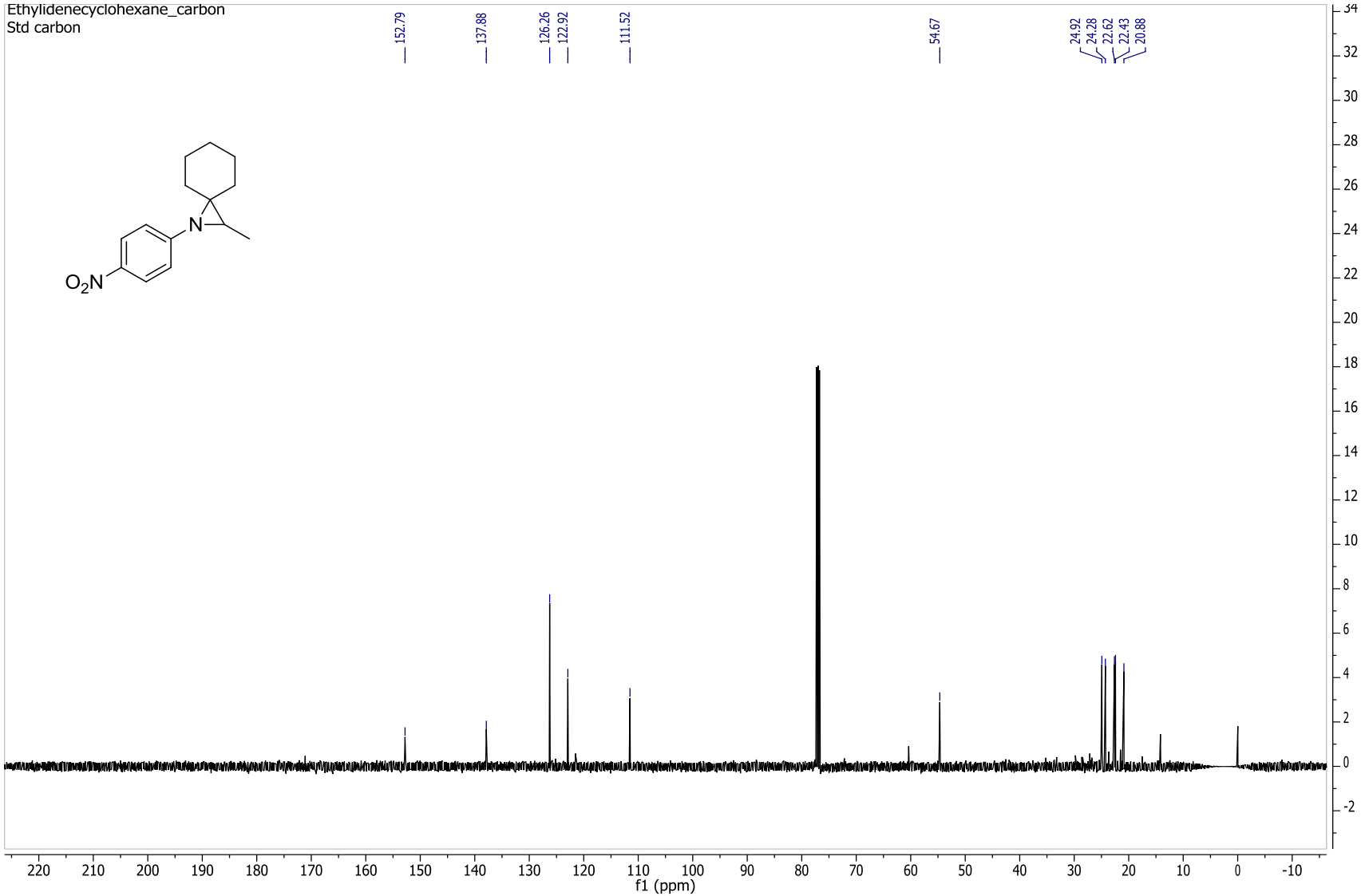

^{13}C NMR spectrum of 6.6

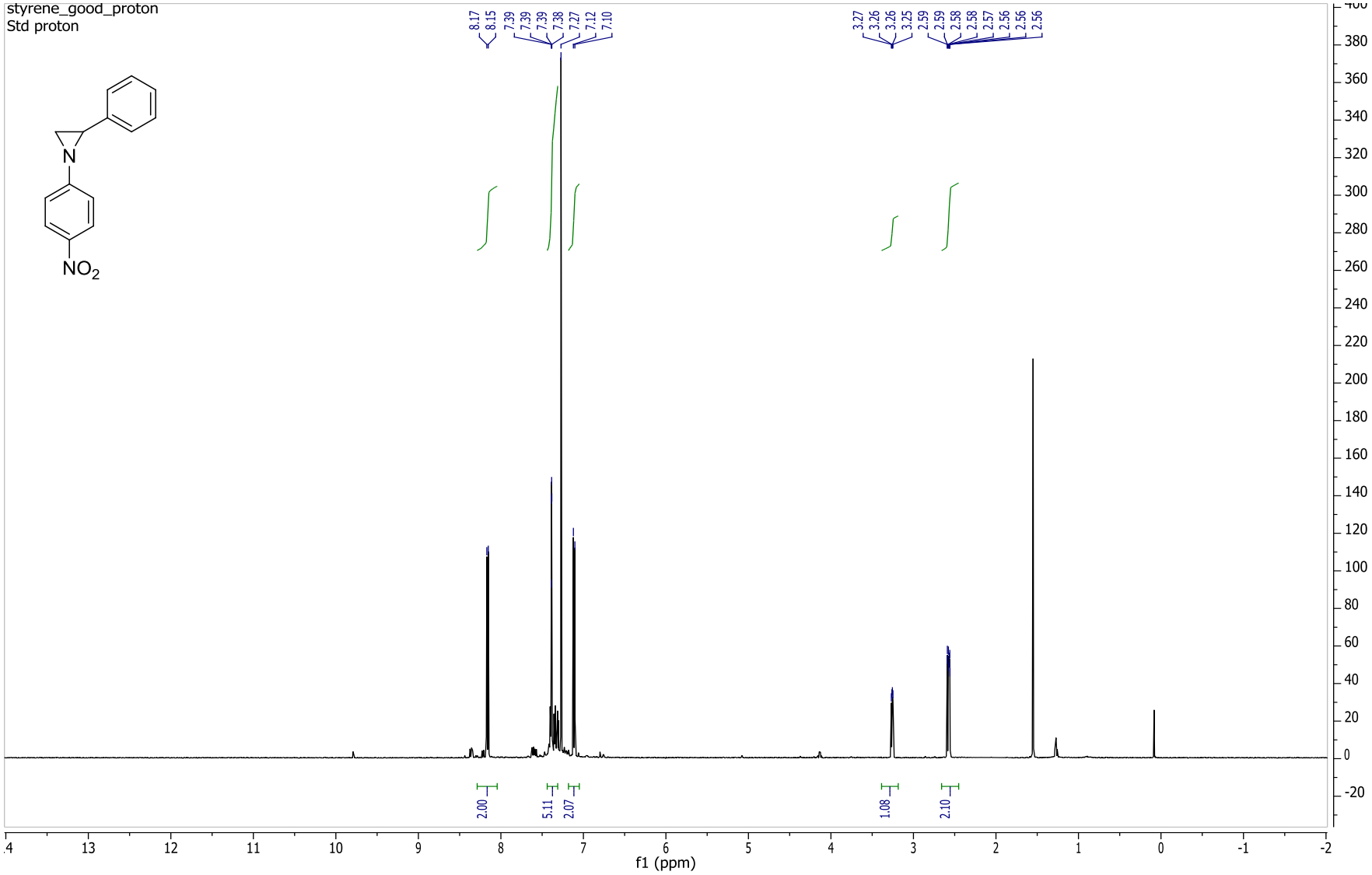

^{1}H NMR spectrum of 6.8

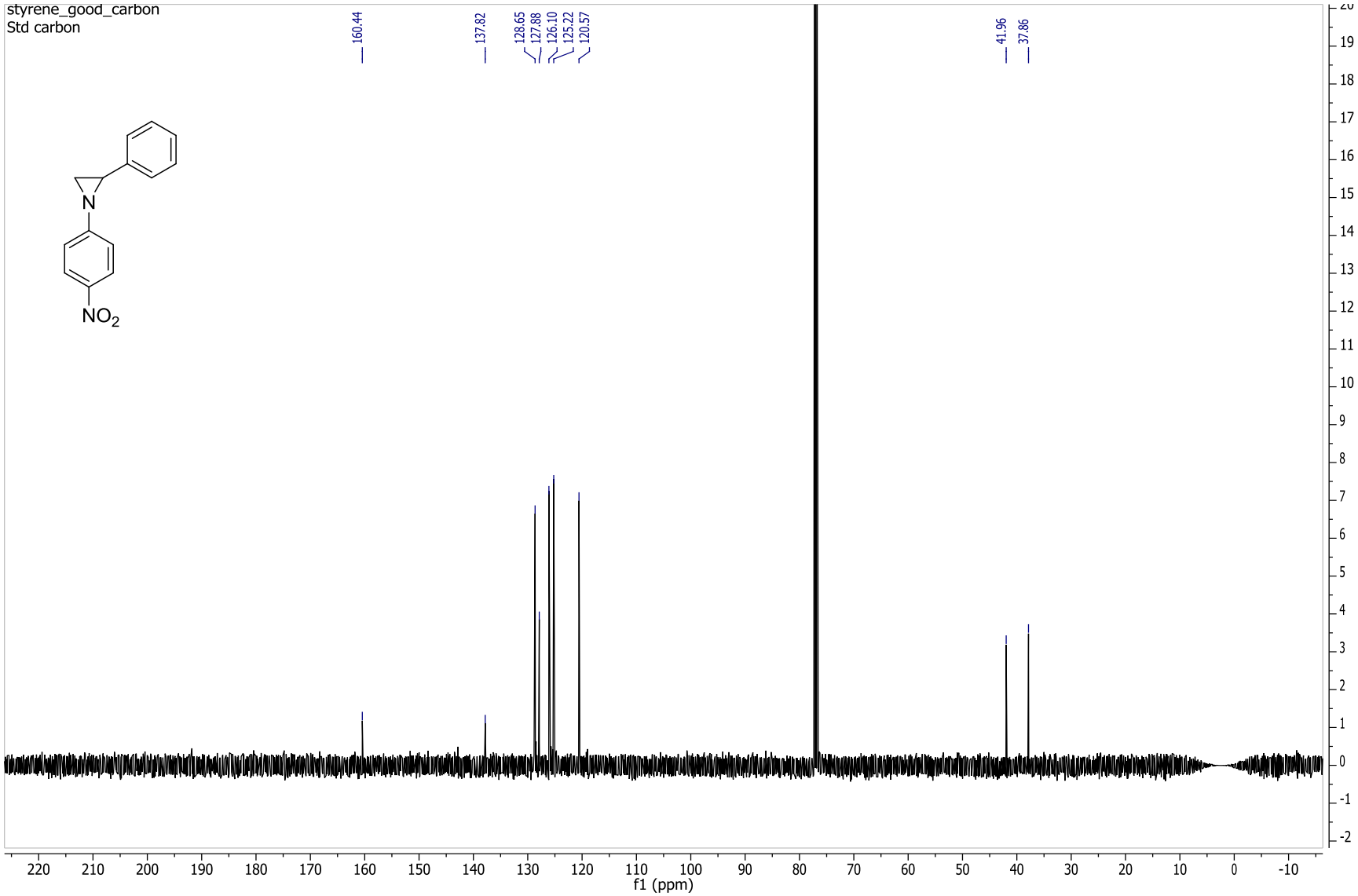

^{13}C NMR spectrum of 6.8

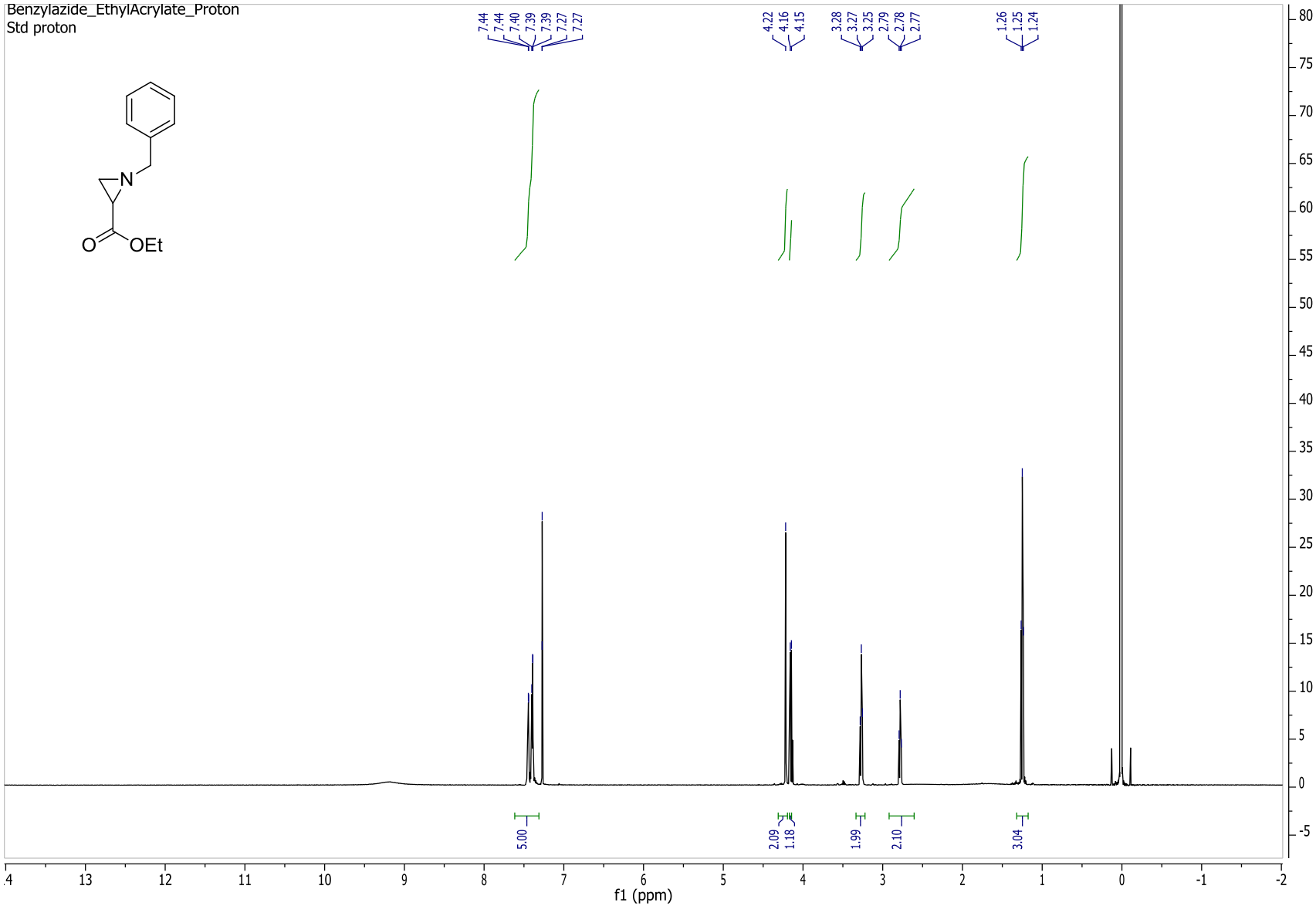

^{1}H NMR spectrum of 6.7

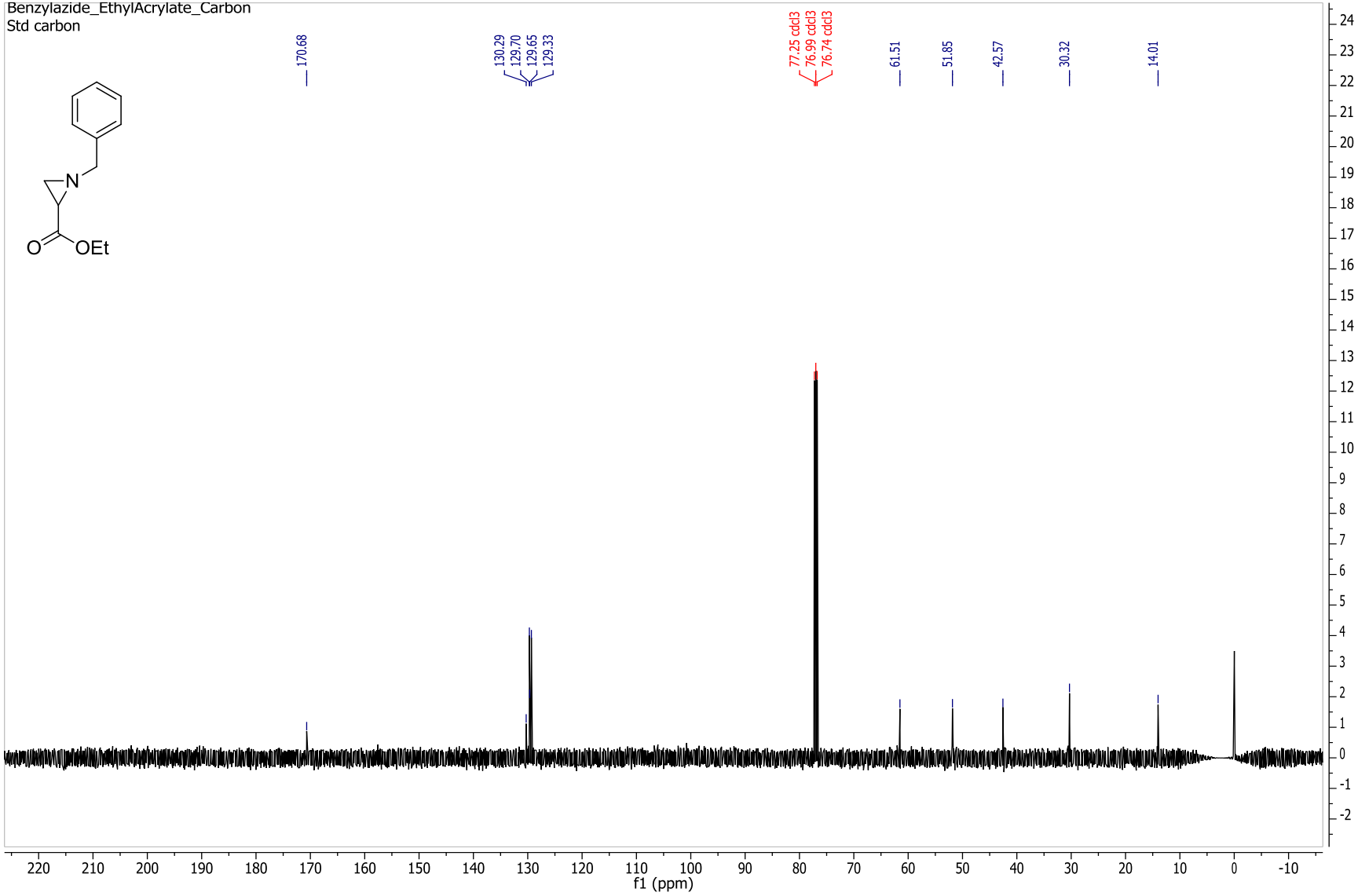

^{13}C NMR spectrum of 6.7

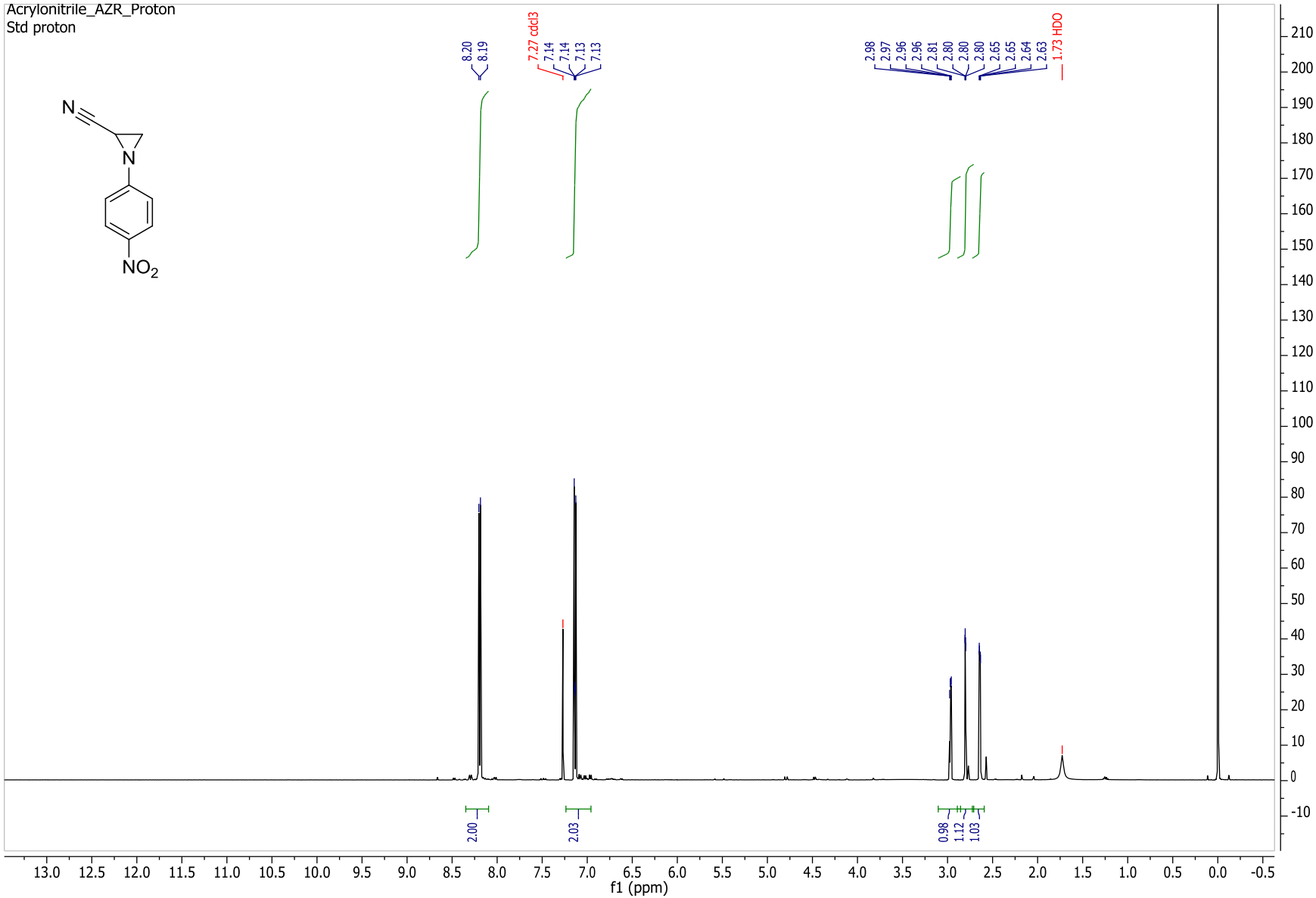

^{1}H NMR spectrum of 6.10

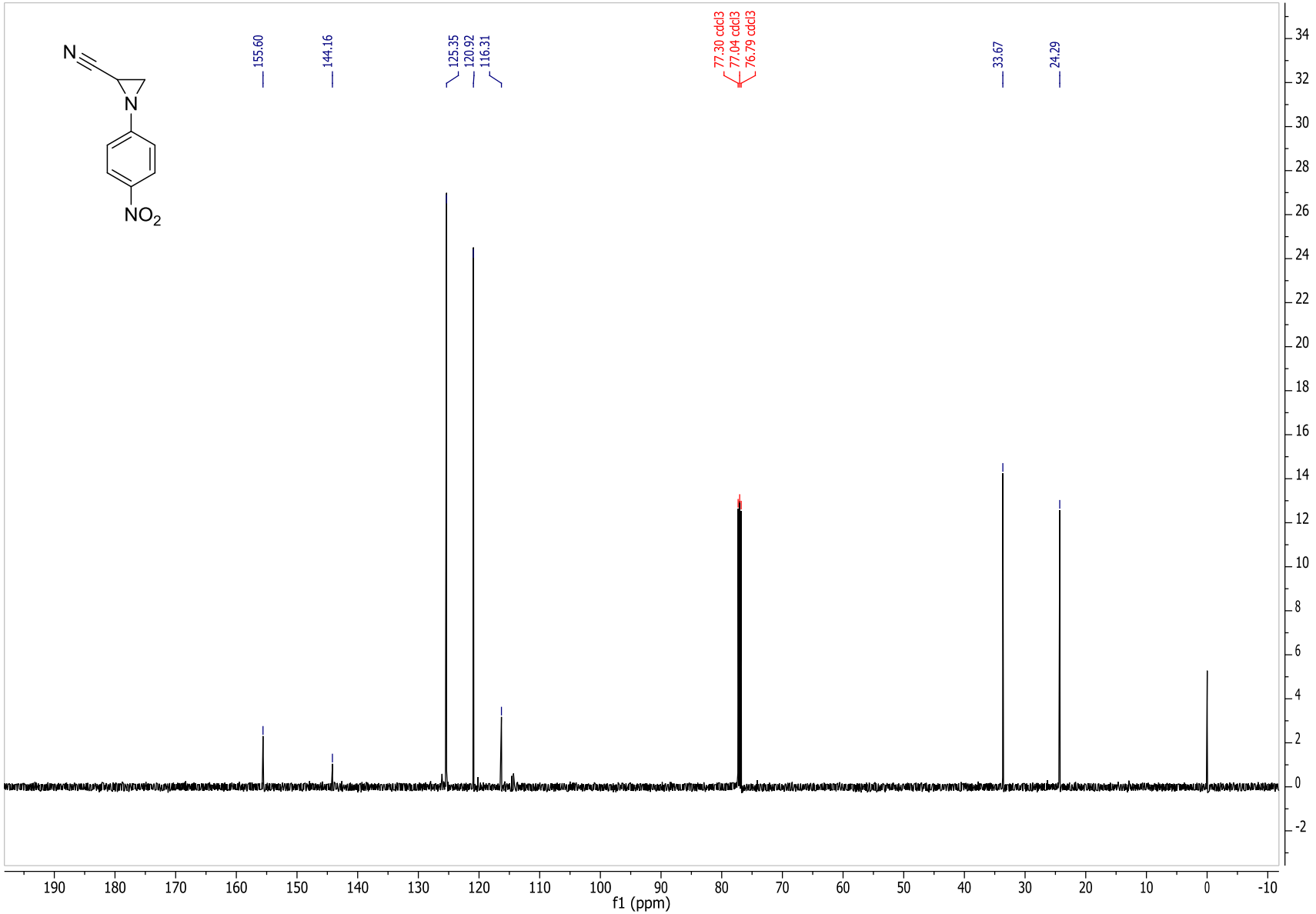

^{13}C NMR spectrum of 6.10

Vita

Ashesh S. Belapure was born in Mumbai, India in 1982. After graduating from highschool, he attended Gujarat University in Ahmedabad, India where he earned a B.Sc. in chemistry with distinction. He then attended University of Pune, Pune, India where he obtained M.Sc. in organic chemistry with first class. He then enrolled in graduate studies at the University of Tennessee under the guidance of Dr. Shane Foister where he obtained Ph.D in organic chemistry.